UNIVERSITY OF CALIFORNIA,
IRVINE

Identifying Synthetic Lethal Interactions in *VHL*-Deficient CC-RCC

DISSERTATION

submitted in partial satisfaction of the requirements
for the degree of

DOCTOR OF PHILOSOPHY

in Molecular Biology and Biochemistry

by

Jordan M. Thompson

Dissertation Committee:
Professor Olga V. Razorenova, Chair
Professor David Fruman
Professor Aimee Edinger

2017

DEDICATION

To my wife Jessica.
I couldn't have done it without you.
Proverbs 31:28-29

TABLE OF CONTENTS

LIST OF FIGURES

LIST OF TABLES

ACKNOWLEDGMENTS

I would like to thank everyone that has supported me and contributed to making this thesis possible. My parents, Mike and Kim Thompson, for putting me through my undergraduate studies at UCSB and constantly pushing me to grow and become the best that I can be. I could not have asked for better parents. Thanks to my brothers Justin and Nathan, who have been and continue to be my role models in life. Thank you for all of your advice and support.

Novi and Stephan, thank you for taking Jessica and I into your house and allowing us to live with you during the beginning of my PhD. Thank you for accepting me as a son, I am so glad to be a part of your family. Thank you to all of Abbalove. You guys have been amazing friends and Jessica and I are so grateful to have you in our lives. We love you guys and we are so thankful for all of your encouraging words and support.

To all of the undergraduate and graduate students who helped me and contributed to this thesis: Quy Nguyen, Manpreet (Sunny) Singh, Bach Tran, Matthew Pavesic, Alejandro (Alex) Alvarez, Monika Singha, Tingting Ge, Kevin Nguyen, Nguyen Dinh, Yuqian (Chen) Zheng, and James Collin Hickey. I literally could not have done it without your support and contributions to my projects. To Quy, Sunny, Matt, Alex, and Monika thank you especially for all of your hard work. I could not have asked for better undergrads or friends. Mentoring you was a privilege and one of the favorite parts of my PhD. I would also like to thank Adam, Christine, and Matthias for their friendship and advice over the years.

Thank you to my amazing labmates Luke Nelson and Dr. Heather Wright. You guys are not only amazing scientists, but also awesome people. Thanks for all the fun times going to the University Club and all of your advice throughout the years on my projects. I wish you both the best in all your future endeavors.

I would like to thank my advancement and dissertation committee members: Dr. David Fruman, Dr. Aimee Edinger, Dr. Marian Waterman, and Dr. Hung Fan. Your time and advice are greatly appreciated. Thank you to all of the labs that participate in our Joint Lab Meetings, your advice and critiques have definitely improved the quality of my research.

Thank you to Oncogene, Molecular Cancer Therapeutics, Small GTPases, and the Yale Journal of Biology and Medicine Journals for the permission to include my published manuscripts in this thesis. I would also like to thank the Cancer Biology & Therapeutics program and the NCI for their financial support through the CBT T32 training grant (2T32CA009054-36A1).

I would like to express my deepest appreciation for my committee chair Olga Razorenova for accepting me into her lab and mentoring me over the last six years. Thank you for your patience and advice. You have shaped me into a better scientist and I am extremely grateful that I joined your lab. Thank you for letting me be a part of your research.

CURRICULUM VITAE

JORDAN M. THOMPSON

EDUCATION

M.S. in Biotechnology, 2017
Department of Molecular Biology & Biochemistry
University of California, Irvine
GPA: 3.99

B.S. in Pharmacology, 2009
Graduated with Honors
University of California, Santa Barbara
GPA: 3.64

CURRENT POSITION

Dissertation Research
06/2013 – Present PhD, December 2017
Department of Molecular Biology & Biochemistry
University of California, Irvine
Olga Razorenova, PhD
GPA: 3.99

Investigating chemical synthetic lethal interactions in Clear Cell Renal Cell Carcinomas (CC-RCC) deficient in the tumor suppressor von Hippel Lindau. Identified and validated a novel synthetic lethal interaction between VHL-deficiency and ROCK1 inhibition. Expanded these results to include Rho inhibitors and identified statins, or HMG-CoA Reductase Inhibitors, as also being synthetically lethal with VHL-deficient RCC. Using VHL-deficient CC-RCC matched lines as a model system to analyze new synthetic lethal interactions and their effects on CC-RCC viability, proliferation, migration, and signaling using molecular biology techniques and mouse models of CC-RCC.

RESEARCH TRAINING

GRADUATE

01/2013-04/2013 **Research Rotation**
UC Irvine, Department of Molecular Biology & Biochemistry
Irene Pedersen, PhD

Investigated the antineoplastic properties of miRs as well as their potential for use in generating induced pluripotent stem cells through two specific aims: characterized anti-miR library screens for novel tumor suppressor miRs and assisted with the development of a miR induced pluripotent stem cell procedure.

09/2012-12/2012 **Research Rotation**
UC Irvine, Department of Developmental & Cell Biology
Aimee Edinger, PhD

Evaluated the potential of novel FTY720 analogs as cancer therapies through two specific aims: to evaluate the relative activity of a panel of FTY720 analogs in cell lines derived from different cancer classes, and to assess whether differences in compound activity can be attributed to differences in their stability or phosphorylation.

INDUSTRY

02/2011-08/2012 **Sr. Professional**
Biomaterials R&D Department
Allergan Medical, Santa Barbara

Developed physical analytical methods using SEM, mechanical testers, and rheometers to characterize specific device properties. Developed chemical analytical methods for use in the detection and quantification of compounds of interest using HPLC and UV Vis. Led a matrix team of 8 people focused on reverse engineering medical devices culminating in a comprehensive technical report and training for the marketing and sales teams. Coordinated the project management of the project, developed new tests, wrote the technical report, created the training presentations, conducted the training with multiple regions, and served as a subject matter expert to regulatory, marketing, and sales. Assisted with training and development of materials for a new product launch. Served as a subject matter expert during training with new principal investigators.

10/2009-02/2011 **Professional**
Biomaterials R&D Department
Allergan Medical, Santa Barbara

Led a formulation group focused on the development of next generation biocompatible constructs. Correlated in vivo and in vitro test results to show project success. Assisted histology and analytical groups in developing and validating protocols. Invented and developed a novel material with an estimated total market potential for medical applications over $400M / year and approximately $1B / year in potential non-medical uses resulting in 14 patent applications. Developed 7 prototypes for 3 new technology platforms that were presented to corporate and executive management at Allergan.

Led a matrix team of 5 individuals including senior associate, associate, and technician level personnel. Managed 3 CRO's with a total annual budget of over $300k. Successfully completed 2 top tier corporate projects on-time.

04/2009-10/2009 **Research Associate**
Allergan Medical
Adecco Group, Santa Barbara

Assisted in developing new biomaterials for use in next generation aesthetic and implant products via synthesis, formulation, fabrication, and characterization. Developed histological assays for the tissue materials science group for use in evaluating the success of different biomaterial formulations. Developed test methods and protocols for characterizing the morphological and mechanical properties of the biomaterial formulations. Developed and expanded an existing in-house biomaterial process with new formulations.

UNDERGRADUATE

05/2007-09/2009 **Research Assistant**
University of California, Santa Barbara, Chemistry Department
Kalju Kahn, PhD

Designed and maintained a Computational Chemistry Database used as an aid in the analysis and publication of new molecular basis set methods in Drug Design. Created a web site for analyzing conformer energies in more than 15 molecules using ten synchronous scripts that access a database containing ten tables per molecule.

Responsible for developing new laboratory procedures for graduate and undergraduate biochemistry lab classes. Developed new procedures involving SDS PAGE and native gel electrophoresis, diffusion blotting and electroblotting, dialysis, and fluorescent markers. Developed and implemented protein-binding studies utilizing attachment of fluorescently labeled protein to target protein recovered from western blotting. Purified Proteins for MALDI mass spectrometry using dialysis from western blot extracts

TEACHING ASSISTANCESHIPS (University of California, Irvine)

2017, fall quarter BS45: Aids Fundamentals (lecture)
BS45: Introduction to Computational Biology (lecture)
2015, winter quarter M130L: Advanced Molecular Biology Techniques Laboratory
M125: Molecular Biology of Cancer (lecture)
2014, spring quarter M116L: Molecular Biology Laboratory
M125: Molecular Biology of Cancer (lecture)
2014, winter quarter M116L: Molecular Biology Laboratory
BIO99: Molecular Biology of Cancer (lecture)

PUBLICATIONS

Thompson JM, Alvarez A, Singha MK, Pavesic MW, Nguyen QH, Nelson LJ, Fruman DA, Razorenova OV. Inhibition of small GTPase isoprenylation by statins is synthetically lethal with von Hippel-Lindau loss in Clear Cell Renal Cell Carcinoma. MolCanTher. **Submitted.**

Thompson JM, Landman J, Razorenova OV. Targeting the RhoGTPase / ROCK pathway for the treatment of VHL / HIF pathway-driven cancers. Small GTPases. 2017;1248.

Thompson JM, Nguyen QH, Singh M, Pavesic MW, Nesterenko I, Nelson LJ, et al. Rho-associated kinase 1 inhibition is synthetically lethal with von Hippel-Lindau deficiency in clear cell renal cell carcinoma. Oncogene. Nature Publishing Group; 2016;36:1080–9.

Thompson JM, Nguyen QH, Singh M, Razorenova O. Approaches to Identifying Synthetic Lethal Interactions in Cancer. Yale J Biol Med. 2015;88:145–55.

Idica, A., **Thompson, J.**, Munk Pedersen, I., and Kadandale, P. 2015. Using Undergraduate Molecular Biology Labs to Discover Targets of miRNAs in Humans. CourseSource.

PRESENTATIONS

Thompson JM, Alvarez A, Singha MK, Pavesic MW, Nguyen QH, Razorenova OV. (**2017**) Statin Inhibition of Rho/ROCK is synthetically lethal in VHL-deficient CC-RCC.

- Presented at Campus Wide Symposium on Basic Cancer Research, **poster presentation**.

Thompson JM, Alvarez A, Singha MK, Pavesic MW, Nguyen QH, Razorenova OV. (**2017**). Statin Inhibition of Rho/ROCK is synthetically lethal in VHL-deficient CC-RCC.

- Presented at Cancer Biology and Therapeutics Research in Progress Series, **oral presentation**.

Thompson JM, Nguyen QH, Singh M, Razorenova OV. (**2016**) Small Molecule Screen in VHL-Deficient CC-RCC Reveals a Synthetic Lethal Interaction with ROCK Inhibition.

- Presented at Campus Wide Symposium on Basic Cancer Research, **poster presentation**.

Thompson JM, Nguyen QH, Singh M, Razorenova OV. (**2015**) ROCK1 inhibition is Synthetically Lethal with VHL loss in Clear Cell Renal Cell Carcinoma.

- Presented at Department of Molecular Biology and Biochemistry Research in Progress Seminar, **oral presentation**.

Thompson JM, Nguyen QH, Singh M, Pavesic MW, Razorenova OV. (**2015**). Investigating the Synthetic Lethal Effect of ROCK Inhibition in VHL-Deficient Clear Cell Renal Cell Carcinoma.

- Presented at Cancer Biology and Therapeutics Research in Progress Series, **oral presentation**.

Thompson JM, Nguyen QH, Singh M, Razorenova OV. (**2015**) Small Molecule Screen in VHL-Deficient CC-RCC Reveals a Synthetic Lethal Interaction with ROCK Inhibition.

- Presented at Campus Wide Symposium on Basic Cancer Research, **poster presentation**.

Thompson JM, Nguyen QH, Singh M, Razorenova OV. (**2015**) Investigating the Synthetic Lethal Effect of ROCK Inhibition in VHL-Deficient Clear Cell Renal Cell Carcinoma.

- ❖ Presented at Department of Molecular Biology and Biochemistry Research in Progress Seminar, **oral presentation**.

Thompson JM, Nguyen QH, Singh M, Razorenova OV. (**2015**) Small Molecule Screen in VHL-Deficient CC-RCC Reveals a Synthetic Lethal Interaction with ROCK Inhibition.

- ❖ Presented at Molecular Biology & Biochemistry Departmental Retreat, **poster presentation**.

Thompson JM, Nguyen QH, Singh M, Pavesic MW, Razorenova OV. (**2015**) Small Molecule Screen in VHL-Deficient CC-RCC Reveals a Synthetic Lethal Interaction with ROCK Inhibition.

- ❖ Presented at Chao Family Comprehensive Cancer Center Retreat, **poster presentation**.

Thompson JM, Nguyen QH, Singh M, Razorenova OV. (**2014**) Small Molecule Screen in Clear Cell Renal Cell Carcinoma Reveals Synthetic Lethal Interactions with VHL Deficiency.

- ❖ Presented at Campus Wide Symposium on Basic Cancer Research, **poster presentation**.

Thompson JM, Nguyen QH, Razorenova OV. (**2014**) Small Molecule Screen in Clear Cell Renal Cell Carcinoma Reveals Synthetic Lethal Interactions with VHL Deficiency.

- ❖ Presented at Department of Molecular Biology and Biochemistry Research in Progress Seminar, **oral presentation**.

Thompson JM, Nguyen QH, Razorenova OV. (**2014**) Small Molecule Screen in Clear Cell Renal Cell Carcinoma Reveals Synthetic Lethal Interactions with VHL Deficiency.

- ❖ Presented at Department of Molecular Biology & Biochemistry Retreat, **oral and poster presentation**.

AWARDS

2015-2017	Cancer Biology and Therapeutics T32 Fellowship, National Cancer Institute
2015	Best Poster Presentation – Campus Wide Symposium on Basic Cancer Research
2014	Best Poster Presentation – Molecular Biology & Biochemistry Retreat
2012	Francisco J. Ayala Graduate Fellowship, UC Irvine
2009	Faculty Research Assistance Program Award, UC Santa Barbara
2005-2009	UCSB Honors Program

ABSTRACT OF THE DISSERTATION

Identifying Synthetic Lethal Interactions in VHL-Deficient CC-RCC

By

Jordan M. Thompson

Doctor of Philosophy in Molecular Biology and Biochemistry

University of California, Irvine, 2017

Professor Olga Razorenova, Chair

Clear Cell Renal Cell Carcinoma (CC-RCC) is a devastating disease in its metastatic manifestation with a 5-year survival rate of 11.7%. The loss of the tumor suppressor von Hippel-Lindau (VHL) has been shown to drive the initiation and progression of CC-RCC. Since most of the currently approved FDA therapies act on a patient's endothelial cells to reduce angiogenesis, instead of directly on the tumor, new targeted therapies are needed to treat this disease. One method for identifying targeted and tumor specific therapies is by identifying synthetic lethal interactions with the most common mutations in the cancer.

We conducted an annotated chemical library screen in a CC-RCC cell line with and without *VHL* re-expressed and identified seven potential synthetic lethal interactions. Validation of these potential hits confirmed that inhibition of Rho Kinase (ROCK) 1 is synthetically lethal with *VHL*

loss in CC-RCC. We then confirmed the interaction both genetically via siRNA knockdown and with multiple ROCK inhibitors. The synthetic lethality interaction effect between ROCK1 inhibition and VHL loss is dependent on the overactivation of HIFs that occurs upon *VHL* loss. Furthermore, treatment with the ROCK inhibitor Y-27632 inhibited tumor growth *in vivo* in a subcutaneous xenograft model using 786-O CC-RCC cells.

While ROCK inhibitors have great potential to become CC-RCC therapeutics, with the exception of Fasudil approved in Japan and China for treating cerebral vasospasm and pulmonary hypertension, the existing inhibitors are currently limited to topical applications for glaucoma. Statins, HMG CoA Reductase inhibitors, can disrupt the Rho/ROCK pathway at doses administered for treating hypercholesterolemia. We have confirmed the synthetic lethal effect of statin treatment in *VHL*-deficient CC-RCC. The effect is cytostatic at low nanomolar doses and becomes cytotoxic as the dose is increased into the low micromolar. The addition of both Mevalonate and Geranylgeranyl pyrophosphate (GGPP) can fully rescue the effect. Increasing ROCK activity with arachidonic acid only partially rescues the effect suggesting that statins act through more synthetic lethal partners beyond the Rho/ROCK pathway. *In vivo,* treatment with Fluvastatin decreased tumor initiation and caused tumor regression in established tumors in subcutaneous xenograft models using 786-O CC-RCC cells.

Combined, these studies identify ROCK inhibitors and HMG CoA Reductase inhibitors as promising new therapies for treating *VHL*-deficient CC-RCC and the biomarkers (VHL/HIF pathway) by which patients can be stratified for clinical trials.

CHAPTER ONE: INTRODUCTION

Opening Statement

The studies presented within this dissertation focus on the identification of novel synthetic lethal interactions in *von Hippel-Lindau* (*VHL)* deficient Clear Cell Renal Cell Carcinoma (CC-RCC). This work first presents the approaches that can be used to identify synthetic lethal interactions. Second, it presents the results from our chemical synthetic lethality screen and the initial validation of the seven hits identified. Third, it presents studies showing the full validation of the synthetic lethal interaction between Rho-associated coiled coil forming protein serine/threonine kinase 1 (ROCK1) inhibitors and *VHL* loss in CC-RCC. Fourth, the potential for the use of ROCK inhibitors in other cancers is examined. This potential is due to the finding that Hypoxia Inducible Factors (HIF) expression is sufficient to trigger the synthetic lethal effect. Lastly, statins, HMG-CoA Reductase inhibitors, are also shown to be synthetically lethal with *VHL* loss in part due to ROCK1 inhibition. Statins act by inhibiting the mevalonate synthesis preventing isoprenylation of small GTPases and disrupting intracellular trafficking of small GTPases. Together, the work presented identifies promising new therapies for treating *VHL*-deficient CC-RCC.

Overview of Kidney Cancer in the United States

There are currently over 375,000 people living with renal cancer in the US today making it one of the most prevalent forms of cancer[1]. The incidence rate is slowly increasing at 1.4% each year with over 63,000 new cases predicted in 2017. Luckily, improved diagnostic tools and increased surveillance have resulted in earlier detection resulting in a decrease in overall mortality by about 0.7% each year[1,2]. Early detection is vital for improving a patient's diagnosis and currently about 65% of patients are diagnosed with localized disease. Localized cancer, which is confined to the initial site, has a high 5-year survival rate of 92.6%. Regional cancer, which has spread to local lymph nodes, has a 5-year survival rate of 66.7%. Unfortunately, the 5-year survival rate of patients with distant or metastasized disease is fewer than 11.7%[1]. Since a patient only needs one kidney to survive, surgery to remove part or the entire affected kidney is often curative in localized disease[1]. For the remaining third of patients, who do not have localized disease upon diagnosis, chemotherapy is often administered. The effectiveness of the given therapy depends upon the type of kidney cancer that the patient has.

Kidney cancer consists of tumors that have formed from the pelvis or from the renal parenchyma. About 90% of all kidney cancers are adenocarcinomas that arise from the renal parenchyma that are referred to as Renal Cell Carcinomas (RCC)[22]. A number of therapies have been developed and approved by the U.S. Food and Drug Administration (FDA) for treating advanced stage, or regional/distant, RCC. These therapies can be separated into two categories: angiogenesis inhibitors and immunomodulators (Table 1.1). Angiogenesis inhibitors typically act by reducing the tumor's blood supply. Immunomodulating drugs act by stimulating the immune system in order to activate the patient's defense mechanisms against the tumor. Immunomodulating drugs were the first class to be approved by the FDA.

Table 1.1 The current list of FDA approved therapies for advanced stage RCC.

Mechanism	Drug Name	Trade Name	Target	Approval	Use	Type	Route
Immunotherapy	Interleukin-2	Aldesleukin	IL-2 Receptor	1992	1°	Cytokine	IV
	Nivolumab	Opdivo	PD-1 Receptor	2015	2°	Monoclonal Antibody	IV
Angiogenesis Inhibitors	Axitinib	Inlyta	VEGF and PDGFR	2012	2°	Small Molecule	Oral
	Sorafenib Tosylate	Nexavar	VEGF and PDGFR	2005	1°	Small Molecule	Oral
	Sunitinib Malate	Sutent	VEGF and PDGFR	2006	1°	Small Molecule	Oral
	Pazopanib Hydrochloride	Votrient	VEGF and PDGFR	2009	1°	Small Molecule	Oral
	Bevacizumab + IFN-α	Avastin	VEGF	2009	1°	Monoclonal Antibody	IV
	Lenvatinib	Lenvima	VEGF and FGFR	2016	2°	Small Molecule	Oral
	Cabozantinib	Cabometyx	VEGF and HGFR	2016	2°	Small Molecule	Oral
	Temsirolimus	Torisel	mTOR	2007	1°	Small Molecule	IV
	Everolimus	Afinitor	mTOR	2009	2°	Small Molecule	Oral

IV stands for intravenous injection.1° indicates first line treatment and 2° indicates that the drug is approved for treatment in patients who are refractory for a primary treatment.

Currently FDA Approved Therapies for CC-RCC

Immunotherapy

Immunomodulating drugs act by enhancing the body's ability to react and recognize cancer cells and this form of therapy, immunotherapy, is traditionally considered to be a standard of care for cancer patients with advanced or metastatic disease. There have been at least 58 different studies of immunotherapies for advanced stage RCC[3]. There are two immunotherapies that are currently approved for the treatment of advanced stage RCC including Interleukin-2 (IL-2) approved in 1992[4] and Nivolumab approved in 2015[5]. Cytokines, like IL-2, work by activating the immune system to strengthen its response to the patient's cancer cells. IL2-based immunotherapy has been shown to prolong overall patient survival to 17.5 months[6], but it has limited efficacy and is associated with significant morbidity and some mortality. Nivolumab is an inhibitor of the programmed cell death 1 (PD-1) receptor. PD-1 is a cell surface receptor that is expressed on

activated T-cells and its activation can inhibit the T-cells response to cancer cells. Nivolumab is a monoclonal antibody blocking PD-1. Since only a small subset of patients undergo full remission with immunotherapies, there is a clear need for improved biomarkers that accurately predict sensitivity.

While systemic therapy was originally limited to cytokines like IL-2, in 2005 the FDA approved the first targeted therapy: Sorafenib Tosylate which acts predominantly as an angiogenesis inhibitor[7]. There are two main pathways that are targeted by FDA approved targeted therapies: Vascular Endothelial Growth Factor (VEGF) and molecular Target of Rapamycin (mTOR).

VEGF Inhibitors

As shown in Table 1.1, there seven VEGF inhibitors currently approved in the US for RCC treatment including six small molecule inhibitors Axitinib, Sorafenib Tosylate, Sunitinib Malate, Pazopanib Hydrochloride, Lenvatinib, Cabozantinib, and one monoclonal antibody Bevacizumab. These therapies predominantly act to inhibit the VEGF cascade that occurs in RCC patients with overexpressed Hypoxia Inducible Factors (HIFs). HIFs become constitutively activated early in the pathogenesis of RCC due to the loss or mutation of the E3 ubiquitin ligase von Hippel-Lindau (VHL) that targets the alpha subunit of HIF[8]. VEGF and receptor tyrosine kinases (RTKs) like the Platelet derived Growth Factor (PDGFR) and Epidermal growth factor receptor (EGFR) are HIF target genes, and HIF overactivation results in the overexpression and overactivation of its downstream RTKs[9]. This signaling cascade induces angiogenesis which in turn supplies the growing tumor with nutrients and oxygen[10]. As the tumor grows more cancer cells escape from the original tumor and intravasate into the blood stream increasing the risk of metastasis[10]. By blocking the tumor's blood supply with angiogenesis inhibitors both tumor growth and metastasis

are inhibited until drug resistance develops. VEGF inhibitors were the first class of targeted therapy developed and approved for treating RCC.

As indicated in Table 1, three of the Receptor Tyrosine Kinase Inhibitors (RTKis) have been approved for first line treatment: Sorafenib, Sunitinib, and Pazopanib. These first line prolong overall survival to 19.3 months[11], 29.3, and 28.4 months respectively[12]. Second line RTKi Axitinib has been shown to prolong overall survival to 13.6 months in Sorafenib-refractory patients and to 29.9 months in cytokine-refractory patients[13].

The two most recently approved receptor tyrosine kinase inhibitors, RTKis, for treating CC-RCC include Lenvatinib and Cabozantinib. Along with inhibiting VEGF, both Lenvatinib and Cabozantinib also target additional RTKs that have been linked to RTKi drug resistance. Accordingly, upregulation of fibroblast growth factor receptor (FGFR) signaling has been shown to contribute to resistance to VEGFR inhibitors[14], and Lenvatinib inhibits PDGFR, VEGFR, and FGFR. In RTKi refractory patients, Lenvatinib prolonged overall patient survival to 18.4 months in comparison to 17.5 months for Everolimus-treated patients. Combination treatment with both Lenvatinib and Everolimus was able to prolong overall patient survival to 25.5 months[15]. Overactivation of the hepatocyte growth factor receptor (HGFR, or MET) pathway has been also implicated in VEGFR inhibitor resistance[16,17], and Cabozantinib inhibits both VEGFR and MET. Treatment with Cabozantinib prolonged overall survival to 21.4 months in RTKi refractory patients over Everolimus treatment, which only prolonged survival to 16.5 months. The approval of both Lenvatinib and Cabozantinib offers new options to overcome resistance to current RTKi, and further clinical trials are underway.

While VEGF and other RTKs are directly activated in RCC by the constitutive activation of HIFs after *VHL* loss, it has been shown that mTOR is an upstream agonist of HIF expression making mTOR inhibitors appealing for the treatment of RCC.

mTOR Inhibitors

There are two mTOR inhibitors that are currently approved for the treatment of advanced stage RCC (Table 1): Temsirolimus and Everolimus. First line mTORi Temsirolimus is approved for poor-prognosis metastatic CC-RCC patients and prolongs overall survival to 10.9 months as compared to cytokine-based immunotherapy, which prolongs overall survival to 7.3 months[18]. Second line mTORi Everolimus increases overall survival of RTKi-refractory metastatic CC-RCC patients by 14.8 months[19]. These therapies inhibit mTOR signaling, which is often overactivated in CC-RCC[20]. mTOR is a key regulator of cellular metabolism and is an upstream HIF regulator: overactivation of mTOR causes an increase in HIF transcription[21]. mTOR is known to regulate both cell growth and proliferation by driving fatty acid synthesis, the pentose phosphate pathway, and increasing glucose uptake and glycolysis[21]. The mTOR pathway can also be activated by RTK signaling creating a feedback loop[22]. Treatment with mTOR inhibitors reduces HIF-α transcription, helping to ameliorate the constitutive activation of HIFs after *VHL* function has been lost. Beyond single agent targeted therapies, combination treatments with targeted therapies and immunotherapies have shown some success in patients.

Combination Therapies

Combining VEGF inhibitors or mTOR inhibitors with immunotherapy has been successful, or at least well tolerated and a number of clinical trials have been successful in combining other VEGF inhibitors with cytokines. For instance, Sorafenib tested in combination with IFNα was better than either treatment alone[23–25]. Until recently, combination therapy of multiple VEGF

inhibitors or VEGF inhibitors and mTOR inhibitors resulted in excessive toxicities in phase I clinical trials[26–28]. These severe toxicities may be due to these drugs primarily acting in a similar fashion as angiogenesis inhibitors to reduce the signaling cascade caused by HIF hyperactivation. Fortunately, in 2016, the FDA approved the use of Lenvatinib plus Everolimus for patients who are refractory for anti-angiogenic therapy with advanced CC-RCC as a second line therapy. So far, this combination has been the only successful and FDA approved combination of RTKi and mTORi. The combination resulted in an increased progression free survival of 9.1 months longer than everolimus alone (14.6 months vs 5.5 months) and a 10.1 month increase in overall survival (25.5 months vs 15.4 months)[29]. Unfortunately, many of the patients quickly develop resistance to the currently approved targeted therapies[22,30], and there is some evidence that the therapies act more on endothelial cells to inhibit angiogenesis rather than the tumor cells[22,30].

Even with the increases in overall patient survival attained through combination therapies and the newly approved RTK and PD-1 inhibitors, there is still an unmet need for novel targeted therapies that will increase patient survival beyond the 5 and 10-year mark, preferably without significant decreases in patients' overall quality of life. One method of identifying such therapies has been through identifying synthetic lethal interactions (reviewed in [31]). Synthetic lethality occurs when the inhibition, loss, or mutation of one of two genes separately does not harm a cell, but when altered together causes cell death. Within CC-RCC, one of the main drivers of tumor initiation and progression is the loss of VHL, which occurs in over 90% of CC-RCC patients[32].

The Role of *VHL* in the Progression of CC-RCC

VHL is a tumor suppressor protein that is named after the two scientists who contributed to its identification and association with VHL Disease: Eugen von Hippel and Arvid Lindau. In 1904, von Hippel first identified a rare disorder of the retina and later, in 1927, Lindau

connected this retina disorder to hemangioblastomas in the cerebellum and spine. The *VHL* gene was identified through genetic studies of patients with VHL disease in 1993[33]. VHL disease is a heritable autosomal-dominant neoplastic syndrome with an incidence of 1 in 36,000[34] that is associated with the development of renal cysts (60 to 70% of patients), with some cysts progressing to CC-RCC (40% of patients), spinal cord (60 to 80% of patients) and retinal (60% of patients) hemangioblastomas (tumors originating from the vasculature), and pheochromocytoma (adrenal gland tumors) (5% of patients)[33,35]. Patients with VHL disease are born lacking one functional copy of the *VHL* gene, and during their lifetime lose a second functional copy due to mutation, deletion, or promoter hypermethylation in certain tissues, triggering cancer development. The disease is divided into distinct subtypes based on *VHL* status[36]. Type 1 VHL disease is associated with deletions and mutations in *VHL* that completely disrupt its function and are associated with high risk of CC-RCC and hemangioblastoma formation. Type 2 VHL disease is further split into three additional subsets, 2A-C, and is associated with *VHL* missense mutations[37]. Type 2A is associated with hemangioblastoma, pheochromocytoma, and a low risk for CC-RCC; type 2B is associated with hemangioblastoma, pheochromocytoma, and CC-RCC; whereas type 2C is associated with pheochromocytoma only[32,36].

VHL loss of function due to deletions, mutations, and promoter hypermethylation occurs in over 90% of sporadic CC-RCC cases[32]. The frequency of *VHL* mutations in CC-RCC tumors ranges from about 46% to 82% depending on the study[38,39], and loss of heterozygosity occurs in up to 98% of cases[40]. In addition, *VHL* promoter hypermethylation occurs in about 10 to 20% of CC-RCC tumors[41–43]. Accordingly, *VHL* loss of function occurs by multiple mechanisms and is a hallmark of sporadic CC-RCC tumors, which has been shown to be a major driver of the disease.

In both hereditary RCC (associated with VHL disease) and sporadic RCC multiple studies have confirmed that the majority of patients have lost *VHL*[44]. *VHL* is an E3 ubiquitin ligase that results in the degradation/inhibition of its targets. The best-known targets of VHL are the Hypoxia Inducible Factor alpha subunits (HIF-α) (diagram shown in Figure 1.1). Hydroxylation of the conserved prolines in the HIF-α proteins can only occur in the presence of oxygen and Fe^{2+}[45,46]. VHL targets HIF-α for degradation through the ubiquitin degradation pathway under normoxia via binding of two hydroxylated prolines. Loss of *VHL* or removal of cofactors (e.g. Fe^{2+}) results in stabilization of HIF-α in normoxic conditions. Hypoxia, or the loss of *VHL* in CC-RCC results in the accumulation and activation of HIF-α[45], which heterodimerizes with constitutively expressed HIF-β forming a functional transcription factor. This then results in the increased expression of HIF-α target genes, which promote cancer cell survival, growth, and metastasis.[47] There are two predominant forms of HIF-α: HIF-1α and HIF-2α. While some of their targets overlap, HIF-1α has been characterized as having more tumor suppressor target genes while HIF-2α has predominantly oncogenic target genes[44]. Furthermore, some CC-RCC tumors lose HIF-1α in the progression of the disease while retaining HIF-2α expression indicating that HIF-2α is critical for CC-RCC development[44,48]. The change in signal transduction between *VHL*-deficient CC-RCC tumors and healthy cells that contain *VHL* can be exploited to identify new and promising chemotherapeutic agents that will specifically kill *VHL* deficient cancerous cells with minimal side effects. These promising therapies are identified in the course of synthetic lethality screens.

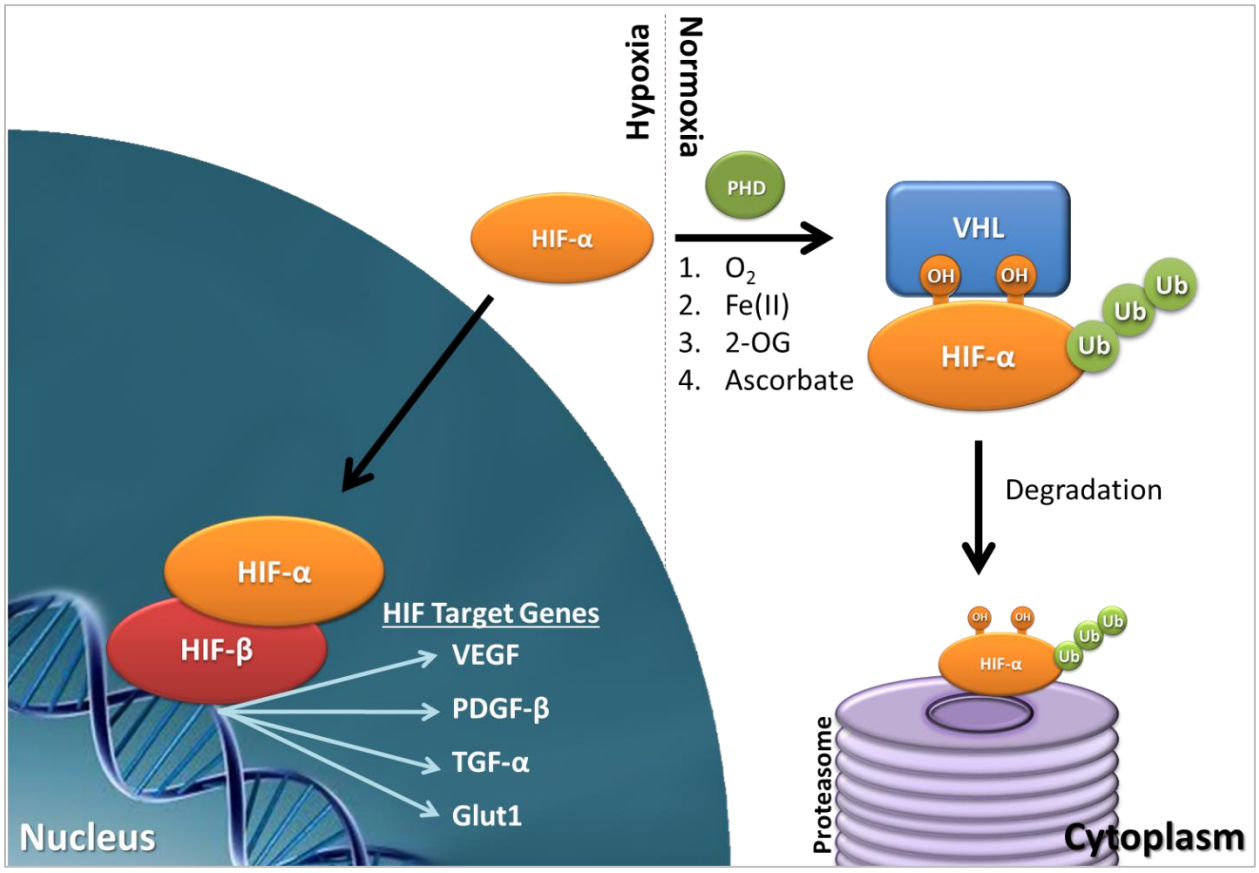

Figure 1.1 HIF Pathway Overview. Under normal oxygen conditions (right), normoxia, prolyl hydroxylases (PHD) hydroxylate HIF-α on two proline residues creating a binding site for VHL. VHL binds to the hydroxylated HIF-α and targets it for degradation via the proteasome. When oxygene is limiting in hypoxia (left), or VHL function is lost/impaired like in CC-RCC, HIF-α can translocate to the nucleus and bind HIF-β. Together the heterodimer binds to hypoxia response elements in the DNA and activate the transcription of HIF target genes.

Synthetic Lethality Concept

Synthetic Lethality occurs when the individual alteration (mutation, deletion, inhibition, overactivation) of two genes independently does not affect cell survival or proliferation, but the simultaneous alteration of both genes results in a cytotoxic or cytostatic effect. Synthetic lethality and approaches to studying synthetic lethality are examined more closely in Chapter Two and in Thompson et al. 2015[49]. In order to identify novel synthetic lethal interactions in *VHL*-deficient CC-RCC we used Sigma's Library of Pharmacologically Active Compounds (LOPAC) and performed a screen using the matched RCC4 cell lines (where the only difference between the two cell lines is whether *VHL* is expressed) as shown in Figure 1.2. The LOPAC is an annotated chemical library that contains 1280 compounds. We conducted the primary screen using fluorescence intensity as a surrogate for cell counting. To do so, the matched RCC4 lines RCC4 and RCC4VHL were transduced with a plasmid expressing enhanced yellow fluorescent protein (EYFP). Thus, the brighter the fluorescence intensity, in the well, the greater the numbers of cells present. The results from the screen were normalized to the vehicle control for each compound and seven hits were identified. Representative results from the screen are shown in Figure 1.3 where the decrease in yellow brightness in each well represents the decrease in fluorescence intensity that was measured, and the results are quantified in dose response curves.

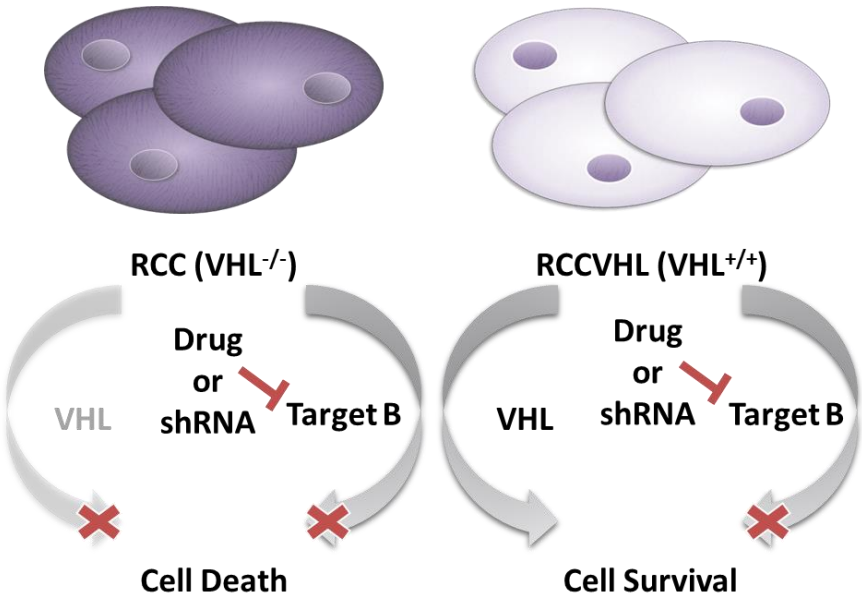

Figure 1.2. Overview of Synthetic lethality model for *VHL*-deficient CC-RCC. Matched RCC and RCCVHL cell lines are tested against drug or shRNA libraries to identify synthetic lethal interactions that kill *VHL*-deficient RCC while sparing *VHL*-expressing RCCVHL.

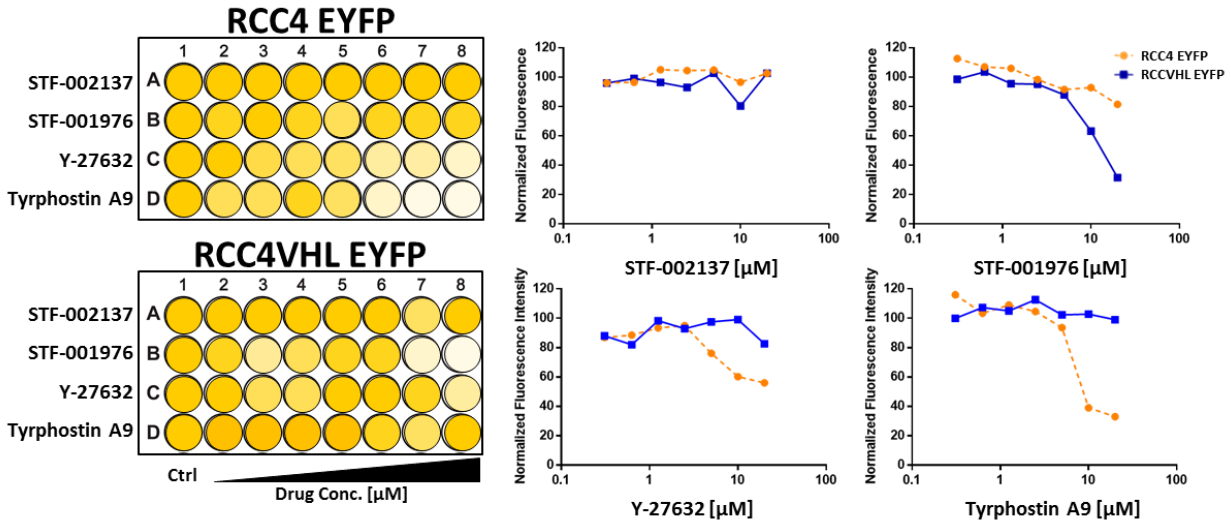

Figure 1.3. Overview of the LOPAC Library Screen showing representative results. A artistic representation of the results from the synthetic lethality screen is shown for the fluorescence intensity measurements on the left with stronger intensity indicated by brighter yellow, and the same results shown as dose response curves on the right compiled using the actual results from the screen. STF-002137 and STF-001976 are representative of negative hits. STF-002137 does not kill either line, whereas STF-001976 inhibits the *VHL*-expressing RCC4VHL EYFP greater than the *VHL*-deficient RCC4 EYFP. Y-27632 and Tyrphostin A9 were two of the hits that were obtained from the LOPAC screen, in which the *VHL*-deficient RCC4 EYFP cell line was selectively inhibited more than 50% in comparison to the less effected RCC4VHL EYFP cell line.

The primary LOPAC screen identified seven compounds that could potentially be synthetically lethal with *VHL* loss in CC-RCC. These compounds included Y-27632, Dequalinium dichloride, Indirubin-3'-oxime, Kenpaullone, SU 9516, Tyrphostin 23, and Tyrphostin A9. The results of this screen are analyzed in depth in Chapter 3. Our best hit from the screen was Y-27632, which inhibits both Rho-associated protein kinases (ROCK) 1 and ROCK2. ROCK is a major regulator of cytoskeleton remodeling downstream of the small GTPase Rho. ROCK phosphorylates its substrates regulating their activity in many cellular processes including actin filament stabilization, actin-membrane linkage, stress fiber formation, actin-network assembly, and microtubule dynamics[50]. ROCK1 and ROCK2 share a 92% identity within their kinase domain[51] and are differentially expressed throughout the tissues with ROCK1 being expressed in the organs including the liver, kidney and lung, whereas ROCK2 is predominantly expressed in the muscle and brain[51]. In Chapter 4, and published in Thompson et al. 2016[52], we present the validation that was conducted to confirm that inhibition of ROCK1 is synthetically lethal with *VHL* loss in CC-RCC. Within this study, we confirm that the synthetic lethal interaction is through ROCK1 and not ROCK2 by genetically knocking down both targets using two independent small interfering RNAs (siRNAs). The interaction between ROCK1 and *VHL* loss is both cytostatic and cytotoxic. The effect is dependent on HIF expression within the CC-RCC line, with HIF-1α overexpression sensitizing the CCRCC cells to ROCK inhibition to a greater degree than HIF-2α overexpression (Figure 1. for VHL and ROCK pathway overview). These findings have important implications about the potential use of ROCK inhibitors in other cancers where HIFs are overactive. These findings are examined more closely in Thompson et al. 2017.[53]

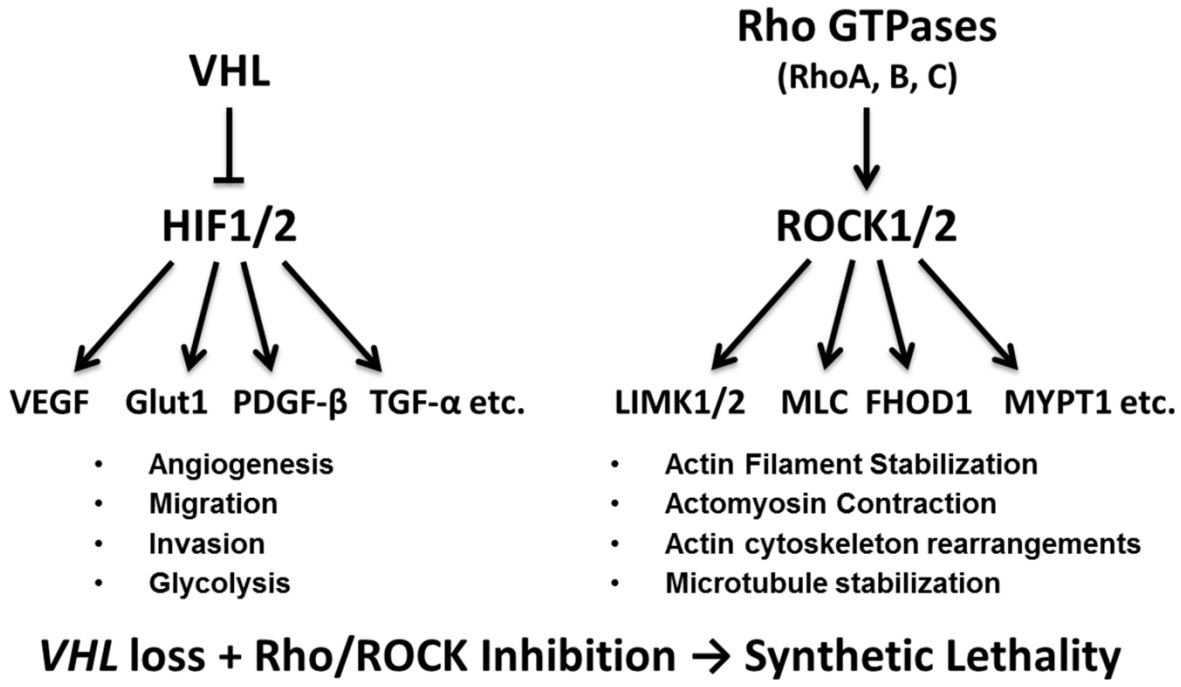

Figure 1.4. Overview of VHL/HIF and Rho/ROCK signaling pathways. VHL, left, is a part of an E3 ubiquitin ligase complex that targets HIF-1α and HIF-2α for degredation. The loss of VHL stabilizes HIFs, leading to elevated expression of a multitude of HIF-target genes, involved in angiogenesis, migration, invasion, glycolysis, etc. ROCK signaling, right, is dependent on activation by RhoGTPases that bind to ROCK1 and ROCK2. ROCK family kinases are major regulators of actin organization within the cell controlling actin filament stabilization, actomyosin contraction, acting cytoskeleton rearrandements, microtubule stabilization, etc. The combination of *VHL* loss leading to HIF overactivation and Rho/ROCK pathway inhibition triggers synthetic lethality.

The identification of a synthetic lethal interaction between ROCK inhibitors and *VHL* loss in CC-RCC led us to hypothesize that inhibition of Rho, the direct upstream regulator of ROCK, would also be synthetically lethal with *VHL* loss. The Rho family GTPases, RhoA, RhoB, and RhoC, directly regulate ROCK1&2 activation. Since ROCK inhibition is synthetically lethal with *VHL* deficiency, we hypothesized that inhibiting Rho would also lead to synthetic lethality with *VHL* loss. We further hypothesized that RhoC is critical for the proliferation of *VHL*-deficient CC-RCC, and can be utilized for specifically targeting CC-RCC tumors. Our rationale was threefold. First, high ROCK and RhoC expression are predictive of poor patient survival[54]. Second, RhoC might interact directly with VHL and ROCK1, as well as have ubiquitin (Ub) modifications,

accordingly to www.signaling-gateway.org and www.phosphosite.org. Lastly, our preliminary data indicates that knocking down RhoC by siRNA causes synthetic lethality with *VHL* loss (personal communication with Luke Nelson). Based on these findings, we hypothesized that treatment with HMG-CoA Reductase inhibitors, also known as statins, as an indirect way to inhibit Rho signaling, would also cause synthetic lethality. Statins are used in a large part of the population to treat hypercholesterolemia. Treatment with statins decreases mevalonate synthesis reducing both cholesterol synthesis and isoprenoid intermediates. A large body of evidence supports that statins can disrupt intracellular trafficking of small GTPases like Rho by inhibiting their isoprenylation[55–57]. Furthermore, disruption of mevalonate synthesis by statins has been shown to inhibit ROCK signaling in patients[57]. While statins have been traditionally used to treat high cholesterol[58] in order to reduce risk of cardiovascular disease, a growing body of literature now shows that statins have "pleiotropic", off-target non-cholesterol related, effects that are responsible for reducing the risk of many types of cancer[59,60]. Indeed, our findings showed that it is the inhibition of small GTPase isoprenylation, and not decreased cholesterol synthesis, which is responsible for the synthetic lethal effect with statins. Our findings with statins are detailed in depth in Chapter 5 and published in Thompson et al. 2017.

Closing Statement

These studies identify two new potential types of therapy for treating *VHL*-deficient CC-RCC including ROCK inhibitors and statins. As statins are already taken by a large portion of the human population, they also provide a mechanism for how statin use is correlated with decreased risk for developing CC-RCC[61]. Furthermore, these studies not only provide new therapeutic approaches, but identify biomarkers that can be used to stratify patients based on predicted sensitivity to the treatment like the HIF/VHL pathway.

CHAPTER TWO: APPROACHES TO IDENTIFYING SYNTHETIC LETHAL INTERACTIONS IN CANCER

Introduction

A major challenge in developing new anticancer therapies is not to identify compounds that kill cancer cells, but instead to identify compounds that have large therapeutic index such thatthe dose that causes tumor regression produces minimal toxicity in normal tissue. Many cancer therapies have a low therapeutic index, producing numerous side effects that greatly reduce a patient's quality of life. Further elucidation of the unique differences between cancer and normal tissue can allow for the development of targeted therapies with fewer side effects. During malignant progression, cancer cells acquire multiple mutations including the activation of proto-oncogenes, the inactivation of tumor suppressors, and other additional genetic or epigenetic alterations resulting in a drastically transformed genome[62,63]. Indeed, most of the hallmarks of cancer are associated with changes to the cancer cell's genetic makeup in order to enable it to endlessly proliferate[64]. These changes create a weakness that can be exploited to specifically target and kill cancer cells while sparing normal cells[63,65]. Traditional chemotherapy, including DNA damaging agents, and irradiation treatment both rely on this principle. Most cancer cells have defects in their cell cycle checkpoints where DNA would normally be repaired before replication[66,67]. Thus, radiotherapy and DNA damaging agents target DNA in the continuously

dividing cancer cells, causing cell death. Normal cells, with their intact cell cycle checkpoints, repair the damage before dividing[66,67]. However, these therapies often have serious side effects, often to highly proliferative tissues like hair, gut, and blood, and greatly reduce a patient's quality of life[68]. Synthetic lethality exploits the specific changes within the cancer at a single gene level to selectively enhance toxicity in tumor but not healthy tissue.

Synthetic Lethality

Synthetic lethality is defined as the interaction between two co-essential genes such that inhibiting the function of either gene separately results in cell survival, but inhibiting the function of both genes results in cell death (Figure 2.1)[31,69,70]. Inhibition of a gene may be achieved by chemical or genetic means. For instance, the genetic inhibition of a gene's function may occur through RNAi, mutation, deletion, epigenetic changes, or perturbations of upstream regulators. Chemical inhibition of the gene's function may be achieved by treatment with a chemical compound. The inhibition of co-essential genes can occur at any level and the loss of function does not have to occur in the same manner for both co-essential genes. For example, one gene can be lost due to deletion and the other inhibited by a chemical compound. While synthetic lethality is best known in the context of loss-of-function mutants[70], other perturbations including gene overexpression[71,72], epigenetic changes[73], and cell extrinsic differences[74,75] can cause these interactions to occur[31] (Figure 2.1). In identifying genes that are synthetically lethal within each cancer type we gain an understanding of the molecular biology of those cancers and how it can be specifically exploited. There are multiple approaches that have been successfully used to identify synthetic lethal interactions in cancer.

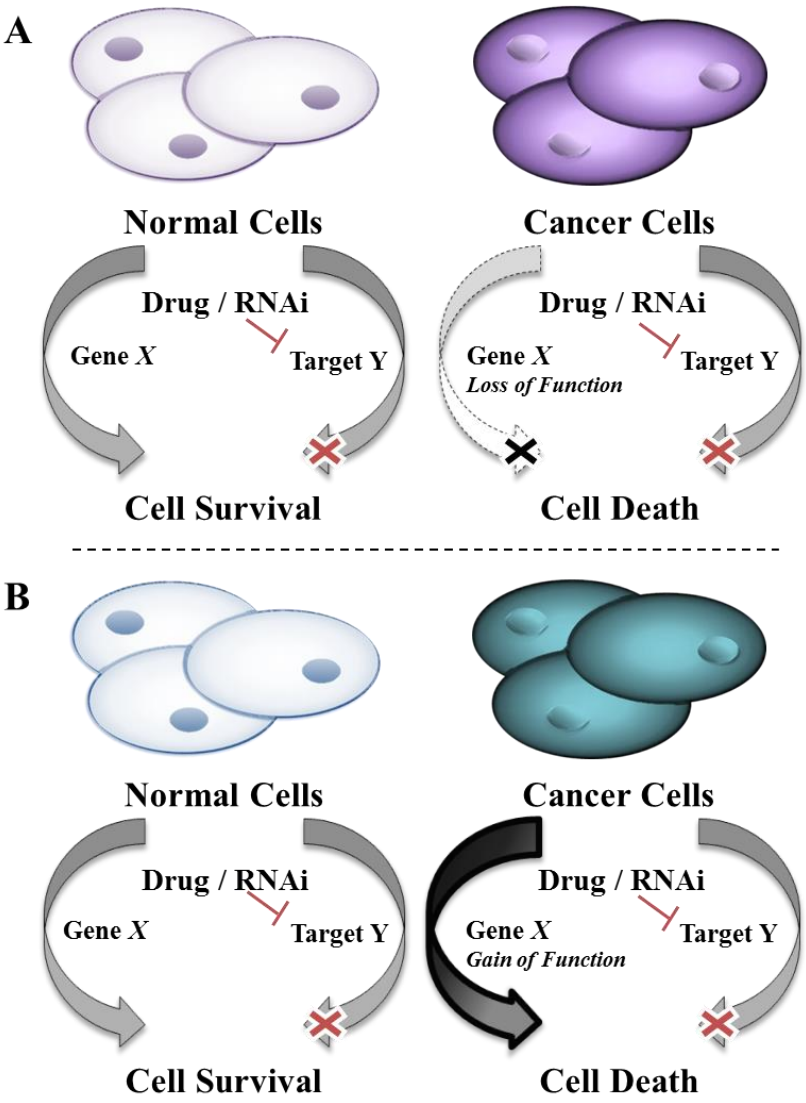

Figure 2.1 Synthetic lethal interactions spare normal cells while selectively killing cancer cells. (**A)** In the loss of function phenotype cancer cells have lost the function of gene X due to genetic loss, epigenetic changes, cell extrinsic changes, and more. When cells that express gene X are treated to inhibit gene X's synthetic lethal partner target Y they remain viable, but cancer cells lacking gene X die. **(B)** In the gain of function phenotype, also called synthetic dosage lethal, cancer cells have an overexpression or overactivation of gene X due to oncogenic mutation, generation of fusion proteins, changes in upstream regulators, epigenetic changes, cell extrinsic changes, and more. When cells with wild type gene X are treated to inhibit gene X's synthetic lethal partner target Y they survive, but cancer cells with the gene X gain of function die.

Different Approaches to Identify Synthetic Lethal Interactions

Hypothesis-Driven Approach

It is possible to identify synthetic lethal interactions using a candidate or hypothesis-driven approach if the alterations to the molecular pathways in the cancer of study are well established. For instance, if a tumor suppressor is frequently lost and the resulting changes to the gene expression profile are known, then it may be possible to use RNA interference (RNAi) or chemical compounds to inhibit the genes that are expected to be upregulated to compensate for the loss. This may result in a synthetic lethal interaction. Mutations in the BReast CAncer early onset (*BRCA*) 1 and *BRCA2* genes are known to occur frequently in breast and ovarian cancers. Knowing that BRCA1/2 are involved in Homologous Recombination (HR) and DNA double-strand break repair, both Byant *et al.*[76] and Farmer *et al.*[77] hypothesized that inhibition of Poly (ADP-Ribose) Polymerase (PARP), responsible for DNA single-strand break repair, would be synthetically lethal with loss of *BRCA1/2*. This hypothesis is based on the knowledge that *PARP* deficiency results in spontaneous single-strand breaks at the DNA replication fork, which require HR for repair. Cells deficient in *BRCA1*/*2* are unable to provide HR for repair of DNA single- and double-strand breaks caused by chemical or genetic PARP inhibition, causing synthetic lethality. The synthetic lethal interaction was extended to *in vivo* studies, followed by clinical studies where treatment of *BRCA1/2*-deficient tumors with a DNA damaging agent combined with a PARP inhibitor, extended patient survival over chemotherapy alone[78,79].

Synthetic lethal interactions may also explain why particular chemical compounds have increased efficacy in cancers characterized with specific genetic alterations. While clinical trials for PARP inhibitors in ovarian cancer were successful in increasing progression free survival by 62% overall [80], in a follow-up analysis of the same study it found that the *BRCA1/2*-deficient group

had a much higher rate of 82%[81]. Another study by Leibowitz *et al.*[82] hypothesized that NonSteroidal Anti-Inflammatory Drugs (NSAIDs) are highly effective in preventing colorectal tumorigenesis due to a synthetic lethal interaction with the loss of the Adenomatous Polyposis Coli (*APC*) gene. While NSAIDs were able to activate cell death pathways in both cancer and normal cells, *APC* deficiency triggered the activation of BH3 Interacting-Domain (BID), a death agonist in extrinsic apoptotic pathway, resulting in synthetic lethality[82]. In situations where putative targets cannot be identified, a screening based approach is necessary.

Screening Based Approaches

Most large-scale approaches investigating synthetic lethal interactions in cancer rely on the comparison of drug or RNAi treatment in "matched" cell lines (Figure 2.2). Matched cell lines are generated so that their only difference is in the expression/activation status of the gene of interest. In studying a loss-of-function phenotype (Figure 2.1A), the parental cancer cell line may have lost the expression of a gene, have inactivating mutations, or have been treated with an extrinsic factor (like a chemical compound) such that the activity of the gene is lost. In this model, a matched cell line could be generated from a parent cancer cell line deficient in the gene by overexpressing it (Figure 2.2A). Next, multiple cell lines with and without expression of the gene could be compared (Figure 2.2B). Finally, one could inactivate the gene in a cell line expressing it (Figure 2.2C). In studying a gain-of-function phenotype (Figure 2.1B) the parental cancer cell line may have acquired a new gene fusion, oncogenic mutation resulting in constitutive activation, overexpression of the gene, or have been treated with an extrinsic factor (like a receptor ligand) such that the gene's activity would increase. In this model, a matched cell line could be generated from a parent cancer cell line with an overactive gene by inactivating it (Figure 2.2D). Next, multiple cancer cell lines with and without the increase in the gene's activity might be investigated

(Figure 2.2E). Additionally, the gene could be overexpressed in the parent cell line expressing it at a normal level (Figure 2.2F). Finally, a cell extrinsic factor like a receptor ligand could be used to treat the cells with low receptor activity such that activity of the receptor would increase (Figure 2.2F). These matched cell lines often differ in the activity of a single gene, and one of them represents a cancer cell line characterized by a specific gene alteration, and the other represents a cancer cell line characterized by the absence of that alteration. In this respect, the latter simulates the normal tissue where genetic alterations are absent. Once the matched cell lines have been generated they can be used in high throughput screens. These screens can be separated into two categories: chemical libraries and genome-wide interference. Chemical libraries include both annotated and non-annotated libraries where the targets of the chemical compounds are known and unknown respectively. Genome-wide interference screens have been conducted successfully using siRNA, shRNA, and CRISPR.

Many chemical library screens rely on the usage of chemical compounds with unknown molecular targets. These screens usually contain tens of thousands of different compounds, which greatly increases the chances of getting a "hit". A hit is a compound that is synthetically lethal within cancer cells containing the gene alteration being studied. The difficulty of these screens is in identifying the molecular target of the hit. Genome-wide interference screens rely on the use of siRNA, shRNA, or CRISPR libraries in order to inhibit genes involved in every molecular pathway within cells. Smaller libraries can be useful if specific pathways are established. Genome-wide interference screens suffer from the need to identify chemical compounds that inhibit the molecular targets identified before the interaction can be utilized in clinical trials. If the compounds are not available their development can be long and arduous. The use of an annotated chemical library can offer both a small molecule compound and the molecular target assuming the hit is acting through

the predicted target. This chapter will investigate multiple case studies for each approach, the screens involved, the methods of validation the studies used, and the synthetic lethal interactions identified. Our goal is to present the merits of each approach and the context in which they have been successfully applied.

Chemical Library Screens

The use of large non-annotated chemical libraries (Figure 2.3A), wherein the molecular targets of the drugs are unknown, have been an effective method for discovering synthetically lethal interactions in a number of different cancers including Renal Cell Carcinomas (RCC)[83,84] and ovarian cancer[85]. Most chemical library screens rely on fluorescently labeled matched cell lines and measure fluorescence intensity as a surrogate for cell count as a high-throughput viability assay. Following the identification of hits, an investigation of the actual drug targets and mechanism of action is required. Often an additional screen is necessary to accomplish this. If the drug class has been previously investigated and its targets have been established, then confirmation that the drug is acting "on-target" can be performed using RNAi to knockdown the putative target. Annotated chemical libraries, in which the targets of the drugs are known, can be useful tools for identifying synthetic lethal interactions. Since annotated libraries are often small (hundreds of chemical compounds) in comparison to non-annotated libraries (tens of thousands of compounds), the benefit from knowing the molecular target of a compound may be offset by the reduced chance in identifying hits from a screen. Likely for this reason, the use of non-annotated chemical library screens appears to be more frequently described in the literature. Below we discuss two papers where screens using non-annotated chemical libraries were employed.

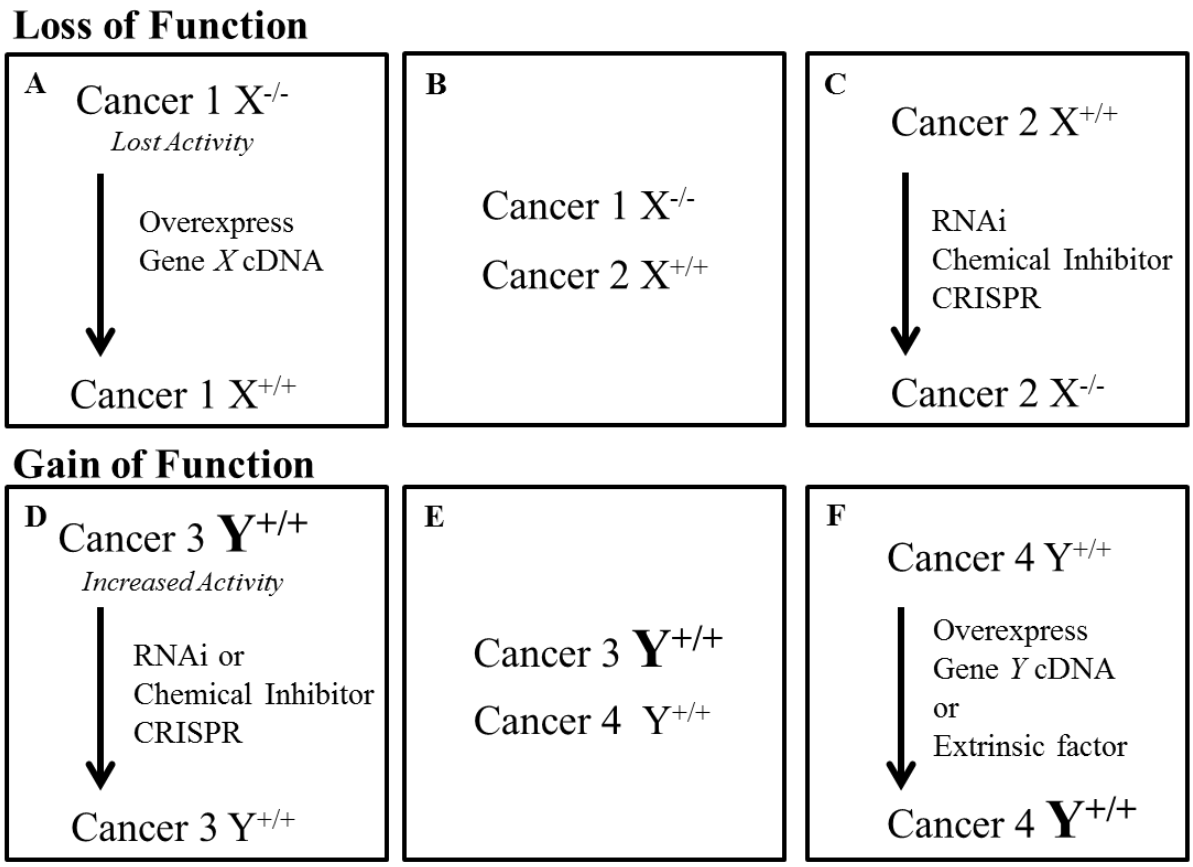

Figure 2.2. Approaches to generating matched cell lines for synthetic lethality screens. There are multiple approaches to generate matched cell lines if a loss of function **(A-C)** or a gain of function **(D-F)** of a specific gene is studied. For studying synthetic lethal interactions in cancer cells that have lost expression of a gene: **(A)** The cDNA for the gene can be re-expressed in the deficient cell line, **(B)** multiple cancer lines both expressing and deficient in the gene can be investigated, or **(C)** cancer lines that express the gene can be treated to inactivate the gene. For studying synthetic lethal interactions in cancer cells with oncogenic mutations that increase activity of the gene or create a new gene fusion (like BCR-ABL) multiple approaches can be used: **(D)** cells can be treated with RNAi or a chemical inhibitor in order to reduce the expression back to normal levels; **(E)** multiple cancer lines both with and without the mutation could be investigated; **(F)** or the mutation can be introduced or the gene can be overexpressed within a cancer line that does not already contain it or has normal expression of it. In addition to this an extrinsic factor could be used induce the activity of the gene.

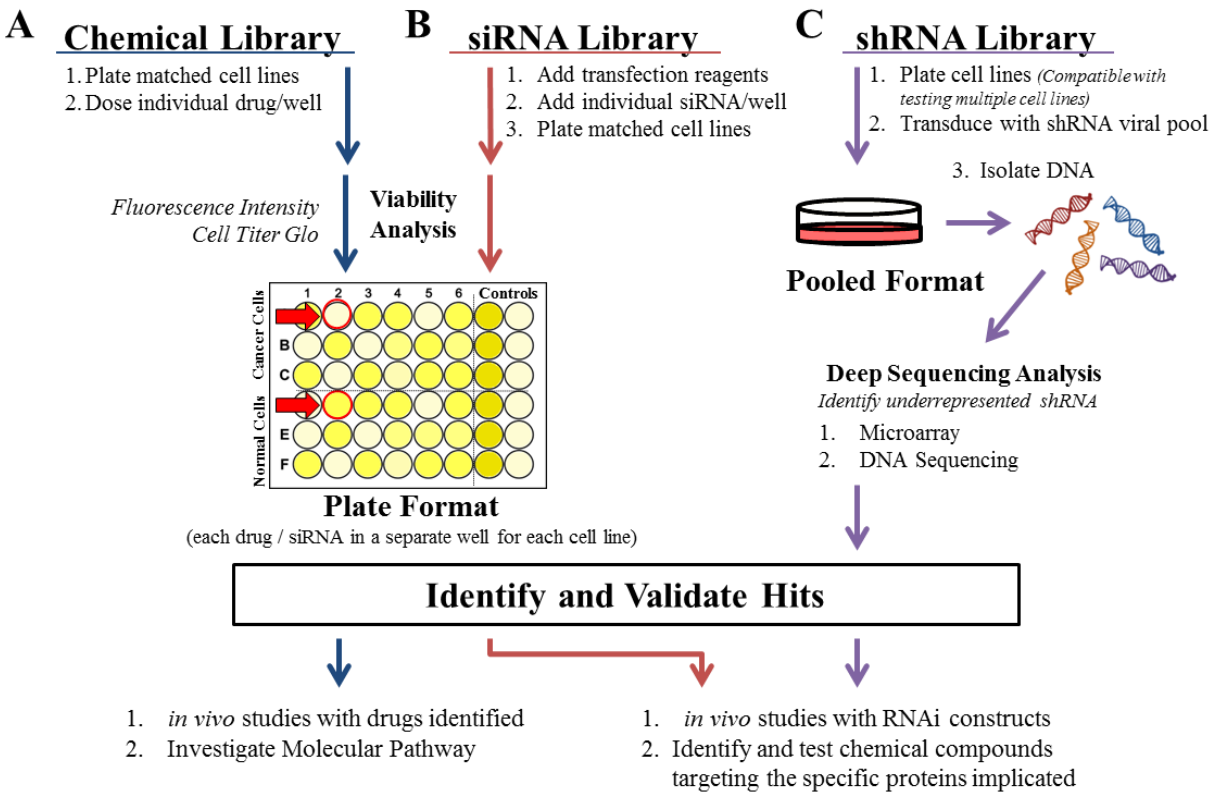

Figure 2.3. Approaches to investigating synthetic lethal interactions. (A) Chemical Library screens are conducted using matched cell lines in a plate format wherein each drug is dosed separately to both lines. Fluorescence intensity from GFP or eYFP labeled cell lines can be used as a surrogate for cell count to make the assay high-throughput. **(B)** siRNA library screens are also conducted in a plate format. Libraries are often custom ordered and contain individual siRNA and transfection reagent plated out to each well. The matched cell lines can then be plated to duplicate plates and analyzed following incubation using a high-throughput method like Cell Titer Glo. Hits from screens performed using the plate format **(A and B)** are identified by comparing the normalized values of each well between the two matched cell lines. A hit, indicated by the red arrows, kills cancer cells while sparing the matched normal cell line. **(C)** The shRNA library approach is most often performed by transducing matched cell lines with a shRNA viral pool, although plated approaches can be conducted similar to the siRNA library approach. The pooled approach is more conducive for studying multiple cell lines and relies on deep sequencing analysis to identify hits. A hit is identified by analyzing for shRNA that are lost after transduction library in cancer cell lines and not normal cell lines, since synthetic lethal interactions will result in the cells death. Once hits have been identified and validated in each screen the approaches **(A, B, C)** split. With a chemical library screen **(A)** *in vivo* studies can be readily initiated while the investigation into the molecular pathway is conducted. For siRNA and shRNA screens **(B, C)** *in vivo* studies can also be initiated using shRNA constructs while small molecules are investigated and developed.

The first paper exploited the fact that inactivation of the tumor suppressor Von Hippel Lindau (*VHL*) has been shown to occur in over 70% of RCC[44]. The inactivation of VHL results in abrogation of its E3 ubiquitin ligase activity and overexpression of its targets. Turcotte *et al.*[83] utilized a library of 64,000 chemical compounds to identify synthetic lethal interactions in *VHL*-deficient RCC (Figure 2.1A). The screen used a *VHL*-deficient RCC4 parent cell line and matched RCC4-VHL cell line obtained by overexpression of *VHL* cDNA (Figure 2.2A). Both matched lines stably expressed Enhanced Yellow Fluorescent Protein (EYFP), and fluorescence was used to monitor cell number. The matched lines were treated in parallel with the chemical library in a plate format (Figure 2.3A). Clonogenic assays, in which the cells were plated at low densities and allowed to form colonies, were used to confirm their hits. The authors observed that *VHL*-deficient RCC cells treated with the hit STF-62247 accumulated intracytoplasmic vesicles more readily than RCC-VHL cells, causing RCC cell death. The synthetic lethal effect of STF-62247 was also confirmed *in vivo* using multiple matched RCC lines. Since the molecular target of STF-62247 was unknown the authors utilized a yeast deletion pool to identify the target. This additional screen confirmed that STF-62247 was disrupting the trans-golgi network stimulating the maturation of autophagosomes to autolysosomes selectively in the *VHL*-deficient RCC.

The second paper aimed at the identification of chemical compounds that would re-sensitize cancer cells to DNA damaging agents such as ionizing radiation (IR) or Cisplatin. These agents cause DNA intrastrand crosslinks and are effective in treating a wide variety of cancers with perturbed DNA repair pathways including ovarian cancer[86]. Eventually, the cancer cells evolve to acquire drug resistance through various mechanisms including activation of DNA repair pathways like the Fanconi Anemia (FA) pathway[87]. For example, DNA damaging agents are initially efficacious in ovarian cancer, but most patients relapse with resistant disease that is no

longer sensitive to the treatment[88]. Jacquemont *et al.*[85] utilized a library of 16,000 chemical compounds to identify hits that would inhibit the overactive FA pathway thus re-sensitizing cancer cells to DNA damaging agents (Figure 2.1B). The parent PD20 fibroblast cell line is Fanconi Anemia Group D2 (*FANCD2*)-deficient, causing FA pathway disfunction. The PD20-EGFP-FANCD2 cell line utilized for the screen was obtained by overexpression of Enhanced Green Fluorescent Protein (EGFP) labeled version of the wild type (WT) *FANCD2* cDNA. This overexpression made the PD20-EGFP-FANCD2 cell line resistant to DNA damaging agents. The chemical compound screen was performed using 96-well plates seeded with PD20-EGFP-FANCD2 cells treated and untreated with IR (Figure 2.2F, extrinsic factor). Cells were dosed with the ICCB bioactives and Commercial Diversity Set 1, Chembridge DiverSet, and NINDS II chemical compound libraries. The plates were imaged using EGFP microscopy to identify hits that selectively reduced EGFP-FANCD2 foci formation by greater than 50% in IR treated cells, which indicates that the hit reduces DNA repair events, causing restoration of sensitivity to the IR treatment. From the 43 hits obtained, 26 hits also successfully reduced EGFP-FANCD2 foci formation in cells treated with Cisplatin. Fifteen hits were then validated in multiple ovarian cancer cell lines. Since the FA pathway is known to be involved in DNA repair and homologous recombination (HR), in a followup study the HR efficiency was tested using a GFP-based reporter system, where GFP expression was correlated with HR events. The majority of the drugs acted by indirectly inhibiting the HR process (like the compound Bortezomib) or by directly inhibiting FANCD2 foci formation.

Taken together, non-annotated chemical library screens, as described above, can be an effective means to identify synthetic lethal interactions within individual matched cell lines. This method is not suited to studying a large number of cell lines in parallel since it relies on the plate

format. One advantage that chemical library screens have in comparison to RNAi or CRISPR based screens (see below) is that chemical compounds tend to inhibit families of targets whereas RNAi is specific for individual members within the family. Different interactions can be identified with both approaches since some genes within the same family might be redundant and inhibiting a single gene would not cause synthetic lethality in an RNAi screen. In contrast, inhibiting the whole family by a chemical compound might be too cytotoxic in a chemical library screen, wherein inhibiting a single member may have been synthetically lethal. Overall this approach is suited for studying specific cancer lines, generates a large number of hits, and provides compounds that can be used *in vivo,*but requires establishment of molecular targets.

siRNA Library Screens

The siRNA library screen relies on a plate format wherein each siRNA is transfected separately in its own well (Figure 2.3B), which makes it very similar to the format described above for the chemical library (Figure 2.3A). In some screens, multiple siRNAs targeting a gene are pooled into the same well (called a siRNA pool, usually comprised of 4 individual siRNAs). Cell Titer-Glo luminescent cell viability assay from Promega is often used to assess viability and identify hits. Both studies investigated below rely on the addition of extrinsic factors to generate matched cell lines. Once hits have been identified, *in vivo* studies can be conducted using RNAi constructs and chemical compounds for the established targets can be investigated.

In the first study Kranz *et al.*[89] performed a genome-wide siRNA screen to sensitize the human glioblastoma cell line U251MG treated with Tumor necrosis factor-Related Apoptosis-Inducing Ligand (TRAIL) to apoptosis (Figure 2.1B). TRAIL is an important ligand in the death receptor-mediated apoptosis pathway, which is often inactivated in cancers including

glioblastoma[90,91]. This screen was performed in a 384-well format using matched U251MG cells both with and without TRAIL treatment (Figure 2.2F, extrinsic factor) and Dharmacon's SMART-pool siRNA library targeting 5,000 genes with 4 pooled siRNAs per target in each well (Figure 2.3B). Plates were analyzed using the Cell Titer-Glo viability assay to identify hits. Validation of the hits from the screen was performed, using the same system, by transfecting individual siRNAs for every gene hit instead of transfecting siRNA pools. *FAT1* was chosen for further investigation since all 4 individual siRNAs resulted in decreased survival in response to TRAIL. This synthetic lethal interaction was also identified in five additional cell lines. The authors found that FAT1 is linked to the extrinsic apoptosis pathway, and that it impedes Caspase-8 recruitment to the Death-Inducing Signaling Complex (DISC) in a ubiquitin-independent mechanism. Synthetic lethality of FAT1 with TRAIL treatment was confirmed by knocking out *FAT1* using CRISPR/Cas9-mediated genome engineering.

In the second study, Josse *et al.*[92] performed a siRNA library screen to identify genes that are synthetically lethal with TOPoisomerase I (TOP1) inhibition in the breast cancer line MDA-MB-231 (Figure 2.1A). TOPoisomerases (TOPs) are enzymes that reverse the supercoiling of DNA that occurs during replication and transcription[93]. Inhibition of TOPs has been shown to be an effective means for killing constitutively proliferating cancer cells[94]. Inhibitors trap the TOP enzyme on the DNA and result in stalled replication forks and transcriptional complexes, causing DNA double strand breaks. Importantly, TOP1 inhibitors are in clinical trials or approved for ovarian cancer, colorectal cancer, breast cancer, and more[93,94]. The siRNA screen was performed using parallel 384-well plates of matched MDA-MB-231 cells treated with the TOP1 inhibitor Camptothecin (CPT) or vehicle control (Figure 2.2C, chemical compound). The Qiagene human druggable genome library version 4.1, targeting 7,000 genes with 4 individual siRNAs per gene,

was transfected into cells. Cell Titer-Glo was used to assess viability and identify hits (Figure 2.3B). Forty-two hits were identified that selectively killed CPT treated MDA-MB-231 while sparing vehicle treated cells. To validate the top hits, the effects of the siRNAs were investigated with varying CPT concentrations and with additional siRNAs for over 40 of the candidate genes. One of the top hits was Ataxia Telangiectasia Mutated (*ATM*). Since *ATM* and Rad3-related protein kinase (*ATR*) function in parallel, and ATR inhibitors have already been developed and are in clinical trials, the authors confirmed that ATR inhibitors are synthetically lethal with TOP1 treatment. The authors found that ATR and its downstream target Chk1 are crucial factors in repairing DNA lesions that occur when TOP1 is inhibited. This synthetic lethal interaction was confirmed *in vivo* in mice with COLO205 colon cancer xenografts, and combination treatment with ATR and TOP1 inhibitors was more effective than individual treatment for either drug.

In summary, the siRNA approach, like the chemical library approach, is limited by the plate format since each siRNA or siRNA pool must be transfected into an individual well (Figure 2.3B, plate format) as compared to the shRNA library approach (discussed below) where shRNAs are transduced in a viral pool (Figure 2.3C, pooled format). Thus, the plate format limits the number of cancer types that can be investigated concurrently, but the screen can be performed using a high-throughput viability assay like Cell Titer-Glo. Hits can later be validated in additional cell lines. When performing secondary siRNA screens each gene must be targeted with multiple non-pooled individual siRNAs to avoid false positives from off-target effects. The study by Josse *et al.*[92] investigated over 7 individual siRNAs for their top hits in order to identify the best candidates for further analysis. Overall the siRNA approach is well suited to investigating individual matched cell lines where understanding the specific genes involved within the synthetic lethal interaction is important.

shRNA Library Screens

The use of shRNA libraries (Figure 2.3C) can aid in identifying the key molecular pathways that a tumor is dependent on for survival. There are a number of common strategies when performing shRNA screens. First, most screens consist of shRNA virus pools, which makes the approach applicable for studying multiple cancer lines in parallel, although a plate format with individual shRNAs per well can also be used[95] similar to siRNA screens (Figure 2.3B). The readout from the pooled screen is often in the form of deep sequencing[96] or a microarray[97]. The hits from the screens are then validated by performing viability assays using the individual shRNAs. Viability assays are often conducted using a kit like Cell Titer-Glo or clonogenic assays. The process of identifying the mechanism of action and chemical compounds targeting the gene hits is then different for each study.

In the first example, Etemadmoghadam *et al.*[97] performed shRNA library screening on 102 cancer cell lines including ovarian, colon, pancreas, lung, and other cancer types to investigate synthetic lethality with Cyclin E1 (*CCNE1*) amplification (Figure 2.1B). Overexpression of the *CCNE1* oncogene occurs in multiple cancers and is associated with poor prognosis in high-grade serous ovarian cancer [98,99]. CCNE1 overexpression results in increased proliferation through decreased regulation of the S phase cell cycle checkpoint [100]. The authors obtained microarray data of shRNA experiments from the Integrative Genomics Portal and the data was analyzed using the GenePattern module ScorebyClassComp and GENE-E software. The shRNA library contained a pool of 54,020 shRNAs targeting 11,194 genes. All cancer cell lines were divided into *CCNE1* amplified/overexpressing or normal *CCNE1* copy number/expression representing matched cell lines (Figure 2.2E). Each cancer type was analyzed separately. The relative abundance of each shRNA sequence in the matched cell lines was compared since shRNAs causing synthetic lethality

should be eliminated from *CCNE1* amplified/overexpressing cells. The screen identified 835 genes that were essential for survival in *CCNE1*-amplified or overexpressing cancer cell lines and 25 high confidence hits. The authors validated the results of the shRNA screen by performing an siRNA screen for their top 115 hits plus an additional 27 candidate genes. For the siRNA screen SK-OV-3 (*CCNE1*-unamplified cells) and OVCAR-3 (*CCNE1*-amplified cells) (Figure 2.2E) were plated in parallel and viability was measured using the Cell Titer-Glo assay in a plate format (similar to Figure 2.3B). Among the best hits were Cyclin-dependent kinase 2, BRCA1, and other genes involved in DNA damage repair (including HR) and cell division. Based on this screen and the chemical library screen by Jacquemont *et al.*[85] (see above) the authors used the chemical compound Bortezomib to target the FA pathway and disrupt HR. Bortezomib was synthetically lethal with *CCNE1* amplification in multiple ovarian cancer cell lines.

In the second example, Hoffman *et al.*[96] identified synthetic lethal interactions in Brahma Related Gene 1 (*BRG1*)-deficient cancers (Figure 2.1A) using an epigenome-focused shRNA screen to identify epigenetic cancer dependencies. Epigenetic disregulation caused by alterations in the chromatin remodeling complex SWItch/Sucrose Non Fermentable (SWI/SNF) are important in tumorigenesis[101]. Inactivation of *BRG1*, a DNA-dependent ATPase and part of the SWI/SNF complex, is associated with increased cell proliferation, dysregulation of cell cycle checkpoints, and poor clinical prognosis[102]. Matched lines for *BRG1* were obtained from the Cancer Cell Line Encyclopedia and consisted of a panel of 58 human cancer cell lines differing in their *BRG1* status (Figure 2.2B). In order to study epigenetics-based synthetic lethality the authors constructed a DEep COverage DEsign shRNA library (DECODER) containing 6,500 shRNAs, with 17 shRNAs per gene, to specifically target enzymes involved in epigenetic regulation. The DECODER lentiviral pool was transduced into each cell line in duplicate. The relative abandance of each

shRNA was measured by Illumina GA2X-based next generation sequencing of each shRNA's barcode in *BRG1*-deficient and expressing cell lines. Hits were shRNAs that were selectively eliminated from *BRG1*-deficient cells. From this screen the gene with the strongest synthetic lethal effect was BRahMa (*BRM*), a catalytic subunit of the SWI/SNF chromatin remodeling complex and paralog of *BRG1*. The authors hypothesized that BRM compensates for BRG1 loss in the deficient cancer cell lines. To confirm this the authors then showed that cancer lines with homozygous loss of *BRG1* are more dependent on *BRM* than those with heterozygous loss. To further confirm the synthetic lethal interaction between *BRG1* and *BRM* the authors introduced an inducible shRNA targeting *BRM* into several *BRG1*-deficient and WT cell lines. *BRM* knockdown in *BRG1*-deficient cells caused irreversible growth arrest and significant induction of repressive H3K9me3 histone methylation marks. The synthetic lethal interaction was confirmed *in vivo* using an inducible shRNA for *BRM* in *BRG1*-deficent lung cancer xenografts of NCI-H1299.

In the third example, Scholl *et al.*[95] identified a synthetic lethal interaction in Kirsten RAt Sarcoma (*KRAS*) oncogene dependent cancer cells using a subset of the Broad Institute TRC shRNA Library that consists of 5,024 shRNAs (Figure 2.1B). Oncogenic *KRAS* mutations occur within most human cancers[103–105] and drive tumorigenesis by increasing proliferation, anabolism, evasion of apoptosis and the immune system, and by stimulating metastasis[103–105]. The authors hypothesized that oncogenic KRAS mutations cause secondary dependencies on genes that can then be exploited for causing synthetic lethal interactions. The shRNA screen was conducted in the Acute Myeloid Leukemia (AML) cell lines NOMO-1 (mutant KRAS), THP-1 (WT KRAS), fibroblasts (WT KRAS), and human mammary epithelial cells (WT KRAS) (Figure 2.2E). Similar to the siRNA plate format approach (Figure 2.3B) the screen was conducted in a 384-well plate format in which each well was transduced with a single shRNA. Cell Titer-Glo was used to

determine cell viability for each well. The top candidate gene *STK33*, a member of the calcium/calmodulin-dependent protein kinase subfamily of serine/threonine protein kinases, was then validated in additional matched AML lines (Figure 2.2E). The authors then tested the consequence of *STK33* knockdown in multiple non-AML cancer types. The synthetic lethal interaction was only observed in cancers that are dependent on mutant KRAS for viability and proliferation. The interaction was confirmed *in vivo* using inducible shRNA targeting *STK33* in pancreatic, breast, lung, and colon cancer xenografts. Further investigation has shown that in mutant KRAS cells, STK33 acts through S6K1-induced inactivation of Bcl-2-associated death promoter to suppress the mitochondia-mediated apoptosis and promote survival.

The shRNA approach requires redundancy in order to rule out false positive hits, since each individual shRNA has varying levels of efficacy in different cell types due to target transcript variation, shRNA design, and varying degrees of off-target effects. Overall this approach allows for the investigation of synthetic lethality in a large number of cancer cell lines in parallel through pooled viral libraries and generates a large number of hits. These methods require the use of microarray or DNA sequencing, which can be cost prohibitive; small molecule compounds targeting the identified genes may not be readily available.

CRISPR Library Screens

A new approach to genome editing was discovered in bacteria and archaea through the identification of clustered repeat sequences in 1987 that was later named CRISPR, or Clustered Regularly Interspaced Short Palindromic Repeats by Jansen *et al.*[106] in 2002. CRISPR serves as a bacterial immune system against bacteriophages. Invading viral DNA is incorporated into the bacterial host genome between the CRISPR repeat sequences, which can then be used to

specifically target the viral DNA for degradation[107]. The CRISPR system is now a powerful tool for specifically editing the genome[108] and can be applied to identifying synthetic lethal interactions (Figure 2.4).

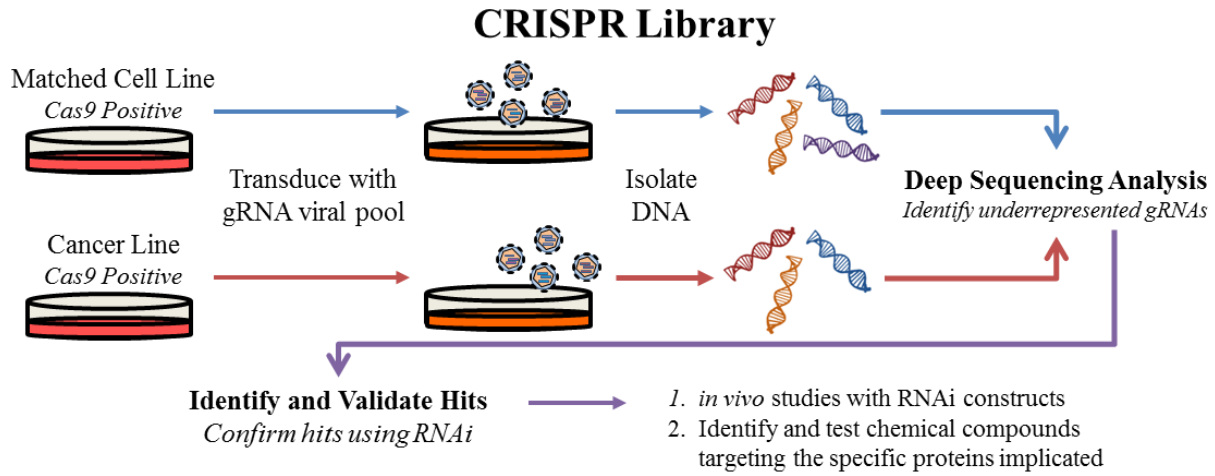

Figure 2.4. An overview of the CRISPR approach for Synthetic Lethality Screens. Matched cell lines stably expressing Cas9 are transduced with the gRNA library in a pooled virus format to produce a library of single cell mutants. The mutant library for each line is then screened for synthetic lethal interactions by isolating DNA and identifying underrepresented gRNA sequences in the cancer cell line which are not lost in the matched normal cells. Interactions identified from the screen are then investigated and validated using RNAi. Small molecules interacting with the targets of interest can be developed and inducible RNAi constructs may be used for *in vivo* studies.

Hiroko *et al.*[109] performed a genome wide CRISPR screen in mouse cells to identify genes that confer susceptibility to *Clostridium septicum* alpha-toxin. The aim of this study was to identify genes that when targeted would confer resistance to the toxin. While not technically identifying synthetic lethal interactions, since the screen identified genes that resulted in survival when targeted by guide RNAs (gRNAs) (reverse of Figure 2.1B), this study exemplifies how a CRISPR based approach could be conducted for studying synthetic lethal interactions in cancer. The CRISPR system generates bi-allelic mutations in each targeted gene resulting in a loss of function phenotype. Lentiviral CRISPR-Cas9 constructs that target 19,150 mouse protein-coding genes were generated using 87,897 gRNAs. The gRNA library covered 94.3% of the genome with at

least 2 gRNAs per gene. Mouse Embryonic Stem Cells (mESC) were transduced with the lentiviral CRISPR pool and were treated with or without alpha-toxin for 5 days (Figure 2.2F). The surviving cells were analyzed by deep sequencing to detect which genes had been lost. In a synthetic lethality screen, the gRNA could be barcoded allowing for hits to be identified by detecting underrepresented gRNA in the cancer population that are still present in the matched (WT) cell line (Figure 2.4). The authors identified 13 genes associated with alpha-toxin resistance and validated genes that were targeted by at least two independent gRNAs. Four validated hits conferring resistance to alpha-toxin were *B4galt7, 1700016K19Rik, Cstf3* and *Ext2*. The authors verified B4galt7 and Ext2 by re-introducing the full-length cDNA into the corresponding gene knockout cell lines, which resulted in sensitivity to the toxin being restored. No further molecular analysis was conducted, and the results were not pursued yet with *in vivo* studies or chemical compound studies.

One major advantage to using a CRISPR library is that the system provides for greater efficiency with fewer off-target effects when compared to an RNAi screen. As such the need for redundant targeting of the same gene is reduced. CRISPR screens, like shRNA library screens, are well suited for studying multiple cell lines in parallel since a pooled viral library can be employed. This is also a disadvantage since the screen will then rely on costly microarray or deep sequencing to identify hits. Since CRISPR is a relatively new system, it is likely that synthetic lethal screens using this approach will become more frequent.

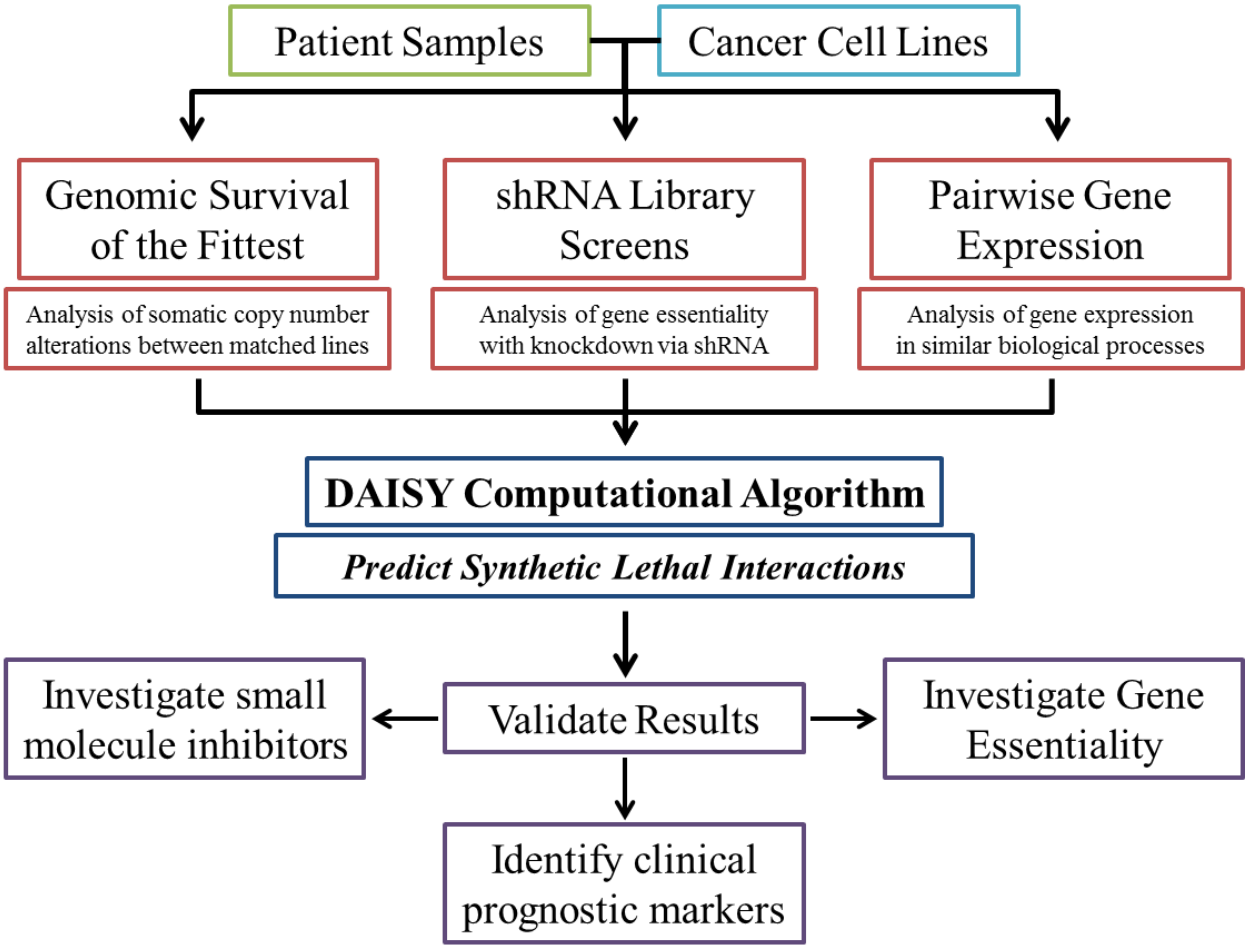

Figure 2.5. DAISY is a computational program that scans large genomic data sets from cell lines and patient samples to identify synthetic lethal interactions. DAISY uses three approaches that independently interpret multiple data sets. The first approach is called survival of the fittest (SoF), which examines genomic DNA data sets for gene co-inactivation and somatic copy number alterations. The second approach analyzes the essentiality of a potential synthetic lethal gene pair using databases from shRNA screens. The last approach uses gene expression data sets to search for genes that are expressed in the similar biological processes by analyzing pairwise gene expression. Predicted synthetic lethality pairs are then tested and validated using *in vitro* gene essentiality assays. If drugs targeting the identified synthetic lethal gene pairs are available then *in vitro* drug screens can be performed. The expression pattern of the synthetic lethal gene pairs can also be assessed for potential use as biomarkers for clinical prognosis.

The DAISY Approach

Most computational approaches to identifying synthetic lethal interactions on a global level have been performed in yeast[70,110] and then applied to human cancer by investigating the effect in their human orthologs. Combining multiple approaches into a single screen can be an effective way to computationally identify synthetic lethal interactions on a global scale in human cancer. The data mining synthetic lethality pipeline, known as DAISY, is an approach published by Arnon *et al.*[111]. It consists of a data-driven computational screen for identifying synthetic lethal pairs through the analysis of cancer genomic data (Figure 2.1A). DAISY is a combination of three inference strategies: Survival of the Fittest (SoF), shRNA functional examination, and pairwise gene co-expression (Figure 2.5). The authors also analyzed Synthetic Dosage Lethality (SDL), which is the overexpression of a gene that leads to the essentiality of a second gene, making a SDL pair (Figure 2.1B). DAISY statistically infers synthetic lethal interactions from data sets generated from cancer cell lines and patient samples (Figure 2.2B, 2E).

The first approach, SoF, is based on the assumption that cells with reduced expression of synthetic lethal gene pairs will not survive in a heterogeneous cell population. Since cancer cells with the inactivation of two synthetically lethal genes will not survive, by studying the Somatic Copy Number Alteration (SCNA) of a specific gene from the pooled populations of multiple cell lines, and comparing it to the average change in all other genes, a synthetic lethal interaction can be inferred. The co-inactivation of synthetically lethal genes should occur less frequently than the average. This is similar to the shRNA screen approach wherein microarray or sequencing is used to identify which shRNAs have been lost from the pooled population with the exception that it is on a much larger scope: each gene investigated is being compared to every other gene across multiple cell lines and patient samples. The second approach is a shRNA functional examination

and relies on three separate shRNA library screens in 46, 9, and 92 cancer cell lines to identify genes that become essential due to the knockdown of another gene. Each separate screen comprised an individual data set including the SCNA and gene expression profiles for each cancer cell line examined within the screen. This relies on the hypothesis that synthetically lethal genes will be simultaneously lost from the viral pool in multiple cancer cell lines. The third approach is pairwise gene co-expression analysis, which is based on the assumption that synthetic lethal pairs are involved in closely related biological processes. The combined analysis of the three approaches analyzed over 535 million gene pairs. A hit from the DAISY screen is defined as two genes in which the inactivation of one renders the other essential for survival.

DAISY's effectiveness was evaluated against previously identified synthetic lethal gene pairs, including the partners of *PARP1*, *VHL*, MutS protein Homolog 2 (*MSH2*), and *KRAS*. The validation was performed on 7,276 gene pairs that were tested in six large screens. *PARP1* and *BRCA1/BRCA2*, as well as *MSH2* and Dihydrofolate reductase were successfully confirmed as synthetic lethal pairs. Daisy's predictive ability was also used to identify genes that become essential with *VHL* deficiency. 44 genes were predicted, and a small siRNA screen was performed to test the validity of the prediction. DAISY identified 3.83 times more synthetically lethal genes than the follow-up siRNA screen. This indicates that additional validation is needed for predicted pairs to eliminate false positives.

The predictive ability of the combined DAISY approach was then used to generate genome-wide networks of synthetic lethal and SDL interactions in cancer. Over 2,000 synthetic lethal genes and over 3,000 SDL genes were identified in both normal and cancer cells. The identified gene pairs were also investigated in a large study based on clinical samples and cancer cell lines to test gene essentiality, clinical prognosis potential, and drug efficacy.

DAISY does have its limitations. It can only be applied to cancer cells since it relies on large genomic mutation data sets, which at times can be hard to work with because of their inaccuracy. It does not account for epigenetic or posttranslational regulation that can alter synthetic lethal and SDL interactions. DAISY's predictive power can be utilized to identify novel co-essential gene pairs, which may lead to new and improved therapeutics for treating cancer.

Conclusions and Outlook

Harnessing synthetic lethal interactions to create novel cancer specific therapies is a rapidly growing part of cancer biology. The specificity of these interactions will allow for improved overall survival while also increasing patient quality of life. Synthetic lethality allows for the exploitation of cancer specific mutations that are not "druggable" by identifying interactions with other co-essential genes. It provides an explanation for why some drugs have increased efficacy in specific cancer types and may even provide new clinically relevant diagnostic markers. With the discovery and implementation of CRISPR it is very likely that studies will be conducted using CRISPR libraries. Future computational based genome-wide inference studies like DAISY could be a powerful tool for mining the myriad of public data sets available to identify synthetic lethal interactions in specific cancer types. Other screens could identify synthetic lethal interactions using a microRNA library approach. As technology advances and sophisticated approaches become easier to conduct, it might be possible for synthetic lethal screens to be extended to personalized medicine.

CHAPTER THREE: LOPAC SYNTHETIC LETHALITY SCREEN

Introduction

Developing Novel Targeted Therapies for CC-RCC

One of the biggest trials faced by scientists is not to develop anticancer drugs that kill cancer cells, but instead to identify drugs that will kill cancer cells at concentrations that do not harm the patient taking them. One way to identify new drugs that specifically target cancer cells and spare normal cells is by identifying synthetic lethal interactions. In this chapter, the term "synthetic lethality" will be used in relation to simultaneous mutation/inhibition of two genes, which results in decreased proliferation (synthetic sick[112]) as well as cell death. Multiple synthetic lethality screens have been conducted in CC-RCC to identify novel drugs that specifically target von Hippel-Lindau (*VHL*) deficient CC-RCC[52,83,84,113–115]. These studies focus on synthetic lethal interactions with *VHL* loss because functional loss of *VHL* has been shown to occur in up to 90% of CC-RCC patients and is a major driver of the disease[44]. These screens have identified multiple targets including the stimulation of autophagy[83]; inhibition of Glut1[84], CDK6[113], MET[113], MEK1[113], protein translation[114,115], and inhibition of ROCK1[52] and are summarized in Table 3.1.

Table 3.1. Targets of published synthetic lethal interactions with *VHL*-deficient CC-RCC.

Drug / Inhibitor	Mechanism	Reference
STF-31	Inducing autophagy	Turcotte et al. 2008
STF-62247	Inhibit Glut1	Chan et al. 2011
219476 and shRNA	Inhibition of CDK6	Bommi-Reddy et al. 2008
shRNA	Knockdown cMET (HGFR)	
shRNA	Knockdown of MEK1	
VerracarinA	Decreased protein translation	Woldemichael et al. 2012
Omacetaxine Mepesuccinate	Decreased protein translation	Wolff et al. 2015
Chromomycin A3	Unknown	Sutphin et al. 2007
Y-27632, RKI 1447	Inhibition of ROCK1	Thompson et al. 2016

This table shows a list of synthetic lethal interactions identified with *VHL* loss in CC-RCC, the method of inhibition, and the corresponding reference.

The previous synthetic lethality screens employed RCC lines that had lost *VHL* and the same cell lines transduced with a wild type cDNA for *VHL* to create a matched RCCVHL line[83]. The matched lines were then tested in chemical and shRNA library screens to identify novel synthetic lethal targets that result in cell death in *VHL*-deficient RCC and spare RCC expressing *VHL*. We conducted a synthetic lethality screen using Sigma's LOPAC, which is an annotated chemical library containing 1280 compounds. The LOPAC screen identified seven compounds: Y-27632, Dequalinium dichloride, Indirubin-3'-oxime, Kenpaullone, SU 9516, Tyrphostin 23, and Tyrphostin A9. The annotated targets for these hits included ROCK, Potassium (K^+) Channels, CDK, PDGFR, and EGFR (Figure 3.1a). Y-27632's inhibition of ROCK is further explored and validated in Chapter 4. A secondary screen was conducted using both the primary screen's fluorescence intensity assay and clonogenic assays to confirm the hits. Following the secondary screen, we then genetically knocked down the LOPAC annotated targets of each hit to see if the hit was "on target" as described by LOPAC. Our results confirmed synthetic lethal interactions

with inhibition or knockdown or ROCK1, CDK2, EGFR, and PDGFR β. While Y-27632 worked well as a small molecule inhibitor of ROCK1, further investigation is needed to identify compounds with greater potency and specificity for targeting CDK2, EGFR, and PDGFR β.

Results

Identification of Synthetic Lethal Interactions with Sigma's LOPAC

In order to identify novel synthetic lethal interactions, we utilized Sigma's LOPAC. In the primary screen RCC4 and RCC4VHL cells, labeled with enhanced yellow fluorescent protein (EYFP), were screened in parallel in 384-well plates for chemical toxicity using LOPAC. After plating, the compounds were added the next day in varying concentrations prepared by serial dilution: 20, 10, 5, 2.5, 1.25, 0.625, and 0.313μM concentrations. Fluorescence intensity, a surrogate indicator of cell growth/viability, was measured four days following plating and exposure to the compounds. Hits from the screen were identified by calculating the maximum inhibition for both the RCC4 and RCC4VHL cell lines and selecting compounds that inhibited RCC4 greater than 50% while not inhibiting RCC4VHL past 50%. This criterion was used to select for compounds that have differential toxicity depending on *VHL* status within the matched cell lines. Seven hits were obtained in the primary LOPAC Screen (Figure 3.1a).

The seven hits identified in the primary screen included the ROCK inhibitor Y-27632, the potassium (K^+) channel inhibitor Dequalinium dichloride, the EGFR inhibitor Tyrphostin 23, the PDGFR inhibitor Tyrphostin A9, and three CDK inhibitors: Indirubin-3'-oxime, Kenpaullone, and SU 9516 (Figure 3.1b-h). For the secondary validation, we decided to proceed with only one CDK inhibitor: SU 9516. The secondary validation included replicating the initial assay used in the primary screen, and conducting clonogenic colony assays in multiple CC-RCC genetic backgrounds.

a

Name	LOPAC Annotated Mode of Action
Y-27632 dihydrochloride	Highly potent, cell-permeable, and selective Rho-associated coiled-coil forming protein serine/threonine kinase (ROCK) inhibitor. Also inhibits ROCK2 with equal potency. The inhibition is competitive with respect to ATP.
Dequalinium dichloride	Selective blocker of apamin-sensitive K^+ channels
Indirubin-3'-oxime	Cyclin dependent kinase (CDK) inhibitor; competes with ATP for catalytic subunit binding
Kenpaullone	Potent inhibitor of CDK1/cyclin B, CDK2/cyclin A, CDK2/cyclin E, and CDK5/p25
SU 9516	Cdk2 inhibitor; induces apoptosis in colon cancer cells
Tyrphostin 23	Protein tyrosine kinase EGFR inhibitor
Tyrphostin A9	Selective PDGF tyrosine kinase receptor inhibitor

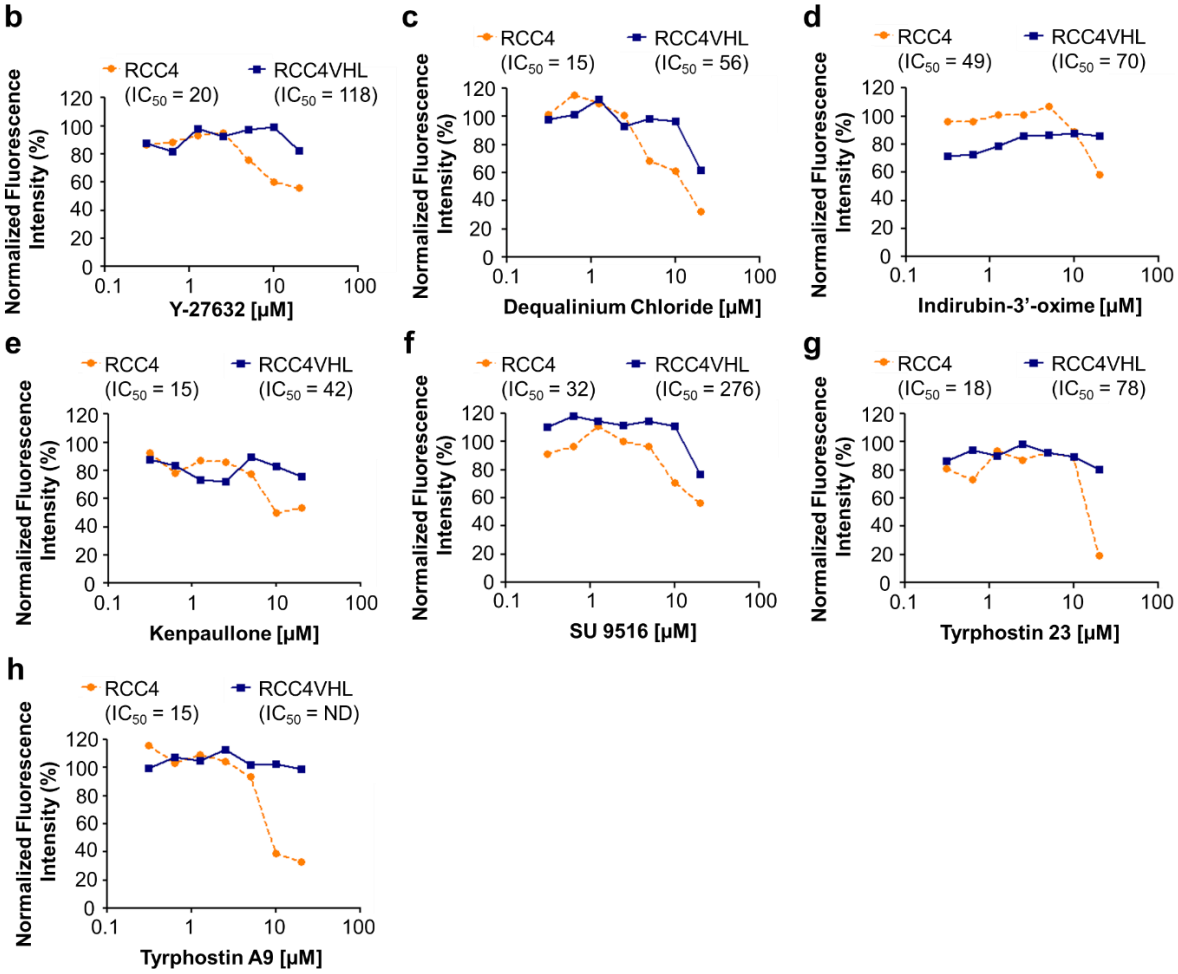

Figure 3.1. The results of a LOPAC library primary screen, which identified seven chemical compounds that specifically target *VHL*-deficient CC-RCC. (**a**) The annotated mode of action of seven chemical compound hits as described in the LOPAC database. Each compound hit is listed with its main target of action. **(b-h)** Dose response curves were generated for each compound hit IC_{50} values are shown, ND – non-determined. RCC4 and RCC4VHL were treated with (**b**) Y-27632, (**c**) Dequalinium dichloride, (**d**) Indurubin-3'-oxime, (**e**) Kenpaullone, (**f**) SU 9516, (**g**) Tyrphostin 23, and (**h**) Tyrphostin A9 for 96 hours. Each chemical compound was administrated at 0.125μM and up to 20μM. Normalized fluorescence intensity of EYFP-labeled RCC4 and RCC4VHL cells served as a surrogate measure of a cell number per well of a 384-well plate. The statistics were not derived since the screen was done with one well per compound concentration.

Validation of the LOPAC Hits via Secondary Screen

We conducted a secondary screen to validate the hits using the fluorescence-based viability assay in the RCC4 EYFP matched cell lines and using clonogenic assay with the RCC4, RCC10, and 786-O matched lines. Using the fluorescence-based viability assay we were able to confirm that each of the hits was selective against the *VHL*-deficient RCC4 EYFP line for at least one dose (Figure 3.2). Y-27632 (Figure 3.2a) showed the greatest difference with a 3x higher IC_{50} at 46µM in RCC4VHL EYFP over 16µM in RCC4 EYFP. The difference in IC_{50}'s was about 2 for the other hits tested including Dequalinium dichloride (Figure 3.2b), SU 9516 (Figure 3.2c), Tyrphostin 23 (Figure 3.2d), and Tyrphostin A9 (Figure 3.2e). We confirmed VHL and HIF expression via western blot (Figure 3.2f). To further validate these hits, we conducted clonogenic assays.

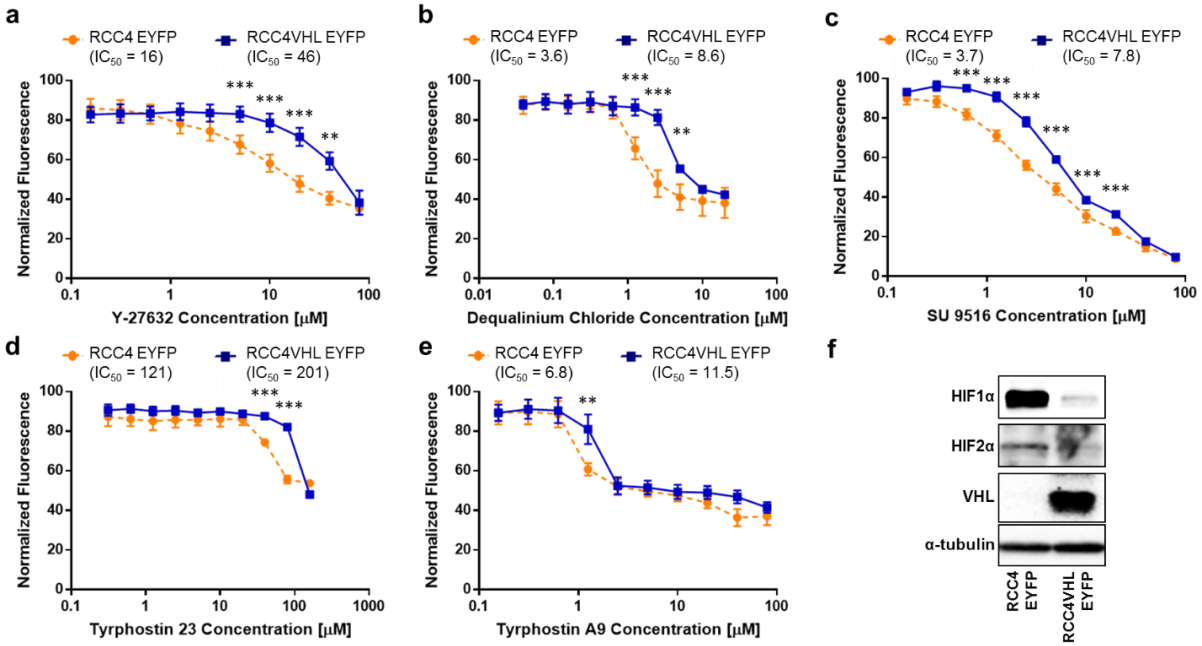

Figure 3.2. Chemical synthetic lethality confirmed in the secondary screen with the hits from the LOPAC. The LOPAC hits were validated in the RCC4 and RCC4VHL matched cell lines, showing selective toxicity towards *VHL*-deficient cells. Normalized fluorescence intensity of EYFP labeled RCC4 with and without VHL treated with (**a**) Y-27632, (**b**) Dequalinium dichloride, (**c**) SU 9516, (**d**) Tyrphostin 23, and (**e**) Tyrphostin A9 for 72 hours. Each dose within each experiment was tested in quadruplicate, and each experiment was repeated three times. Statistical analysis was conducted using a paired t-test for each dose between the matched lines. (** $p < 0.01$, *** $p < 0.001$) (**f**) Western blot showing VHL status and HIF expression in the RCC4 EYFP matched lines. α-Tubulin served as a loading control.

Next, we tested whether the synthetic lethal effect could be reproduced in multiple matched CC-RCC cell lines with different genetic backgrounds including RCC4, RCC10, and 786-O matched cell lines. Similar to the fluorescence based viability assay, Y-27632 showed the best difference in IC_{50} with the RCC4VHL at 51μM and RCC4 at 12μM. Once again, the other compounds while showing statistically significant differences for at least one dose, showed limited differences in IC_{50} between the matched lines (Figure 3.3b-e). Western blot analysis was conducted to confirm HIF and VHL expression in the RCC4 matched cell lines (Figure 3.3f). We observed similar results for both the RCC10 matched line (Supplemental Figure 3.1) and the 786-O matched line (Supplemental Figure 3.2). In both lines, Y-27632 was the best hit and the other compounds had less than a 3x difference in IC_{50} between the *VHL*-deficient line and *VHL* line. Since the compounds did show at least selectiveness against the *VHL*-deficient lines for at least one dose we wanted to test if knocking down the annotated target for each compound could replicate the effect to see if the drugs are acting on-target.

Confirmation that the LOPAC Hits are Acting On-Target.

We next sought to test if the hits from the LOPAC screen are acting on target by conducting siRNA clonogenic assays using the annotated targets listed by LOPAC (Figure 3.1a). We were able to identify the main target of the effect for four of our hits (Figure 3.4). Based on the siRNA clonogenic assay Y-27632 acts through ROCK1 and not ROCK2, as knockdown of ROCK1 replicated the effect and knockdown of ROCK2 had no effect. Similarly, knockdown of CDK2 and EGFR also replicated the effects for SU 9516 and Tyrphostin 23 respectively. Knockdown of PDGFR β replicated the effect of Tyrphostin A9, while knockdown of PDGFR α did not. This indicates that the effect of Tyrphostin A9 is through PDGFR β. The knockdowns were confirmed by qRTPCR (Supplemental Figure 3.3). Unfortunately, we were unable to confirm the knockdown

of PDGFRα so the result is not conclusive for Tyrphostin A9. We were also unable replicate the effects of Dequalinium dichloride by knocking down the Apminin-sensitive potassium channels KCNN1 and KCNN3 (Supplemental Figure 3.4). Knockdown of KCNN1 actually doubled the survival of RCC4 cells while not affecting RCC4VHL cells. We did not confirm knockdown of KCNN1 or KCNN3 by qRT-PCR however, so these results are inconclusive. It may be that Dequalinium dichloride is acting off-target, potentially through PKC[116], which still needs to be explored. Taken together, the results from the secondary screen and siRNA clonogenic assays confirm that Y-27632 is a valid hit from the LOPAC screen, which we discuss in Chapter 4. The other hits that still need to be explored include SU 9516, Tyrphostin 23, and Tyrphostin A9.

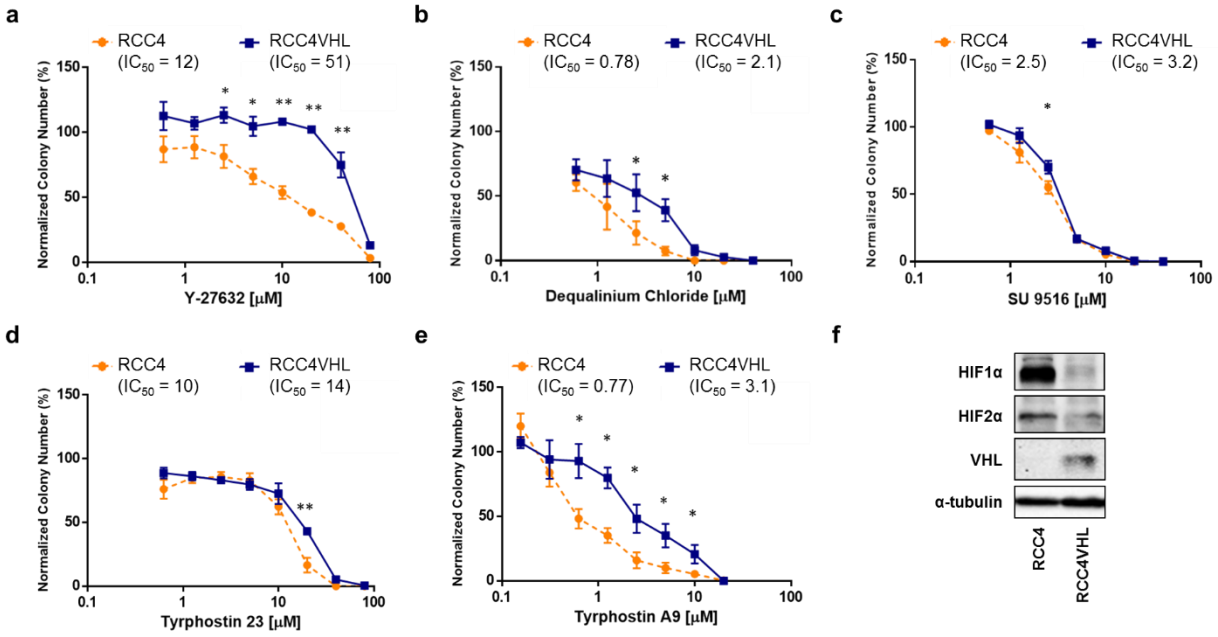

Figure 3.3. Clonogenic Assays confirm the synthetic lethal interactions identified by the LOPAC Screen. Clonogenic assays in RCC4 matched cell lines confirm the synthetic lethal interaction between *VHL* loss and (**a**) Y-27632, (**b**) Dequalinium dichloride, (**c**) SU 9516, (**d**) Tyrphostin 23, and (**e**) Tyrphostin A9 for at least one dose tested for each compound. Each dose within each experiment was tested in duplicate, and each experiment was repeated three times. IC_{50s} are indicated. Statistical analysis in (**a-e**) was performed using a paired t-test between the matched cell lines at each dose (* $p < 0.05$, ** $p < 0.01$), SEMs are shown. (**e**) Western blot showing VHL status and HIF expression in the RCC4 matched lines. α-Tubulin served as a loading control.

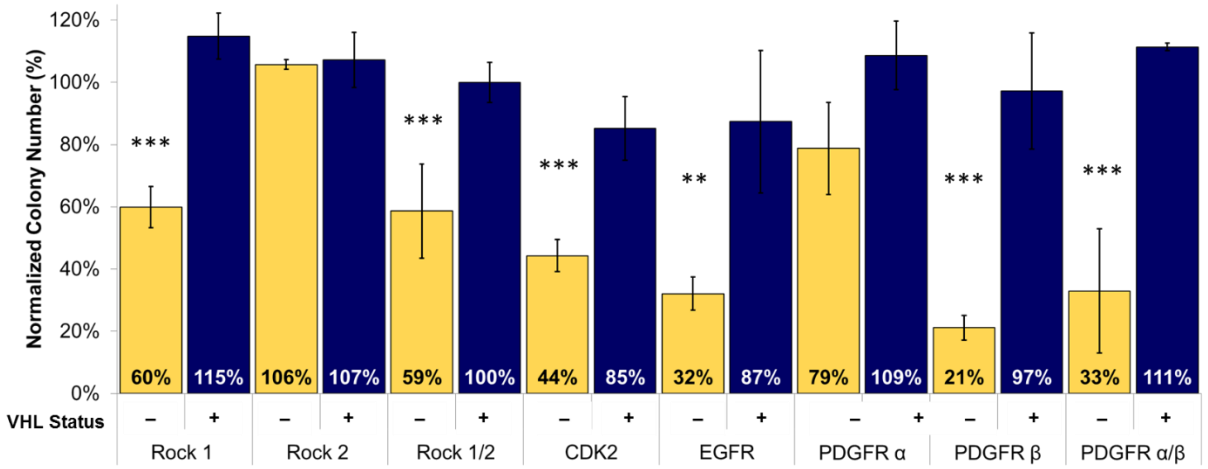

Figure 3.4. Genetic Knockdown of LOPAC Annotated Targets confirms On Target Effect for Y-27632, SU 9516, Tyrphostin 23, and Tyrphostin A9. siRNA clonogenic colony assays were conducted using the matched RCC4 cell line for the main annotated targets for some of the hits from the LOPAC screen. Knockdown of ROCK1, CDK2, EGFR, and PDGFR β triggered a synthetic lethal effect in the *VHL*-deficient RCC4 cell line indicating that these are the interacting partners with *VHL* in the synthetic lethal effect.

Discussion

In this study, we conducted an annotated chemical library screen and identified seven potential hits. Each of the hits was tested in a secondary screen using the fluorescence based viability assay and clonogenic assays in multiple CC-RCC matched cell lines. From these hits, we were able to validate the ROCK inhibitor Y-27632 as a target for further study (explored in depth in Chapter Four). ROCK inhibition is synthetically lethal in multiple CC-RCC genetic backgrounds and we were able to confirm that synthetic lethality occurs through ROCK1 and not ROCK2. The other hits, while showing limited success at specific doses, did not have as great of a selectivity towards the *VHL*-deficient CC-RCC lines. On the other hand, the siRNA studies suggest that CDK2, EGFR, and PDGFR-β are synthetic lethality partners with *VHL* and more specific chemical inhibitors might be more suitable for future synthetic lethality studies.

One of our hits, Tyrphostin A9, targets the PDGFR pathway that is already targeted by FDA approved therapies. Receptor Tyrosine Kinase inhibitors are the major class of targeted

therapeutics that is approved for treating advanced CC-RCC, and multiple approved RTKis target PDGFR, including Axitinib, Sorafenib Tosylate, Sunitinib Malate, Pazopanib Hydrochloride. Our study shows that part of the mechanism of action of these drugs may come from a synthetic lethal interaction between *VHL* loss and PDGFR β inhibition. The current view is that the predominant effect of these therapies is mediated by the inhibition of endothelial cells and not tumor cells[22,30]. Based on this, more potent and selective inhibitors of PDGFR β may have the potential to serve as viable therapies for CC-RCC, but additional testing is needed to confirm their effect on tumor cell survival independent of endothelial cell targeting.

One of the synthetic lethal interactions identified occurs between EGFR inhibition and *VHL* loss. EGFR is an interesting target that has been widely investigated for use in treating CC-RCC without success (review in [117]). Overactivation of EGFR has been linked to higher tumor grade and stage[118]. Interestingly, phosphorylated EGFR has been shown to be a VHL target[119]. Thus, upon *VHL* loss in CC-RCC active EGFR is no longer degraded, accumulates, and activates its downstream pathways similar to HIFs. Furthermore, EGFR can increase HIF-1α translation via activation of the PI3K/AKT pathway[120]. Altogether, EGFR inhibitors seem like a good therapy, but further investigation is needed to determine why EGFR inhibitors have not been successful in the clinic.

Of note, three of our hits are CDK inhibitors. In 2008, Bommi-Reddy et al. performed an shRNA based synthetic lethality screen and identified CDK6 as being synthetically lethal with *VHL* loss[113], which they also confirmed using the CDK4/6 inhibitor 219476. Our hits, Indirubin-3'-oxime, Kenpaullone, and SU 9516 target multiple CDKs, but also have reported non CDK off targets. Indirubin-3'-oxime targets GSK3β in addition to targeting CDK1, CDK2, CDK4, and CDK5[121]. Besides targeting CDK1, CDK2, and CDK5 Kenpaulone has been shown to target GSK-

3β, ERK2, and c-Src[122]. SU 9516 targets PKC, p38, PDGFR, and EGFR in addition to CDK1, CDK2, and CDK4[123]. These off-target effects may be the reason for the discrepancy between the secondary screen results and the siRNA clonogenic assay for CDK2 knockdown. Knockdown of CDK2 resulted in a 56% reduction in colony number in the *VHL*-deficient RCC4 cell line while the RCC4VHL only decreased by 15%. In the secondary screen SU 9156 only showed small differences between the two lines and our tests with Indirubin-3'-oxime and Kenpaulone (data not shown) showed the same effect. Additional testing is still required to determine which CDKs are involved in the synthetic lethal effect. We hypothesize that a CDK inhibitor that is more potent and more specific for CDK1, CDK2, and CDK4/6 may serve as an effective therapy.

In summary, we have identified and confirmed one new synthetic lethal interaction between ROCK1 and VHL in CC-RCC. Similarly, knockdown of CDK2, EGFR, and PDGFR β with siRNA had a synthetic lethal effect with *VHL* loss in CC-RCC, which still needs to be confirmed with multiple siRNAs to account for off-target effects. It is important to keep in mind that the LOPAC compounds have off-target effects that likely limits their synthetic lethal effect and additional more specific compounds need to be tested.

Materials and Methods

Cell culture and chemical treatments.

The CMV-EYFP labeled RCC4±VHL matched cell lines were previously described[124]. Cells were grown in Dulbecco's Modified Eagle's Medium (DMEM; Caisson Labs #25-500, North Logan, UT) + 10% Fetal Bovine Serum (FBS; Omega Scientific #FB-12, Tarzana, CA) + 1% Penicillin/Streptomycin (Caisson Labs #25-512). in 5%CO_2, 21%O_2 at +37ºC. All compounds were diluted in Dimethyl Sulfoxide (DMSO) and serially diluted for each experiment.

Cell viability assay based on measurements of fluorescence intensity.

RCC4 EYFP and RCC4VHL EYFP were plated at 5,000 cells per well in black 96-well tissue culture plates in FBS-free DMEM media. The following day, DMSO vehicle or varying compound concentrations were prepared in 20% FBS DMEM by serial dilution and an equal volume was added to the cells. Cells were incubated for 72 hours. Wells were washed with Phosphate Buffered Saline (PBS). Then, 100μL of PBS was added to each well and fluorescence intensity was measured on a BioTek Synergy HT Microplate Reader (Winooski, VT) at 488nm. Each experiment was performed three times in quadruplicate per treatment.

Clonogenic cell survival assay.

Clonogenic assays were performed by serially diluting cells to 300 cells/ml and adding 1ml to each 60mm plate for 300 cells/plate with 2 ml of complete DMEM. The next day after cells had attached DMSO or the compounds, prepared by serial dilution at 4x the proper concentrations, was added to each plate to bring the volume to 4ml total. Cells were incubated for 10 days for the RCC4 matched lines and 7 days for the RCC10 and 786-O matched lines. Cells were then washed with PBS and fixed with Crystal Violet staining solution (0.1% Crystal Violet, 0.3% Glacial Acetic acid, 95% ethanol) for 15min. The plates were washed again in PBS and the colonies were counted on each plate. Each experiment was performed three times in duplicate per treatment.

Gene knockdowns by siRNAs.

RCC4±VHL were plated at 200,000 cells per well of a 6-well plate in FBS-free DMEM. The following day the cells were transfected with 6 μL DharmaFECT1 (Dharmacon, Lafayette, CO) and up to 2 nM siRNA accordingly to manufacturer's protocol. The siRNAs for ROCK1 (SASI_Hs01_00065573), ROCK2 (SASI_Hs01_00204253), CDK2 (SASI_Hs01_00060175),

EGFR (SASI_Hs01_00215449), KCNN1 (SASI_Hs01_00030339), KCNN3 (SASI_Hs01_00085793) and MISSION(R) Universal Negative Control #1 siRNA were obtained from Sigma (St. Louis, MO). The following day, transfected cells were plated for the clonogenic cell survival assay. Replicate plates were lysed after 72 hours and ROCK1 and ROCK2 expression analyzed by Western blot.

Western blot analysis.

After treatments, cells were lysed and Western blot was conducted as previously described[125]. Proteins were visualized using primary antibodies recognizing HIF1α (BD Biosciences, #610959, San Jose, CA), HIF2α (Novus Biological, #NB100-122, Littleton, CO), α-tubulin (Fitzgerald, #10R-842, North Acton, MA), VHL (Cell Signaling, #9661, #2738, Danvers, MA), and Horseradish peroxidase conjugated Goat anti-Rabbit IgG and Goat anti-Mouse IgG secondary antibodies (Thermo Scientific, #31460, #31430). Blots were imaged using a Bio Rad ChemiDoc XRS$^+$ (BioRad, Hercules, CA).

Quantitative reverse transcription-polymerase chain reaction (qRT-PCR) analysis.

Following siRNA knockdown for the siRNA colony assays cells were plated for the clonogenic assay and the remainder were collected for RNA isolation using the TRI Reagent (Sigma Aldrich #T9424) following the manufacturer's protocol. cDNA was synthesized using Superscript II reverse transcriptase (Invitrogen #18064014) following the manufacturer's protocol. qRT-PCR was performed using Power SYBR Green (Thermo Fisher #4367660) on an ABI ViiA7 qPCR machine. Primer sequences for ROCK1 (F' 5' AAGTGAGGTTAGGGCGAAATG 3', R' 5' AAGGTAGTTGATTGCCAACGAA 3'), ROCK2 (F' 5' TTGCTCTGGATGCAATACACTC 3', R' 5' TCTCGCCCATAGAAACCATCA 3'), CDK2 (F' 5' CCAGGAGTTACTTCTATGCCTGA 3', R' 5' TTCATCCAGGGGAGGTACAAC 3'), EGFR

(F’ 5’ AGGCACGAGTAACAAGCTCAC 3’, R’ 5’ ATGAGGACATAACCAGCCACC 3’), PDGFRβ (F’ 5’ TGATGCCGAGGAACTATTCATCT 3’, R’ 5’ TTTCTTCTCGTGCAGTGTCAC 3’) were obtained from PrimerBank. The TBP primer used was F’ 5’ CCCGAAACGCCGAAT 3’ and R’ 5’GACTGTTCTTCACTCTTGGCTC 3’.

Growth curves and statistical analysis.

Dose response and cell growth curves were generated using GraphPad Prism. IC_{50} values were calculated by transforming the X axis using X=Log(X), normalizing the transformed data to the vehicle control with 0 as 0%, and then fitting the normalized transformed data with a nonlinear trend line either using a normalized response ("log(inhibitor) vs. normalized response") or a variable slope ("log(inhibitor) vs. normalized response – Variable slope”). The correct nonlinear trendline was selected using GraphPad’s comparison of fits, which directly compares both fit lines statistically using an extra sum-of-squares F test. The fit line is not shown in the figures. The IC_{50} values for each experiment were then calculated from the Best-fit values. Statistical analysis was conducted in Minitab 16 using a paired t-test or ANOVA between cell lines with a p-value of less than 0.05 considered statistically significant. All error bars represent the SEMs.

Supplemental Figures

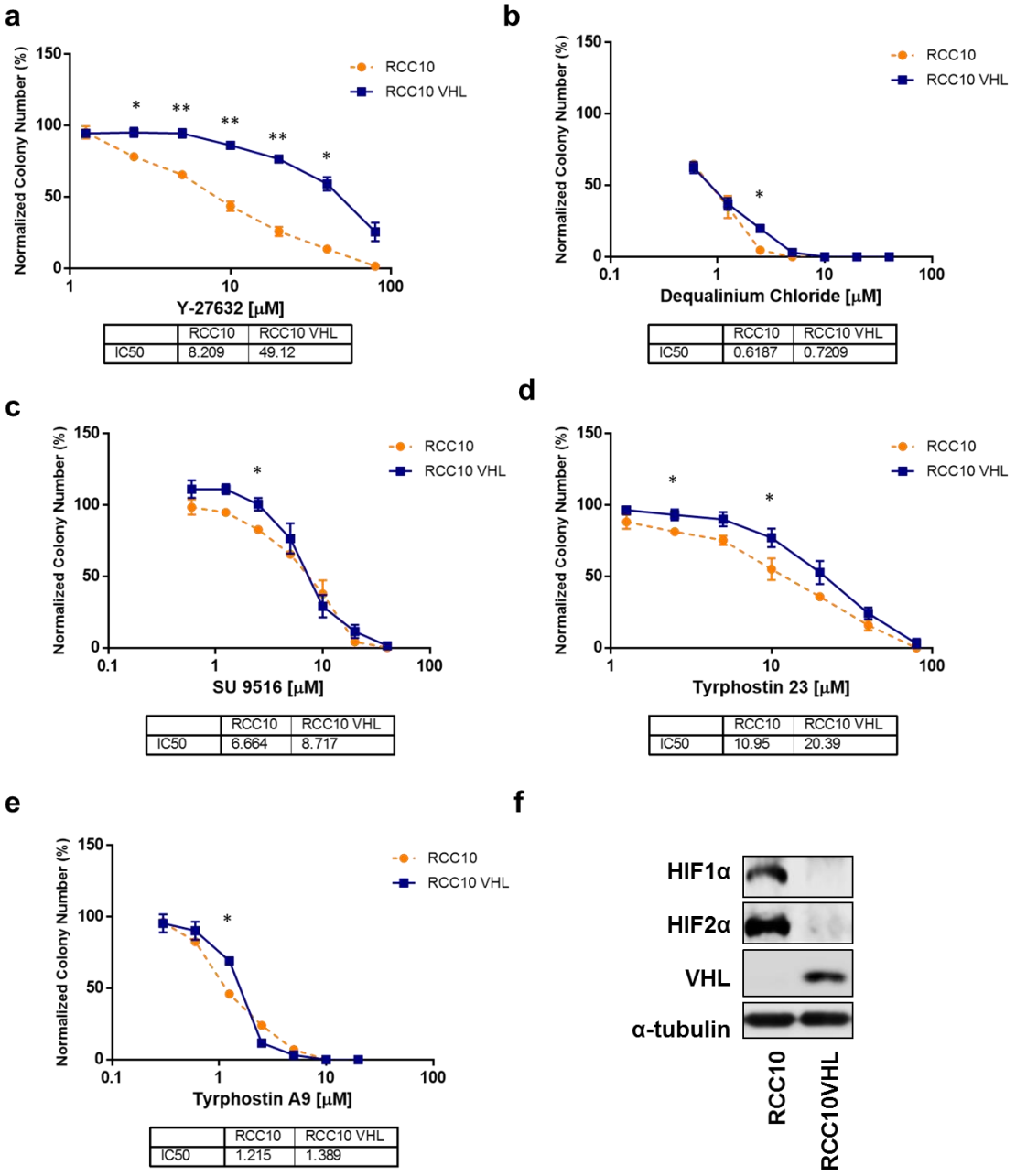

Supplemental Figure 3.1. Clonogenic Assays confirm the synthetic lethal interactions identified by the LOPAC Screen. Clonogenic assays in RCC10 matched cell lines confirm the synthetic lethal interaction between *VHL* loss and (**a**) Y-27632, (**b**) Dequalinium dichloride, (**c**) SU 9516, (**d**) Tyrphostin 23, and (**e**) Tyrphostin A9 for at least one dose tested for each compound. Each dose within each experiment was tested in duplicate, and each experiment was repeated three times. IC_{50s} are indicated. Statistical analysis in (**a-e**) was performed using a paired t-test between the matched cell lines at each dose (* $p < 0.05$, ** $p < 0.01$), SEMs are shown. (**e**) Western blot showing VHL status and HIF expression in the RCC4 matched lines. α-Tubulin served as a loading control.

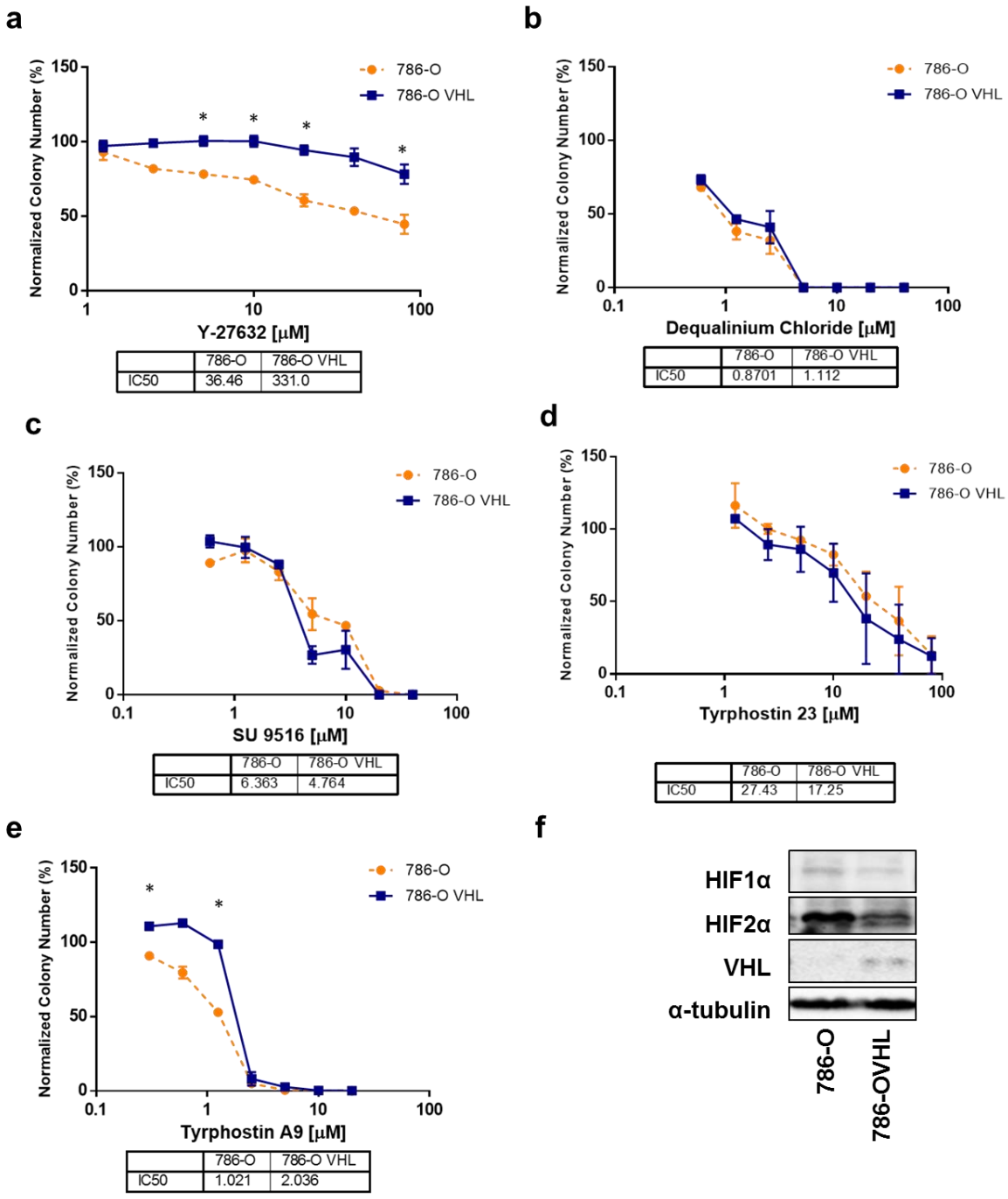

Supplemental Figure 3.2. Clonogenic Assays confirm the synthetic lethal interactions identified by the LOPAC Screen. Clonogenic assays in 786-O matched cell lines confirm the synthetic lethal interaction between *VHL* loss and (**a**) Y-27632, (**b**) Dequalinium dichloride, (**c**) SU 9516, (**d**) Tyrphostin 23, and (**e**) Tyrphostin A9 for at least one dose tested for each compound. Each dose within each experiment was tested in duplicate, and each experiment was repeated three times. IC_{50s} are indicated. Statistical analysis in (**a-e**) was performed using a paired t-test between the matched cell lines at each dose (* $p < 0.05$, ** $p < 0.01$), SEMs are shown. (**e**) Western blot showing VHL status and HIF expression in the RCC4 matched lines. α-Tubulin served as a loading control.

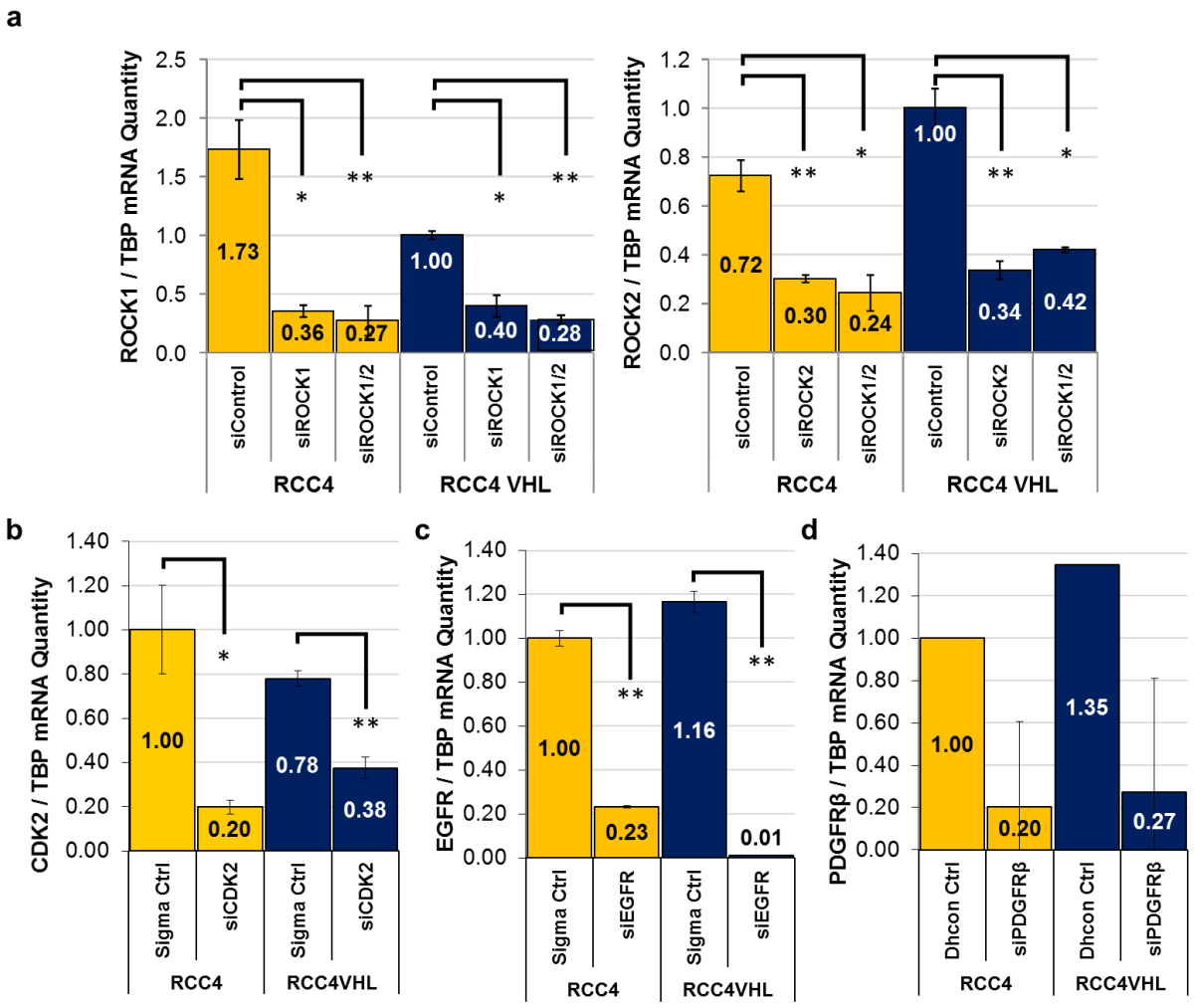

Supplemental Figure 3.3. qPCR Analysis confirms the knockdown of LOPAC targets. The degree of each target knockdown by its specific siRNA (as indicated) was assessed by QRT-PCR. (**a**) Although the starting ROCK1 expression is lower in RCC4VHL cells compared to RCC4 (siCtrl), the expression is equal in both cell lines upon siROCK1 or siROCK1/2 transfection. (**b**) The knockdown of CDK2 in the RCC4VHL was slightly reduced in comparison to the RCC4 cells. (**c**) The knockdown in the RCC4VHL cells was far better than the knockdown in RCC4. (**d**) Both RCC4 and RCC4VHL cell lines showed high variability with less reliable results. The data was normalized to siControl (Sigma Ctrl or Dharmacon siControl) in the RCC4 cell line for each experiment. Samples were tested in triplicate and the experiment was repeated at least two times. Statistical analysis in (**a-d**) was performed using a paired t-test between the treatments as indicated (* $p < 0.05$, ** $p < 0.01$), SEMs are shown.

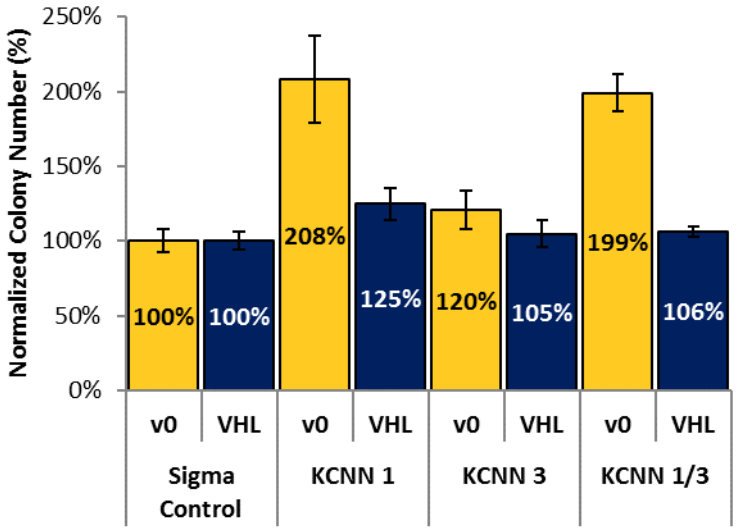

Supplemental Figure 3.4. Knockdown of Apamin sensitive potassium channels does not replicate Dequalinium dichloride effect. siRNA clonogenic colony assays were conducted using the matched RCC4 cell line for the main annotated targets for some of the hits from the LOPAC screen. Knockdown of KCNN1 increased the survival of RCC4 cells while not affecting RCC4VHL cells. Knockdown of KCNN3 did not affect either RCC4 or RCC4VHL indicating that Dequalinium dichloride is acting off-target.

CHAPTER FOUR: ROCK1 INHIBITION IS SYNTHETICALLY LETHAL WITH VHL DEFICIENCY IN CC-RCC

Introduction

Renal cancer is the most deadly of all genitourinary cancers with 62,700 new cases and 14,240 deaths projected to occur in 2016[126]. While surgical resection is often curative at early stages, metastatic renal cancer remains a devastating disease with a 5-year survival rate of less than 20%[126,127]. The poor survival rate is due to renal cancer's resistance to radiotherapy[128], chemotherapy[127], and traditional immunotherapy[127], which has been linked to multidrug resistance mechanisms[129] and the lack of common solid tumor mutations[130].

Clear Cell Renal Cell Carcinomas (CC-RCCs) account for 90% of all renal cancer cases, and the tumor-suppressor *VHL* is functionally lost in up to 90% of CC-RCC tumors[32]. *VHL* loss occurs early in the disease and drives its pathogenesis[32]. *VHL* is an E3 ubiquitin ligase that targets multiple proteins for proteasomal degradation, including the Hypoxia Inducible Factor (HIF) α subunits and the Epidermal Growth Factor Receptor (EGFR)[119]. Thus, upon *VHL* loss, CC-RCCs upregulate expression of EGFR and other Receptor Tyrosine Kinases (RTKs), as well as HIFs, in turn upregulating proangiogenic genes, like Vascular Endothelial Growth Factor (VEGF). As a

consequence, CC-RCCs are highly vascularized and aggressive. Accordingly, the majority of approved CC-RCC therapies inhibit angiogenesis. The RTK inhibitors (RTKi) sunitinib[131], sorafenib[11], and axitinib[13], which block VEGFR and Platelet Derived Growth Factor Receptor (PDGFR), prolong progression-free survival for a median of 5 months when compared to placebo[11,132] or standard of care treatments like interferon α[133]. Another class of CC-RCC therapeutics is represented by mammalian target of rapamycin inhibitors (mTORi) everolimus[19] and temsirolimus[134], which prolong progression-free survival for a median of 3 months when used as single agents compared to standard of care. While these treatments offer significant clinical benefit, resistance to both RTKi and mTORi therapeutics develops quickly creating the need for new and improved therapeutics[22,30,135].

In this study, we relied on a "synthetic lethality" approach to identify new therapeutics for *VHL*-deficient CC-RCC. A large body of evidence supports the use of synthetic lethality screens for identifying specific chemical compounds or small hairpin RNAs (shRNAs) that cause cell death and/or inhibit cell proliferation in combination with a particular cancer mutation[31,49]. The principle underlying such screens is that cancer cells with a specific mutation will be more sensitive to targeted inhibition of a certain pathway than normal cells that are do not the same mutation. Thus, the resulting synthetic lethality compounds represent excellent candidates for therapies that target mutation-bearing cancer cells, but spare normal tissues. Several synthetic lethality screens have been conducted in CC-RCC to date[83,84,113–115,124]. Each of these screens utilized the loss of the *VHL* tumor suppressor to identify compounds that are selectively targeting *VHL*-deficient CC-RCCs. The synthetic lethality screens relied on "matched" cell lines, which were created by introducing either a vector control or the wild-type *VHL* cDNA to *VHL*-deficient CC-RCC[49]. These matched cell lines were then used in chemical or shRNA library screens to

identify chemical compounds or shRNAs that selectively target *VHL*-deficient CC-RCCs, while sparing their *VHL*-reconstituted "matched" counterparts. While both unannotated chemical library[83,84,114,115,124] and shRNA[113] screens have been conducted, to date no screens have been conducted using an annotated chemical library.

In this study, we screened the annotated Library of Pharmacologically Active Compounds (LOPAC). This approach simultaneously revealed the exact molecular pathways responsible for selective targeting of *VHL*-deficient cells, and chemical compounds that inhibit them. Herein we report a chemical hit identified in a LOPAC screen, Y-27632 an inhibitor of the Rho-associated coiled-coil-containing protein kinase *(*ROCK) that selectively targets VHL-deficient CC-RCC. The ROCK proteins are regulated by the small GTP-binding protein Rho and are best known for their role in regulating cell morphology and motility by controlling actin-myosin contractile force[136]. This role is mediated through phosphorylation of their downstream substrates, including Myosin Light Chain (MLC), Myosin Light Chain 2 (MLC2), MYosin Phosphatase Target 1 (MYPT1), and LIM Kinases (LIMK)[136]. ROCK signaling is commonly upregulated in bladder[137], testicular[138], breast[139], prostate[140], and renal cancer[54], and has been shown to contribute to tumor metastasis in bladder[137], breast[141], and prostate cancer[140]. In addition, certain ROCK substrates induce cell proliferation[140], apoptosis[142], and inhibit autophagy[143]. The two ROCK isoforms, ROCK1 and ROCK2, are differentially expressed throughout the body with ROCK1 being expressed ubiquitously and ROCK2 being expressed predominantly in the brain, muscle, heart, and lungs[144]. Although the two isoforms are highly homologous and have redundant functions, they also have unique functions and substrates[136].

In the present study, we show that ROCK inhibitors selectively target *VHL*-deficient CC-RCC to reduce cell proliferation, induce cell death, and block migration, which is mediated through

inhibition of ROCK1 and not ROCK2. Our studies also reveal that HIF over-activation caused by *VHL* loss is both necessary and sufficient to cause synthetic lethality with ROCK inhibitors. Importantly, treatment with ROCK inhibitors blocks tumor growth *in vivo*, validating ROCK inhibitors as potential therapeutics for *VHL*-deficient CC-RCC.

Results

Identification of chemical hit Y-27632 targeting VHL-deficient CC-RCC.

To identify novel chemical compounds that selectively target *VHL*-deficient CC-RCC, we screened the LOPAC composed of 1,280 compounds annotated with their protein targets (Chapter 3), which allowed us to identify not only the chemicals, but also the molecular pathways necessary for survival/proliferation of *VHL*-deficient CC-RCC. The screen utilized the RCC4±VHL matched cell lines. RCC4 cells lack both alleles of *VHL* and as a consequence HIF1α and HIF2α expression and activity are dramatically elevated compared to cell lines expressing *VHL* tumor suppressor[32,145,146]. RCC4VHL cells were generated by stably transfecting full-length wild type *VHL* cDNA to RCC4[46]. Both RCC4 and RCC4VHL cells were labeled with Enhanced Yellow Fluorescent Protein (EYFP) and the matched cell lines were treated in parallel with the LOPAC compounds at concentrations ranging from 0.3μM to 20μM in 384-well plates. Fluorescence intensity, a surrogate measure of cell numbers per well, was measured 96 hours following the treatment. The ROCK inhibitor Y-27632 (structure shown in Supplemental Figure 4.1a) was identified in this screen and selectively targeted *VHL*-deficient RCC4 while sparing RCC4VHL. The structures of the other two ROCK inhibitors, used later in this study, are shown in Supplemental Figure 4.1b,c. We validated Y-27632 as a "hit" by fluorescence-based viability assay (Figure 4.1a). To further validate Y-27632 as a chemical hit we conducted clonogenic assays

on RCC4 and RCC4VHL cell lines (Figure 4.1b and Supplemental Figure 4.2a). Importantly, *VHL*-deficient RCC4 cells were 4-5 times more sensitive to Y-27632 treatment than RCC4VHL in both assays (Figure 4.1a-b).

Treatment with ROCK inhibitor Y-27632 selectively targets VHL-deficient CC-RCCs of multiple genetic backgrounds.

Next, we tested if the synthetic lethality effect could be reproduced in multiple genetic backgrounds. We repeated the clonogenic assays in two more *VHL* matched CC-RCC cell lines based on RCC10 expressing both HIF1α and HIF2α and 786-O expressing only HIF2α (Figure 4.1c-d and Supplemental Figure 4.2b-c). Similar to the results obtained in RCC4, Y-27632 treatment specifically targeted the *VHL*-deficient RCC10 and 786-O cell lines, while sparing the CC-RCCVHL. Y-27632 treatment not only reduced colony numbers selectively in *VHL*-deficient CC-RCC (Supplemental Figure 4.2a-c), but also caused reduced colony staining intensity due to a reduction in cell numbers per colony (Supplemental Figure 4.2d-f). For each CC-RCC/CC-RCCVHL cell line pair the IC_{50} for *VHL*-deficient CC-RCC was approximately five times lower than for CC-RCCVHL (Figure 4.1b-d). VHL expression in each CC-RCCVHL cell line was confirmed by Western blot analysis, and it caused a reduction in HIF1α and HIF2α expression compared to the respective CC-RCC cell line (Figure 4.1e).

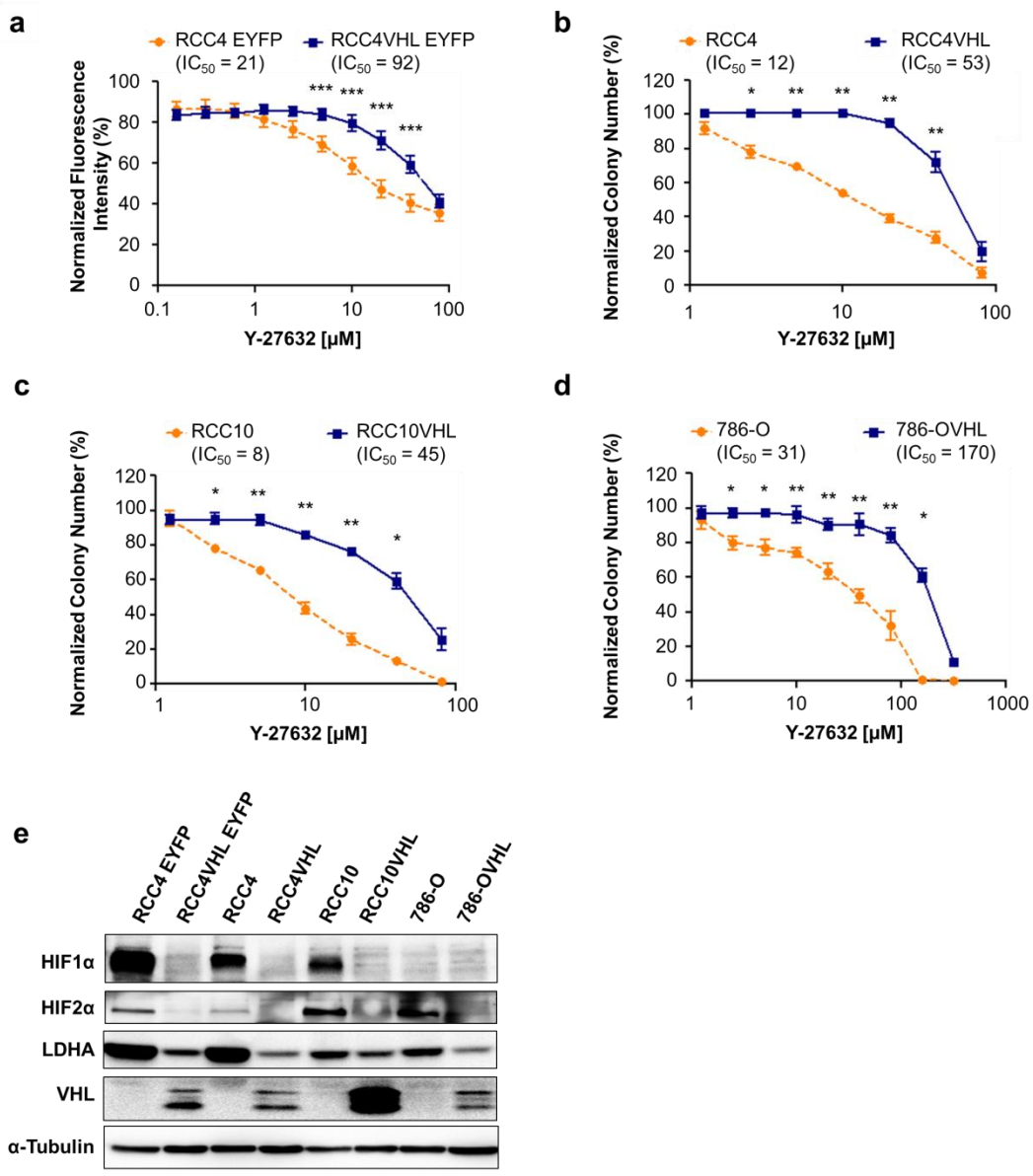

Figure 4.1. The ROCK inhibitor Y-27632 causes synthetic lethality with *VHL* loss in multiple CC-RCC cell lines. (**a**) The LOPAC hit Y-27632 was validated in the RCC4-EYFP and RCC4VHL-EYFP matched cell lines, showing selective toxicity towards *VHL*-deficient cells. Each dose of Y-27632 within each experiment was tested in quadruplicate, and the experiment was repeated three times. Fluorescence intensity of EYFP-labeled cells was used as a surrogate for cell number. (**b-d**) Clonogenic assays in (**b**) RCC4±VHL, (**c**) RCC10±VHL, and (**d**) 786-O±VHL matched cell lines confirming that Y-27632 causes synthetic lethality with *VHL* loss in multiple CC-RCC genetic backgrounds. Each dose of Y-27632 within each experiment was tested in duplicate, and the experiment was repeated three times. IC_{50s} are indicated. Statistical analysis in (**a-d**) was performed using a paired t-test between the matched cell lines at each dose (* $p < 0.05$, ** $p < 0.01$, *** $p < 0.001$), SEMs are shown. (**e**) Western blot showing the effect of VHL re-expression in CC-RCC cell lines on HIF1α and HIF2α expression, and the expression of their downstream target LDHA. α-tubulin serves as a loading control.

Y-27632's ability to inhibit ROCK activity was assayed via Western blot analysis of MYPT1 Thr^{696} phosphorylation (ROCK substrate[50]). Y-27632 treatment for 2 hours was effective at inhibiting MYPT1 phosphorylation (Supplemental Figure 4.3). Interestingly, *VHL*-deficient CC-RCC have decreased basal MYPT1 phosphorylation in comparison to CC-RCCVHL. Together these results indicate that Y-27632 inhibits ROCK in CC-RCC and selectively targets *VHL*-deficient CC-RCC while sparing *VHL*-reconstituted CC-RCC in multiple genetic backgrounds.

Synthetic lethality occurs through inhibition of ROCK1.

We aimed to confirm that the synthetic lethal effect of Y-27632 is "on-target" through blocking ROCKs as annotated in LOPAC. Since Y-27632 inhibits both ROCK family members: ROCK1 and ROCK2, we sought to determine which ROCK was responsible for the synthetic lethal effect. To do this we knocked down ROCK1 or ROCK2 with selective siRNAs. To control for the off-target effects of the siRNAs we used two siRNAs to knockdown ROCK1 (siROCK1#1, siROCK1#2) and two to knockdown ROCK2 (siROCK2#1, siROCK2#2). Our data showed that knockdown of ROCK1, but not ROCK2, reduced the colony forming ability and colony size of *VHL*-deficient RCC4 cells, sparing RCC4VHL cells, thus mimicking the effect of Y-27632 treatment (Figure 4.2a, Supplemental Figure 4.4). The ROCK1 and ROCK2 knockdowns were confirmed by Western blot analysis. Importantly, the knockdowns were equal or greater in the RCC4VHL cells for each siRNA used (Figure 4.2b-c). These data were reproduced in 786-O and 786-OVHL matched cell lines (Supplemental Figure 4.5). In summary, siRNA knockdown of ROCK1, but not ROCK2, selectively inhibits colony formation of *VHL*-deficient CC-RCC.

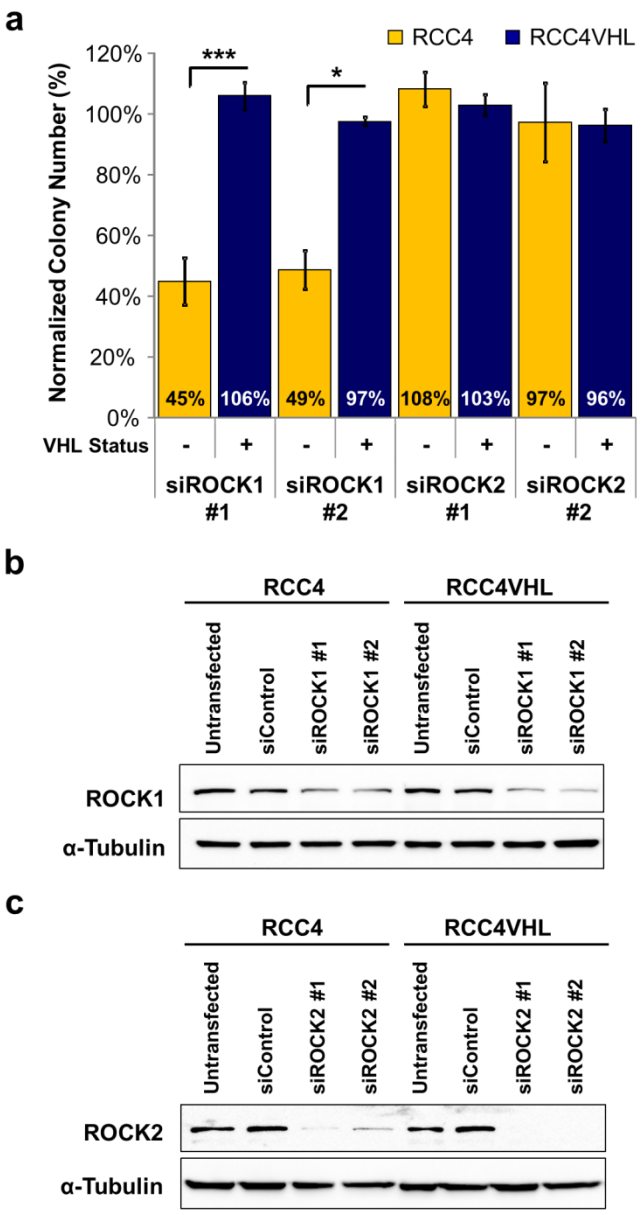

Figure 4.2. Synthetic lethality of Y-27632 with *VHL* loss is mimicked by siRNA downregulation of ROCK1, not ROCK2. RCC4±VHL matched cell lines were transfected with siRNAs targeting ROCK1, ROCK2, or non-targeting siRNA control (siControl). Two different siRNAs per target were used. Twenty-four hours after transfection cells were plated for a clonogenic assay. Each transfection was done in triplicate, followed by clonogenic assays conducted in triplicate, and the experiments were repeated three times except siROCK2#2 (n=2). (**a**) Transfection with siROCK1, but not siROCK2, resulted in significant reduction in RCC4 colony numbers in comparison to RCC4VHL. Thus, ROCK1 downregulation mimics the effect of Y-27632 treatment on viability of RCC4 cells, making it a likely target for Y-27632 causing synthetic lethality effect. Statistical analysis was performed using a paired t-test between the matched cell lines for each siRNA (* $p < 0.05$, *** $p < 0.01$), SEMs are shown. (**b-c**) The degree of each target knockdown by its specific siRNA (as indicated) was assessed by Western blot.

RKI 1447 and GSK 429286 ROCK inhibitors target VHL-deficient CC-RCC.

Since there are several commercially available ROCK inhibitors, and all of them differ in their potency and selectivity towards ROCK1 versus ROCK2, we tested two additional ROCK inhibitors in clonogenic assays: RKI 1447 (structure shown in Supplemental Figure 4.1b) and GSK 429286 (structure shown in Supplemental Figure 4.1c). Since RKI 1447 showed the strongest potency it was tested in all three matched cell lines. RKI 1447, similar to Y-27632 treatment and ROCK1 knockdown, selectively reduced the number of colonies and cells per colony in the *VHL*-deficient CC-RCC (Figure 4.3a-c, Supplemental Figure 4.6). The potencies of Y-27632, RKI 1447, and GSK 429286 were compared in RCC10±VHL in Figure 4.1c, Figure 4.3b, and Supplemental Figure 4.7 respectively. The overall inhibitor potencies based on IC_{50s} are as follows: RKI 1447 (0.8μM) > GSK 429286 (6.4μM) > Y-27632 (8.2μM). Since GSK 429286 was less potent than RKI 1447 we did not test it further. We also observed that repeat, daily, treatment with 2μM RKI 1447 led to an enhanced synthetic lethal effect in each of the *VHL*-deficient CC-RCC, while minimally affecting matched *VHL*-expressing CC-RCCVHL (Figure 4.3d-f). For visual comparison, representative images were obtained on day 14 of treatment for RCC4 and 786-O, and day 9 of treatment for RCC10 (Supplemental Figure 4.8). Thus, multiple ROCK inhibitors specifically target *VHL*-deficient CC-RCC.

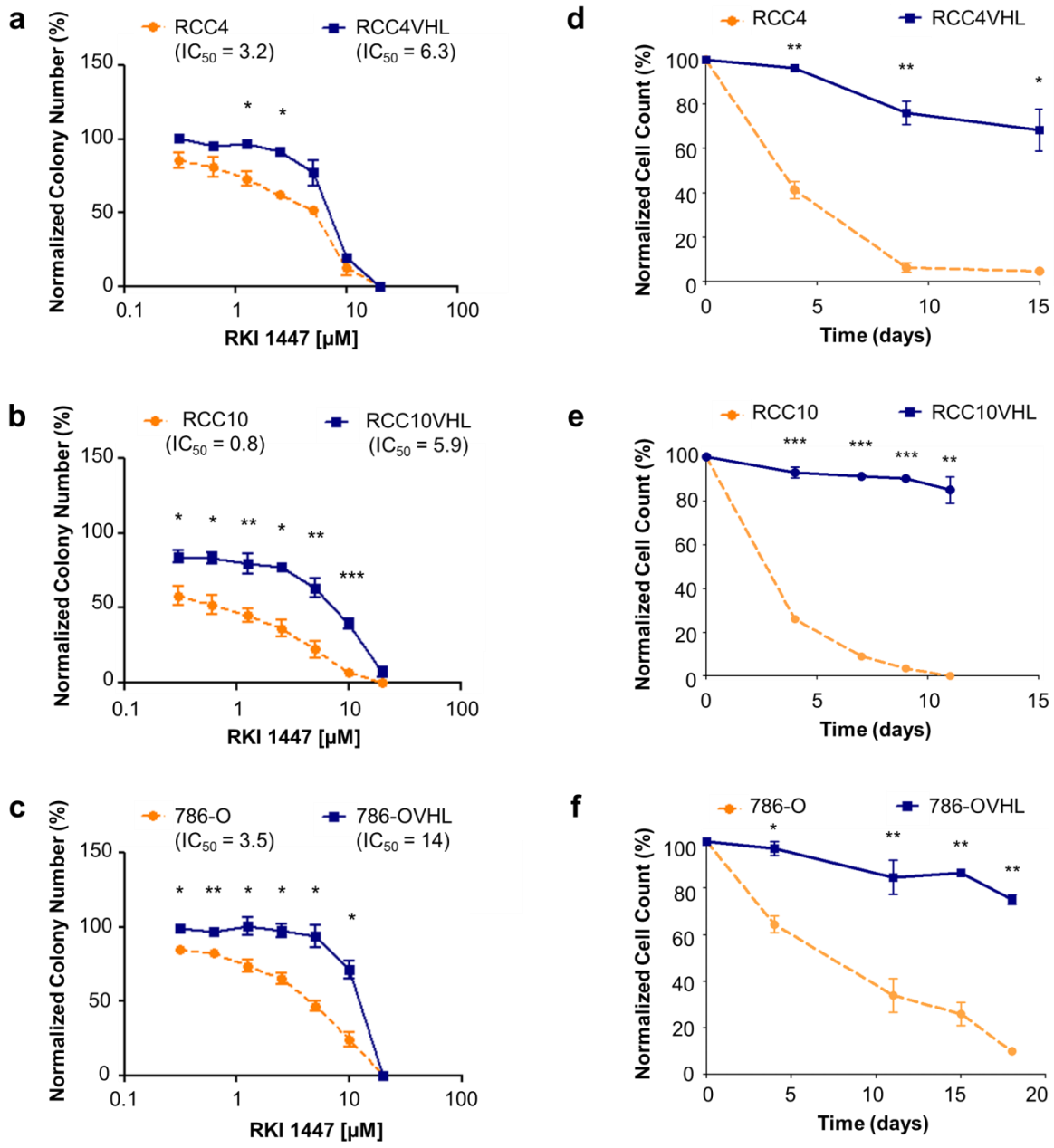

Figure 4.3. ROCK inhibitor RKI 1447 causes synthetic lethality with *VHL* deficiency similar to Y-27632. Clonogenic assays in RCC4±VHL (**a**), RCC10±VHL (**b**) and 786-O±VHL (**c**) matched cell lines confirmed the synthetic lethality of ROCK inhibitors with *VHL* loss. Each dose of RKI 1447 within each experiment was tested in duplicate, and each experiment was repeated three times. (**d-f**) Long term repeat administration of RKI 1447 enhanced the synthetic lethality effect. Repeated daily treatment of RCC4±VHL (**d**), RCC10±VHL (**e**) and 786-O±VHL (**f**) with 2μM RKI 1447 caused *VHL*-deficient RCC cell numbers to decline, while RCCVHL cells continued to proliferate. Daily treatment with DMSO was used as a control. Cells were counted and passaged at 1:10 when the DMSO-treated *VHL*-expressing cells became >80% confluent. Statistical analysis was performed using a paired t-test between the matched cell lines at each dose (* $p < 0.05$, ** $p < 0.01$, *** $p < 0.001$), SEMs are shown.

Treatment with ROCK inhibitors reduces CC-RCC proliferation and induces cell death.

The results from the clonogenic assays pointed to both cell death (reduced colony numbers) and proliferation defect (reduced colony size) as biological outcomes of Y-27632 treatment (Figure 4.1b-d, Supplemental Figure 4.2). To confirm these biological outcomes, we assessed cell cycle progression using a FITC-Bromodeoxyuridine (BrdU) assay. Treatment of RCC4 and RCC4VHL cells with Y-27632 at 10μM, 20μM, and 40μM resulted in an increase in the apoptotic/debris population and a decrease in the S phase and G_0/G_1 phase populations, but the effects were more pronounced in RCC4 than in RCC4VHL (Figure 4.4a, Supplemental Figure 4.9). To determine if apoptosis was responsible for the increase in the apoptotic/debris population we assessed if Y-27632 stimulated caspase 3 cleavage in CC-RCC cells by Western blot analysis. Our results show that Y-27632 induced caspase 3 cleavage in both RCC4 and RCC4VHL, but did not induce caspase 3 cleavage in RCC10±VHL or 786-O±VHL over the basal level, thus ruling out apoptosis as a cause of selective cell death in *VHL*-deficient CC-RCC (Supplemental Figure 4.10).

To confirm that Y-27632 treatment induces cell death, we treated RCC4 and RCC4VHL cells with 20μM Y-27632 for 24 hours and then stained the cells with propidium iodide (PI). Imaging of the RCC4 cells showed a 5.4-fold increase in the number of PI-positive dead cells, while RCC4VHL showed a 1.5-fold increase (Figure 4.4b, Supplemental Figure 4.11a). Additionally, siRNA knockdown of ROCK1, but not ROCK2, resulted in a more than 5-fold increase in PI-positive dead cells (Figure 4.4c, Supplemental Figure 4.11b). Together these results indicate that ROCK1 inhibition induces cell death and blocks proliferation in *VHL*-deficient CC-RCC.

Figure 4.4. ROCK inhibition in *VHL*-deficient CC-RCC cells decreases proliferation, induces cell death, and blocks cell migration. (**a**) BrdU assay revealed that Y-27632 treatment is both cytotoxic and cytostatic in RCC4. RCC4 cells acquired a large fraction of apoptotic/debris cells and greatly reduced the S phase upon treatment with Y-27632 for 72 hours as opposed to RCC4VHL. The graph shows the representative experiment of two experiments performed. (**b**) RCC4 cells treated with 20μM Y-27632 for 24 hours showed a more than five-fold increase in cell death while RCC4VHL were minimally affected. Cells were stained with the vital dye PI and imaged at 4x. The number of PI-positive cells was then counted for each field. The data was normalized to DMSO-treated cells. (**c**) Knockdown of ROCK1, but not ROCK2, induces cell death in the *VHL*-deficient RCC4. 48 hours post siRNA transfection, RCC4±VHL cells were stained with PI and imaged. Knockdown of ROCK1 resulted in over a 5-fold increase in PI-positive cells. The data was normalized to siControl-transfected cells. Each experiment in (**b**-**c**) was performed in triplicate. (**d**) ROCK inhibition blocks CC-RCC migration in a transwell assay. Cells were normalized to a DMSO vehicle control for each experiment. RCC10 or 786-O cells were treated with Y-27632, RKI 1447 or DMSO vehicle (as indicated) for 6 hours. The assay was performed in duplicate and repeated three times. Statistical analysis in (**b**-**d**) was performed using a paired t-test comparing each dose to the negative control (* $p < 0.05$, ** $p < 0.01$, *** $p < 0.001$), SEMs are shown.

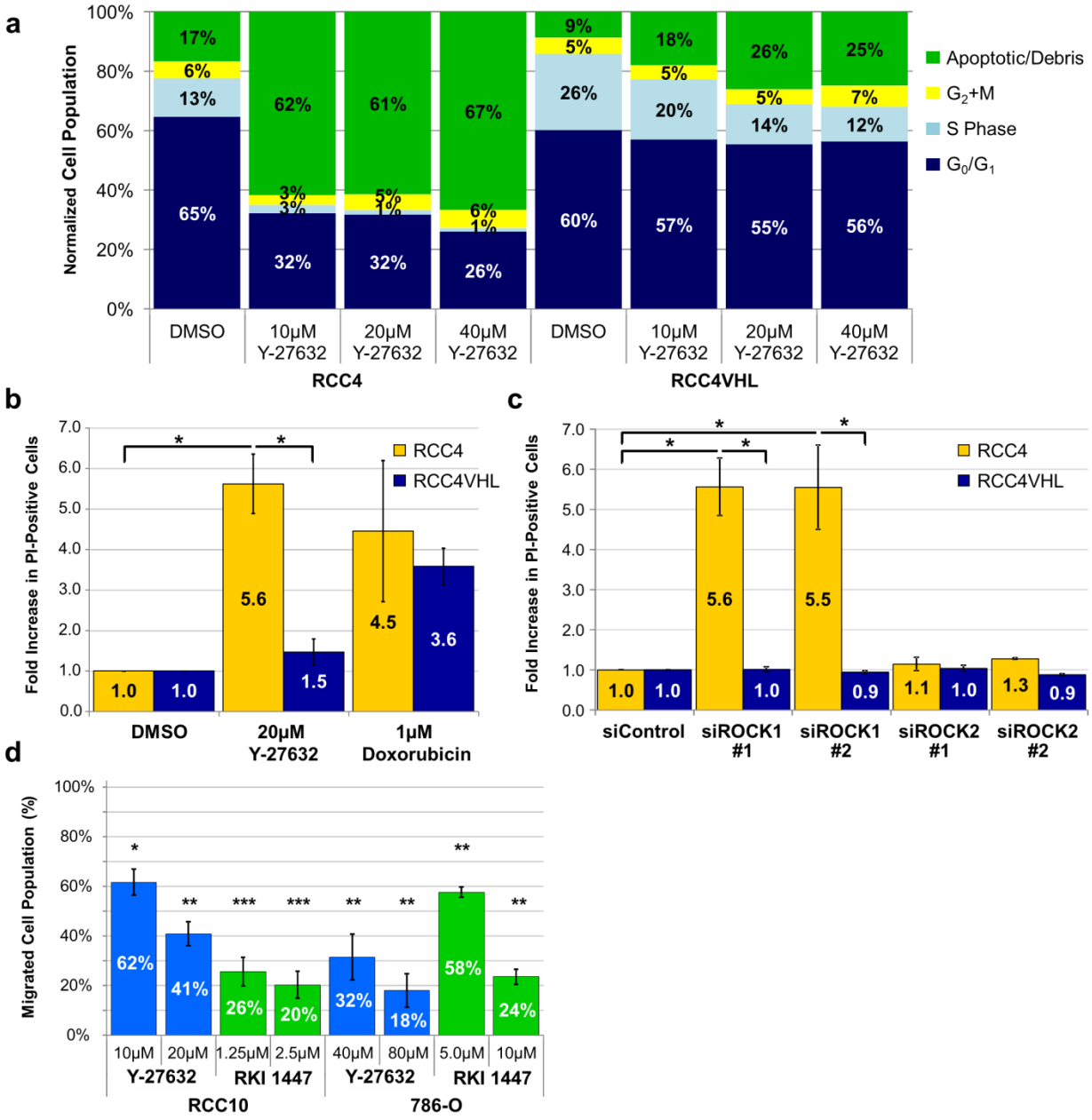
a
Normalized Cell Population
100%
80%
60%
40%
20%
0%
17%
6%
13%
65%
62%
3%
3%
32%
61%
5%
1%
32%
67%
6%
1%
26%
9%
5%
26%
60%
18%
5%
20%
57%
26%
5%
14%
55%
25%
7%
12%
56%
Apoptotic/Debris
G2+M
S Phase
G0/G1
DMSO
10μM Y-27632
20μM Y-27632
40μM Y-27632
DMSO
10μM Y-27632
20μM Y-27632
40μM Y-27632
RCC4
RCC4VHL
b
Fold Increase in PI-Positive Cells
7.0
6.0
5.0
4.0
3.0
2.0
1.0
0.0
RCC4
RCC4VHL
1.0
1.0
5.6
1.5
4.5
3.6
DMSO
20μM Y-27632
1μM Doxorubicin
c
Fold Increase in PI-Positive Cells
RCC4
RCC4VHL
1.0
1.0
5.6
1.0
5.5
0.9
1.1
1.0
1.3
0.9
siControl
siROCK1 #1
siROCK1 #2
siROCK2 #1
siROCK2 #2
d
Migrated Cell Population (%)
100%
80%
60%
40%
20%
0%
62%
41%
26%
20%
32%
18%
58%
24%
10μM
20μM
1.25μM
2.5μM
40μM
80μM
5.0μM
10μM
Y-27632
RKI 1447
Y-27632
RKI 1447
RCC10
786-O

ROCK inhibition blocks CC-RCC migration.

Due to the known role of ROCKs in the regulation of cell adhesion, migration, and invasion[141,147,148], we decided to assess the contribution of ROCKs to CC-RCC migration. First, we noticed that treatment with Y-27632 results in a change in cell morphology (cells become elongated and spindly), likely due to ROCKs role in regulating actin cytoskeleton reorganization and actomyosin contraction[136] (Supplemental Figure 4.12). When we stopped the compound treatment at 48 hours, cells reverted to their non-elongated phenotype (Supplemental Figure 4.12). Second, both Y-27632 and RKI 1447 caused a dramatic reduction of RCC10 and 786-O cell migration in a transwell migration assay (Figure 4.4d). To rule out the cytotoxic/proliferation-inhibitory effect of Y-27632 and RKI 1447 on migrating cells, we conducted all of the migration experiments at short 6-hour time points. At 6 hours, the live cell numbers were assessed by PI vital dye exclusion flow cytometry and no changes were detected (Supplemental Figure 4.13). Thus, ROCK inhibitors have the potential to reduce CC-RCC primary tumor growth through their cytotoxic and cytostatic effects and may inhibit metastasis by blocking cell migration.

Figure 4.5. The synthetic lethal interaction between *VHL* loss and ROCK inhibition is HIF-dependent. (**a**) Western blot showing the efficiency of ARNT knockdown by shRNA (shARNT) in *VHL*-deficient RCC4 and RCC10. The scrambled shRNA was used as a control (shScr). ARNT inhibition causes a decrease in HIF1α and HIF2α activity as evidenced by the decrease in expression of a HIF-target gene LDHA. (**b**) Clonogenic assay showing that CC-RCCs transduced with shARNT exerted resistance to ROCK inhibition in comparison to shScr transduced CC-RCCs. In that respect, CC-RCCs transduced with shARNT behaved similarly to the cell lines with reintroduced *VHL*. Each treatment was normalized to the DMSO control. (**c**) Cells from the CC-RCC±VHL were treated with Y-27632 at the indicated concentrations, plated for clonogenic assays, and replicate plates were subjected to either normoxia (21% O_2) or hypoxia (2% O_2). Each assay was performed in duplicate and repeated three times. Colony numbers were normalized to the vehicle control. RCC4VHL, RCC10VHL, and 786-OVHL cells were sensitized to ROCK inhibition in hypoxia. Statistical analysis was performed using a paired t-test (* $p < 0.05$, ** $p < 0.01$, *** $p < 0.001$), SEMs are shown. (**d-e**) Clonogenic assay showing that HIF-1α expression sensitizes 786-O cells to Y-27632 (**d**) and RKI 1447 (**e**). Each dose was compared statistically using a one-way ANOVA followed by Tukey's Posthoc. Tie bars indicate significant differences with a p-value < 0.01. (**f**) Clonogenic assay showing that non-degradable HIF1α and HIF2α expression are sufficient to induce the synthetic lethal effect with 20μM Y-27632 treatment. Statistical analysis was conducted using a one-way ANOVA ($p < 0.001$) followed by Tukey's Posthoc. There were 3 statistically significant groups: 786OVHL > 786O, 786OVHL HIF2a > 786OVHL HIF1a, 786O HIF1a.

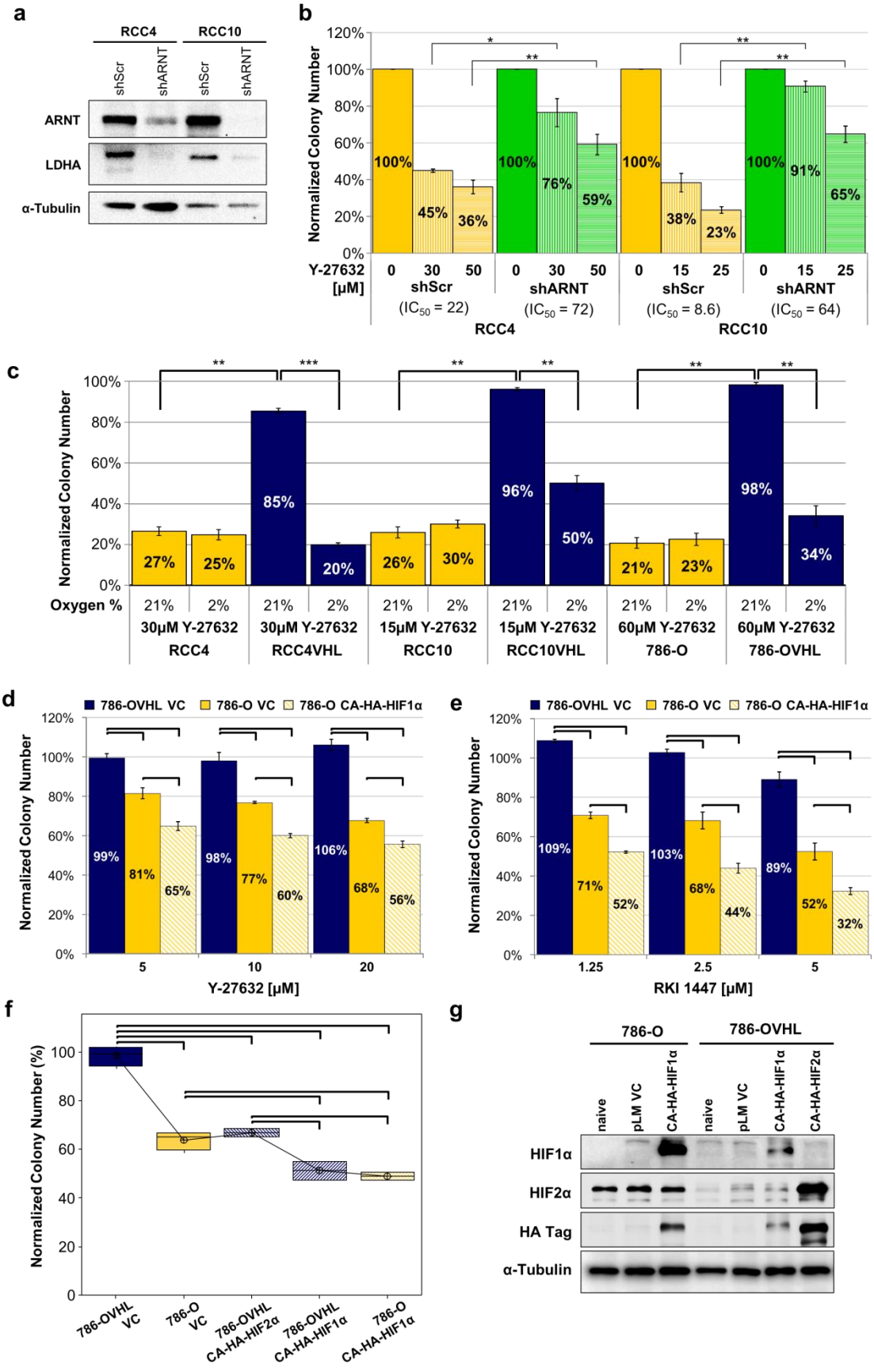
a
RCC4
RCC10
shScr
shARNT
shScr
shARNT
ARNT
LDHA
α-Tubulin
b
Normalized Colony Number
120%
100%
80%
60%
40%
20%
0%
100%
45%
36%
100%
76%
59%
100%
38%
23%
100%
91%
65%
Y-27632 [μM]
0 30 50 0 30 50 0 15 25 0 15 25
shScr
shARNT
shScr
shARNT
(IC50 = 22)
(IC50 = 72)
(IC50 = 8.6)
(IC50 = 64)
RCC4
RCC10
c
Normalized Colony Number
100%
80%
60%
40%
20%
0%
27%
25%
85%
20%
26%
30%
96%
50%
21%
23%
98%
34%
Oxygen %
21% 2% 21% 2% 21% 2% 21% 2% 21% 2% 21% 2%
30μM Y-27632
RCC4
30μM Y-27632
RCC4VHL
15μM Y-27632
RCC10
15μM Y-27632
RCC10VHL
60μM Y-27632
786-O
60μM Y-27632
786-OVHL
d
786-OVHL VC
786-O VC
786-O CA-HA-HIF1α
Normalized Colony Number
120%
100%
80%
60%
40%
20%
0%
99%
81%
65%
98%
77%
60%
106%
68%
56%
5
10
20
Y-27632 [μM]
e
786-OVHL VC
786-O VC
786-O CA-HA-HIF1α
Normalized Colony Number
120%
100%
80%
60%
40%
20%
0%
109%
71%
52%
103%
68%
44%
89%
52%
32%
1.25
2.5
5
RKI 1447 [μM]
f
Normalized Colony Number (%)
100
80
60
40
20
0
786-OVHL VC
786-O VC
786-OVHL CA-HA-HIF2α
786-OVHL CA-HA-HIF1α
786-O CA-HA-HIF1α
g
786-O
786-OVHL
naive
pLM VC
CA-HA-HIF1α
naive
pLM VC
CA-HA-HIF1α
CA-HA-HIF2α
HIF1α
HIF2α
HA Tag
α-Tubulin

Synthetic lethality between ROCK inhibition and VHL deficiency is dependent on HIFs.

One of the best-studied consequences of *VHL* loss/mutation in CC-RCC is the massive stabilization and activation of HIF1α and HIF2α[18-20] (Figure 4.1e). Thus, we hypothesized that the synthetic lethal effect between ROCK inhibition and *VHL* deficiency would be dependent on HIF activation. To test this hypothesis, we acquired RCC4 and RCC10 cell lines where we stably knocked down HIFβ, also known as Aryl hydrocarbon Receptor Nuclear Translocator (ARNT) with a specific shRNA. Since ARNT forms a heterodimer with either HIF1α or HIF2α, and is essential for HIF transcriptional activity, its knockdown inhibited HIF activity. This resulted in a reduction of the Lactate DeHydrogenase A (LDHA) HIF target gene expression (Figure 4.5a). As predicted, knockdown of ARNT in the *VHL*-deficient RCC4 and RCC10 cell lines had a protective effect against Y-27632 treatment (Figure 4.5b), mimicking *VHL* reintroduction. These results indicate that synthetic lethality between ROCK inhibition and *VHL* deficiency is dependent on HIF activation.

To further confirm our findings, cells from the matched cell lines RCC4±VHL, RCC10±VHL, and 786-O±VHL were treated with Y-27632, plated for clonogenic assays, and replicate plates were subjected to either normoxia (21% O_2, low HIF level and activity) or hypoxia (2% O_2, high HIF level and activity). Each Y-27632 treatment was normalized to the DMSO vehicle control in both normoxia and hypoxia groups. The normalized colony numbers for Y-27632-treated *VHL*-deficient CC-RCC cell lines were not affected by oxygen concentration (Figure 4.5c). In contrast, CC-RCCVHL were sensitized to Y-27632 treatment in hypoxia having reduced colony-forming ability in hypoxia compared to normoxia (Figure 4.5c). Hypoxic induction of HIF1α and HIF2α was confirmed by Western blot analysis (Supplemental Figure

4.14). These results confirm that the synthetic lethal interaction between ROCK inhibition and *VHL* deficiency is HIF dependent.

Since 786-O cells were the most resistant to Y-27632 out of the three matched cell lines tested (Figure 4.1b-d) and they do not express HIF1α, while RCC4 and RCC10 do, we hypothesized that HIF1α re-expression in 786-O would sensitize them to Y-27632. To test this hypothesis, we generated a 786-O cell line expressing a non-degradable constitutively active HA-tagged HIF1α (CA-HA-HIF1α). The 786-O CA-HA-HIF1α cells showed increased sensitivity to both Y-27632 (Figure 4.5d) and RKI 1447 (Figure 4.5e) when compared to the 786-O vector control expressing cell line. Additionally, we generated 786-OVHL cells expressing either the CA-HA-HIF1α or CA-HA-HIF2α. Expression of either HIF1α or HIF2α in 786-OVHL was sufficient to cause the synthetic lethal effect with ROCK inhibition, with 786-OVHL CA-HA-HIF1α showing a more pronounced effect than 786-OVHL CA-HA-HIF2α (Figure 4.5f-g). Altogether these results indicate that the synthetic lethal interaction of VHL loss with ROCK inhibition is due to the resulting constitutive activation of HIF in *VHL*-deficient CC-RCC.

Y-27632 inhibits tumor growth in vivo.

786-OT1 cells were isolated from a 786-O tumor grown in a RAG1 mouse and re-established *in vitro* to acquire a cell sub-line capable of fast growth *in vivo*. 786-OT1 were injected subcutaneously (sc) into the right flank of 18 RAG1 mice. After the tumors reached ~500 mm^3, the mice were randomized and either daily treated with a vehicle control (PBS) or 10 mg/kg Y-27632 via intraperitoneal (ip) injection for 18 days. Y-27632 was selected for *in vivo* experiments based on abundant literature reporting its maximum tolerated dose and treatment regimens in mouse experiments[148–151] in comparison to RKI 1447 used in a single study[147]. Tumor size was measured every day during treatment, and tumor volume constantly increased in the control group

(n = 9), whereas tumor volume remained static in the Y-27632 group (n = 9) (Figure 4.6). The treatment was well tolerated with no weight loss in the mice (Supplemental Figure 4.15). The antitumor effects of Y-27632 support the concept that ROCK inhibitors can be used to selectively target *VHL*-deficient CC-RCC *in vivo*.

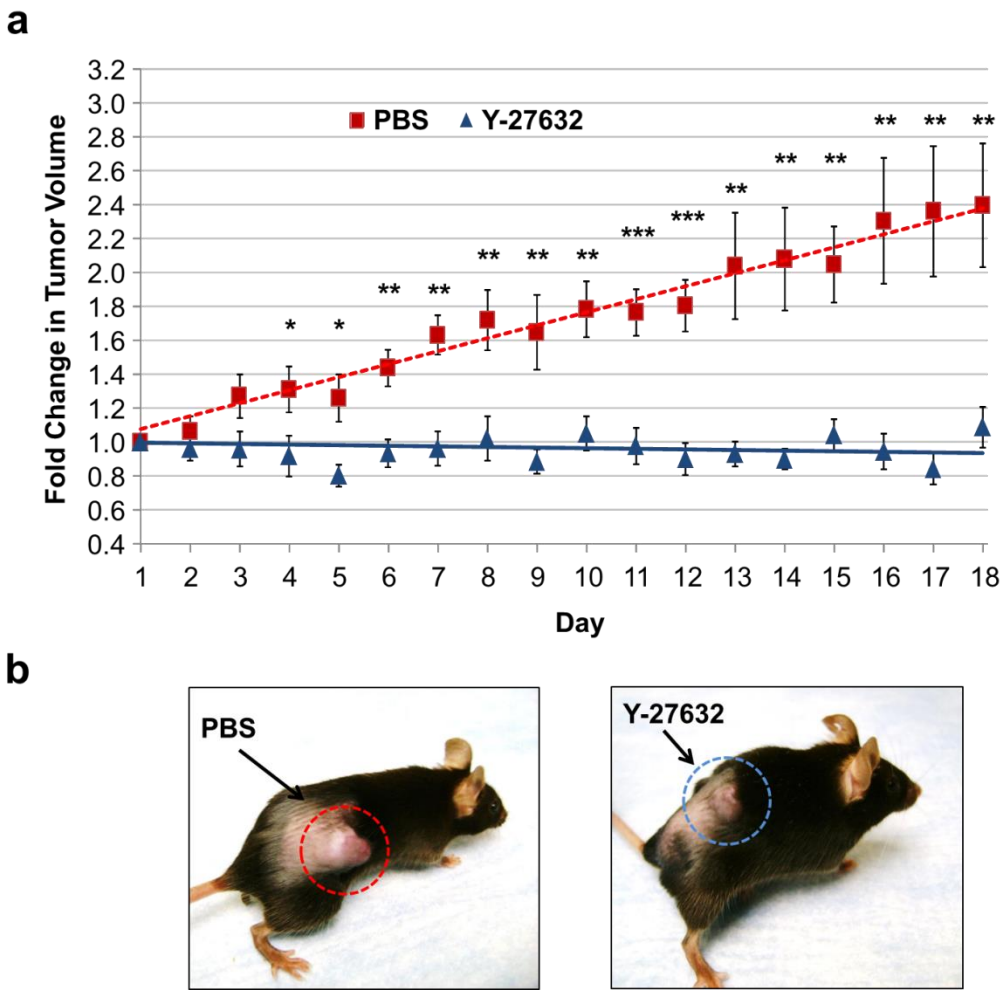

Figure 4.6. Y-27632 inhibits tumor growth *in vivo*. (**a**) 5 x 10^6 786-OT1 cells were injected into the right flank of 18 NOG mice. After one month, mice were randomized into two groups. Mice were treated daily with PBS vehicle (n = 9) or 10 mg/kg Y-27632 (n = 9) by ip injection. The fold change in tumor volume was analyzed statistically using a One-way ANOVA with treatment as the factor (*p < 0.05, **p < 0.01, ***p < 0.005), SEMs are shown. The solid line represents the linear trend fit of the data for each treatment group. (**b**) Representative images of a control mouse (top) and a Y-27632-treated mouse (bottom) on day 14 of treatment are shown.

Discussion

In this study, we identified a synthetic lethal interaction between the ROCK inhibitor, Y-27632, and the loss of VHL in CC-RCC. We have focused on validating ROCK inhibitors *(*Y-27632 and RKI 1447), which exhibited cytotoxic and cytostatic effects on VHL-deficient CC-RCC, making them candidate novel therapeutics for CC-RCC. First, the vast majority of CC-RCCs have lost *VHL* expression/function[32] making over 90% of CC-RCC potentially sensitive to ROCK inhibition. Second, we have shown that the ROCK inhibitor Y-27632 suppresses CC-RCC tumor growth *in vivo*. Third, ROCK inhibitors reduce CC-RCC cell migration, indicating that they may have the potential to inhibit CC-RCC metastasis. Finally, ROCK1 and ROCK2 knockout mice are viable, indicating that both are dispensable under physiological conditions[136], predicting no normal tissue toxicity. Since we have shown that synthetic lethality of ROCK inhibition with *VHL* deficiency occurs primarily through ROCK1, one future direction would be to acquire ROCK inhibitors specifically targeting ROCK1 and not ROCK2.

Previous synthetic lethality studies of *VHL* deficiency have identified "hits" being HIF-dependent[84,124] and HIF-independent[83,113]. Our data in Figure 4.5 indicates that the synthetic lethal interaction of ROCK inhibitors with *VHL* loss is HIF-dependent. Exposure of *VHL*-reconstituted CC-RCC to hypoxia conferred sensitivity to ROCK inhibitors, while the knockdown of *ARNT* in *VHL*-deficient CC-RCC conferred resistance to ROCK inhibitors. Re-expression of non-degradable HIFs also sensitized 786-OVHL cells to ROCK inhibition. Importantly, *VHL*-deficient CC-RCC patient's tumors differ in their repertoire of HIF subunits: 69% of patients express both HIF1α and HIF2α, while 31% express only HIF2α[44]. ROCK inhibition is synthetically lethal in both tumor types; although the cell lines RCC4 and RCC10 expressing both HIF1α and HIF2α are more sensitive to ROCK inhibition than 786-O expressing HIF2α only. In support of the role of

HIF1α in the sensitization to ROCK inhibition the same increase in sensitivity to ROCK inhibitors was observed in the cell lines expressing HIF1α (786-OVHL HIF1α and 786-OHIF1α) over those only expressing HIF2α (786-O and 786-OVHL HIF2α).

The dependence of the synthetic lethal effect of ROCK inhibition on HIF overexpression is important since ROCK inhibitors may serve as potential therapeutics for other types of solid tumors besides CC-RCC where both HIF and ROCK are overactive. In addition to CC-RCC[54], ROCK overexpression occurs commonly in multiple cancer types[152] including lung[144], breast[139,141], osteosarcoma[153], and prostate cancer[140]. On the other hand, a large fraction of solid tumors possesses hypoxic regions (where HIFs are stabilized[47]) or stabilize HIF1α and HIF2α by *VHL* independent mechanisms, including Phosphatase and TENsin homolog (*PTEN*)-loss or Harvey Rat Sarcoma Viral Oncogene Homolog (H-Ras) activation[47,48]. Thus, we predict that ROCK inhibitors will be effective against several more tumor types besides CC-RCC.

The crosstalk between HIF and ROCK has been investigated previously[154–157]. On the one hand, two studies show that RhoA and ROCK1 are HIF target genes in breast cancer[154] and trophoblast cells[155]. In addition, *Turcotte et al.* showed that RhoA expression and activity are hypoxia inducible in renal cancer, although it does not depend on HIF activity[156]. If this regulation is maintained in renal cancer, the loss of *VHL* would be predicted to induce ROCK1 upregulation. We do not see increased ROCK1 expression (Figure 4.2b-c, Supplemental Figure 4.5) and actually observe decreased phosphorylation of the ROCK substrate MYPT1 in *VHL*-deficient cells (Supplemental Figure 4.3), thus not supporting this type of regulation. On the other hand, multiple studies show that the Rho/ROCK pathway stimulates HIF activity by multiple mechanisms, which are likely to be cell type specific[156–158]. This data for CC-RCC is missing and the crosstalk needs to be investigated.

In summary, ROCK1 inhibition is synthetically lethal with *VHL* loss in CC-RCC, and ROCK inhibitors could serve as novel therapeutics for the disease. ROCK inhibitors would complement currently approved angiogenesis inhibitors since ROCK inhibitors selectively induce tumor cell death, reduce proliferation and migration, ultimately leading to inhibition of tumor growth and potentially metastasis.

Materials and Methods

Cell culture and chemical treatments.

The CMV-EYFP labeled RCC4±VHL matched cell lines were previously described[124]. Cells were grown in Dulbecco's Modified Eagle's Medium (DMEM; Caisson Labs #25-500, North Logan, UT) + 10% Fetal Bovine Serum (FBS; Omega Scientific #FB-12, Tarzana, CA) + 1% Penicillin/Streptomycin (Caisson Labs #25-512). in 5%CO_2, 21%O_2 at +37ºC. Y-27632 and GSK 429286 were obtained from Tocris (Minneapolis, MN). RKI 1447 was obtained from Selleck Chemicals (Houston, TX). All compounds were diluted in DiMethyl SulfOxide (DMSO) and serially diluted for each experiment.

Cell viability assay based on measurements of fluorescence intensity.

RCC4 EYFP and RCC4VHL EYFP were plated at 5,000 cells per well in black 96-well tissue culture plates in FBS-free DMEM media. The following day, DMSO vehicle or varying compound concentrations were prepared in 20% FBS DMEM by serial dilution and an equal volume was added to the cells. Cells were incubated for 72 hours. Wells were washed with Phosphate Buffered Saline (PBS). Then, 100μL of PBS was added to each well and fluorescence intensity was measured on a BioTek Synergy HT Microplate Reader (Winooski, VT) at 488nm. Each experiment was performed three times in quadruplicate per treatment.

Clonogenic cell survival assay.

Clonogenic assays were performed plating 300 cells/plate as previously described[145].

Long term repeat treatment experiments.

RCC4 EYFP, RCC4VHL EYFP, 786-O and 786-OVHL were plated at $5x10^4$ cells per well into a 6-well plate and treated with vehicle (DMSO) or 2μM RKI 1447 daily. Each day the media was aspirated and fresh media with DMSO vehicle or 2μM RKI 1447 was added to each well. When the vehicle control plate was at 80% confluency, the cells were passaged 1:10 into new plates. Due to different growth kinetics each cell line was passaged and counted at different time points: RCC4 on day 4, 9, and 15; RCC10 on 4, 7, 9, 11; and 786-O on 4, 11, 15, and 18.

Gene knockdowns by siRNAs.

RCC4±VHL were plated at 200,000 cells per well of a 6-well plate in FBS-free DMEM. The following day the cells were transfected with 6 μL DharmaFECT1 (Dharmacon, Lafayette, CO) and up to 2 nM siRNA accordingly to manufacturer's protocol. The siRNAs for ROCK1 (#1: SASI_Hs01_00065573 and #2: SASI_Hs01_00065570), ROCK2 (#1: SASI_Hs01_00204253 and #2: SASI_Hs01_00204251), and MISSION(R) Universal Negative Control #1 siRNA were obtained from Sigma (St. Louis, MO). The following day, transfected cells were plated for the clonogenic cell survival assay. Replicate plates were lysed after 72 hours and ROCK1 and ROCK2 expression analyzed by Western blot.

Western blot analysis.

After treatments, cells were lysed and Western blot was conducted as previously described[125]. Proteins were visualized using primary antibodies recognizing HIF1α (BD Biosciences, #610959, San Jose, CA), HIF2α (Novus Biological, #NB100-122, Littleton, CO), α-tubulin (Fitzgerald, #10R-842, North Acton, MA), MYPT1-P Thr696 (EMD Millipore, #ABS45,

Temecula, CA), MYPT1, (Abcam, #ab32393, Cambridge, MA), Cleaved Caspase 3, VHL (Cell Signaling, #9661, #2738, Danvers, MA), ROCK1, ROCK2 (Thermo Scientific, #PA5-22262, #PA5-21131, Grand Island, NY); and Horseradish peroxidase conjugated Goat anti-Rabbit IgG and Goat anti-Mouse IgG secondary antibodies (Thermo Scientific, #31460, #31430). Blots were imaged using a Bio Rad ChemiDoc XRS$^+$ (BioRad, Hercules, CA).

PI-immunofluorescence staining.

RCC4±VHL cells were cultured in the presence of DMSO, 20μM Y-27632, or 1μM Doxorubicin. After 24 hours, 1 μg/ml PI was added to each well and the cells were imaged on a Nikon TI-E at 4x and the PI-positive cells were counted per field. For the siRNA experiments, siRNAs were transfected at 5 nM following Dharmafect's protocol and imaged at 10x after 48 hours. Each transfection was conducted in triplicate.

Transwell migration assay.

8.0μm Polyethylene terephthalate Transwells (Corning, Corning, NY) were coated with Fibronectin as previously described[125]. 70,000 RCC10 or 35,000 786-O cells were used per transwell.

Cell cycle analysis.

10^5 cells were seeded per well of a 6-well plate and treated the following day with vehicle (DMSO) or Y-27632 for 72 hours. BrdU analysis was performed using the FITC BrdU Flow Kit (BD Biosciences, Catalog #559619) following the manufacturer's protocol.

shRNA expression constructs, lentivirus packaging, and infection of target cells.

HEK 293T cells were transfected with lentiviral plasmids (pLKO.1shARNT: 5'AAATAAACCATCTGACTTCTC3' (OpenBiosystems, Huntsville, AL)) or

pLKO.1shScrambled (Addgene, Cambidge, MA, #1864) along with packaging plasmids, pVSVG and ΔR8.2, as previously described[159].

Tumor growth analysis.

Briefly, 18 RAG1 (B6.129S7-Rag1^{tm1Mom}/J, Jackson Labs) mice (11–20 weeks old) were injected sc into the right flank with 5x10^6 786-OT1 cells. Before each injection, cells were resuspended in 50 μl PBS/matrigel (BD Bioscience # 354248) mixture at 50/50 ratio. One-month post-injections, when the tumors had reached the size of ~500mm^3, littermates were randomized into two groups. 10 mg/kg Y-27632 or PBS diluent was administered ip daily for 18 days. Tumor size was measured daily with a digital caliper. On day 18 the mice were sacrificed. Tumor volume was calculated using the formula: V=(a)(b^2/2), where "a" is the shorter measurement of length/width. Every measurement for each mouse was normalized to the day 1 measurement to show the fold change over time. Statistical analysis was performed using a one-way ANOVA between the two groups per day.

Growth curves and statistical analysis.

Dose response and cell growth curves were generated using GraphPad Prism. IC_{50} values were calculated by transforming the X axis using X=Log(X), normalizing the transformed data to the vehicle control with 0 as 0%, and then fitting the normalized transformed data with a nonlinear trend line either using a normalized response ("log(inhibitor) vs. normalized response") or a variable slope ("log(inhibitor) vs. normalized response – Variable slope"). The correct nonlinear trendline was selected using GraphPad's comparison of fits, which directly compares both fit lines statistically using an extra sum-of-squares F test. The fit line is not shown in the figures. The IC_{50} values for each experiment were then calculated from the Best-fit values. Statistical analysis was

conducted in Minitab 16 using a paired t-test or ANOVA between cell lines with a p-value of less than 0.05 considered statistically significant. All error bars represent the SEMs.

Supplemental Figures

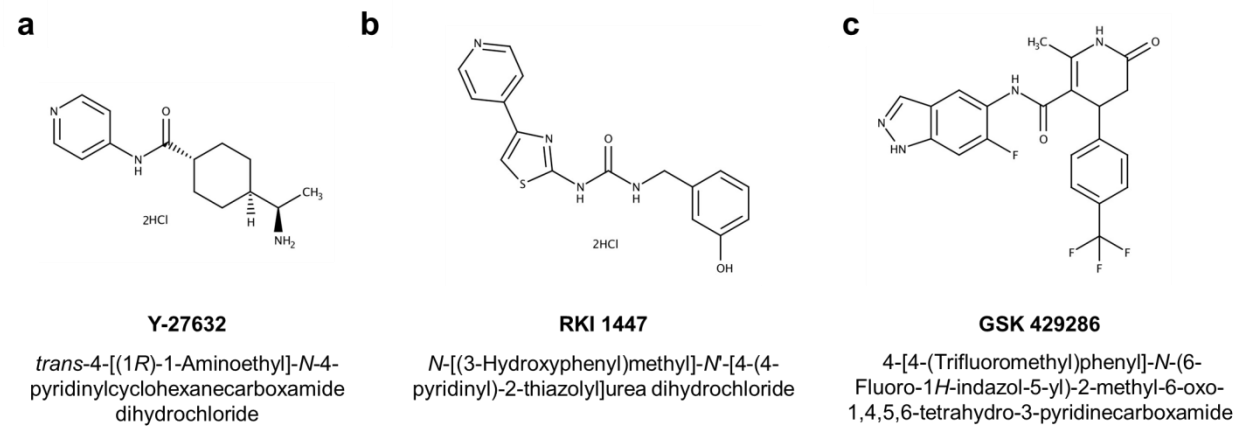

Supplemental Figure 4.1. The chemical structures and chemical names for Y-27632 (a), RKI 1447 (b), and GSK 429286 (c) ROCK inhibitors used in this study.

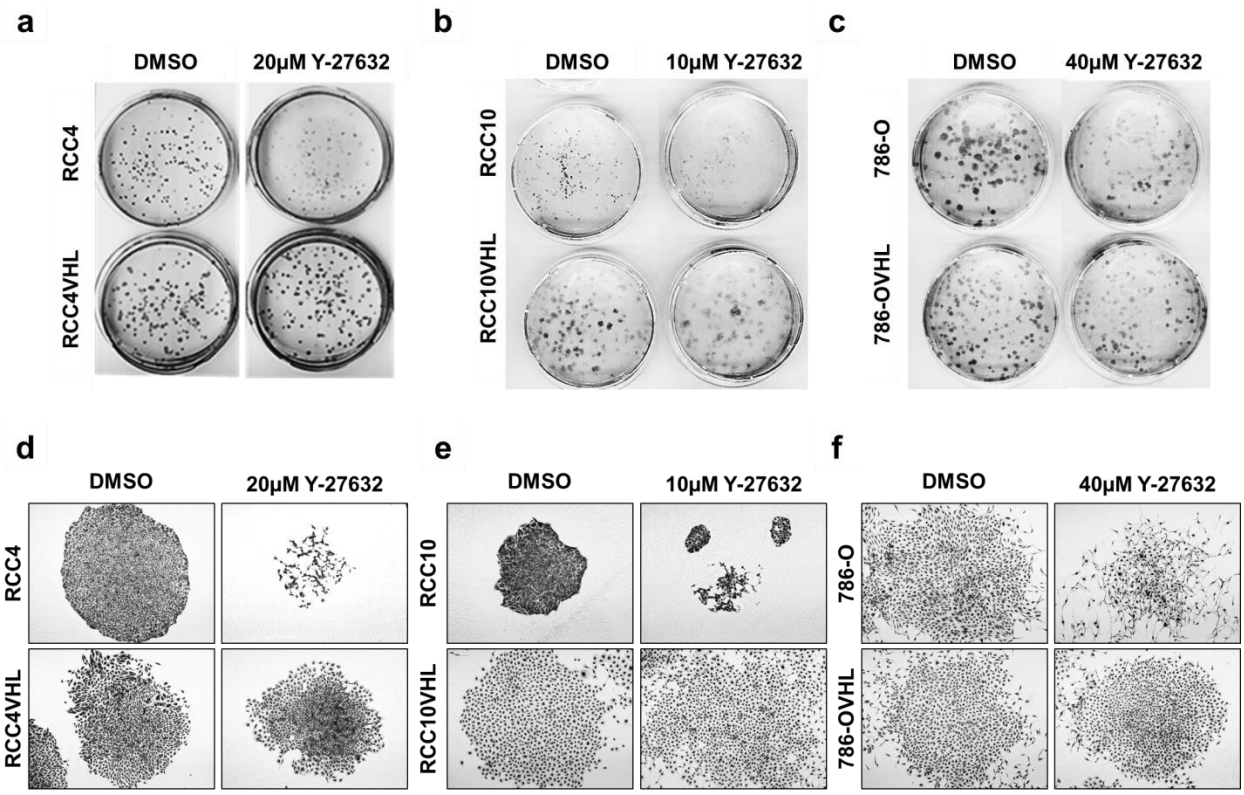

Supplemental Figure 4.2. The ROCK inhibitor Y-27632 causes synthetic lethality with *VHL* loss in multiple CC-RCC cell lines. (**a**-**c**) Treatment with Y-27632 reduces the colony forming ability of *VHL*-deficient RCC4, RCC10, and 786-O. Representative plates from the clonogenic assays quantified in Figure 1b-d are shown for the indicated Y-27632 concentrations for RCC4±VHL (**a**), RCC10±VHL (**b**), and 786-O±VHL (**c**) matched cell lines. (**d**-**f**) Treatment with Y-27632 reduces *VHL*-deficient CC-RCC's proliferation as shown by the decrease in cell number making up each colony. Representative colonies from the clonogenic assays quantified in Figure 1b-d are shown for the indicated Y-27632 concentrations for RCC4±VHL (**d**), RCC10±VHL (**e**), and 786-O±VHL (**f**) matched cell lines.

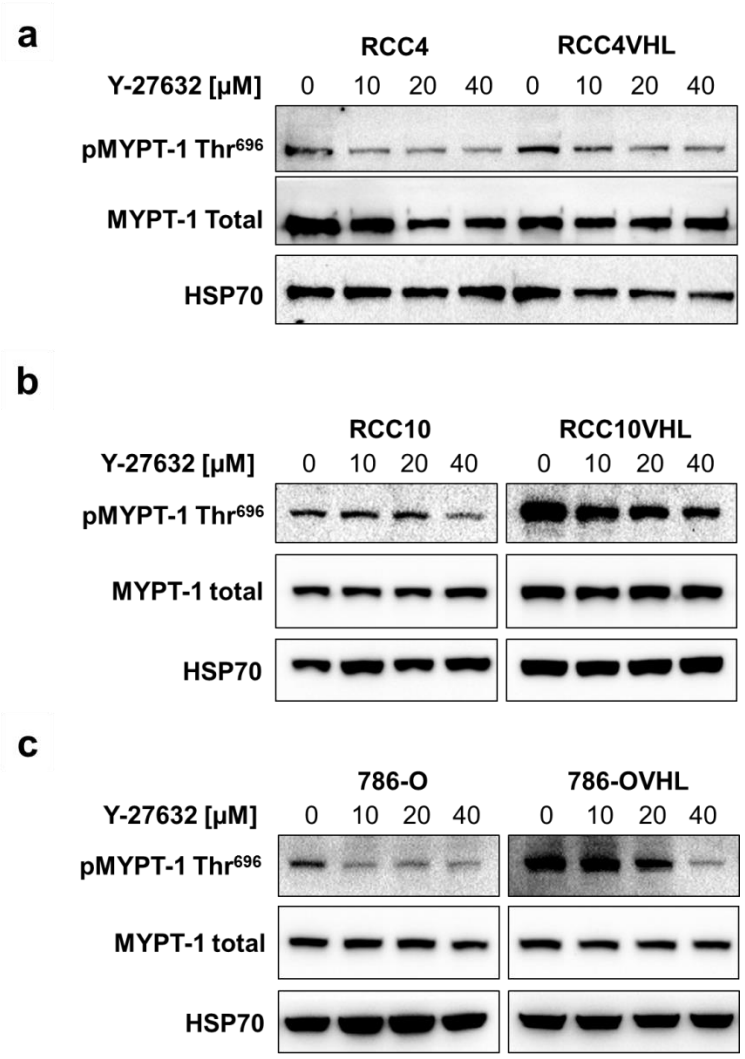

Supplemental Figure 4.3. Y-27632 treatment inhibits ROCK activity. Western blot shows the decrease in phosphorylation of ROCK target MYPT1 at Thr^{696} upon treatment with 20μM Y-27632 for 2 hours for RCC4±VHL (**a**), RCC10±VHL (**b**), and 786-O±VHL (**c**). RCC10±VHL and 786-O±VHL lysates were run on the same gel and processed as part of the same Western blot. α-Tubulin and HSP70 served as a loading control.

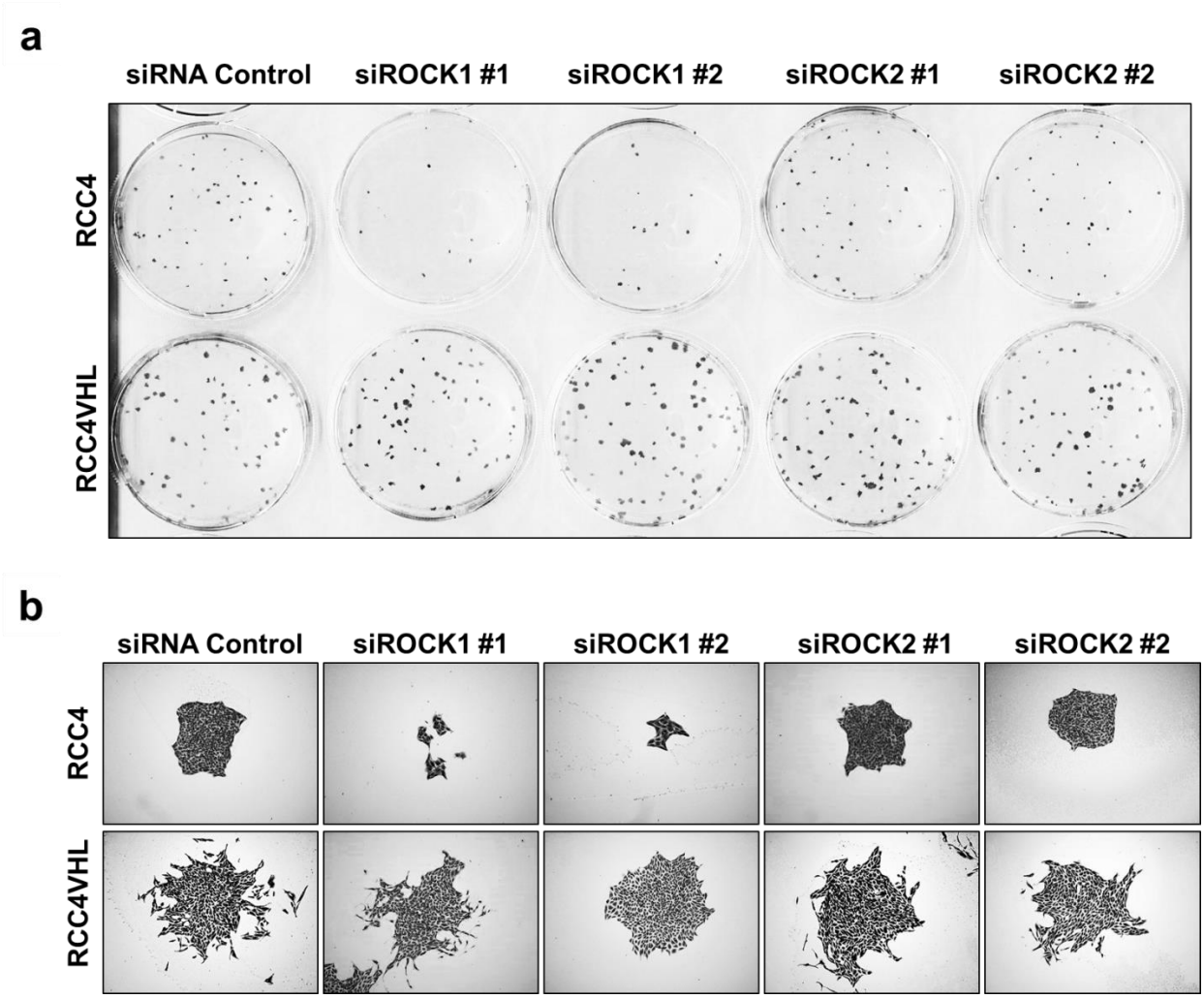

Supplemental Figure 4.4. Synthetic lethality of Y-27632 with *VHL* loss is mimicked by siRNA downregulation of ROCK1, not ROCK2. Representative plates (**a**) and colonies (**b**) from the RCC4 and RCC4VHL clonogenic assays are shown for each transfection as indicated.

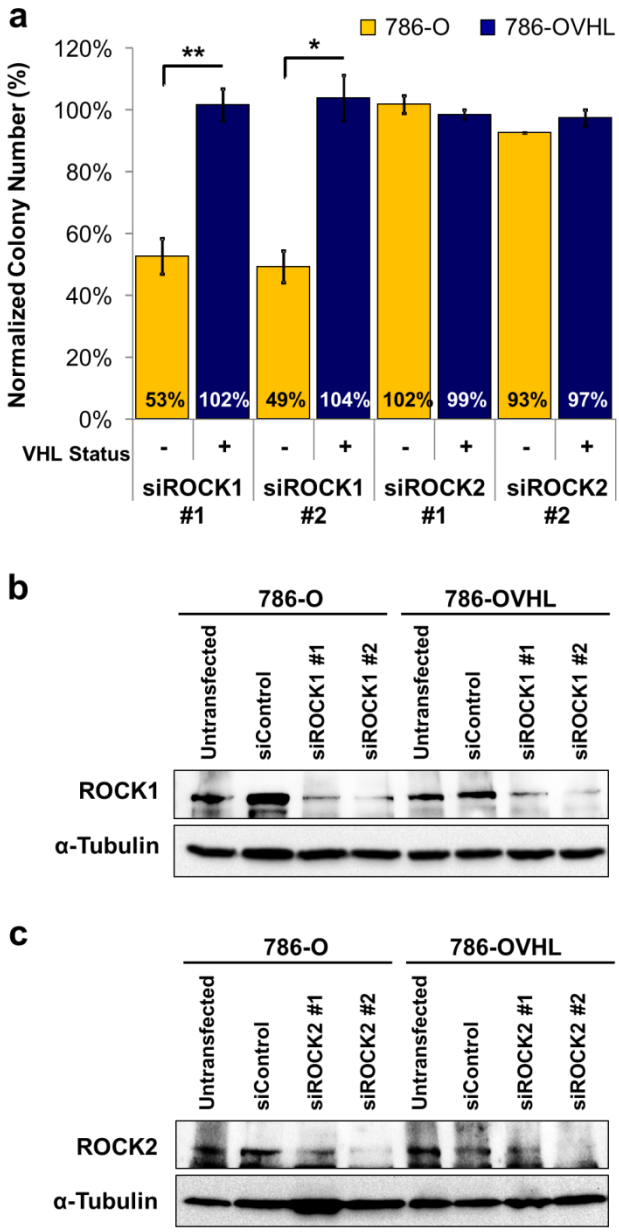

Supplemental Figure 4.5. Synthetic lethality of Y-27632 with *VHL* loss is mimicked by siRNA downregulation of ROCK1, but not ROCK2 in the 786-O matched cell line. 786-O±VHL matched cell lines were transfected with siRNAs targeting ROCK1, ROCK2, or non-targeting siRNA control (siControl). Two different siRNAs per target were used. Twenty-four hours after transfection cells were plated for a clonogenic assay. Each transfection was done in triplicate, followed by clonogenic assays conducted in triplicate, and the experiments were repeated two times. (**a**) Transfection with siROCK1, but not siROCK2, resulted in significant reduction in 786-O colony numbers in comparison to 786-OVHL. Statistical analysis was performed using a paired t-test between the matched cell lines for each siRNA (* $p < 0.05$, ** $p < 0.01$), SEMs are shown. (**b**-**c**) The degree of each target knockdown by its specific siRNA (as indicated) was assessed by Western blot.

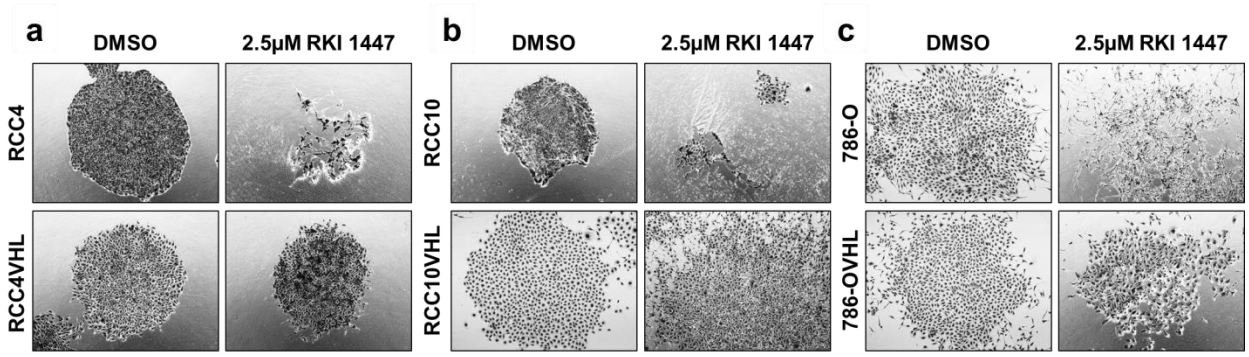

Supplemental Figure 4.6. Treatment with 2.5μM RKI 1447 reduces *VHL*-deficient CC-RCC's proliferation as shown by the decrease in cell number making up each colony for RCC4±VHL (**a**), RCC10±VHL (**b**), and 786-O±VHL (**c**) matched cell lines. Representative colonies from the clonogenic assays quantified in Figure 4a-c are shown as indicated.

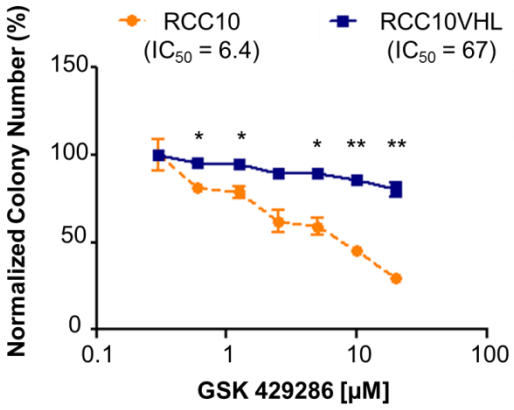

Supplemental Figure 4.7. ROCK inhibitor GSK 429286 causes synthetic lethality with *VHL* deficiency similar to Y-27632 and RKI 1447 in RCC10±VHL matched cell lines. Each dose of GSK 429286 within each experiment was tested in duplicate, and the experiment was repeated two times. Statistical analysis was performed using a paired t-test between the matched cell lines at each dose (* $p < 0.05$, ** $p < 0.01$), SEMs are shown.

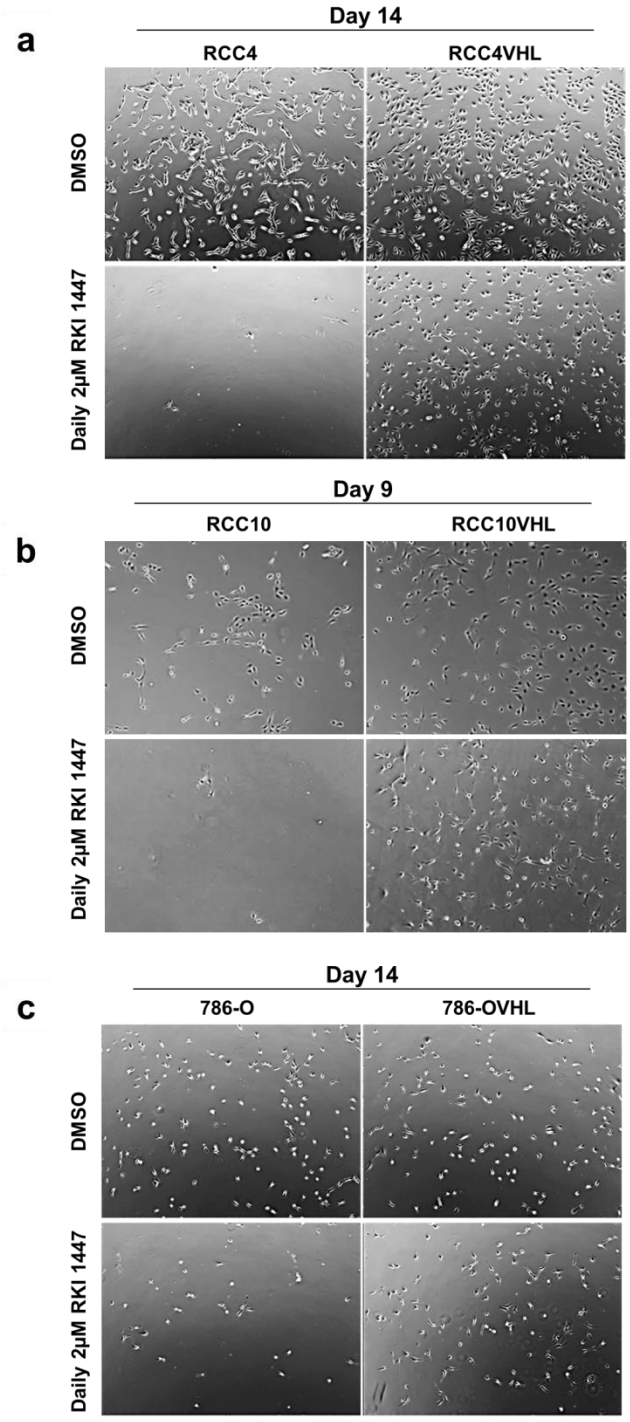

Supplemental Figure 4.8. Long term repeat administration of RKI 1447 enhances the synthetic lethality effect. Representative images of RCC4±VHL (**a**), RCC10±VHL (**b**) and 786-O±VHL (**c**) cells showing the decline in CC-RCC cell numbers while CC-RCCVHL cells continued to proliferate. The day the images were taken is indicated for each cell line.

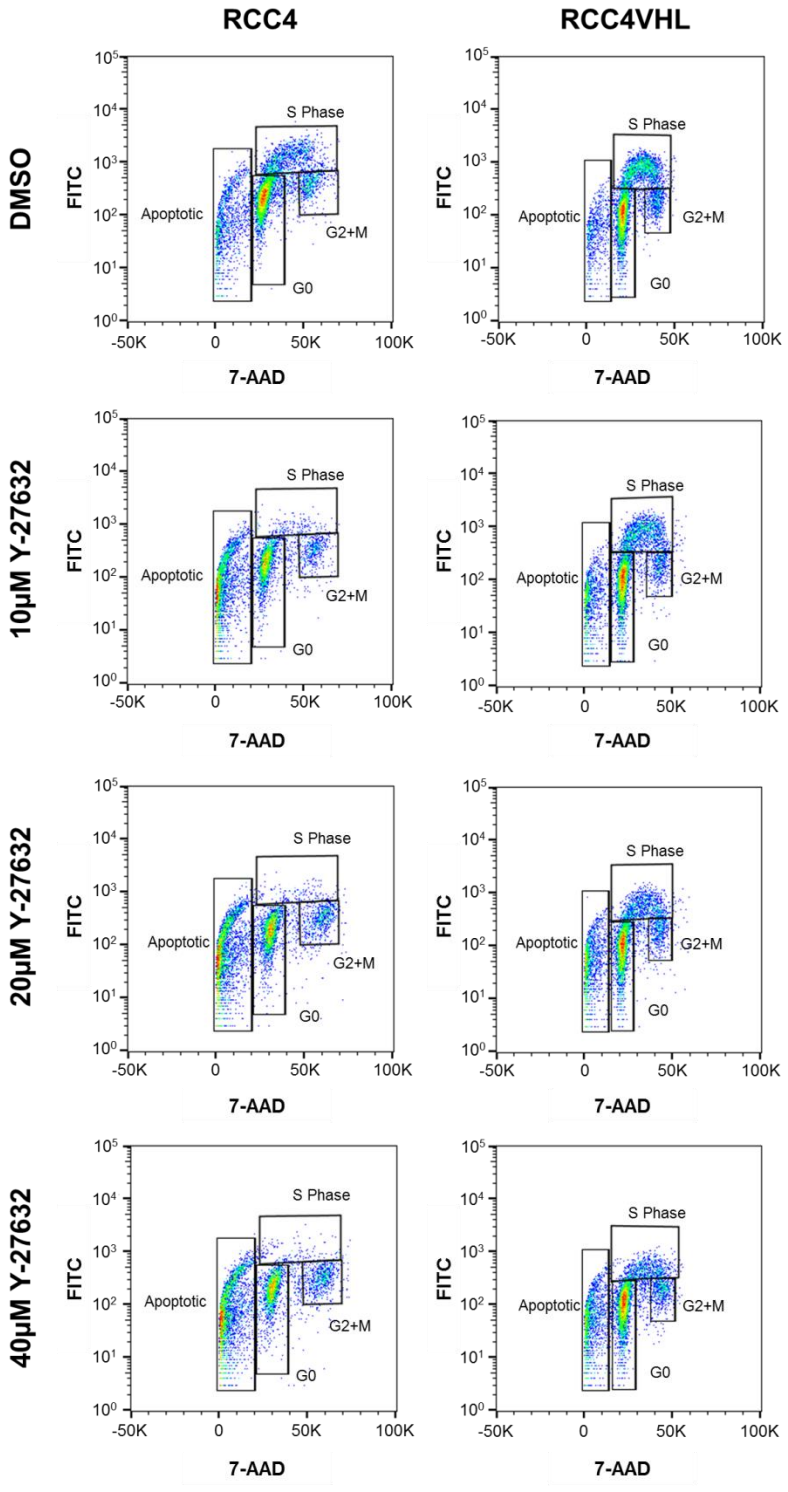

Supplemental Figure 4.9. ROCK inhibition in *VHL*-deficient CC-RCC cells inhibits proliferation and induces cell death. Representative FACS plots from the FITC BrdU assay done on RCC4 and RCC4VHL cells at several Y-27632 concentrations (as indicated) and quantified in Figure 4a. Voltages and gates were set based on the DMSO vehicle control for each cell line.

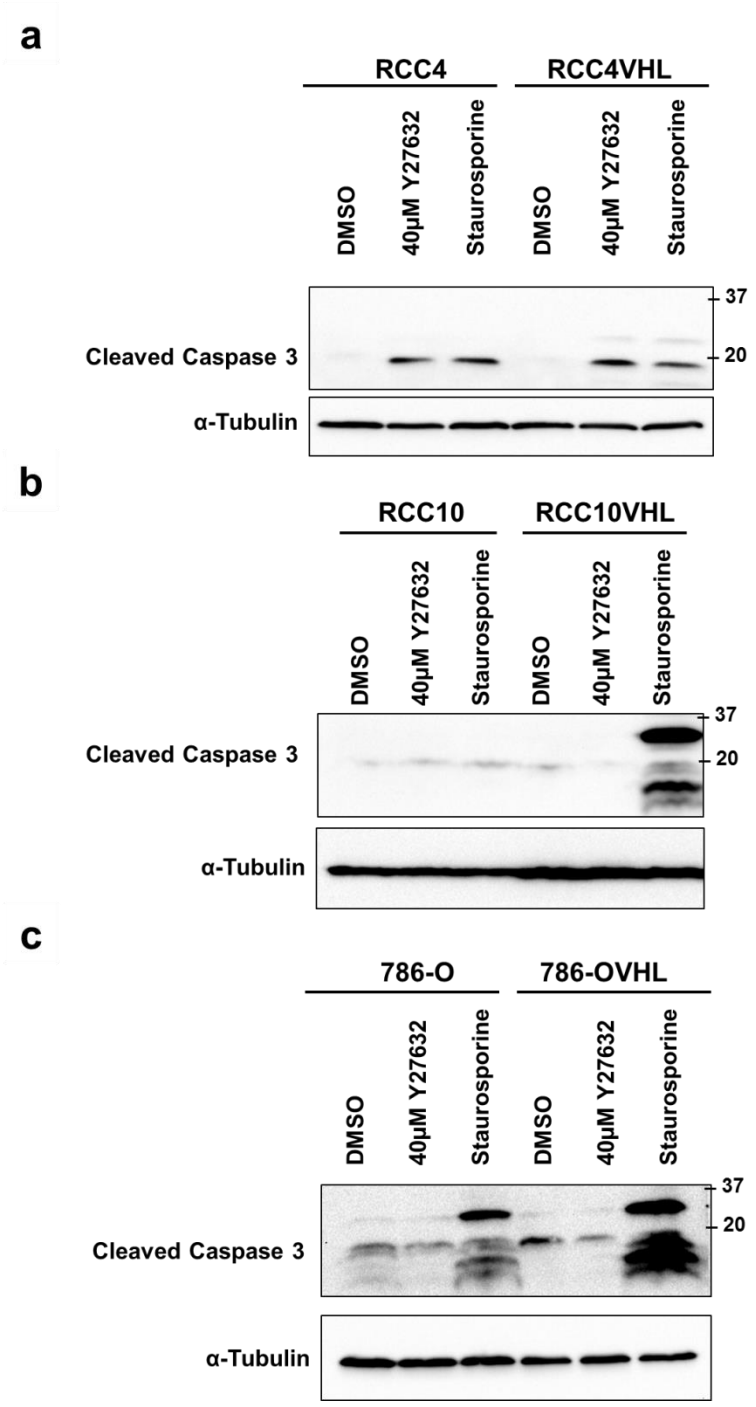

Supplemental Figure 4.10. ROCK inhibition induces caspase 3 cleavage in RCC4, RCC4VHL, and RCC10 cells. Cells were treated with 40μM Y-27632 or DMSO vehicle for 48 hours, lysed, and caspase 3 cleavage (19kDa) was assessed by Western blot. Treatment with 2μM Staurosporine for 4 hours was used as a positive control for Caspase 3 cleavage. α-Tubulin was used as a loading control.

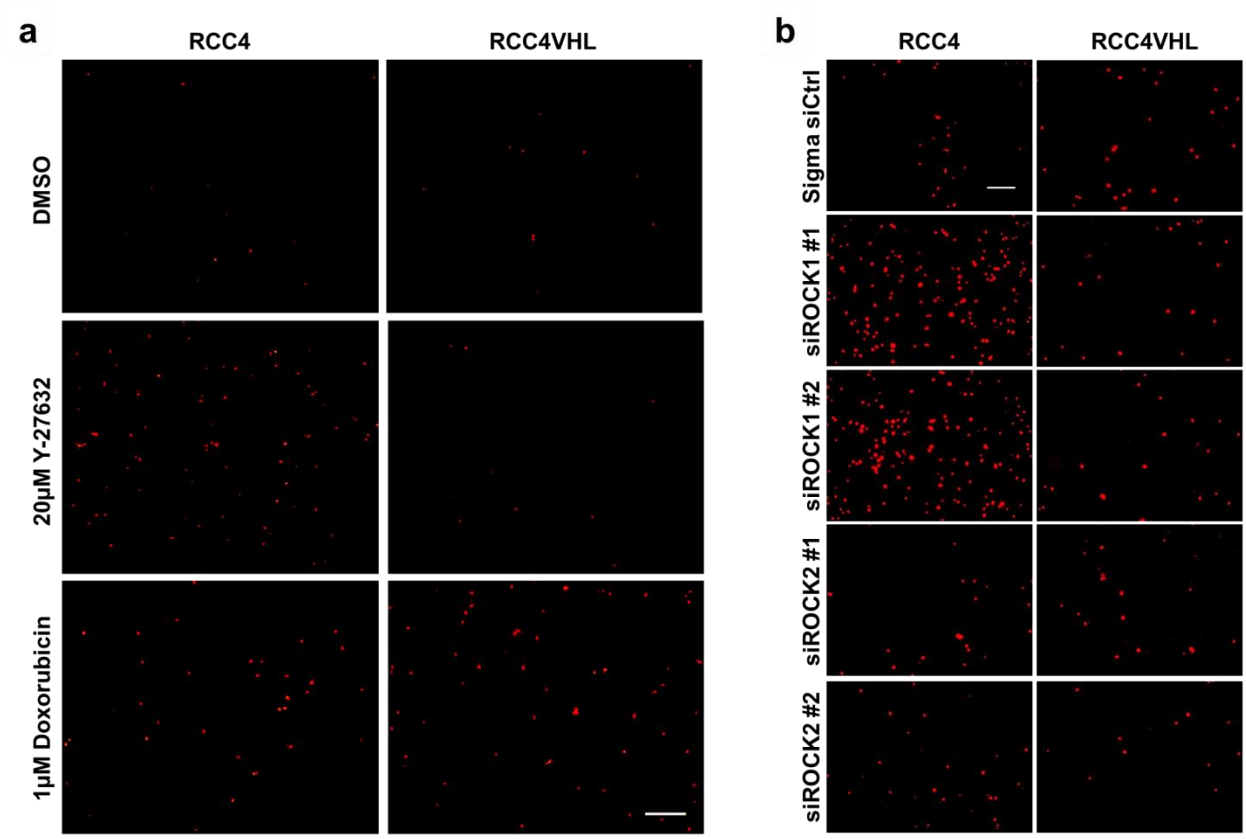

Supplemental Figure 4.11. ROCK inhibition by Y-27632 or siRNA in *VHL*-deficient CC-RCC cells induces cell death. (**a**) Representative images of PI-positive RCC4 and RCC4VHL cells treated with 20μM Y-27632 for 24 hours. Doxorubicin was used as a control inducing cell death in a non-VHL-specific manner. Images were taken at 4x magnification. Scale bar, 100μm. (**b**) Representative images of PI-positive RCC4 and RCC4VHL cells at 48 hours after control non-targeting siRNA transfection or siRNA targeting ROCK1 or ROCK2 transfection as indicated (two siRNAs per each target). Images were taken at 10x magnification. Scale bar, 200μm. Each experiment in (**a**-**b**) was repeated 3-4 times.

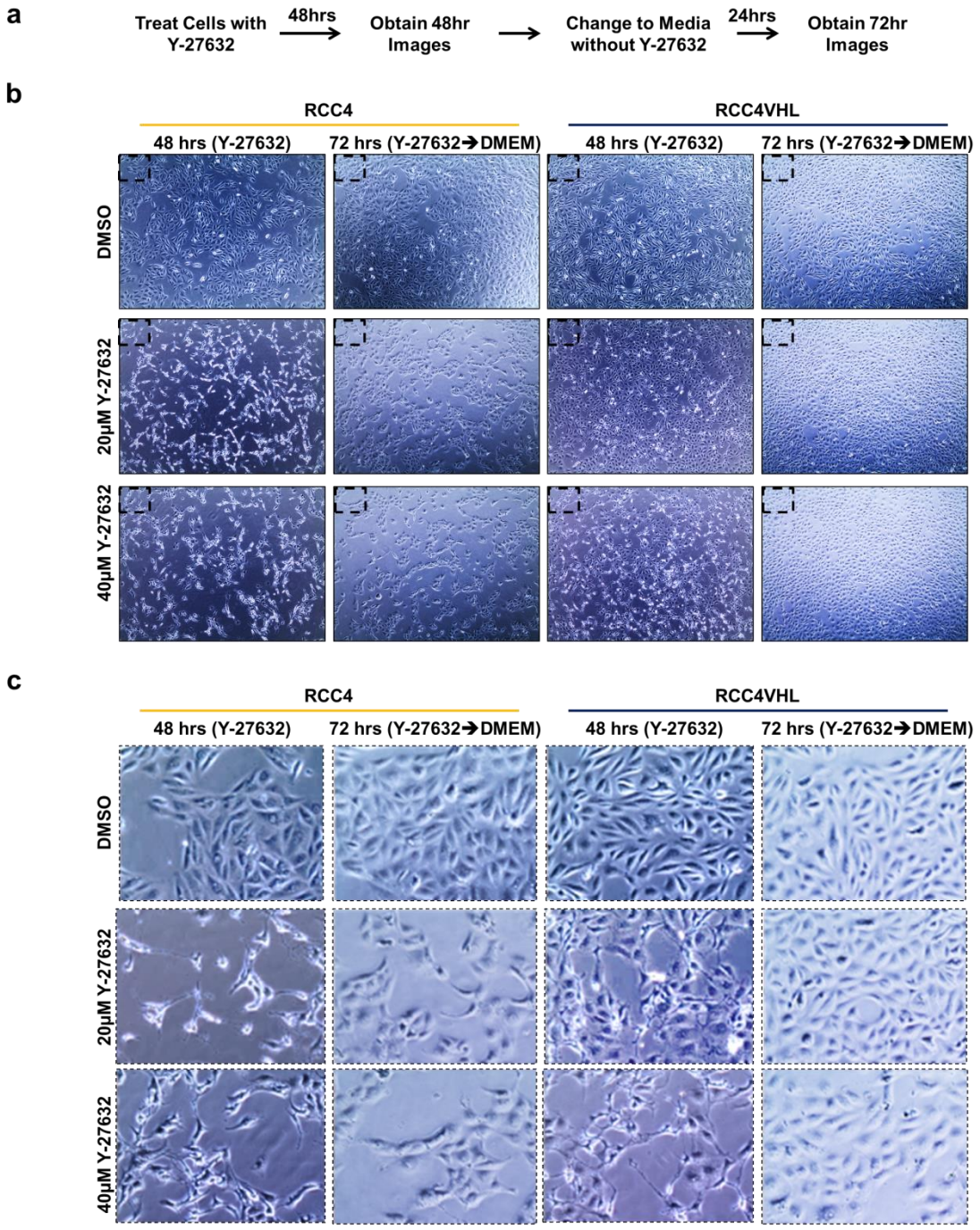

Supplemental Figure 4.12. The morphological changes induced by Y-27632 treatment are reversible when compound treatment is stopped. (**a**) The timeline of Y-27632 treatment for examining the change in morphology. The cells were plated and allowed to attach overnight. The cells were then treated with 20μM or 40μM Y-27632. Representative images of the cells were obtained after 48 hours of Y-27632 treatment and then a media change was performed. After 24 hours images were taken again for morphological comparison. (**b**) Representative images of cells at the indicated time points. (**c**) Close ups of top left areas in the dotted boxes shown in (**b**).

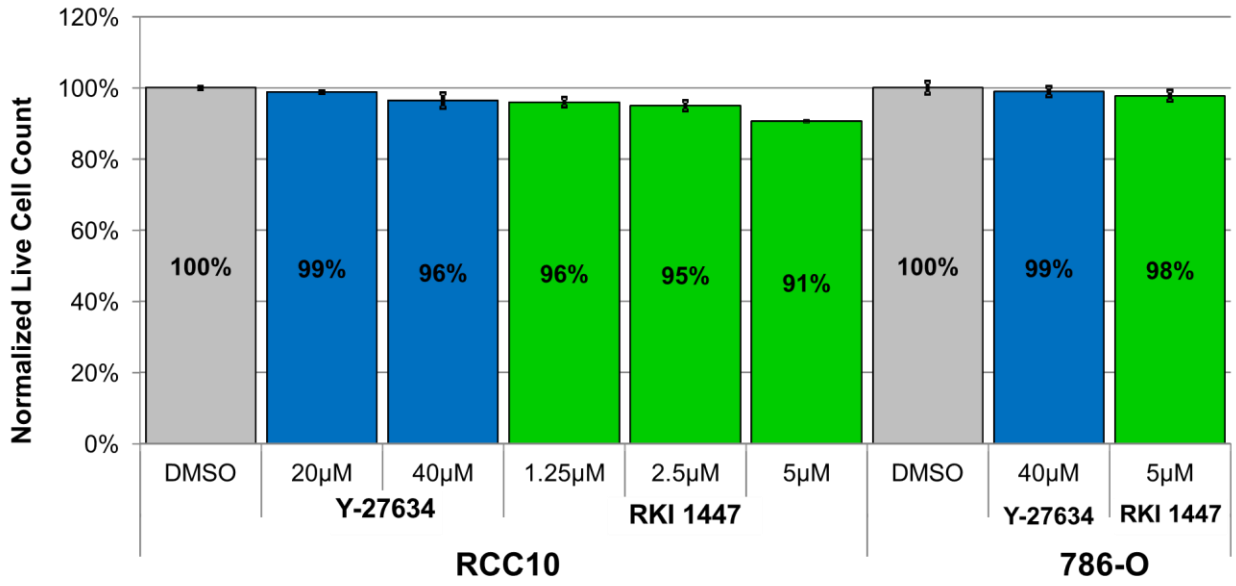

Supplemental Figure 4.13. Treatment with ROCK inhibitors at the concentrations used in the migration assays in Figure 4d for 6 hours does not affect RCC10 and 786-O cell survival or proliferation. PI vital dye exclusion was assessed via flow cytometry and used to measure the number of viable cells. Samples were collected for 60 seconds in order to obtain cell counts and then gated for PI-negative live cells. Each treatment was normalized to the DMSO vehicle control. Each treatment was conducted in duplicate and the experiment was repeated two times.

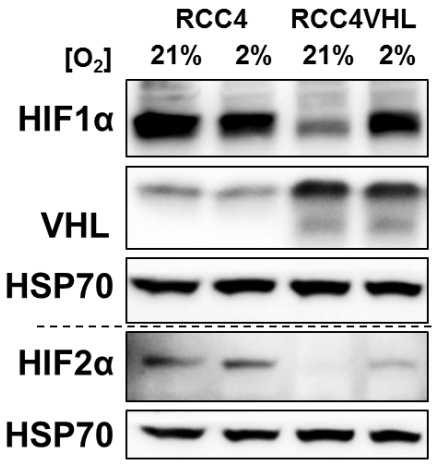

Supplemental Figure 4.14. Western blot showing that RCC4VHL stabilize both HIF1α and HIF2α under hypoxia (2% O_2 for 16 hours). The dotted line indicates a separate Western blot conducted using the same protein lysates. HSP70 was used as a loading control.

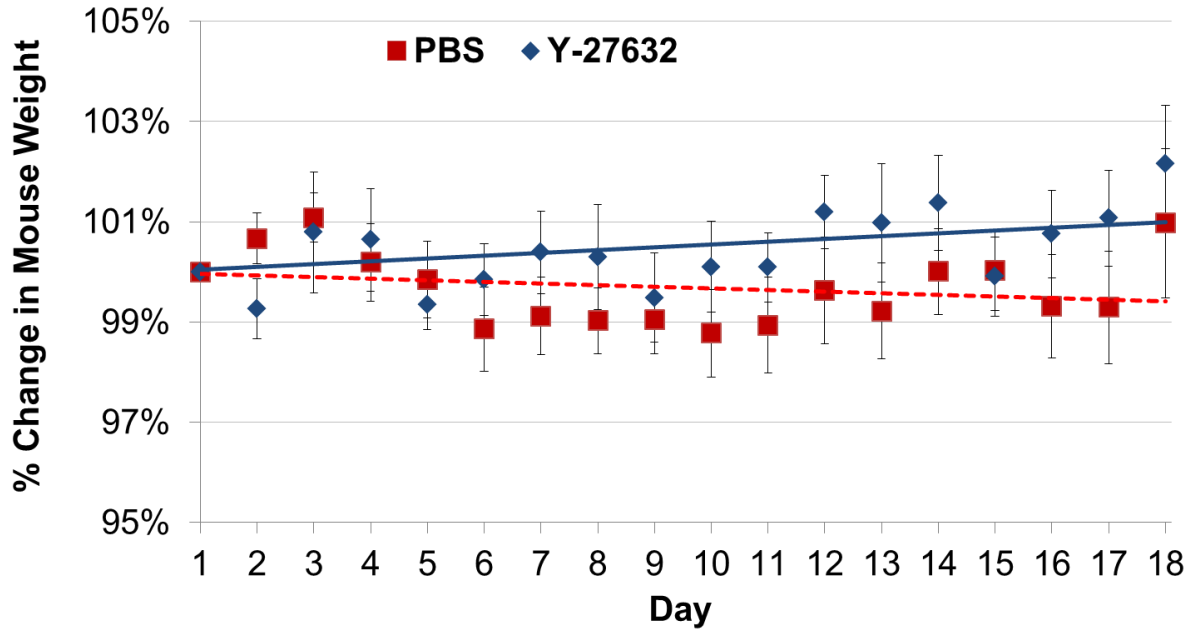

Supplemental Figure 4.15. Y-27632 treatment does not reduce mouse weight over the course of treatment. Mice were treated daily with PBS vehicle (n = 9) or 10 mg/kg Y-27632 (n = 9) by ip injection for 18 days. Mouse weight was monitored daily.

CHAPTER FIVE: TARGETING THE MEVALONATE PATHWAY SUPPRESSES VHL-DEFICIENT CC-RCC THROUGH A HIF-DEPENDENT MECHANISM

Introduction

CC-RCC is a life-threatening condition, especially in its metastatic manifestation. It is resistant to both radiation and chemotherapy[160], and although a recently introduced programmed death-1 inhibitor based immunotherapy shows promise with 25% of metastatic CC-RCC patients responding, the median overall survival remains at 2 years[5]. In addition, toxicity to normal tissues is a limiting factor for current treatments. Thus, it is of primary importance to identify new therapeutics and their target pathways to successfully treat CC-RCC. Identified in 1993 as the tumor-suppressor gene affected in von Hippel-Lindau disease[161], the *VHL* gene is lost in 80-90% of CC-RCC[39]. The goal of this study is to therapeutically target this large group of *VHL*-deficient CC-RCCs using a synthetic lethality approach.

A large body of evidence supports the use of synthetic lethality screens for identifying specific compounds or small interfering RNAs (siRNAs) that cause cell death in combination with a particular cancer mutation[31,49]. Several synthetic lethality screens have been conducted in *VHL*-deficient CC-RCC to date[52,83,84,113–115,124]. Previously we conducted a chemical library screen and

identified Y-27632 as a top hit; we also found that inhibition of Y-27632's target ROCK1 is synthetically lethal with *VHL* loss[52]. VHL is a part of the E3 ubiquitin ligase complex that targets the α subunits of Hypoxia Inducible Factors 1 and 2 (HIF1 and HIF2) transcription factor for degradation in the presence of oxygen (in normoxia)[33]. The loss of *VHL* in CC-RCC results in the overactivation of HIFs and overexpression of their downstream targets. Accordingly, our data also indicate that Y-27632 treatment is synthetically lethal to HIF pathway overactivation.

While multiple ROCK inhibitors have shown success in topical treatments for glaucoma[162], systemic treatments were conducted only with two ROCK inhibitors - Fasudil[163] and AT13148[164]. Fasudil was approved in Japan for treatment of cerebral vasospasm complicating intracranial hemorrhage[163]; and AT13148 is currently in a phase I clinical trial (NCT01585701) for solid tumors other than CC-RCC. Thus, systemic use of ROCK inhibitors has been limited in patients and requires further investigation to determine a therapeutic window for cancer patients. On the other hand, HMG-CoA Reductase inhibitors, also known as statins, can inhibit Rho/ROCK signaling in human patients[165], and their pharmacokinetics and doses are well established, including maximum tolerated doses[166].

Rho GTPases are upstream activators of ROCK[142]. Rho/ROCK inhibition by statins occurs due to reduced synthesis of mevalonate and geranylgeranyl pyrophosphate (GGPP), in turn leading to inhibition of protein isoprenylation[57,165]. This disrupts the intracellular trafficking of small GTPases like Rho, Ras, Rap1a and Rac and their recruitment to the cell membrane required for their activity[56]. Although statins are not specific toward Rho, they are safe and taken by a considerable part of the human population at up to 1mpk [80 mg daily][167]. In addition, Lovastatin was evaluated as an anti-cancer agent for gastric carcinoma[168], anaplastic astrocytoma[169], and glioblastoma multiforme[169] in phase I and II clinical trials, and the maximum tolerated doses were

established as high as 20-35mpk daily for 7 days, with monthly repeats, resulting in responses in 3 out of 18 patients[169]. Similarly, in a phase I study, patients with recurrent or metastatic squamous cell carcinoma of the head and neck or of the cervix, 5-10mpk Lovastatin taken daily resulted in responses in 6 out of 26 patients. Based on the above trials, it has become clear that biomarkers are needed to stratify the patients into responders and non-responders. In addition, studies addressing the mechanism of statins' anti-cancer action are largely absent. Since our studies show that statins trigger synthetic lethality with *VHL* deficiency, *VHL* can be used as a biomarker for tumor sensitivity to statins. Furthermore, the effect is dependent on the overactivation of HIFs upon *VHL* loss, making HIF expression a second potential biomarker. Statin treatment selectively inhibits cell proliferation and induces cell death. Our studies also reveal that this effect occurs due to the disruption of GTPase isoprenylation and partially through the inhibition of Rho/ROCK1 signaling. Statin treatment is effective at inhibiting tumor initiation and tumor growth of established tumors *in vivo*, confirming their potential as therapeutics for treating *VHL*-deficient CC-RCC.

Results

Treatment with statins selectively targets *VHL*-deficient CC-RCCs of multiple genetic backgrounds

Since statins inhibit Rho/ROCK signaling[57,165,170] and we recently showed that ROCK1 inhibition is synthetically lethal with *VHL*-loss in CC-RCC[52] we decided to test if statin treatment would be synthetically lethal with *VHL*-loss. Isogenic cell line pairs were generated from the parental *VHL*-deficient CC-RCC cell lines by re-expressing the full-length wild-type *VHL* cDNA[124]. *VHL* loss causes overexpression of HIF1α and HIF2α in RCC4 and RCC10 cells and HIF2α in 786-O cells, and *VHL* reintroduction causes a decrease in HIF expression (Supplemental

Figure 5.1). We conducted clonogenic assays and showed that both Simvastatin (Figure 5.1a-c, Supplemental Figure 5.2a-c) and Fluvastatin (Figure 5.1d-f, Supplemental Figure 5.2d-i) treatment is synthetically lethal with *VHL* loss. Both RCC4 (Figure 5.1a, d) and RCC10 (Figure 5.1b, e) showed sensitivity to statin treatment and a nearly 15-fold difference in IC_{50} values over respective RCC-VHL cell lines. 786-O (Figure 5.1c, f) showed a 5-fold difference in IC_{50} values over 786-OVHL.

We also tested the effect of two more statins, Lovastatin and Pravastatin, on the colony forming ability of the RCC4±VHL matched cell lines. RCC4 (Supplemental Figure 5.3a) showed sensitivity to Lovastatin treatment and a 9-fold difference in IC_{50} values over RCC4VHL. Since treatment with Pravastatin up to 80μM did not reduce the colony forming ability of both RCC4 and RCC4VHL (Supplemental Figure 5.3b), we assessed the inhibitory effect of each statin on isoprenylation of Rap1a, which depends on the mevalonate pathway. Unprenylated Rap1a was detected by western blot with an antibody specific for unprenylated Rap1a[171] after treatment with all statins but Pravastatin (Supplemental Figure 5.3c), which is consistent with the lack of the effect of Pravastatin on colony forming ability of RCC4 cells. Unlike lipophilic statins Simvastatin, Fluvastatin, and Lovastatin, Pravastatin is hydrophilic and requires a liver-specific transporter OATP1B1[172] to be delivered inside the cells; thus it is likely not delivered to CC-RCC cells. Together, these data indicate that treatment with multiple lipophilic statins is synthetically lethal with *VHL*-loss in several CC-RCC genetic backgrounds.

Treatment with statins is cytostatic and cytotoxic in *VHL*-deficient CC-RCC.

We next sought to determine if the effect of statins on colony forming ability of *VHL*-deficient CC-RCC was caused by cell death, inhibition of proliferation, or both. We treated RCC4±VHL cells with activated Simvastatin at doses ranging from ~600nM to 10μM in a Calcein-

based Live/Dead assay. We found that Simvastatin decreases RCC4 cell proliferation starting at nanomolar doses and increases RCC4 cell death starting at low micromolar doses (Figure 5.2a-c). These results indicate that the effect of Simvastatin on CC-RCC colony forming ability in Figure 5.1a is mostly due to inhibition of cell proliferation and is cytostatic. We confirmed these effects in the 786-O±VHL cells (Supplemental Figure 5.4). Thus, statin treatment is predominantly cytostatic in *VHL*-deficient CC-RCC, but becomes cytotoxic as the concentration increases.

Since each of the RCCVHL cell lines used above was genetically modified to overexpress *VHL*, we then asked if endogenous *VHL* expression could protect against the cytostatic effects of Simvastatin treatment. We compared the sensitivity of four *VHL*-deficient and four *VHL*-expressing kidney cancer cell lines to 5μM Simvastatin by Calcein-based assay. As expected, statistical analysis divided the cell lines into two groups based on *VHL* expression (Figure 5.2d). The *VHL*-deficient RCC4, RCC10, 786-O, and A498 were all more sensitive to Simvastatin treatment in comparison to the *VHL*-expressing ACHN, SN12C, SN12L1, and TK10. VHL expression and HIF expression in these cell lines was confirmed by western blot (Figure 5.2e). Thus, endogenous *VHL* expression is sufficient to protect cells against Simvastatin treatment.

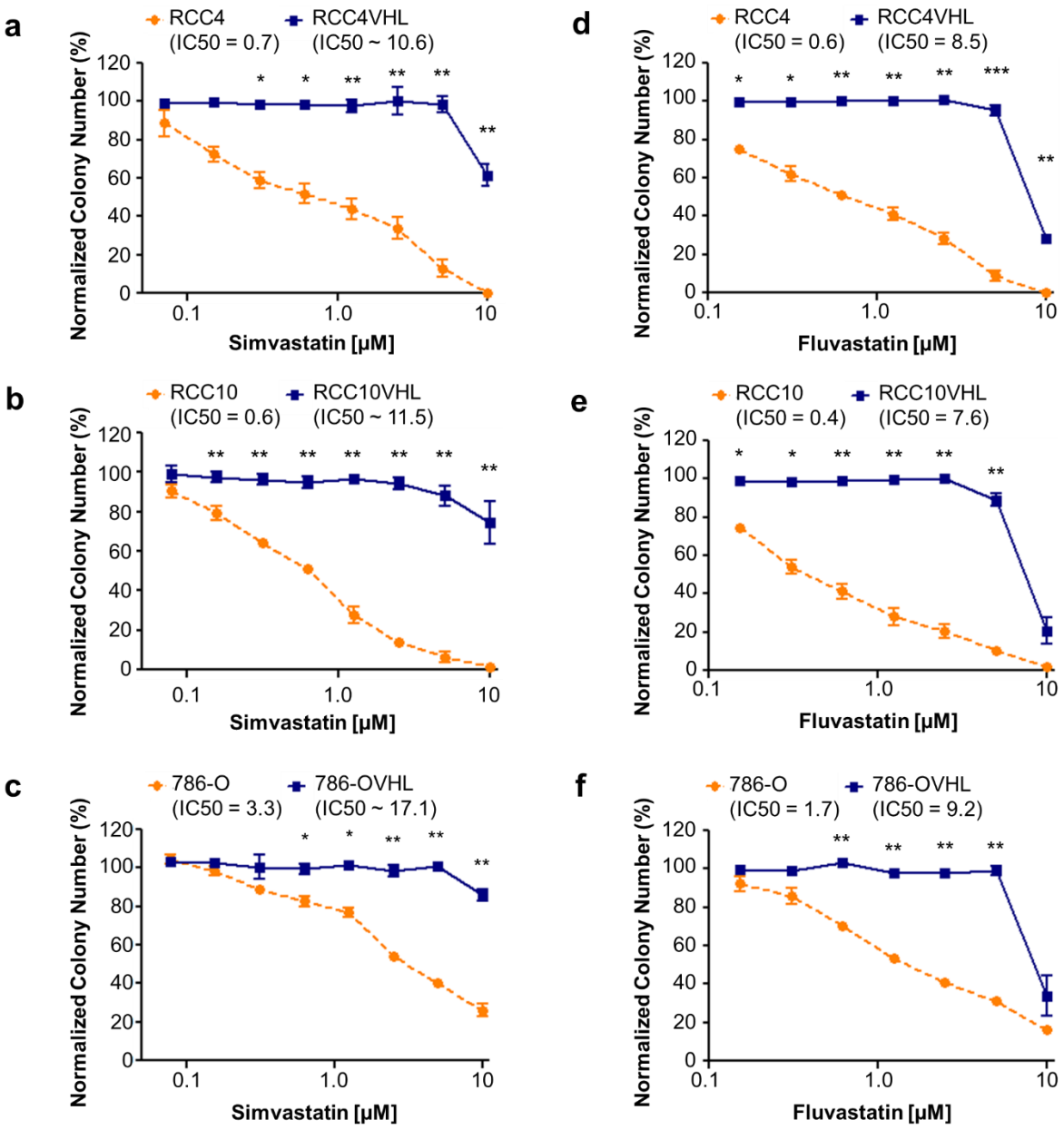

Figure 5.1. Simvastatin and Fluvastatin treatment causes synthetic lethality with *VHL* loss in multiple CC-RCC cell lines. In a clonogenic assay activated Simvastatin (**a-c**) and Fluvastatin (**d-f**) show selective toxicity towards *VHL*-deficient (**a, d**) RCC4, (**b, e**) RCC10, and (**c, f**) 786-O while sparing their *VHL*-expressing isogenic cell line pairs. Data for Simvastatin and Fluvastatin treatments were normalized to 80%DMSO/20%Ethanol and DMSO vehicle controls, respectively. Each dose within each experiment was tested in duplicate, and each experiment was repeated three times for each isogenic cell line pair. IC_{50s} are indicated where "~" corresponds to IC_{50s} extrapolated based on a best fit line of the data. Statistical analysis in (**a-f**) was performed using a paired t-test between the matched cell lines at each dose (* $p < 0.05$, ** $p < 0.01$, *** $p < 0.001$), SEMs are shown.

Synthetic lethality depends on statins' blocking effect on small GTPase isoprenylation.

Next, we sought to confirm that the synthetic lethal interaction between statins and *VHL* loss was due to their inhibition of HMG-CoA reductase (see Supplemental Figure 5.5 for schematic). Since HMG-CoA reductase catalyzes the metabolic step leading to generation of mevalonate, we performed rescue experiments with exogenous mevalonate to see if we could rescue cell proliferation of Fluvastatin-treated RCC4. As expected, 500μM and 1000μM/2000μM mevalonate treatments were able to partially and fully rescue the colony forming ability of Fluvastatin-treated RCC4 (Figure 5.3a). The effectiveness of treatment by statins and rescue by mevalonate was assessed by their effect on Rap1a isoprenylation at 24 hours, which was blocked by Fluvastatin and rescued by mevalonate (Figure 5.3c). Since 500μM mevalonate was able to fully restore Rap1a isoprenylation at 24 hours, but provided just the partial rescue of colony forming ability at 10 days, we assume that mevalonate stability and/or metabolic rate over the prolonged period of time contributes to the partial rescue. Furthermore, the addition of mevalonate to the RCC4±VHL cells treated with high doses of Simvastatin (10 and 20μM) resulted in a partial rescue of proliferation and a complete rescue of cell death in the Live/Dead assay (Supplemental Figure 5.6). BrdU cell cycle analysis revealed that statin treatment selectively decreases S phase progression and increases apoptotic/debris cells in RCC4 cells, but not in RCC4VHL cells (Supplemental Figure 5.7).

Figure 5.2. Statin treatment is cytostatic and cytotoxic in *VHL*-deficient CC-RCC. LIVE/DEAD assay measuring live cell numbers via Calcein staining (**a**) and dead cell numbers via PI staining (**b**) reveals that Simvastatin treatment inhibits RCC4 cell proliferation at nanomolar and micromolar doses, and triggers cell death at higher micromolar doses. RCC4±VHL cells were treated with Simvastatin or vehicle control (80%DMSO/20%Ethanol) for 6 days. Calcein-positive cells in (**a**) were normalized to the vehicle control. Normalized % viability in (**b**) was calculated by dividing the number of dead PI-positive cells by the total number of cells (PI-positive + Calcein-positive), multiplying the result by 100 and subtracting the result from 100%; the resulting viabilities were then normalized to the vehicle control. Statistical analysis in (**a**-**b**) was performed using a paired t-test between the matched cell lines at each dose (* $p < 0.05$, ** $p < 0.01$), SEMs are shown. (**c**) Representative images of LIVE/DEAD assay. (**d**) *VHL*-deficient CC-RCC are more sensitive to Simvastatin treatment than renal cancer cell lines endogenously expressing *VHL*. Cell lines were treated with 5 μM Simvastatin for 6 days and the live cell number was assessed by Calcein staining. The results were normalized to vehicle-treated cells. Statistical significance was determined using a one-way ANOVA followed by Tukey's post-hoc analysis (*** $p < 0.001$), SEMs are shown. The experiment was conducted in duplicate and repeated two times. (**e**) Western blot confirming VHL expression in cell lines used in (**d**), HIF1α and HIF2α expression is also shown. α-tubulin serves as a loading control.

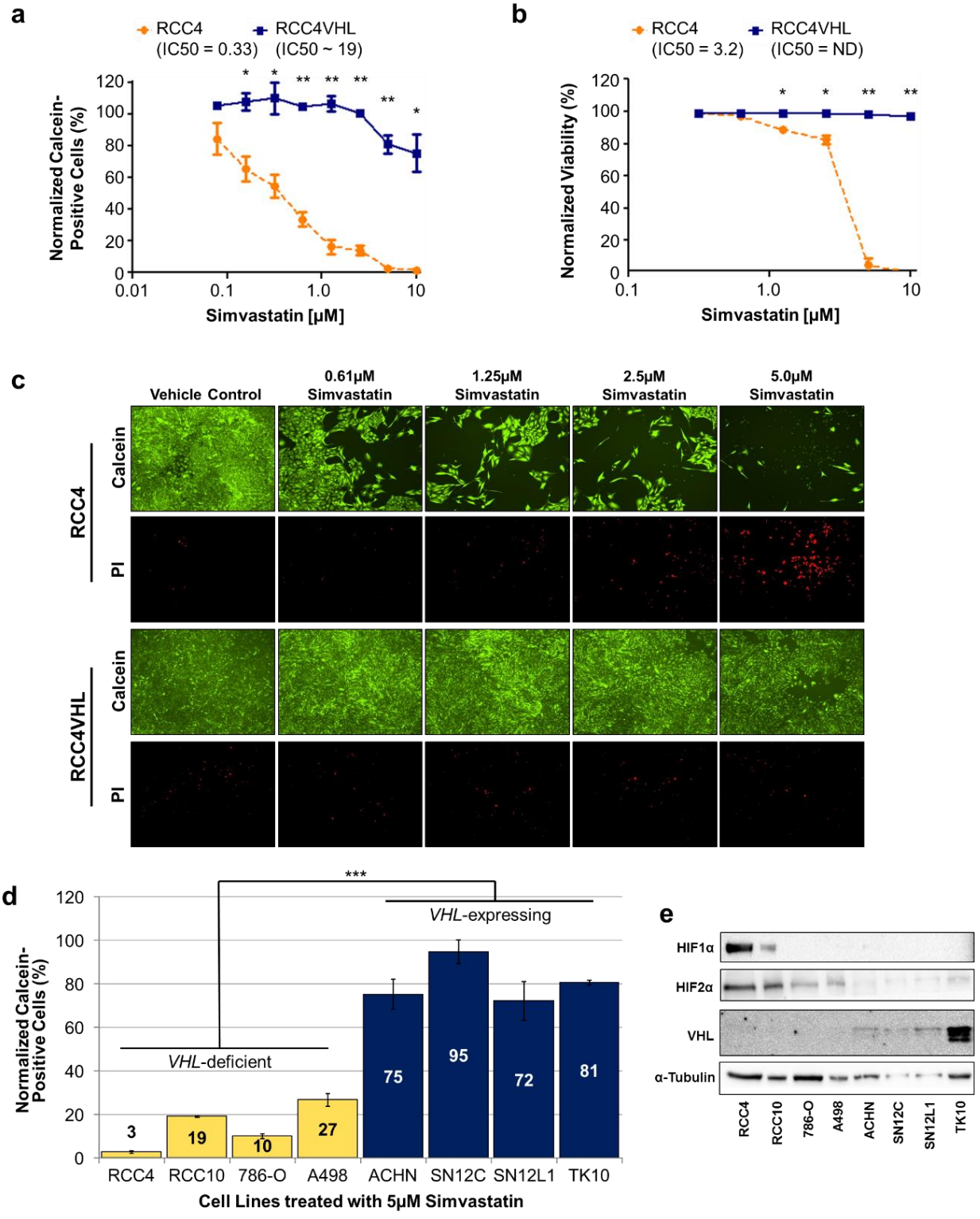
a
RCC4 (IC50 = 0.33)
RCC4VHL (IC50 ~ 19)
Normalized Calcein-Positive Cells (%)
Simvastatin [μM]
b
RCC4 (IC50 = 3.2)
RCC4VHL (IC50 = ND)
Normalized Viability (%)
Simvastatin [μM]
c
Vehicle Control
0.61μM Simvastatin
1.25μM Simvastatin
2.5μM Simvastatin
5.0μM Simvastatin
RCC4
RCC4VHL
Calcein
PI
d
Normalized Calcein-Positive Cells (%)
VHL-deficient
VHL-expressing
***
3
19
10
27
75
95
72
81
RCC4 RCC10 786-O A498 ACHN SN12C SN12L1 TK10
Cell Lines treated with 5μM Simvastatin
e
HIF1α
HIF2α
VHL
α-Tubulin
RCC4 RCC10 786-O A498 ACHN SN12C SN12L1 TK10

Since the mevalonate pathway has multiple downstream metabolic products, we next sought to elucidate which arm of the pathway is involved in the synthetic lethal effect. The best-known arm of the mevalonate pathway affected by statins is the cholesterol synthesis arm, where the last step is conversion of squalene to cholesterol. It is important to note that in our experiments we used medium with the cholesterol-containing serum, which can provide cholesterol to cells exogenously. Since we are seeing the difference in RCC and RCCVHL colony forming ability in that medium, it suggests that this arm of the mevalonate pathway is not important for the synthetic lethal effect. To confirm this, we conducted an additional experiment to rescue endogenous cholesterol synthesis in Fluvastatin-treated RCC4±VHL cells: we added up to 100μM squalene and conducted clonogenic assays. The addition of squalene was unable to rescue the synthetic lethal effect (Supplemental Figure 5.8), confirming that cholesterol synthesis does not contribute to the synthetic lethal effect.

Previous studies have identified the inhibitory effect of statins on small GTPases, including the Rho GTPase and Rap1a GTPase[57,165,171,173] (used as a readout of statin inhibitory action on the mevalonate pathway in Figure 5.3c and Supplemental Figure 5.3C). To be functional, GTPases need to be isoprenylated to translocate to the membrane. One of the arms of the mevalonate pathway generates GGPP, which is used as a substrate for isoprenylation of small GTPases by GGTase (Supplemental Figure 5.5 for schematic). In order to rescue isoprenylation of small GTPases in Fluvastatin-treated RCC4±VHL cells, we added 10μM or 20μM GGPP and conducted clonogenic assays. GGPP treatment led to a partial (10μM) and full (20μM) rescue of colony forming ability (Figure 5.3b). Similar to mevalonate, 10μM GGPP treatment fully rescued the Rap1a isoprenylation at 24 hours as assessed by western blot (Figure 5.3c). Together, these results

indicate that the synthetic lethal effect between statin treatment and *VHL* loss is through inhibition of HMG-CoA reductase and the resulting effect of inhibiting GTPase isoprenylation.

The inhibitory effect of statins on the Rho/ROCK pathway is important for synthetic lethality with *VHL* loss.

Previously we reported that ROCK1 inhibition results in a synthetic lethal interaction with *VHL* loss in CC-RCC[52]. Thus, we hypothesized that inhibition of Rho GTPase isoprenylation and subsequent inhibition of ROCK by statins, is responsible for the synthetic lethality with *VHL* loss. First, we assessed whether treatment with statins causes Rho/ROCK pathway inhibition. We treated the RCC4±VHL cells with Fluvastatin for 24 hours and observed a decrease in phosphorylation of LIMK1 at Thr^{508} and LIMK2 at Thr^{505} (Figure 5.4a). This effect was also replicated in the RCC10±VHL and the 786-O±VHL (Supplemental Figure 5.9).

Second, in order to rescue ROCK pathway activity in Fluvastatin-treated RCC4±VHL cells, we added 100μM Arachidonic acid (AA), which binds and activates ROCK by releasing it from its own autoinhibition[174,175], and conducted clonogenic assays. AA was able to partially rescue the colony forming ability of Fluvastatin-treated RCC4 cells (Figure 5.4b). AA treatment activated ROCK signaling as judged by increased phospho-LIMK1/2 (Figure 5.4c). Together, these results indicate that inhibition of the Rho/ROCK pathway by statins contributes to synthetic lethality with *VHL* loss in CC-RCC.

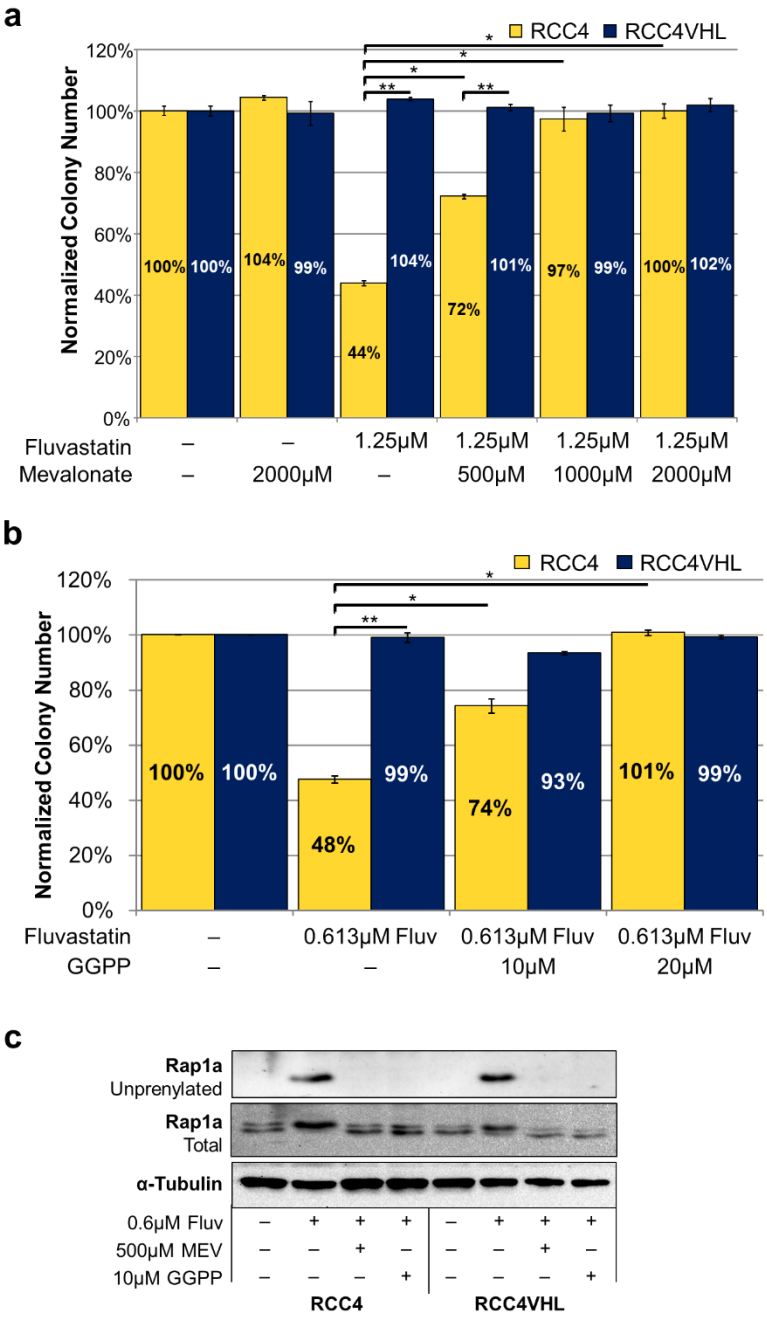

Figure 5.3. The effect of statins on GTPase isoprenylation is important for synthetic lethality with *VHL* loss. (**a-b**) Addition of 1000μM mevalonate (**a**) or 20μM GGPP (**b**) rescues the effect of Fluvastatin on colony forming ability of RCC4 cells. Statistical analysis in (**a-b**) was performed using a paired t-test comparing treatments, and comparing RCC4 to RCC4VHL (* $p < 0.05$, ** $p < 0.01$), SEMs are shown. In (**a-b**) each dose of Fluvastatin or vehicle control (DMSO) within each experiment was tested in duplicate, and the experiment was repeated three times for each isogenic cell line pair. (**c**) Western blot showing that the addition of mevalonate or GGPP rescues the effect of Fluvastatin on GTPase isoprenylation by blocking the appearance of unprenylated Rap1a. α-tubulin serves as a loading control.

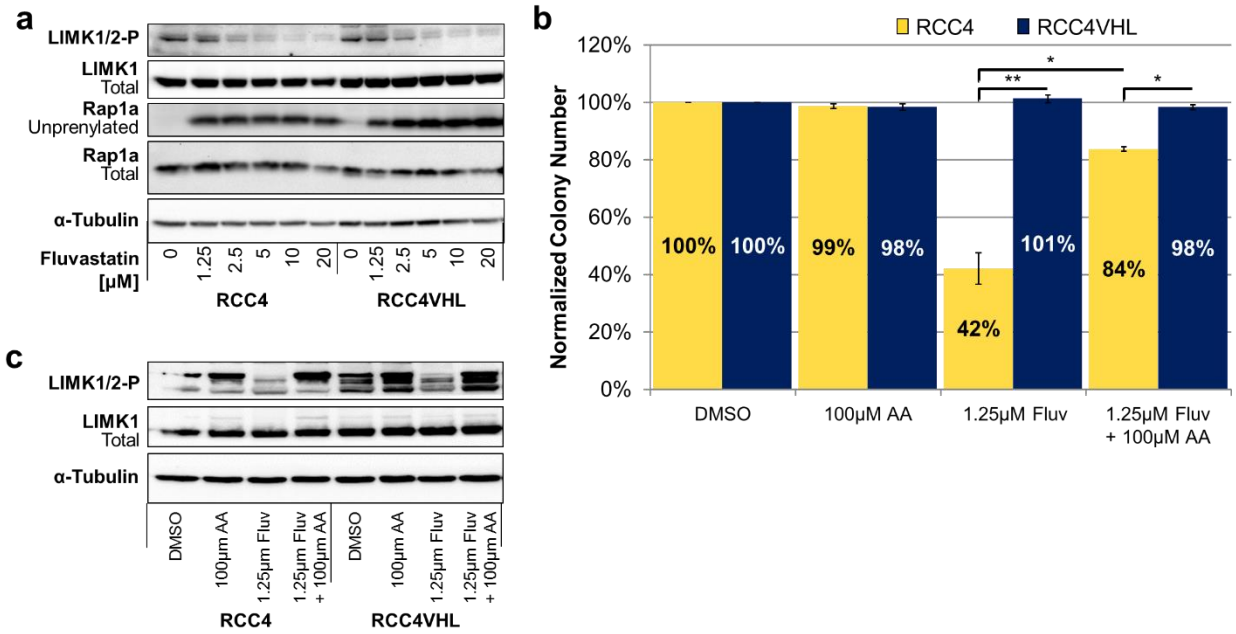

Figure 5.4. The inhibitory effect of statins on the Rho/ROCK pathway contributes to synthetic lethality with *VHL* loss. (**a**) Western blot showing that 24h treatment with Fluvastatin is sufficient to inhibit phosphorylation of LIMK1 (Thr^{508}) and LIMK2 (Thr^{505}) (ROCK substrates) in RCC4±VHL. Unprenylated Rap1a is used as a readout for the disruption of GTPase isoprenylation by treatment with Fluvastatin. (**b**) The effect of Fluvastatin on RCC4 colony forming ability can be partially rescued by administration of 100μM Arachidonic Acid (AA) (ROCK activator). Each dose of Fluvastatin or vehicle control (DMSO) within each experiment was tested in duplicate, and the experiment was repeated three times. Statistical analysis was performed using a paired t-test between the matched cell lines at each dose (* $p < 0.05$, ** $p < 0.01$), SEMs are shown. (**c**) Western blot showing that 24h treatment with Fluvastatin inhibits phosphorylation of LIMK1/2, and co-treatment with AA rescues phosphorylation of LIMK1/2 in the RCC4±VHL. (**a-c**) α-tubulin serves as a loading control.

The synthetic lethal interaction between statin treatment and *VHL* loss is dependent on the activation of HIFs

VHL functions as a substrate-recognition subunit of an E3 ubiquitin ligase complex and binds to hydroxylated forms of HIF1α and HIF2α under normoxic conditions, causing their degradation through the proteasome. Mutation or deletion of *VHL* results in the stabilization and activation of HIF1α and HIF2α[45,46,49,84,119]. To test if the synthetic lethal effect of statin treatment with *VHL* loss is dependent on overactivation of the HIF pathway, we conducted three experiments.

In the first experiment, we knocked down the Aryl Hydrocarbon Receptor Nuclear Translocator (ARNT), which heterodimerizes with both HIF1α and HIF2α and is absolutely required for their activity[176]. We then treated shARNT- and shScramble-transduced CC-RCC cells with Fluvastatin and conducted colony assays. shARNT-transduced RCC4, RCC10, and 786-O cells were all protected from Fluvastatin treatment in comparison to respective shScramble-transduced control cells (Figure 5.5a). Inactivation of HIF signaling by ARNT knockdown was confirmed by western blot, which showed reduced expression of HIF target gene LDHA (Figure 5.5b). The protection of the shARNT-transduced CC-RCC cell lines from Fluvastatin treatment mimics *VHL* reintroduction, indicating that the synthetic lethal effect is dependent on HIF signaling.

In the second experiment, we treated RCC4±VHL, RCC10±VHL, and 786-O±VHL cells with Fluvastatin and subjected them to colony assays in normoxia (21% oxygen) or hypoxia (2% oxygen). Each treatment was then normalized to the DMSO vehicle control. RCCVHL cell lines were sensitized to Fluvastatin treatment in hypoxia having decreased colony-forming ability in hypoxia in comparison to normoxia (Figure 5.5c). Activation of HIF1α and HIF2α and induction

of their downstream targets in hypoxia were confirmed by western blot (Figure 5.5d). The sensitization of the RCCVHL cells to Fluvastatin treatment in hypoxia mimics *VHL* loss, indicating that the synthetic lethal effect is dependent on HIF signaling.

In the third experiment, we used 786-OVHL cell line expressing a non-degradable constitutively active hemagglutinin-tagged HIF1α (CA-HA-HIF1α) or HIF2α (CA-HA-HIF2α) (Figure 5.5e), which sensitized 786-OVHL cells to Fluvastatin treatment in comparison to vector-control cells (Figure 5.5f). Expression of CA-HA-HIF1α in 786-O cells did not further sensitize them to Fluvastatin treatment in comparison to the vector-control cells (Figure 5.5f). Together, these results confirm that the synthetic lethal effect between statins and *VHL* loss is dependent on the resulting stabilization and overactivation of either HIF1α or HIF2α signaling.

Fluvastatin delays tumor initiation and inhibits tumor growth *in vivo*

There are reports suggesting that statins reduce the risk of developing cancer[61,177,178], while other studies suggest that statins could serve as viable therapies for patients after tumors have formed[173,179]. Accordingly, we decided to test if statins delay CC-RCC tumor initiation and also inhibit tumor growth. For *in vivo* studies, we used 786-OT1 cells, which were established from a 786-O-based tumor and are characterized by fast tumor growth kinetics *in vivo* as previously described[52]. 786-OT1 showed similar sensitivity to Fluvastatin *in vitro* as the parental 786-O cell line (Supplemental Figure 5.10). 786-OT1 cells were injected subcutaneously into the right flank of 25 RAG1 mice. The mice were then randomized into three groups and two out of three groups were treated daily with (3% DMSO in PBS) vehicle-control (n=8) or 10mpk Fluvastatin (n=8) via intraperitoneal (ip) injection. The third group was left untreated (n=9) until the tumors reached approximately 300mm^3. Mice were examined daily and palpable tumors were recorded.

Figure 5.5. HIF activation sensitizes CC-RCC to Fluvastatin. (**a**) Clonogenic assay showing that CC-RCC cells transduced with shARNT are protected against Fluvastatin treatment and their colony forming ability is comparable to RCCVHL cells. (**b**) Western blot confirming the downregulation of ARNT in shRNA-transduced cells, accompanied by downregulation of HIF's downstream targets LDHA. Cells transduced with scramble shRNA (shScr) serve as controls. (**c**) RCC±VHL cells were treated with 1.25μM Fluvastatin, plated for clonogenic assays and replicate plates were subjected to either normoxia (21% O_2) or hypoxia (2% O_2) for the duration of the experiment. Colony numbers were normalized to the DMSO vehicle control. RCC4VHL, RCC10VHL and 786-OVHL cells were sensitized to Fluvastatin treatment in hypoxia. (**d**) Western blot showing the induction of HIF1α and HIF2α and their downstream target LDHA in hypoxia (2% O_2, 24h). (**e**) Western blot confirming the overexpression of constitutively active (CA) non-degradable hemagglutinin-tagged HIF1α or HIF2α (CA-HA-HIF1α and CA-HA-HIF2α). Cells transduced with vector-control (VC) serve as controls. Western blots shown a from the same gel. (**f**) Clonogenic assay showing that overexpression of CAHIF1α or CAHIF2α sensitizes the indicated cell lines to Fluvastatin treatment. Each assay in (**a**, **c**, and **f**) was performed in duplicate and repeated three times, and statistical analysis was performed using a paired t-test (* $p < 0.05$, ** $p < 0.01$ and *** $p < 0.001$), SEMs are shown. α-tubulin serves as a loading control in (**b**, **d**, and **e**).

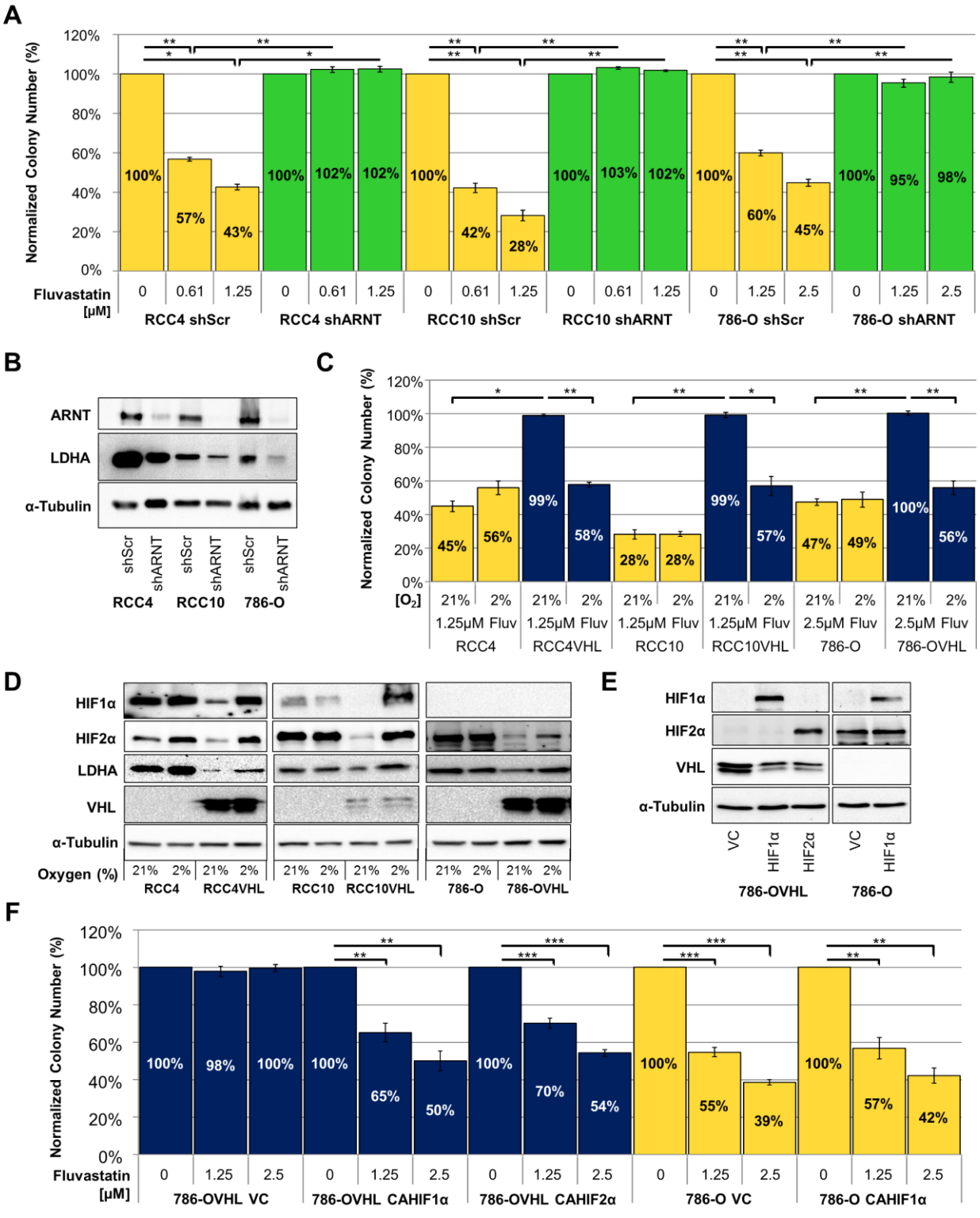
A
Normalized Colony Number (%)
120%
100%
80%
60%
40%
20%
0%
100%
57%
43%
100%
102%
102%
100%
42%
28%
100%
103%
102%
100%
60%
45%
100%
95%
98%
Fluvastatin [μM]
0 0.61 1.25 0 0.61 1.25 0 0.61 1.25 0 0.61 1.25 0 1.25 2.5 0 1.25 2.5
RCC4 shScr
RCC4 shARNT
RCC10 shScr
RCC10 shARNT
786-O shScr
786-O shARNT
B
ARNT
LDHA
α-Tubulin
shScr shARNT shScr shARNT shScr shARNT
RCC4 RCC10 786-O
C
Normalized Colony Number (%)
120%
100%
80%
60%
40%
20%
0%
45%
56%
99%
58%
28%
28%
99%
57%
47%
49%
100%
56%
[O2]
21% 2% 21% 2% 21% 2% 21% 2% 21% 2% 21% 2%
1.25μM Fluv
2.5μM Fluv
RCC4 RCC4VHL RCC10 RCC10VHL 786-O 786-OVHL
D
HIF1α
HIF2α
LDHA
VHL
α-Tubulin
Oxygen (%)
21% 2% 21% 2% 21% 2% 21% 2% 21% 2% 21% 2%
RCC4 RCC4VHL RCC10 RCC10VHL 786-O 786-OVHL
E
HIF1α
HIF2α
VHL
α-Tubulin
VC HIF1α HIF2α VC HIF1α
786-OVHL 786-O
F
Normalized Colony Number (%)
120%
100%
80%
60%
40%
20%
0%
100%
98%
100%
100%
65%
50%
100%
70%
54%
100%
55%
39%
100%
57%
42%
Fluvastatin [μM]
0 1.25 2.5 0 1.25 2.5 0 1.25 2.5 0 1.25 2.5 0 1.25 2.5
786-OVHL VC
786-OVHL CAHIF1α
786-OVHL CAHIF2α
786-O VC
786-O CAHIF1α

Treatment with 10mpk Fluvastatin inhibited tumor initiation as shown by Kaplan Meier curves (Figure 5.6a). Once tumors had formed, tumor size was measured biweekly by calipers; tumor volume increased rapidly in the vehicle-treated control group, while tumor volume in the 10mpk Fluvastatin-treated group increased at a significantly slower rate (Figure 5.6b). While Fluvastatin treatment initially delayed tumor growth in this group, over time resistance developed and the tumors began to grow at the same rate as the control (Figure 5.6b). When tumors reached approximately $300mm^3$ in the third group (at day 54), we began treatments with 15mpk Fluvastatin daily for 21 days. Fluvastatin treatment caused initial weight loss in both groups, but was well tolerated overall (Supplemental Figure 5.11). Tumor size was measured triweekly and while tumor size constantly increased in the control group, treatment with 15mpk Fluvastatin resulted in a significant regression in tumor size (Figure 5.6c). Both treatments resulted in a reduction of tumor weight and size (Figure 5.6d,e). We also confirmed that 10mpk and 15mpk Fluvastatin treatments resulted in increased unprenylated Rap1a in tumor samples by western blot indicative of effective Fluvastatin delivery to tumor tissue (Figure 5.6f). Ki67 and Tunel analysis revealed that 15mpk Fluvastatin treatment resulted in decreased tumor proliferation (Figure 5.6g, Supplemental Figure 5.12a) and an increase in apoptotic cell death (Figure 5.6h, Supplemental Figure 5.12b) *in vivo* at the time of sacrifice. As expected the 10mpk Fluvastatin treatment group was resistant to Fluvastatin treatment at the time of sacrifice and was not significantly different from the control group for both Ki67 and Tunel staining. To confirm that this is due to resistance to Fluvastatin, we reisolated the cell lines for the vehicle control and 10mpk groups from 3 tumors. We conducted the LIVE/DEAD assay on these cells and found that while both were equal sensitive to the cytostatic effect of Fluvastatin treatment (Figure 5.7a,c), the 10mpk group was now resistant to the cytotoxic effect with a ~4x increase in IC_{50} for viability in comparison to the control group

(Figure 5.7b,c). These results confirmed that the 10mpk group had become resistant to Fluvastatin treatment during the experiment.

Figure 5.6. Fluvastatin prevents tumor initiation and inhibits tumor growth *in vivo*. (**a**) 5 x 10^6 786-OT1 cells were injected subcutaneously into 25 RAG1 mice. The mice were then randomized into three groups: vehicle control (n=8), 10mpk Fluvastatin (n=8), and no treatment (n=9). Treatment was administrated immediately for the vehicle control and 10mpk Fluvastain groups. 10mpk Fluvastatin treatment inhibited tumor initiation (**a**) as shown by Kaplan Meier analysis and inhibited tumor growth (**b**). When the "vehicle control" and "no treatment" tumors reached approximately 300mm^3, 15mpk Fluvastatin treatment was initiated for the "no treatment" group, which inhibited tumor growth (**c**). (**d**) Administration of Fluvastatin to both groups (10mpk and 15mpk) resulted in reduced tumor weight in comparison to vehicle-control group at sacrifice. (**e**) Representative images of tumors. (**f**) Western blot showing that 10mpk and 15mpk Fluvastatin treatments resulted in appearance of unprenylated Rap1a in the tumor samples in comparison to the vehicle control, indicating that the drug was effectively delivered to the tumors. Administration of 15mpk Fluvastatin resulted in (**g**) decreased proliferation measured via Ki67 staining and (**h**) increased apoptotic cell death measured via Tunel staining in comparison to vehicle-control group at sacrifice. Statistical analysis in (**a**) was conducted using Log-rank (Mantel-Cox) Test ($p = 0.0007$) and Gehan-Breslow-Wilcoxon Test ($p = 0.0015$). Statistical analysis in (**b**-**c**) was conducted using a paired t-test between doses and a two-way ANOVA comparing the response of each treatment group over time. Statistical analysis in (**d, g, h**) was conducted using a one-way ANOVA comparing treatments. (* $p < 0.05$, ** $p < 0.01$, *** $p < 0.001$) and Dunnett post-hoc with vehicle set as the control group. SEMs are shown.

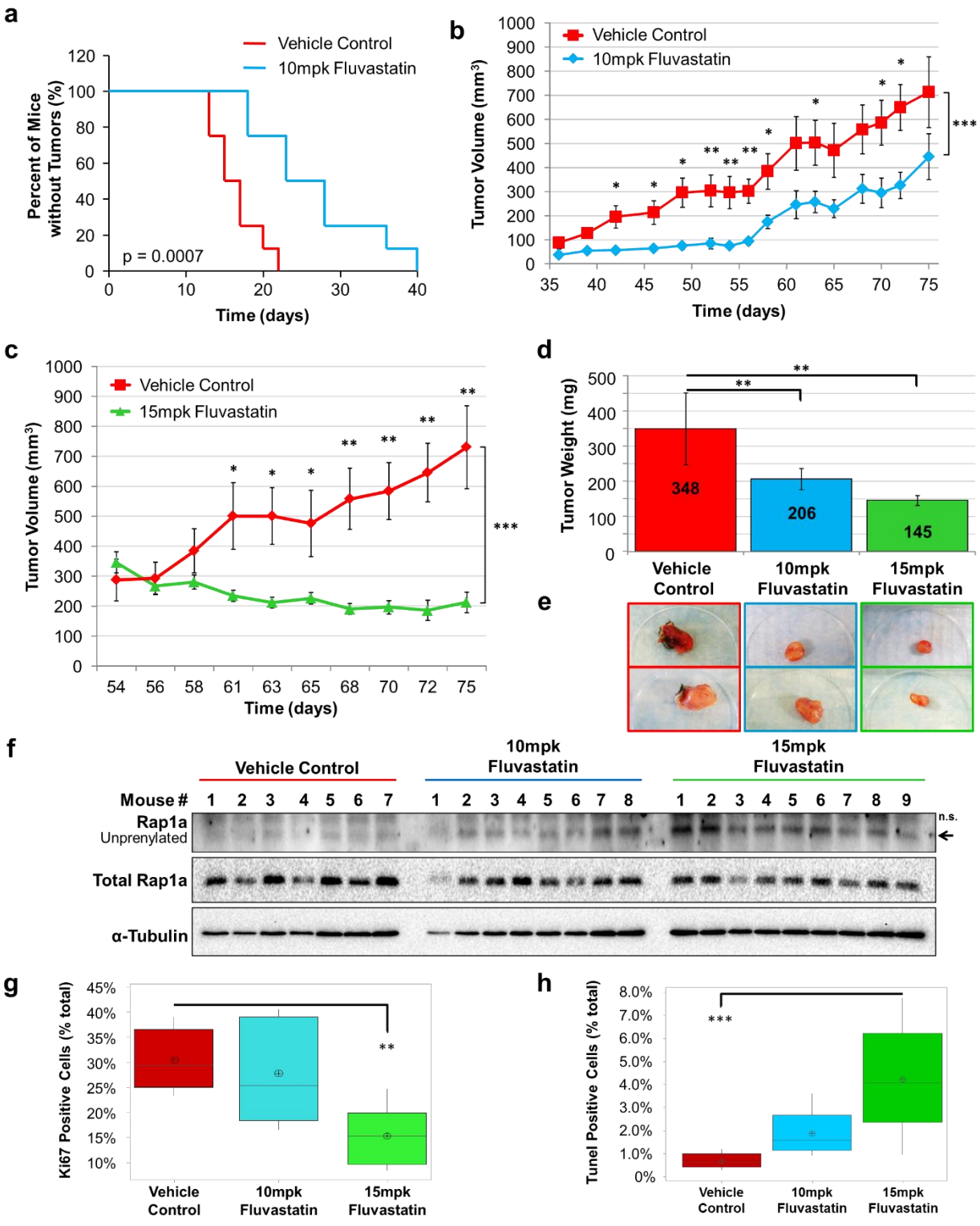
a
Vehicle Control
10mpk Fluvastatin
Percent of Mice without Tumors (%)
p = 0.0007
Time (days)
b
Vehicle Control
10mpk Fluvastatin
Tumor Volume (mm³)
Time (days)
c
Vehicle Control
15mpk Fluvastatin
Tumor Volume (mm³)
Time (days)
d
Tumor Weight (mg)
348
206
145
Vehicle Control
10mpk Fluvastatin
15mpk Fluvastatin
e
f
Vehicle Control
10mpk Fluvastatin
15mpk Fluvastatin
Mouse #
Rap1a Unprenylated
Total Rap1a
α-Tubulin
n.s.
g
Ki67 Positive Cells (% total)
Vehicle Control
10mpk Fluvastatin
15mpk Fluvastatin
h
Tunel Positive Cells (% total)
Vehicle Control
10mpk Fluvastatin
15mpk Fluvastatin

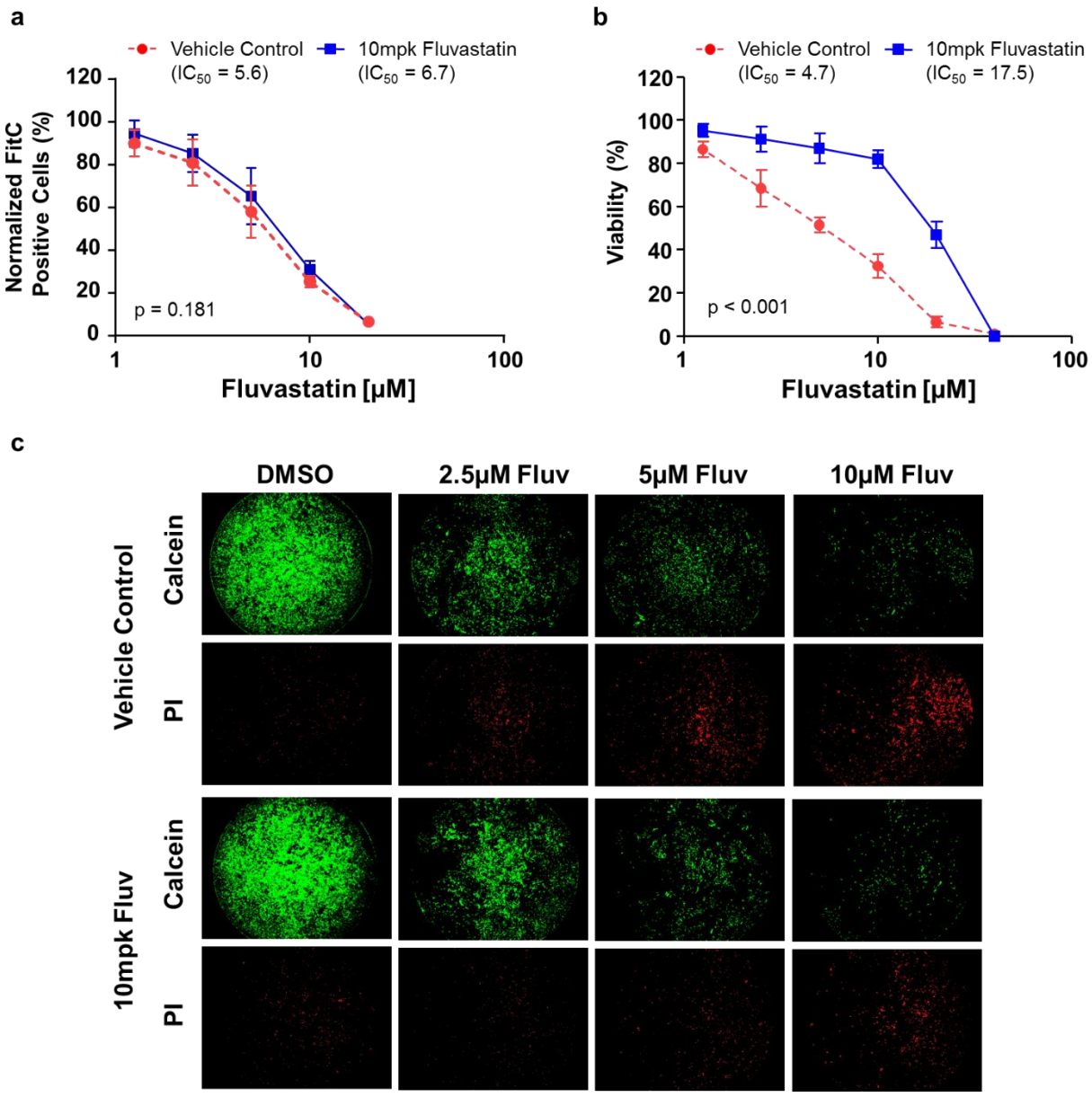

Figure 5.7. The 10mpk Fluvastatin treated group developed resistance to Fluvastatin induced cell death. Cell lines were reestablished *in vitro* for the vehicle control and 10mpk Fluvastatin treated groups. The LIVE/DEAD assay was then performed on the reestablished cell lines treated with Fluvastatin for 5 days. (**a**) Both cell lines were equally sensitive to Fluvastatin's cytostatic effect. (**b**) The 10mpk Fluvastatin treated cells were resistant to the Fluvastatin's cytotoxic effect showing far fewer PI positive cells in comparison to the vehicle control group. (**c**) Representative images obtained at 2x are shown for the LIVE/DEAD assay. Cell lines were reestablished from 3 tumors for each treatment group. Treatments were conducted in triplicate and results are an average from all 3 tumors / group. SEM shown. For a,b we conducted a two-way ANOVA comparing *in vivo* treatment group and Fluvastatin dose and while dose was significant for both ($p < 0.001$), only the difference in viability was statistically significant for the treatment factor.

Discussion

In this study, we have shown that statins may serve as potential therapeutics to target *VHL*-deficient CC-RCC. We have further determined that the therapeutic effect depends on 1) the effects of statins on GTPase isoprenylation, with a significant contribution of Rho/ROCK pathway inhibition mediating the effect; 2) Overactivation of the HIF pathway triggered by the *VHL* loss. Treatment of *VHL*-deficient CC-RCC with statins *in vitro* inhibits proliferation and induces cell death. Accordingly, *in vivo* statins are effective at both preventing tumor initiation and at inhibiting tumor growth of established xenografts, confirming their therapeutic potential.

Multiple synthetic lethal interactions have been identified in *VHL*-deficient CC-RCC, including stimulation of autophagy[83]; inhibition of Glut1[84], CDK6[113], MET[113], MEK1[113], protein translation [114,115], and inhibition of ROCK1 [52]. Interestingly, with the exception of MET inhibition, statin treatment targets each of these synthetic lethality partners of VHL. Statin treatment has been shown to stimulate autophagy[180–182], inhibit glucose uptake and glucose metabolism[183–185], CDKs[55,179,186] (including CDK6[179]), the MEK pathway[187,188], and finally inhibit small GTPases[57] (including the Rho/ROCK pathway[170,173]). Since our studies show only partial reliance on Rho/ROCK pathway inhibition for statin's selective targeting of *VHL*-deficient CC-RCC, we think that the statin's inhibitory effect on other synthetic lethality targets does contribute to the observed therapeutic effect. Furthermore, the statins' inhibitory effect on all of these synthetic lethality targets, except for the inhibition of glucose uptake, can be rescued by GGPP[173,180,186,187], indicating that inhibition of small GTPase isoprenylation is important.

Statins affect isoprenylation of multiple small GTPases, including Rho, Ras, Rap1a, and Rac, disturbing their activity[58]. CC-RCCs are characterized by low (≤ 1%) frequency of K-Ras/N-Ras/H-Ras mutations combined[57], thus making Ras-dependent mechanism unlikely. RhoC and

ROCK expression is increased in CC-RCC, which has been correlated with increased tumor grade and stage, and decreased overall patient survival[54]. The Rac pathway is often stimulated by mutations affecting Rac's upstream regulators in CC-RCC and correlates with tumor invasiveness[189]. Further studies are needed to assess the contribution of specific inhibition of individual small GTPases to synthetic lethality with *VHL* loss.

The majority of patients with CC-RCC lose the function of VHL[32], which results in constitutive activation of HIFs, which is vital to the pathogenesis of the disease. Our finding that the synthetic lethal interaction is dependent on HIF overactivation suggests that other cancer types with overactivation of the HIF pathway might be sensitive to statin treatment. HIF overactivation was documented in a fraction of bladder, brain, breast, colon, ovarian, gastric, lung, melanoma, pancreatic, and prostate cancers[190,191], although the overactivation degree in the majority of cases is significantly less than in *VHL*-deficient CC-RCC. Accordingly, several commonly mutated genes in cancer have been linked to HIF activation in normoxia, including *p53* loss[192,193], H-Ras[47,194] (via PI3K signaling), v-Src[195] and c-Myc[196] overactivation. In some cancer types, like pancreatic, colorectal, and breast cancer[197] overactivation of HIFs in normoxia is achieved by the mutations affecting prolyl hydroxylases (PHDs) that would otherwise hydroxylate HIFα subunits causing *VHL*-mediated degradation[198]. In addition, the majority of solid tumors are characterized by dysfunctional vasculature, leading to regional hypoxia, where HIFs stabilize[47]. Thus, our finding that the synthetic lethal interaction is dependent on HIF signaling suggests that certain patient's tumors might be sensitized to statins, but the stratification based on HIF activity would be required, and more insight acquired into the status of their small GTPase signaling.

For cholesterol reduction in patients, statins are taken daily at ~1 mpk [80 mg daily][167]. For gastric carcinoma[168], anaplastic astrocytoma[169], and glioblastoma multiforme[169] treatment in phase

I and II clinical trials, Lovastatin was taken at maximum tolerated doses: 20-35 mpk daily for 7 days repeated monthly. In this study, we used high doses of Fluvastatin *in vivo* (10mpk and 15mpk), which are close to maximum tolerated doses. The administration of statins at high doses was reported to cause apoptosis of skeletal muscle cells, leading to myopathy, but this side-effect is preventable by the co-administration of ubiquinone[199]. At the same time, the administration of Fluvastatin at low doses of 40 and 80 mg, was reported to reach C_{max} concentrations in the blood of 1.28μM and 3.45μM, respectively[200], that are greater than the IC_{50s} we report for CC-RCC. Moreover, low hypercholesterolemia doses of Rosuvastatin and Atorvastatin can inhibit ROCK activity in patient's leukocytes[170], even though Rosuvastatin is a hydrophilic statin with the reduced uptake in non-hepatic tissues. Thus, statin dosing and regimen for treatment of CC-RCC need to be evaluated in patients and may end up being lower than the maximum tolerated doses.

There is one more study reporting on the effect of statins on kidney cancer proliferation, migration, and tumor growth[201]. The study did not concentrate on *VHL*-deficient CC-RCC and included several types of *VHL*-positive and -negative kidney cancers. Simvastatin was found to inhibit tumor cell proliferation via the inhibition of the AKT/mTOR, ERK, and JAK2/STAT3 pathways at μM doses[201], and tumor growth of A498-based xenografts. Our data show that A498 cells are the least sensitive to statin treatment among the *VHL*-deficient cell lines tested (RCC4, RCC10, and 786-O, Figure 5.2d) and the reported Simvastatin C_{max} concentrations in the blood[166] are lower than for Fluvastatin used in our study (see below). At the same time, we provide additional mechanisms of action for statins in CC-RCC via *VHL* loss and resulting overactivation of the HIF pathway and inhibition of small GTPases, including Rho GTPase. Importantly, Rho GTPase was reported to regulate AKT signaling in melanoma[202], making our findings consistent

with the ones discussed above. We also provide data on tumor initiation in addition to tumor progression.

While a number of epidemiological studies have been conducted on the ability of statins to reduce the risk of CC-RCC, there is conflicting literature on the subject. Although, there are studies showing that people on statins have a lower risk of CC-RCC development[61], and that CC-RCC patients on statins have a better overall survival and lower risk of progression after surgery[177,178], there are two studies which found no correlation of statin intake and CC-RCC recurrence-free and progression-free survival[203,204]. This discrepancy may be explained by the absence of stratification of CC-RCC patients by *VHL* status, difference in pharmacokinetics (maximum blood concentration achieved) for different statins, and intake of lipophilic vs hydrophilic statins, targeting both hepatic and non-hepatic tissues vs mainly hepatic tissue, respectively. Accordingly, although *VHL* is lost in 80-90% of all CC-RCC[32], the *VHL* status of CC-RCC tumors was not taken into consideration in these studies. There is also a considerable variation in C_{max} concentrations in the blood for different statins: for example in one study Fluvastatin reached 448ng/ml [1.09µM], whereas simvastatin only reached 10-34ng/ml [81nM][166]. Finally, lipophilic statins (Atorvastatin, Lovastatin, Simvastatin, Fluvastatin, Cerivastatin and Pitavastatin) tend to target both hepatic and non-hepatic tissues, while the hydrophilic statins (Pravastatin, Rosuvastatin) are more liver-specific[172]. Taking into consideration the above factors, a more careful epidemiologic analysis should be conducted to draw the conclusions.

In addition, we see a conceptual difference between tumors arising in patients already on statins (those tumors should be already statin-resistant), and *VHL*-deficient statin-naïve tumors (those tumors should be statin-sensitive and respond to statin therapy). Accordingly, we propose that *VHL*-deficient CC-RCC patients, who were never on statins before, would benefit from

lipophilic statin intake; and that *VHL*-deficient CC-RCC tumor patients, who are on hydrophilic statins, would benefit from switching to lipophilic statins. Furthermore, patients with VHL disease, lacking one copy of *VHL* at birth, may benefit from taking lipophilic statins to prevent initiation of CC-RCC, hemangioblastoma, and pheochromocytoma[33,35,205].

In conclusion, statin treatment is synthetically lethal with *VHL* loss in CC-RCC, and statins could serve as viable therapies for the disease. Treatment with statins has a profound effect on *VHL*-deficient CC-RCC cells inhibiting proliferation, inducing cell death, and inhibiting both tumor initiation and growth. It is expected that patient stratification by the HIF and small GTPase signaling status will predict the response to lipophilic statin therapy; it is also expected that the reanalysis of the existing epidemiologic data on the CC-RCC initiation taking into account the administrated statin's C_{max}, the lipophilic vs hydrophilic statins, and *VHL* status of the tumor, will generate valuable data. Further studies are needed to evaluate statins as single agent CC-RCC therapeutics or combined with currently approved treatments.

Materials and Methods

Cell culture and chemical treatments.

All cell lines used in this study were grown in Dulbecco's Modified Eagle's Medium (DMEM; Caisson Labs #25-500, North Logan, UT) + 10% Fetal Bovine Serum (FBS; Omega Scientific #FB-12, Tarzana, CA) + 1% Penicillin/Streptomycin (Caisson Labs #25-512) in 5%CO_2, 21%O_2 at +37ºC. 786-OT1 cells are a sub-line of 786-O described in [52]. Simvastatin, Pravastatin, mevalonate, GGPP, squalene (Sigma-Aldrich, St. Louis, MO), Fluvastatin, Lovastatin (Selleck Chemicals, Houston, TX), and Arachidonic acid (MP Biomedicals, Santa Ana, CA). Fluvastatin and Pravastatin were diluted in Dimethyl Sulfoxide (DMSO) and serially diluted for each experiment. Simvastatin and Lovastatin were dissolved in ethanol and activated in 0.1N NaOH by incubation at 50˚C for 2 hours, followed by neutralization with 1N HCl, and dilution to 20mM in DMSO. The vehicle control was subjected to the same process and is approximately 20% ethanol and 80% DMSO.

Clonogenic assay.

Clonogenic assays were performed using 300 cells/plate as previously described [52]. For rescue experiments Fluvastatin (0.6125 or 1.25µM) and metabolite (GGPP [10 and 20µM], or mevalonate [500, 1000, and 2000µM], or squalene [10, 100, and 1000µM]) were dosed together and the clonogenic assays analyzed 10 days after treatment.

LIVE/DEAD cell viability assay.

The LIVE/DEAD cell viability assays were performed by plating 300 cells per well into a 96-well plate, allowing them to attach overnight. The following day statins. On the 6th day Calcein AM fluorescent dye from Thermo Fisher (1:1000) and propidium iodide (PI) from Sigma-Aldrich (1:250) were added to each well, incubated for 10 minutes at 37˚C, and then images were obtained

on a Nikon TI-E at 4x. The live cells (Calcein-positive) and dead cells (PI-positive) were counted per field. Treatments were normalized to vehicle-controls for proliferation calculations. Normalized % viability was calculated by dividing the number of dead PI-positive cells by the total number of cells (Calcein-positive + PI-positive), subtracting the result from 1, and then multiplying by 100%. Treatments were conducted in quadruplicate and each experiment was repeated three times.

Western blot analysis.

After treatments, cells were lysed and western blot was conducted as previously described [52]. Proteins were visualized using primary antibodies recognizing HIF1α, VHL (BD Biosciences, #610959, #564183, San Jose, CA), HIF2α (Novus Biological, #NB100-122, Littleton, CO), α-tubulin (Fitzgerald, #10R-842, North Acton, MA), Phospho-LIMK1 (Thr508)/LIMK2 (Thr505), LIMK1, Rap1a , CDCP1 (Cell Signaling, #3841S, #3842S, #4938S, #4115S, Danvers, MA), unprenylated Rap1a (Santa Cruz Biotechnology, #SC-1482, Dallas, TX), LDHA, CAIX (GeneTex, #GTX101416, #GTX70020, Irvine, CA); and Horseradish peroxidase conjugated Goat anti-Rabbit IgG and Goat anti-Mouse IgG secondary antibodies (Thermo Scientific, #31460, #31430). Blots were imaged using a ChemiDoc XRS$^+$ (BioRad, Hercules, CA).

Cholesterol Detection Assay

The Cholesterol Cell-Based Detection Assay Kit (Cayman Chemical, #10009779, Ann Arbor, Michigan) was performed following the manufacture's protocol. Cells were treated 24hr before fixation. U-18666A, at 1.25μM, served as a positive control.

shRNAs and cDNAs, virus produciton

HEK 293T cells were transfected with lentiviral plasmids (pLKO.1shARNT: 5'AAATAAACCATCTGACTTCTC3' (target sequence, OpenBiosystems, Huntsville, AL)) or

pLKO.1shScr: 5'CCTAAGGTTAAGTCGCCCTCGC3' (target sequence, Addgene, Cambidge, MA, #1864), along with packaging plasmids, pVSVG and ΔR8.2. Virus collection and infection were conducted as previously described[52].

Cell cycle analysis.

50,000 cells were seeded per well of a 6-well plate and treated the following day with vehicle (DMSO) or Fluvastatin for 6 days. BrdU analysis was performed using the FITC BrdU Flow Kit (BD Biosciences, San Jose, CA, #559619) following the manufacturer's protocol.

In vivo experiments

25 RAG1 (B6.129S7-Rag1^{tm1Mom}/J, Jackson Labs) mice (11–20 weeks old) were injected subcutaneously (sc) into the right flank with 5x10^6 786-OT1 cells. Before each injection, cells were resuspended in 50µl of 50%PBS/50%matrigel (BD Bioscience # 354248) mixture. The mice were randomized into three groups: vehicle control (n=8), 10mpk Fluvastatin (n=8), and 15mpk Fluvastatin (n=9). The vehicle control, 3% DMSO in PBS, and 10mpk Fluvastatin treatments were immediately administered intraperitoneally (ip) daily. Mice were checked daily for tumor formation and once palpable tumors had formed, it was recorded and tumor initiation assessed. Kaplan Meier curves were derived using GraphPad software and statistical significance calculated based on a Mantel-Cox test. Starting day 36, when palpable tumors had formed in both groups of mice, tumor size was measured with digital calipers biweekly. Starting day 54, when the tumors in vehicle-control and untreated group were ~300mm^3, we started to administer 15mpk Fluvastatin to the untreated group daily for 21 days. During that part of the experiment, tumor size was measured with calipers triweekly. On day 75 all of the mice were sacrificed, tumors excised and weighted. Tumor volume was calculated using the formula: V=(a)(b^2/2), where "a" is the shorter

measurement of length/width. Statistical analysis was performed using a one-way ANOVA between the two groups per day.

Tumor Sample Processing

Tumor samples were fixed in formalin overnight and stored in 70% ethanol until processing. Tissues were processed on a Leica Tissue Processor (TP1020) following the manufacturer's protocol. Samples were then embedded in paraffin on a Leica EG 1150 embedding/cooling station and microtomed on a Lecia RM2255.

Ki67 Staining

Samples were baked at 65°C overnight and then deparaffinized and rehydrated. Antigen retrieval was performed in 10mM sodium citrate, samples were blocked in goat serum. Cells were then incubated overnight in primary antibody (Genetex, #GTX16667) at 4 °C, followed by incubation for 1 h in secondary antibody (Goat Anti-Rabbit IgG H&L (Alexa Fluor® 488), Abcam, Cambridge, UK, #ab150077) at room temperature. Cell nuclei were counterstain with DAPI using Vectashield with Dapi (VWR, Radnor, PA, #101098-044) then images were obtained on a Nikon TI-E.

Tunel Analysis

Tunel analysis was conducted using the DeadEnd Fluorometric Tunel System (Promega, Madison, WI, #G3250) following the manufacturer's protocol for paraffin-embedded tissue sections. The positive control was prepared by treating 786-O cells with 2µM Staurosporine for 4 hours. The cells were then trypsonized, washed with PBS, and spun down onto slides using a cytospin centrifuge.

Growth curves and statistical analysis

Dose response and cell growth curves were generated using GraphPad Prism. IC_{50} values were calculated by transforming the X axis using X=Log(X), normalizing the transformed data to the vehicle control with 0 as 0%, and then fitting the normalized transformed data with a nonlinear trend line either using a normalized response ("log(inhibitor) vs. normalized response") or a variable slope ("log(inhibitor) vs. normalized response – variable slope"). The correct nonlinear trendline was selected using GraphPad's comparison of fits, which directly compares both fit lines statistically using an extra sum-of-squares F test. The fit line is not shown in the figures. The IC_{50} values for each experiment were then calculated from the best-fit values. Statistical analysis was conducted in Minitab 16 using a paired t-test or ANOVA between cell lines with a p-value of less than 0.05 considered statistically significant. All error bars represent the SEMs. The number of biological replicates is indicated in each figure legend.

Supplemental Figures

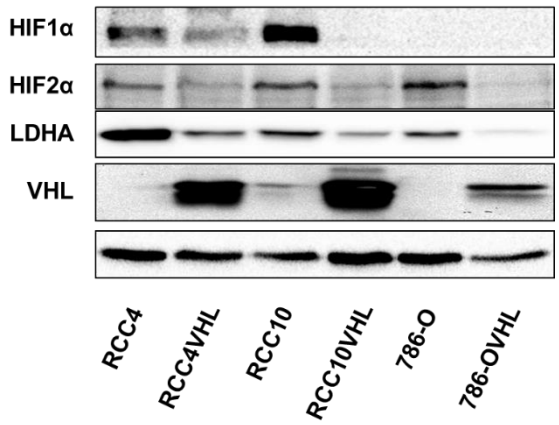

Supplemental Figure 5.1. VHL re-expression blocks HIF expression. Western blot showing the effect of VHL re-expression in CC-RCC cell lines on HIF1α, HIF2α, and LDHA (HIF target gene) expression. α-tubulin serves as a loading control.

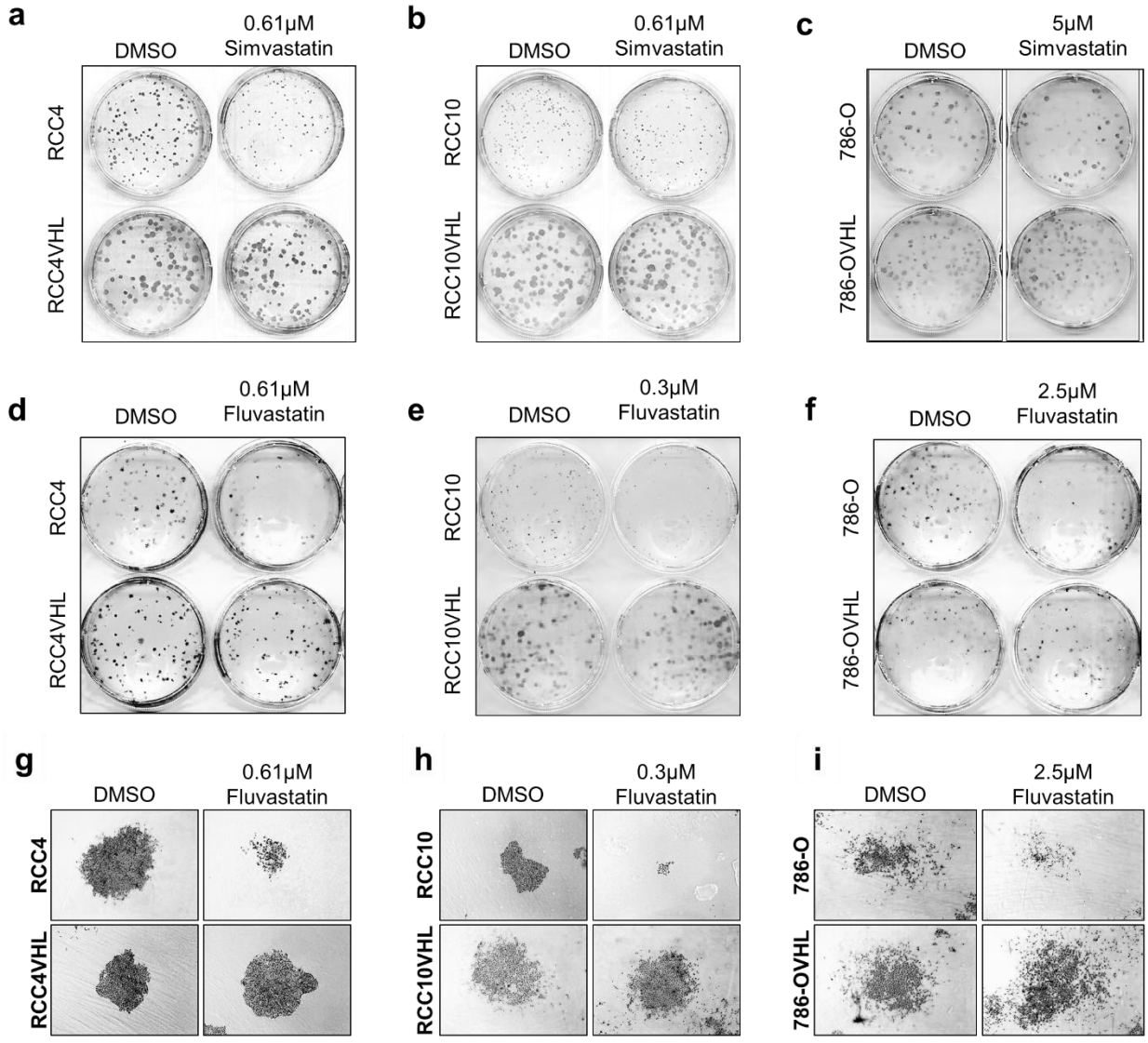

Supplemental Figure 5.2. Simvastatin and Fluvastatin treatment causes synthetic lethality with *VHL* loss in multiple CC-RCC cell lines. Treatment with Simvastatin (a-c) and Fluvastatin (d-f) reduces the colony forming ability of *VHL*-deficient CC-RCC. Representative plates from the clonogenic assays quantified in Figure 5.1 are shown for the indicated compound concentrations for RCC4±VHL (a, d), RCC10±VHL (b, e), 786-O±VHL (c, f) isogenic cell line pairs. (**g**-**i**) Treatment with Fluvastatin reduces *VHL*-deficient CC-RCC's proliferation as shown by the decrease in cell number making up each colony. Representative colonies from the clonogenic assays quantified in Figure 5.1d-f are shown for the indicated Fluvastatin concentrations for RCC4±VHL (**g**), RCC10±VHL (**h**), and 786-O±VHL (**i**) matched cell lines.

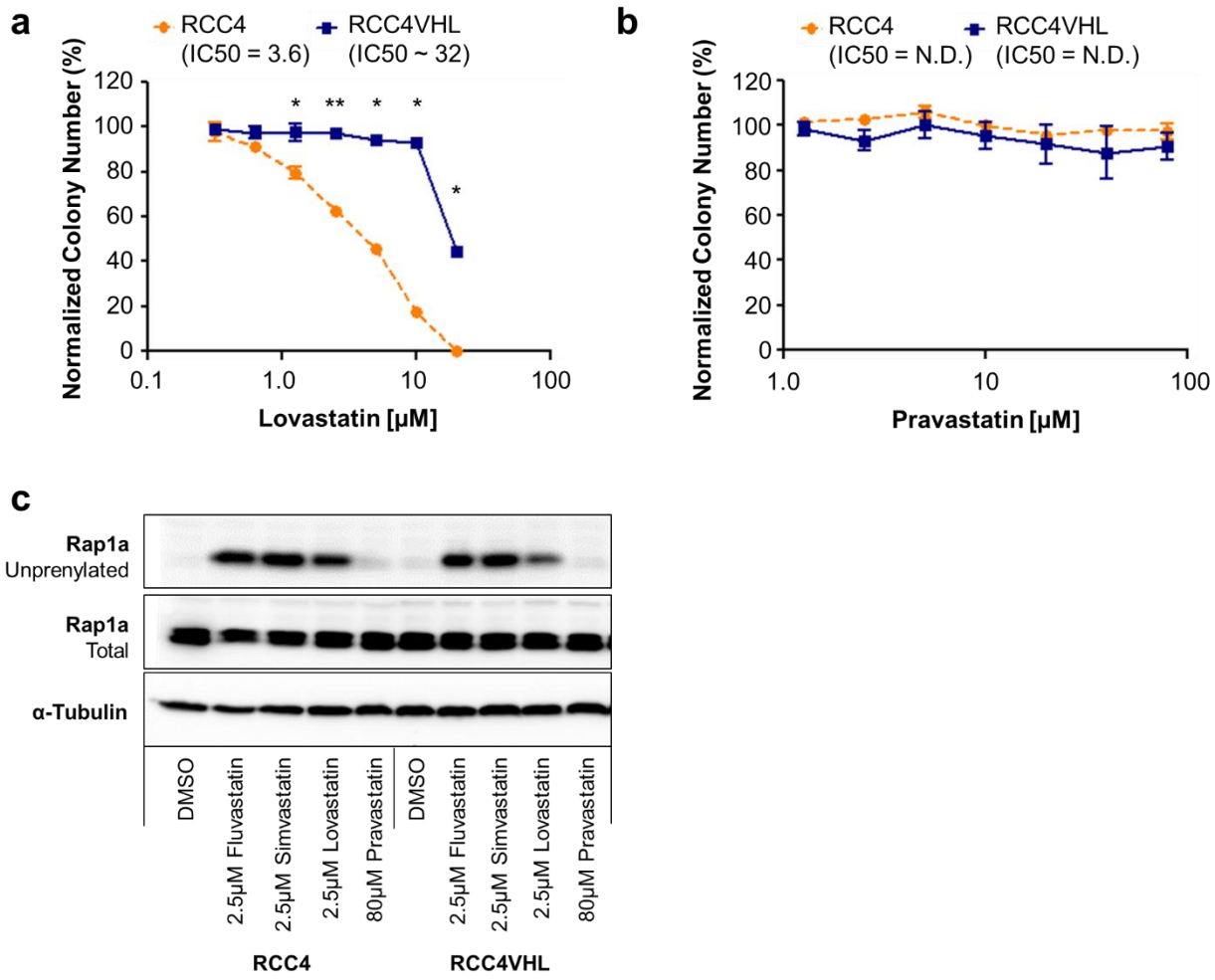

Supplemental Figure 5.3. Lovastatin treatment causes synthetic lethality with *VHL* loss in the RCC4 matched cell line, while Pravastatin does not. Treatment with Lovastatin (a) reduces the colony forming ability of *VHL*-deficient RCC4. (b) Treatment with Pravastatin does not reduce the colony forming ability of either RCC4 or RCC4VHL. Statistical analysis was performed using a paired t-test between the matched cell lines at each dose (* $p < 0.05$, ** $p < 0.01$), SEMs are shown. (c) Western blot showing that Fluvastatin, Simvastatin, and Lovastatin treatments cause the appearance of unprenylated Rap1a, while Pravastatin treatment does not. α-tubulin serves as a loading control.

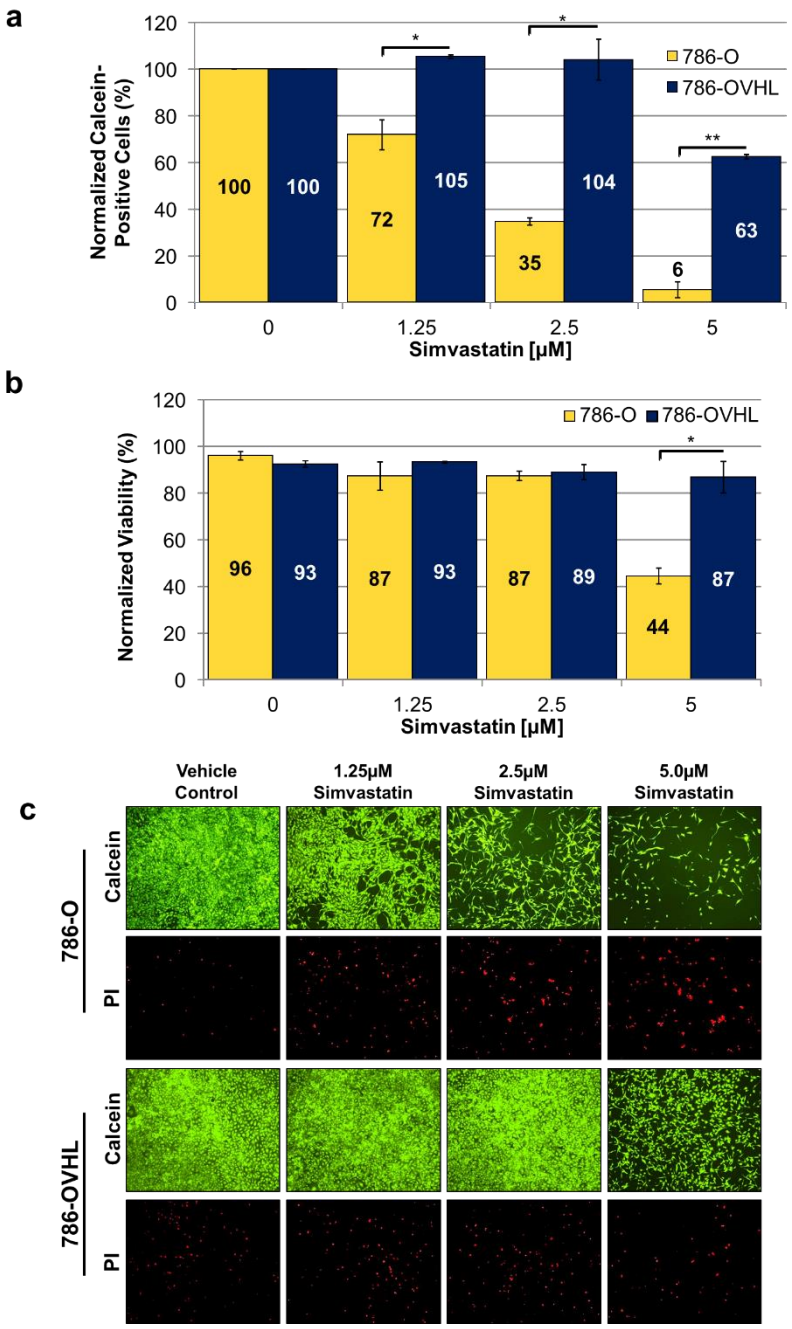

Supplemental Figure 5.4. Statin treatment is cytostatic and cytotoxic in *VHL*-deficient CC-RCC. LIVE/DEAD assay measuring live cell numbers via Calcein staining (**a**) and dead cell numbers via PI staining (**b**) reveals that Simvastatin treatment inhibits 786-O cell proliferation and triggers cell death at low micromolar doses. 786-O±VHL cells were treated with Simvastatin or vehicle control (80%DMSO/20%Ethanol) for 6 days. Calcein-positive cells in (**a**) were normalized to the vehicle control. Normalized % viability in (**b**) was calculated as described in Figure 5.2b. Statistical analysis in (**a**-**b**) was performed using a paired t-test between the matched cell lines at each dose (* $p < 0.05$, ** $p < 0.01$), SEMs are shown. (**c**) Representative images of LIVE/DEAD assay at three Simvastatin doses.

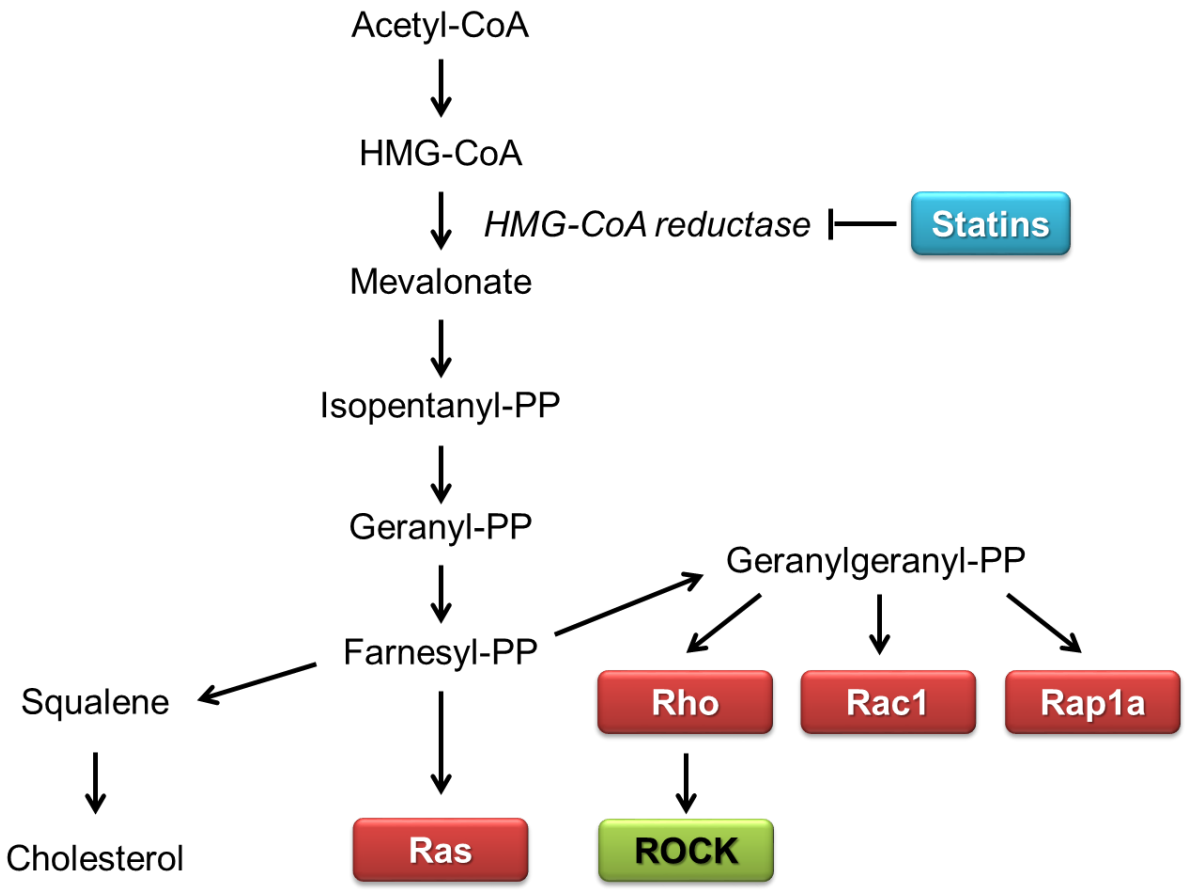

Supplemental Figure 5.5. The mevalonate synthesis pathway. Statins target HMG-CoA reductase, the rate-limiting enzyme in the mevalonate synthesis pathway. Inhibition of mevalonate synthesis decreases the concentration of the isoprenoid geranylgeranyl pyrophosphate, which is required for isoprenylation and intracellular trafficking of GTPases (shown in red). Disruption of GTPase isoprenylation prevents their ability to activate their downstream targets like ROCK. Inhibition of mevalonate synthesis also decreases cholesterol synthesis.

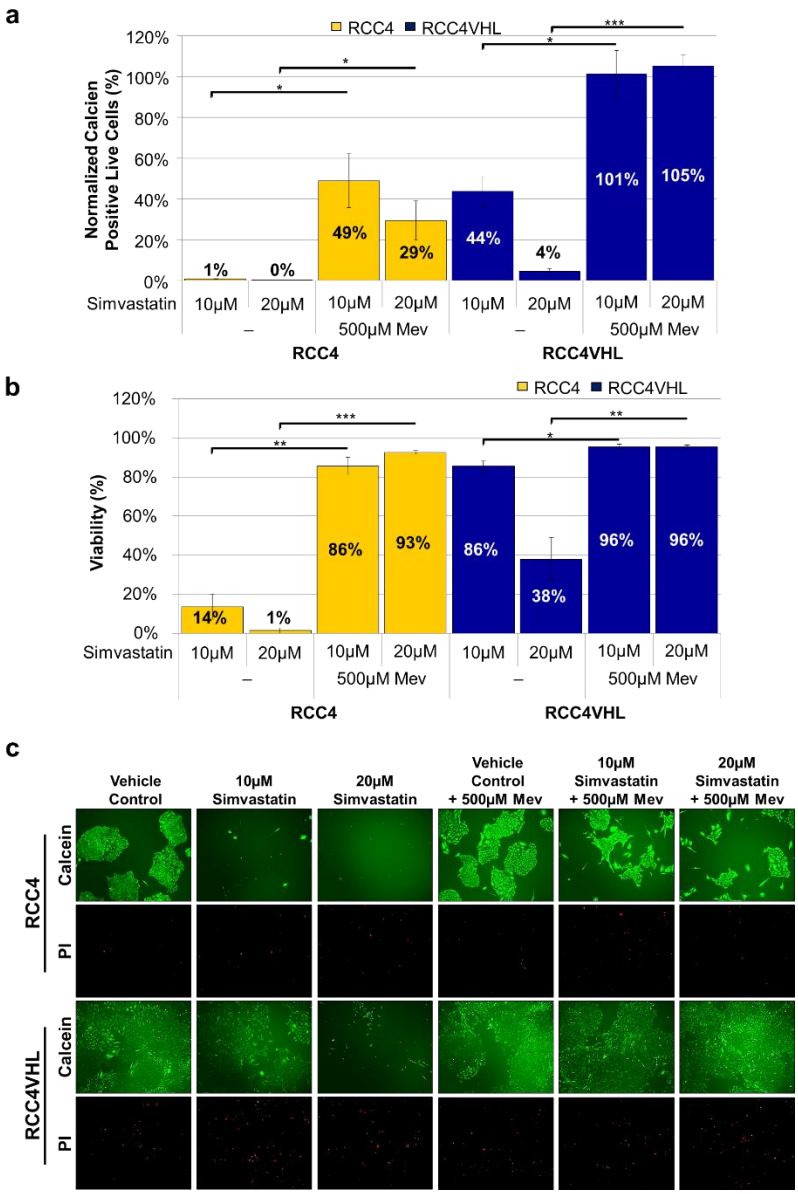

Supplemental Figure 5.6. The cytostatic and cytotoxic effects of Simvastatin can be rescued with Mevalonate. LIVE/DEAD assay measuring live cell numbers via Calcein staining (**a**) and viability via PI staining (**b**) reveals that the coadministration of mevalonate with Simvastatin results in a partial rescue of proliferation in RCC4 cells and a complete rescue in RCC4VHL cells even at high 10 and 20μM doses. LIVE/DEAD assay measuring viability via PI staining (**b**) reveals that the addition of mevalonate completely rescues both RCC4 and RCC4VHL cells from the cytotoxic effects of Simvastatin. (**c**) Representative images of LIVE/DEAD assay with the indicated treatments. RCC4 and RCC4VHL cells were treated with Simvastatin, Simvastatin and mevalonate. or vehicle control (80%DMSO/20%Ethanol) for 6 days. Calcein-positive cells in (**a**) were normalized to the vehicle control. Normalized % viability in (**b**) was calculated as described in Figure 5.2b. Statistical analysis in (**a**-**b**) was performed using a paired t-test between the matched cell lines at each dose (* $p < 0.05$, ** $p < 0.01$, *** $p < 0.001$), SEMs are shown.

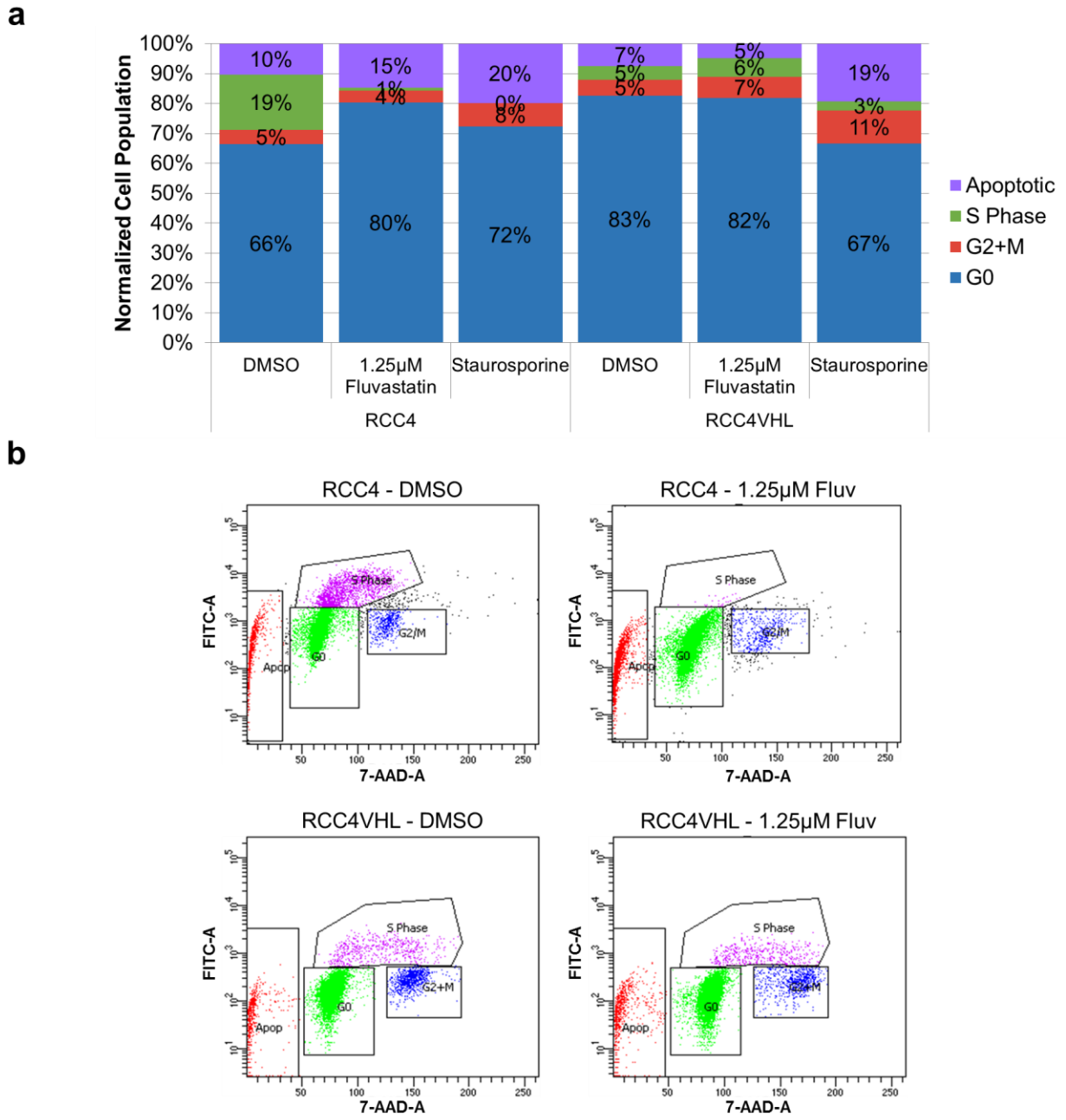

Supplemental Figure 5.7. Statin treatment in *VHL*-deficient CC-RCC cells disrupts cell cycle progression and increases apoptotic/debris cells. (**a**) BrdU assay reveals that statin treatment is both cytotoxic and cytostatic in RCC4. RCC4 cells increase G0 cells, increase apoptotic/debris, and reduce in S phase population upon treatment with Fluvastatin for 6 days as opposed to RCC4VHL. The graph shows the representative experiment of two experiments performed. Treatment with 2μM Staurosporine for 4 hours was used as the positive control. (**b**) Representative flow cytometry plots of the results from the experiment shown in a.

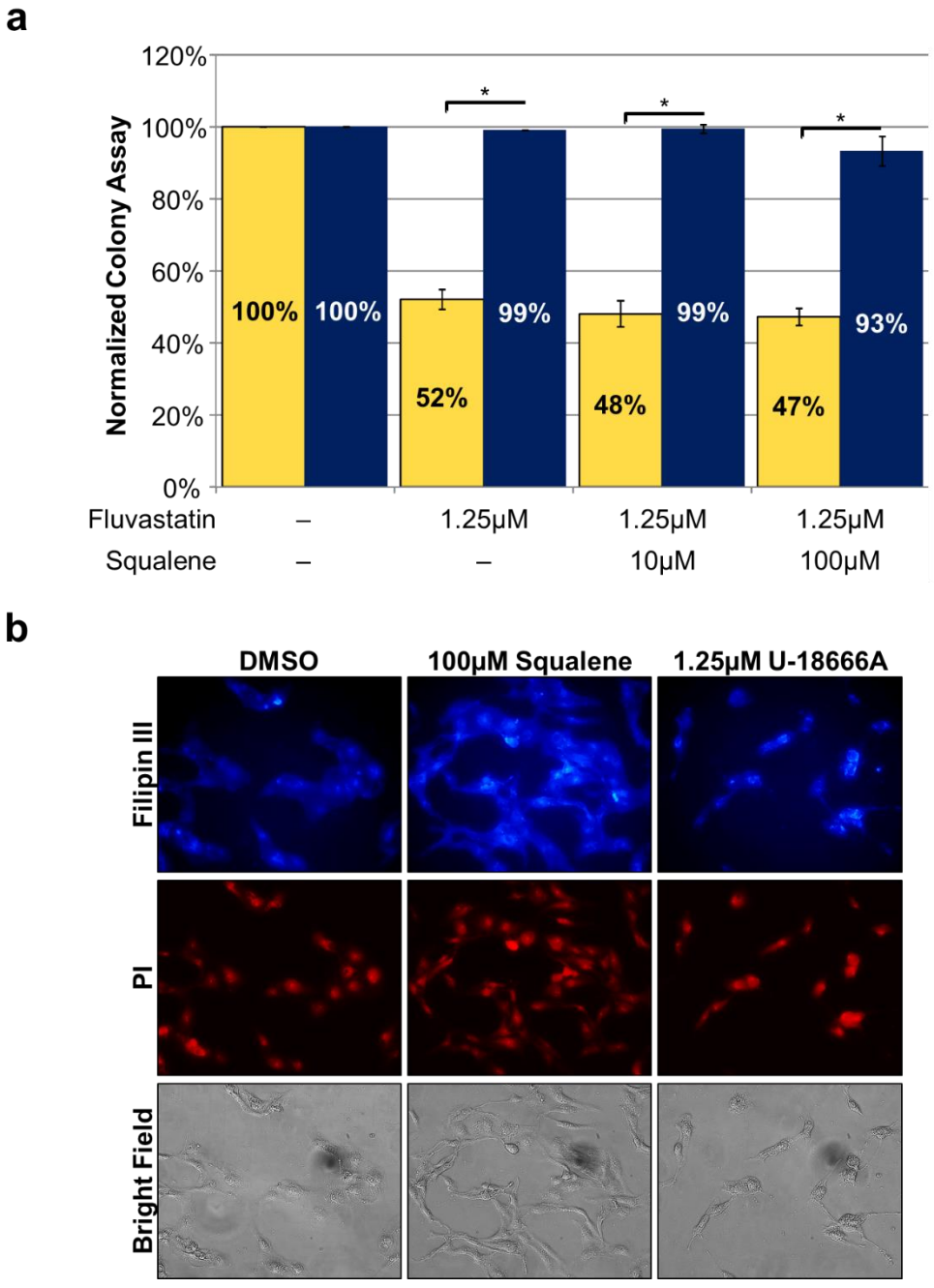

Supplemental Figure 5.8. The effect of statins on cholesterol synthesis is not involved in synthetic lethality with *VHL* loss. (**a**) Addition of up to 1000μM Squalene does not rescue the effect of Fluvastatin on colony forming ability of RCC4 cells. Each dose of Fluvastatin or vehicle control (DMSO) within each experiment was tested in duplicate, and the experiment was repeated two times. Statistical analysis was performed using a paired t-test between the matched cell lines at each dose (* $p < 0.05$), SEMs are shown. (**b**) Squalene is incorporated and converted to

cholesterol in RCC4 cells as shown by increased Filipin III stain intensity in comparison to the DMSO control. U-18666A is a cholesterol trafficking inhibitor (positive control). Propidium Iodide (PI) was used to label cell nuclei.

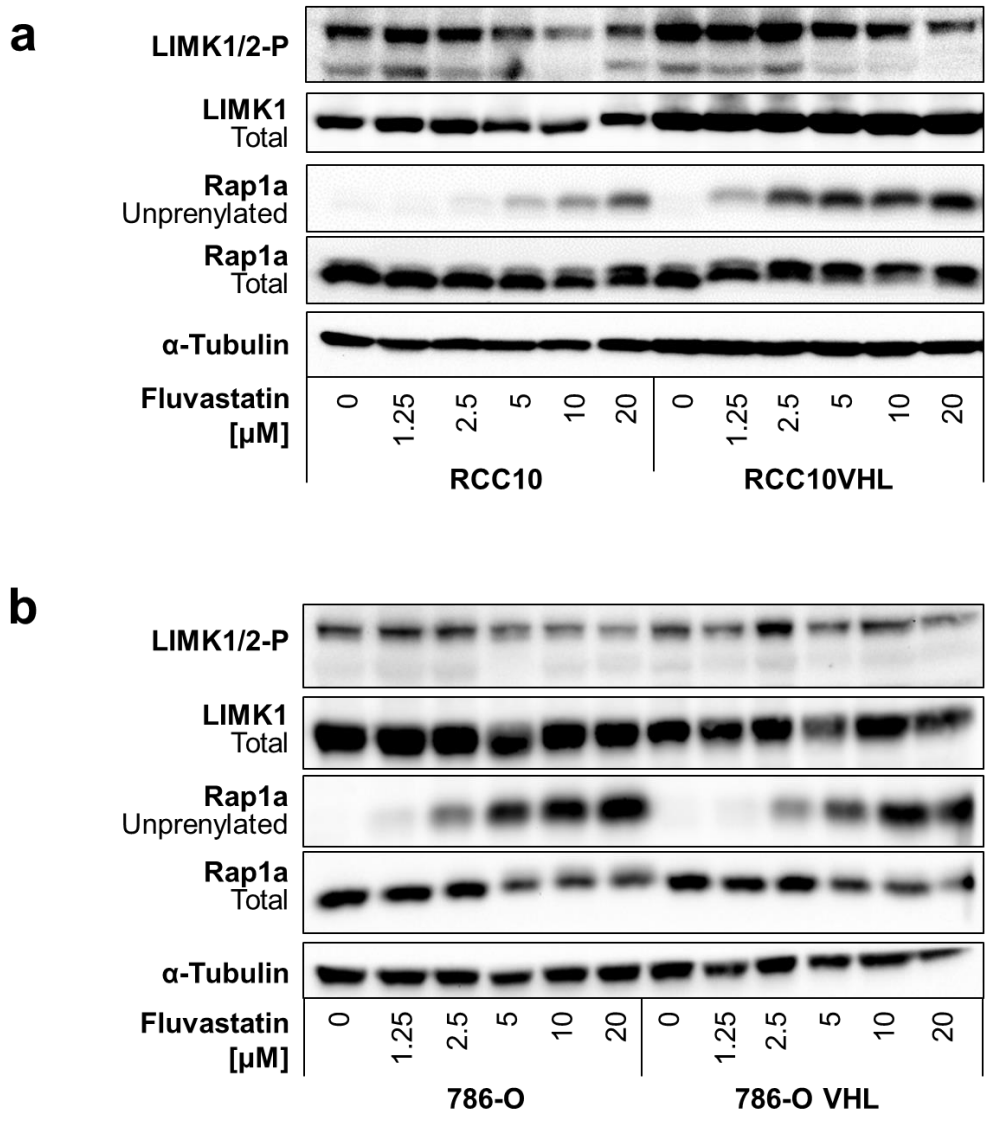

Supplemental Figure 5.9. Treatment with statins inhibits ROCK substrate phosphorylation. Western blot showing that 24h treatment with Fluvastatin is sufficient to inhibit phosphorylation of LIMK1/2 in the RCC10±VHL (**a**) and 786-O±VHL (**b**). Unprenylated RAP1a is used as a readout for the disruption of GTPase isoprenylation by treatment with Fluvastatin. α-tubulin serves as a loading control.

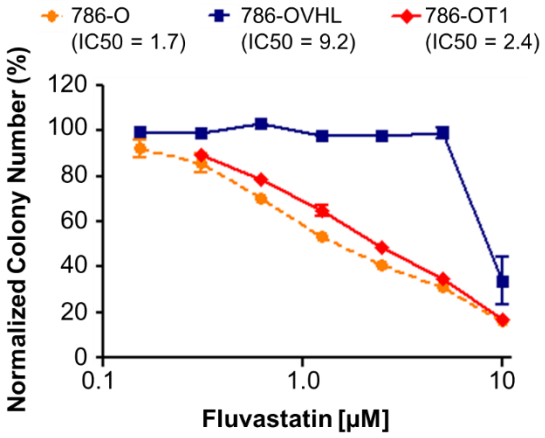

Supplemental Figure 5.10. Fluvastatin causes synthetic lethality with *VHL* loss in 786-OT1 cells similar to 786-O. In a clonogenic assay Fluvastatin shows selective toxicity towards *VHL*-deficient 786-OT1 and 786-O while sparing 786-OVHL cells expressing *VHL*. Each dose within each experiment was tested in duplicate, and each experiment was repeated three times. IC_{50s} are indicated. Statistical analysis was performed using a General Linear Model comparing cell line and treatment followed by Tukey's Post Hoc analysis. A statistically significant difference was observed between 786-OVHL and the two *VHL*-deficient 786-O and 786-OT1 cell lines (*** $p < 0.001$), SEMs are shown.

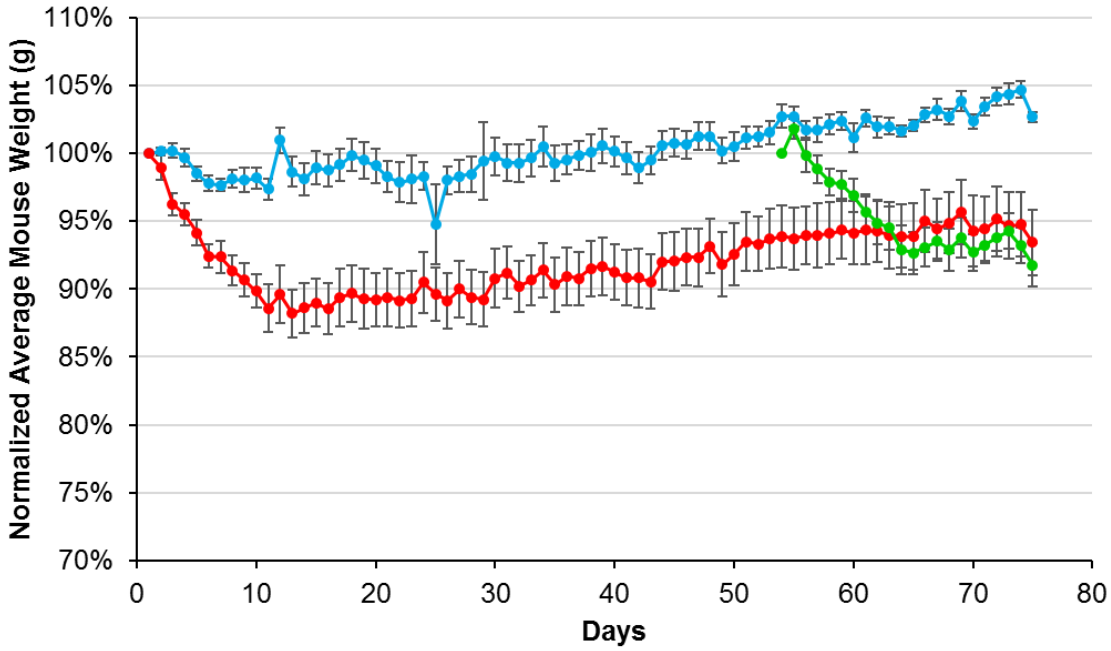

Supplemental Figure 5.11. Fluvastatin treatment causes minimal mouse weight loss during in vivo treatment. Mice were treated daily with PBS/DMSO vehicle (n = 8), 10 mg/kg Fluvastatin (n = 8), or 15mpk Fluvastatin (n=9) by ip injection for up to 75 days. Mouse weight was monitored daily. Fluvastatin treatment causes an initial weight loss upon beginning treatment.

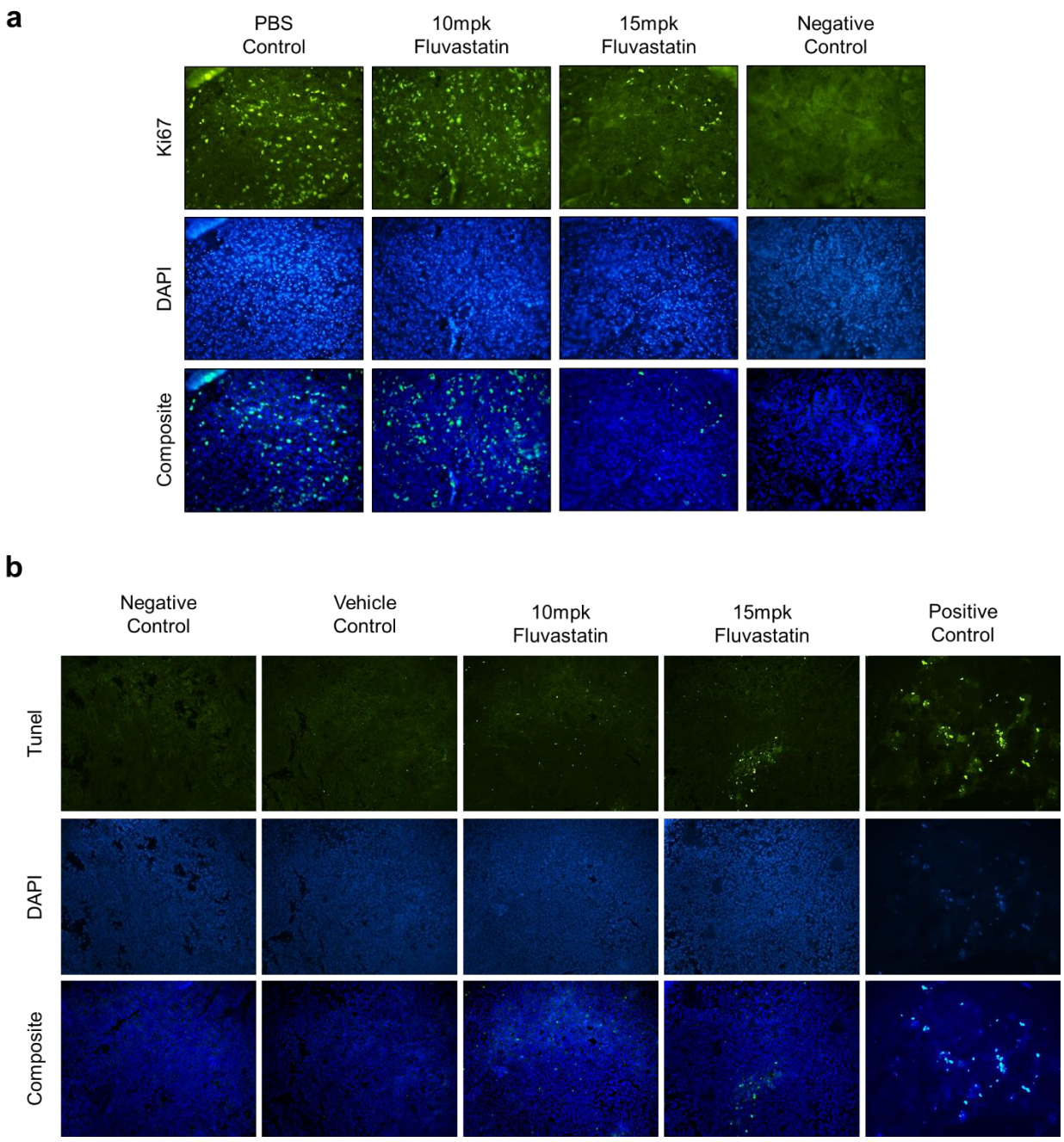

Supplemental Figure 5.12. Fluvastatin inhibits tumor cell proliferation and increases apoptotic cell death *in vivo* at 15mpk. Representative images of (**a**) Ki67 staining with Ki67 in green and DAPI in blue and (**b**) Tunel staining with Tunel in green and DAPI in blue. Images were obtained at 20x.

CHAPTER SIX: CONCLUSIONS AND FUTURE DIRECTIONS

CC-RCC is a devastating disease in its metastatic manifestation with a 5-year survival of less than 15% and approximately one third of patients' tumors will have spread beyond the localized region at the time of diagnosis. Adding to the complexity of treating CC-RCC, traditional chemotherapies, cytokine-based immunotherapy, and radiation therapy have had very limited success in clinic. Current therapies can be differentiated between angiogenesis inhibiting RTKis and mTORi that decrease HIF expression. Next generation therapies revolve around circumventing the rapid resistance that develops to these therapies or in combining currently approved therapies together or with various immunotherapies that are available. With the exception of the newly approved PD-1 inhibitors, which have shown promise, pursuing the same paradigm for treating CC-RCC has had limited success. The focus of this work is to identify new therapies for treating *VHL*-deficient CC-RCC.

We used a synthetic lethality approach in order to identify new molecular targets that when inhibited should not harm healthy, non-tumor, cells that express *VHL*. In Chapter 2 we explored

the different methods that have been employed to successfully identify synthetic lethal interactions in different forms of cancer including chemical compound library screen, shRNA screens, and CRISPR screens. For our own synthetic lethality screen, we used Sigma's annotated LOPAC small molecule library. In Chapter 3, we present the results from the LOPAC screen and the initial validation of the 7 hits that were identified. From the LOPAC screen we identified Y-27632, a ROCK inhibitor, as a top hit.

In Chapter 4, we validated that multiple ROCK inhibitors are synthetically lethal with *VHL* loss in multiple CC-RCC backgrounds and that the effect occurs through ROCK1 and not ROCK2. Inhibition of ROCK1 is both cytotoxic and cytostatic in *VHL*-deficient CC-RCC and treatment with Y-27632 was able to prevent tumor growth *in vivo*. Furthermore, we discovered that the synthetic lethal interaction between ROCK inhibition and *VHL* loss is dependent on HIF signaling and that overexpression of either HIF-1α or HIF-2α is sufficient to cause the effect. These results have important implications for the potential use of ROCK inhibitors in other types of cancer beyond those where *VHL* is lost or mutated and HIFs become overexpressed and overactivated.

Since our data indicate that *VHL* loss causing HIF stabilization sensitizes CC-RCC to ROCK inhibitors, we expect that tumors harboring *VHL* mutations which either completely disrupt VHL function (like those occurring in type 1 VHL disease, e.g. C162F[36]), or specifically disrupt VHL's ability to regulate HIF activity (like those occurring in type 2A disease, e.g. Y98H, Y112H, A149T, T157I, and 2B disease, e.g. Y98N, Y112N[206,207]) will be sensitive to ROCK inhibitors. The resulting overactivation of HIFs in these tumors will make them candidates for ROCK inhibitor-based therapies. Since VHL regulates many targets besides HIFα, including activated epidermal growth factor receptor, RNA Pol II subunits, protein kinase C, and others[119] further

investigation is needed to establish if, in addition to disruption of HIF regulation, disruption of any of these VHL functions by certain missense mutations is important for ROCK inhibitor sensitivity.

Overactivation of HIFs is a frequent event in cancer. Both HIF1α and HIF2α are overexpressed in tumor samples compared to matched normal tissues in multiple cancer types besides CC-RCC including bladder, brain, breast, colon, ovarian, gastric, lung, melanoma, pancreatic, and prostate cancers[190,191]. While HIF activation often occurs in perinecrotic regions of solid tumors that lack adequate vasculature and oxygen supply[47], there are multiple mechanisms by which HIFs are activated under normoxic conditions apart from *VHL* loss. For instance, the loss of *p53* tumor suppressor leads to disruption of human homolog of mouse double minute 2 (HDM2)-mediated degradation of HIFα subunits resulting in HIF overactivation[193]. Similarly, the loss of phosphatase and tensin homolog (PTEN) leads to deregulation of phosphoinositide 3-kinase (PI3K) and protein kinase B (Akt) activity resulting in HIF overactivation[208]. Furthermore, disruption of prolyl hydroxylases (PHDs) by mutations blocks hydroxylation of the HIFα subunits and inhibits VHL-mediated HIFα degradation[46]. Multiple oncogenes that are commonly activated by mutations or overexpressed in cancer have also been shown to result in HIF overactivation, including Ha-ras[194] (via PI3K signaling), v-Src[195], and c-Myc[196]. Although these findings suggest that HIF overactivation occurs frequently in multiple cancers, it is important to keep in mind that the magnitude of HIF activity is often less than in the case of *VHL* loss or hypoxic exposure, which are the main players of the pathway controlling HIF activity[191]. Thus, additional experiments establishing the sensitivity of cancer cell lines with the genetic alterations listed above to ROCK inhibitors in normoxia and hypoxia are required to drive the conclusions on their sensitivity and utility of ROCK inhibitors for their targeting.

Another important factor that needs to be taken into consideration for prediction of sensitivity to ROCK inhibitors is expression of the drug target, ROCK1, in cancers other than CC-RCC. In this respect, elevated ROCK1 expression was reported in breast[139] and prostate[140] cancers at the protein level and lung cancer at the mRNA level[144]. Activating ROCK1 somatic mutations have been also reported in breast and lung cancers[152], affecting the autoinhibitory region of ROCK1, resulting in increased activity even though protein levels remain unchanged. Interestingly, ROCK1 is a HIF-target gene in breast cancer[154], although the regulation likely involves cell-type-specific components since we found ROCK1 expression to be similar in *VHL*-deficient CC-RCC and CC-RCC with re-introduced *VHL*[52]. In addition, overexpression at the mRNA and protein levels of upstream regulators of ROCK – Rho GTPases RhoA and RhoC[51] – occurs in breast, prostate, lung, bladder, colon, ovarian, gastric, melanoma, and pancreatic cancers[209]. While somatic mutations resulting in increased Rho activity are rare[210], regulators of Rho, guanine-nucleotide exchange factors (GEFs), GTPase-activating proteins (GAPs) and guanine-nucleotide dissociation inhibitors (GDIs), can be deregulated in cancer[209] contributing to the activity of the Rho/ROCK pathway. Currently, a specific Rho GTPase inhibitor, Cethrin, was developed for the management of spinal cord injuries compatible with intrathecal delivery[211], but feasibility of its systemic delivery needs evaluation. RhoGTPases can also be targeted indirectly, e.g., by statins (HMG-CoA Reductase inhibitors), which inhibit Rho GTPase isoprenylation and translocation to the plasma membrane[56], although statins are far from being specific towards Rho, and also inhibit Ras and Rac GTPases dependent on isoprenylation[56]. Together, these data suggest that the Rho/ROCK pathway is active and can be targeted in multiple cancer types.

Overall, ROCK and HIF co-activation frequently occurs in a number of cancer types, suggesting that ROCK inhibitors should be effective for targeting those cancers. Accordingly,

ROCK inhibitors have shown an anti-cancer effect in breast[147], prostate[140], ovarian[212], and melanoma[213] cancers both *in vitro* and *in vivo* in mouse models. Recently, AT13148, a multi-kinase inhibitor targeting ROCK and other kinases, has shown an anti-cancer effect in mouse models of breast[164], prostate[164], lung[164], uterine[164], gastric[214], and melanoma[213] types of cancer. Currently, there is an ongoing phase I clinical trial (NCT01585701) of AT13148 administered to breast, prostate, and ovarian cancer patients, which will be evaluated for normal tissue toxicity and possible anti-tumor response. It is likely that the synthetic lethal interaction between ROCK inhibition and HIF overactivation contributes to sensitivity of these forms of cancer to ROCK inhibitors. Additional studies are required to develop reliable markers for prediction of ROCK inhibitor anti-tumor response.

The synthetic lethal interaction between ROCK inhibition and HIF overactivation is important since it justifies ROCK inhibitors as candidate therapeutics for multiple forms of cancer. It is also worth investigating which *VHL* mutations would confer sensitivity to ROCK inhibitors to a degree similar to *VHL* loss in CC-RCC, hemangioblastoma, and pheochromocytoma. Further research is needed to evaluate the impact of the discovered synthetic lethal interaction on sensitivity of other forms of cancer besides CC-RCC to ROCK inhibitors; and develop the plan for patient stratification into ROCK inhibitor-sensitive and -insensitive groups. Upon identifying the synthetic lethal interaction between ROCK1 and VHL we then began to expand our studies to investigate the upstream regulators of ROCK: Rho GTPases.

Overexpression of RhoC and ROCK has been correlated with increased CC-RCC tumor grade, stage, and inversely correlated with overall patient survival[54]. Additionally, VHL has been shown to directly bind RhoC[215] and our own investigations found that VHL can bind RhoA, RhoB, and RhoC and that each Rho can be polyubiquitinated (Luke Nelson, personal communication).

Based on this we hypothesized that inhibiting Rho's would also be synthetically lethal with *VHL* loss. Indeed, knockdown of RhoC in the RCC10 matched cell line triggered the synthetic lethal effect (Luke Nelson, personal communication). Similarly, anti-hypercholesterolemia doses of statins have already been shown to be able to inhibit both Rho and ROCK activity in patients[142]. While the literature is mixed on the usefulness of statins in treating or preventing CC-RCC, multiple studies have found a strong correlation between statin use and decreased risk for CC-RCC[61]. One explanation for the discrepancy observed in the literature is the clear lack of differentiation between the type of statins used in the studies, and the VHL/HIF status of the patients. To this end there is a need for new predictive biomarkers of response (beyond VHL/HIF status) that can be used to stratify patients into responders and non-responders to specific therapies.

Fluvastatin is currently the only statin shown to have a saturable first pass metabolism allowing it to reach low micromolar plasma concentration at the FDA approved hypercholesterolemia doses. Our studies confirmed that the loss of VHL and resulting overactivation of HIFs sensitizes cancer cells to statin treatment. Based on these results and the studies showing statin's ability to inhibit ROCK activity and to reduce CC-RCC risk, we sought to investigate if statins could trigger the synthetic lethal effect with *VHL* loss.

In Chapter 5 we present the results of our investigation showing that statins cause a synthetic lethal effect in *VHL*-deficient CC-RCC. Interestingly, the effect was even more pronounced than that of the ROCK inhibitors resulting in greater therapeutic indexes. Treatment with multiple hydrophobic statins, including Simvastatin, Fluvastatin, and Lovastatin, caused the synthetic lethal effect in multiple CC-RCC genetic backgrounds. We found that treatment with statins is cytostatic at low nanomolar doses and becomes cytotoxic as the dose is increased to low micromolar concentrations. Statin treatment could be rescued with the addition of both Mevalonate

and GGPP, but not Squalene, indicating that the synthetic lethal effect is due to statin's disruption of small GTPase isoprenylation and trafficking to the cellular membrane. Statin treatment was also HIF-dependent similar to ROCK inhibitors, and overactivation of ROCK with arachidonic acid could partially rescue the effect. Treatment with statins *in vivo* resulted in both decreased/delayed initial tumor formation and tumor regression in established tumors although we observed drug resistance in tumors treated with statins for a prolonged period of time. These results indicate that patients taking lipophilic statins may already be benefiting from the synthetic lethal effect, but also that patients who have developed CC-RCC while taking statins would likely be resistant to the therapy.

While the results from our *in vivo* experiments in Chapters 4 and 5 indicate that ROCK inhibitors and hydrophobic statins may be promising therapies it is unlikely that they would be used as single agents in the clinic. Due to this, there is a need to test them in combination with the current standard of care (mTORi, RTKi, and PD-1 inhibitors) to see if any synergistic effects occur. We tested Sorafenib Tosylate (RTKi), Axitinib (RTKi), Everolimus (mTORi), and Gefitinib (EGFR inhibitor) for synthetical lethality using clonogenic assays with the RCC10 and 786-O matched cell lines and did not observe a synthetic lethal effect with any of the compounds (data not shown). We then tested each of the compounds in combination with Y-27632 in RCC10 clonogenic assays and found a better than additive effect in the RCC10 line while RCC10VHL cells had an additive effect (data not shown). This may indicate that a combination therapy including mTORi and ROCKi could be a potential therapy, but these results need to be investigated more thoroughly in multiple CC-RCC matched lines. Additionally, combination treatment of statins with currently approved therapies still needs to be investigated.

In order to extend our findings further investigation into the molecular interaction between Rho/ROCK and VHL is needed. Since statins are more effective than ROCK inhibitors, it is likely that additional small GTPases are involved in the synthetic lethal effect. We expect that additional synthetic lethal partners exist within this group, which might have a better therapeutic window. The use of a small siRNA library to knockdown each of the small GTPases that are isoprenylated by the mevalonate pathway may help elucidate these targets. While the focus of our studies has been on *VHL*-deficient CC-RCC, there are other mutations that play an important role in the progression of the disease.

Another future direction of these projects is to test ROCKi and statins with patient-derived samples in vitro and to establish Patient-Derived Xenograft (PDX) models to use in testing the compounds. The *in vivo* studies conducted in Chapters 4 and 5 were conducted in RAG1$^{-/-}$ mice, which lack T and B cells but still have natural killer (NK) cells. Testing in another mouse background may identify if NK cells were involved in the anti-cancer response. Recently, two new autochthonous models of CC-RCC have been generated in mice. These autochthonous models spontaneously form tumors in the kidney due to homozygous loss of *Vhl*, *Trp53*, and *Rb1* deletion[216] or *VHL* and *Pbrm1*[217]. Use of these models would allow us to investigate the effects of treatment with ROCKi and statins in mice with an intact immune system. It would also serve as a better model for investigating if statin treatment reduces the risk of, or delays, initial tumor CC-RCC tumor formation.

There is a need to identify the molecular pathways the advanced stage RCC depends on for survival. While *VHL* loss has been shown to be an early driver of RCC pathogenesis[32], other genes have also been implicated as drivers of the disease, including overexpression of the Hepatocyte Growth Factor Receptor (*HGFR*)[218] and the loss of the Fructose-1,6-Bisphosphatase (*FBP1*)[219].

Drug library screens to identify drugs that selectively target these mutations could allow for the development of new therapies. Multiple screens have been performed in order to identify drugs that selectively target *VHL*-deficient RCC while sparing the same cell line with *VHL* re-expressed [83,84,113,124], but to date no screens have been conducted for *FBP1* or *HGFR* synthetic lethality. For example, new molecular targets may be identified in drug library screens where both *VHL* and *FBP1* are re-expressed in an RCC cell line that lacks them since both are functionally lost in over 90% of RCC patients.

Improving our understanding of the basic biology that drives RCC development and pathogenesis is vital to developing new therapies. Instead of relying on angiogenesis inhibitors to slow the growth and metastasis of these tumors, there is a need for targeted molecular therapies that will selectively kill the cancerous cells while sparing the patient's healthy tissue.

REFERENCES

1 Howlader N, Noone AM, Krapcho M, Miller D, Bishop K, Kosary CL, Yu M, Ruhl J, Tatalovich Z, Mariotto A, Lewis DR, Chen HS, Feuer EJ, Cronin KA (eds). SEER Cancer Statistics Review, 1975-2014, National Cancer Institute. Bethesda, MD, https://seer.cancer.gov/csr/1975_2014/, based on November 2016 SEER data submission, posted to the SEER web site, April 2017.

2 Chow W, Dong L, Devesa S. Epidemiology and risk factors for kidney cancer. *Nat Rev Urol* 2010; **7**: 245–257.

3 Coppin C, Porzsolt F, Autenrieth M, Kumpf J, Coldman A, Wilt T. Immunotherapy for advanced renal cell cancer. *Cochrane Database Syst Rev* 2004.

4 Rosenberg SA, Yang JC, White DE, Steinberg SM. Durability of complete responses in patients with metastatic cancer treated with high-dose interleukin-2: identification of the antigens mediating response. *Ann Surg* 1998; **228**: 307–319.

5 Motzer RJ, Escudier B, McDermott DF, George S, Hammers HJ, Srinivas S *et al.* Nivolumab versus Everolimus in Advanced Renal-Cell Carcinoma. *N Engl J Med* 2015; : 1803–1813.

6 McDermott DF, Regan MM, Clark JI, Flaherty LE, Weiss GR, Logan TF *et al.* Randomized phase III trial of high-dose interleukin-2 versus subcutaneous interleukin-2 and interferon in patients with metastatic renal cell carcinoma. *J Clin Oncol* 2005; **23**: 133–141.

7 Hutson TE. Targeted therapies for the treatment of metastatic renal cell carcinoma: clinical evidence. *Oncologist* 2011; **16 Suppl 2**: 14–22.

8 Linehan WM, Rubin JS, Bottaro DP. VHL loss of function and its impact on oncogenic signaling networks in clear cell renal cell carcinoma. *Int J Biochem Cell Biol* 2009; **41**: 753–756.

9 Sun M, Shariat SF, Cheng C, Ficarra V, Murai M, Oudard S *et al.* Prognostic factors and predictive models in renal cell carcinoma: A contemporary review. *Eur Urol* 2011; **60**: 644–661.

10 Chambers AF, Groom AC, MacDonald IC. Metastasis: Dissemination and growth of cancer cells in metastatic sites. *Nat Rev Cancer* 2002; **2**: 563–572.

11 Escudier B, Eisen T, Stadler W, Szczylik C, Oudard S, Siebels M *et al.* Sorafenib in Advanced Clear-Cell Renal-Cell Carcinoma. *N Engl JMed* 2007; **456**: 125–134.

12 Motzer RJ, Hutson TE, Cella D, Reeves J, Hawkins R, Guo J *et al.* Pazopanib versus Sunitinib in Metastatic Renal-Cell Carcinoma. *N Engl J Med* 2013; **369**: 722–731.

13 Escudier B, Gore M. Axitinib for the management of metastatic renal cell carcinoma. *Drugs R D* 2011; **11**: 113–126.

14 Criscitiello C, Esposito A, De Placido S, Curigliano G. Targeting fibroblast growth factor receptor pathway in breast cancer. *Curr Opin Oncol* 2015; **27**: 452–6.

15 Motzer RJ, Hutson TE, Glen H, Michaelson MD, Molina A, Eisen T *et al.* Lenvatinib, everolimus, and the combination in patients with metastatic renal cell carcinoma: A randomised, phase 2, open-label, multicentre trial. *Lancet Oncol* 2015; **16**: 1473–1482.

16 Xie Z, Lee YH, Boeke M, Jilaveanu LB, Liu Z, Bottaro DP *et al.* MET inhibition in clear cell renal cell carcinoma. *J Cancer* 2016; **7**: 1205–1214.

17 Choueiri TK, Escudier B, Powles T, Tannir NM, Mainwaring PN, Rini BI *et al.* Cabozantinib versus everolimus in advanced renal cell carcinoma (METEOR): final

results from a randomised, open-label, phase 3 trial. *Lancet Oncol* 2016; **17**: 917–927.
18 McKay RR, Lin X, Albiges L, Fay AP, Kaymakcalan MD, Mickey SS *et al.* Statins and survival outcomes in patients with metastatic renal cell carcinoma. *Eur J Cancer* 2016; **52**: 155–162.
19 Motzer RJ, Escudier B, Oudard S, Hutson TE, Porta C, Bracarda S *et al.* Phase 3 trial of everolimus for metastatic renal cell carcinoma: Final results and analysis of prognostic factors. *Cancer* 2010; **116**: 4256–4265.
20 Lin F, Zhang PL, Yang XJ, Prichard JW, Lun M, Brown RE. Morphoproteomic and molecular concomitants of an overexpressed and activated mTOR pathway in renal cell carcinomas. *Ann Clin Lab Sci* 2006; **36**: 283–293.
21 Sudarshan S, Karam J a., Brugarolas J, Thompson RH, Uzzo R, Rini B *et al.* Metabolism of kidney cancer: From the lab to clinical practice. *Eur Urol* 2013; **63**: 244–251.
22 Rini BI, Atkins MB. Resistance to targeted therapy in renal-cell carcinoma. *Lancet Oncol* 2009; **10**: 992–1000.
23 Eto M, Kawano Y, Hirao Y, Mita K, Arai Y, Tsukamoto T *et al.* Phase II clinical trial of sorafenib plus interferon-alpha treatment for patients with metastatic renal cell carcinoma in Japan. *BMC Cancer* 2015; **15**: 667.
24 Ryan CW, Goldman BH, Lara Jr. PN, Mack PC, Beer TM, Tangen CM *et al.* Sorafenib with interferon alfa-2b as first-line treatment of advanced renal carcinoma: a phase II study of the Southwest Oncology Group. *J Clin Oncol* 2007; **25**: 3296–3301.
25 Escudier B, Pluzanska A, Koralewski P, Ravaud A, Bracarda S, Szczylik C *et al.* Bevacizumab plus interferon alfa-2a for treatment of metastatic renal cell carcinoma: a randomised, double-blind phase III trial. *Lancet* 2007; **370**: 2103–2111.
26 Azad NS, Posadas EM, Kwitkowski VE, Steinberg SM, Jain L, Annunziata CM *et al.* Combination targeted therapy with sorafenib and bevacizumab results in enhanced toxicity and antitumor activity. *J Clin Oncol* 2008; **26**: 3709–3714.
27 Patel PH, Senico PL, Curiel RE, Motzer RJ. Phase I Study Combining Treatment with Temsirolimus and Sunitinib Malate in Patients with Advanced Renal Cell Carcinoma. 2013; **18**: 1199–1216.
28 Rini BI, Garcia J a, Cooney MM, Elson P, Tyler A, Beatty K *et al.* A phase I study of sunitinib plus bevacizumab in advanced solid tumors. *Clin Cancer Res* 2009; **15**: 6277–6283.
29 Kuznar W. Lenvatinib Extends Survival in Metastatic Renal-Cell Carcinoma. *Am Heal drug benefits* 2015; **8**: 18.
30 Buczek M, Escudier B, Bartnik E, Szczylik C, Czarnecka A. Resistance to tyrosine kinase inhibitors in clear cell renal cell carcinoma: from the patient's bed to molecular mechanisms. *Biochim Biophys Acta* 2014; **1845**: 31–41.
31 Chan D a, Giaccia AJ. Harnessing synthetic lethal interactions in anticancer drug discovery. *Nat Rev Drug Discov* 2011; **10**: 351–64.
32 Cowey CL, Rathmell WK. VHL gene mutations in renal cell carcinoma: Role as a biomarker of disease outcome and drug efficacy. *Curr Oncol Rep* 2009; **11**: 94–101.
33 Gossage L, Eisen T, Maher ER. VHL, the story of a tumour suppressor gene. *Nat Rev Cancer* 2014; **15**: 55–64.
34 Lonser RR, Glenn GM, Walther M, Chew EY, Libutti SK, Linehan WM *et al.* Von Hippel-Lindau disease. *Lancet* 2003; **361**: 2059–2067.
35 Maher ER, Neumann HP, Richard S. von Hippel-Lindau disease: a clinical and scientific

review. *Eur J Hum Genet* 2011; **19**: 617–23.
36 Knauth K, Cartwright E, Freund S, Bycroft M, Buchberger A. VHL mutations linked to type 2C von Hippel-Lindau disease cause extensive structural perturbations in pVHL. *J Biol Chem* 2009; **284**: 10514–10522.
37 Kaelin WG. Molecular basis of the VHL hereditary cancer syndrome. *Nat Rev Cancer* 2002; **2**: 673–682.
38 Shuin T, Kondo K, Torigoe S, Kishida T, Kubota Y, Hosaka M *et al.* Frequent somatic mutations and loss of heterozygosity of the von Hippel-Lindau tumor suppressor gene in primary human renal cell carcinomas. *Cancer Res* 1994; **54**: 2852–2855.
39 Nickerson ML, Jaeger E, Shi Y, Durocher J a., Mahurkar S, Zaridze D *et al.* Improved identification of von Hippel-Lindau gene alterations in clear cell renal tumors. *Clin Cancer Res* 2008; **14**: 4726–4734.
40 Gnarra JR, Tory K, Weng Y, Schmidt L, Wei MH, Li H *et al.* Mutations of the VHL tumour suppressor gene in renal carcinoma. *Nat Genet* 1994; **7**: 85–90.
41 Marshall FF. Promoter hypermethylation profile of kidney cancer. *J Urol* 2005; **174**: 484–485.
42 Herman JG, Latif F, Weng Y, Lerman MI, Zbar B, Liu S *et al.* Silencing of the VHL tumor-suppressor gene by DNA methylation in renal carcinoma. *Proc Natl Acad Sci U S A* 1994; **91**: 9700–4.
43 Network CGAR. Comprehensive molecular characterization of clear cell renal cell carcinoma. *Nature* 2013; **499**: 43–49.
44 Gordan J, Lal P, Dondeti V, Letrero R. HIF-α Effects on c-Myc Distinguish Two Subtypes of Sporadic VHL-Deficient Clear Cell Renal Carcinoma. *Cancer Cell* 2008; **14**: 435–446.
45 Ivan M, Kondo K, Yang H, Kim W, Valiando J, Ohh M *et al.* HIFalpha targeted for VHL-mediated destruction by proline hydroxylation: implications for O2 sensing. *Science* 2001; **292**: 464–8.
46 Chan DA, Sutphin PD, Denko NC, Giaccia AJ. Role of prolyl hydroxylation in oncogenically stabilized hypoxia-inducible factor-1α. *J Biol Chem* 2002; **277**: 40112–40117.
47 Semenza GL. Targeting HIF-1 for cancer therapy. *Nat Rev Cancer* 2003; **3**: 721–32.
48 Kapitsinou PP, Haase VH. The VHL tumor suppressor and HIF: insights from genetic studies in mice. *Cell Death Differ* 2008; **15**: 650–659.
49 Thompson JM, Nguyen QH, Singh M, Razorenova O. Approaches to Identifying Synthetic Lethal Interactions in Cancer. *Yale J Biol Med* 2015; **88**: 1–11.
50 Amin E, Dubey BN, Zhang SC, Gremer L, Dvorsky R, Moll JM *et al.* Rho-kinase: Regulation, (dys)function, and inhibition. *Biol Chem* 2013; **394**: 1399–1410.
51 Morgan-Fisher M, Wewer UM, Yoneda A. Regulation of ROCK activity in cancer. *J Histochem Cytochem* 2013; **61**: 185–98.
52 Thompson JM, Nguyen QH, Singh M, Pavesic MW, Nesterenko I, Nelson LJ *et al.* Rho-associated kinase 1 inhibition is synthetically lethal with von Hippel-Lindau deficiency in clear cell renal cell carcinoma. *Oncogene* 2016; **36**: 1080–1089.
53 Thompson JM, Landman J, Razorenova O V. Targeting the RhoGTPase / ROCK pathway for the treatment of VHL / HIF pathway-driven cancers. *Small GTPases* 2017; **1248**.
54 Abe H, Kamai T, Tsujii T, Nakamura F, Mashidori T, Mizuno T *et al.* Possible role of the RhoC/ROCK pathway in progression of clear cell renal cell carcinoma. *Biomed Res* 2008;

29: 155–61.
55 Danesh FR, Sadeghi MM, Amro N, Philips C, Zeng L, Lin S *et al.* 3-Hydroxy-3-methylglutaryl CoA reductase inhibitors prevent high glucose-induced proliferation of mesangial cells via modulation of Rho GTPase/ p21 signaling pathway: Implications for diabetic nephropathy. *Proc Natl Acad Sci U S A* 2002; **99**: 8301–8305.
56 Rikitake Y, Liao JK. Rho GTPases, statins, and nitric oxide. *Circ Res* 2005; **97**: 1232–1235.
57 Liu P, Liu Y, Lin L, Chen J. Evidence for Statin Pleiotropy in Humans: Differential Effects of Statins and Ezetimibe on Rho-Associated Coiled-Coil Containing Protein Kinase Activity, Endothelial Function, and Inflammation. *Inflammation* 2009; **119**: 131–138.
58 Chao-Yung Wang, Ping-Yen Liu JKL. Pleiotropic effects of statin therapy. 2009; **14**: 37–44.
59 Blais L, Desgagné A. 3-Hydroxy-3-Methylglutaryl Coenzyme A Reductase Inhibitors and the Risk of Cancer. *Arch Intern Med* 2000; **160**: 2363.
60 Graaf MR, Beiderbeck AB, Egberts ACG, Richel DJ, Guchelaar HJ. The risk of cancer in users of statins. *J Clin Oncol* 2004; **22**: 2388–2394.
61 Khurana V, Caldito G, Ankem M. Statins Might Reduce Risk of Renal Cell Carcinoma in Humans: Case-Control Study of 500,000 Veterans. *Urology* 2008; **71**: 118–122.
62 Sharma S V, Settleman J. Oncogene addiction: setting the stage for molecularly targeted cancer therapy. *Genes Dev* 2007; **21**: 3214–31.
63 Weinstein IB, Joe AK. Mechanisms of disease: Oncogene addiction--a rationale for molecular targeting in cancer therapy. *Nat Clin Pract Oncol* 2006; **3**: 448–57.
64 Hanahan D, Weinberg R a. Hallmarks of cancer: the next generation. *Cell* 2011; **144**: 646–74.
65 Reddy A, Jr WK. Using cancer genetics to guide the selection of anticancer drug targets. *Curr Opin Pharmacol* 2002; : 366–373.
66 Helleday T, Petermann E, Lundin C, Hodgson B, Sharma R a. DNA repair pathways as targets for cancer therapy. *Nat Rev Cancer* 2008; **8**: 193–204.
67 Hosoya N, Miyagawa K. Targeting DNA damage response in cancer therapy. *Cancer Sci* 2014; **105**: 370–88.
68 Block KI, Koch AC, Mead MN, Tothy PK, Newman R a, Gyllenhaal C. Impact of antioxidant supplementation on chemotherapeutic toxicity: a systematic review of the evidence from randomized controlled trials. *Int J Cancer* 2008; **123**: 1227–39.
69 Hartman J, Garvik B, Hartwell L. Principles for the buffering of genetic variation. *Science (80-)* 2001; **1001**: 1001–1004.
70 Boone C, Bussey H, Andrews BJ. Exploring genetic interactions and networks with yeast. *Nat Rev Genet* 2007; **8**: 437–49.
71 Steckel M, Molina-Arcas M, Weigelt B, Marani M, Warne PH, Kuznetsov H *et al.* Determination of synthetic lethal interactions in KRAS oncogene-dependent cancer cells reveals novel therapeutic targeting strategies. *Cell Res* 2012; **22**: 1227–45.
72 Luo J, Emanuele MJ, Li D, Creighton CJ, Schlabach MR, Westbrook TF *et al.* A genome-wide RNAi screen identifies multiple synthetic lethal interactions with the Ras oncogene. *Cell* 2009; **137**: 835–48.
73 Mair B, Kubicek S, Nijman SMB. Exploiting epigenetic vulnerabilities for cancer therapeutics. *Trends Pharmacol Sci* 2014; **35**: 136–45.

74 Chan N, Pires IM, Bencokova Z, Coackley C, Luoto KR, Bhogal N *et al.* Contextual synthetic lethality of cancer cell kill based on the tumor microenvironment. *Cancer Res* 2010; **70**: 8045–54.
75 Krawczyk PM, Eppink B, Essers J, Stap J, Rodermond H, Odijk H *et al.* Mild hyperthermia inhibits homologous recombination, induces BRCA2 degradation, and sensitizes cancer cells to poly (ADP-ribose) polymerase-1 inhibition. *Proc Natl Acad Sci U S A* 2011; **108**: 9851–6.
76 Bryant H, Schultz N, Thomas H. Specific killing of BRCA2-deficient tumours with inhibitors of poly (ADP-ribose) polymerase. *Nature* 2005; **7**: 913–918.
77 Farmer H, Mccabe N, Lord CJ. Targeting the DNA repair defect in BRCA mutant cells as a therapeutic strategy. 2005; **239**: 236–239.
78 Ellisen L. PARP inhibitors in cancer therapy: promise, progress, and puzzles. *Cancer Cell* 2011; **19**: 165–167.
79 Luvero D, Milani A, Ledermann J a. Treatment options in recurrent ovarian cancer: latest evidence and clinical potential. *Ther Adv Med Oncol* 2014; **6**: 229–39.
80 Ledermann J, Harter P. Olaparib maintenance therapy in platinum-sensitive relapsed ovarian cancer. *... Engl J ...* 2012.
81 Ledermann J, Harter P, Gourley C, Friedlander M, Vergote I, Rustin G *et al.* Olaparib maintenance therapy in patients with platinum-sensitive relapsed serous ovarian cancer: a preplanned retrospective analysis of outcomes by BRCA status in a randomised phase 2 trial. *Lancet Oncol* 2014; **15**: 852–61.
82 Leibowitz B, Qiu W, Buchanan ME, Zou F, Vernon P, Moyer MP *et al.* BID mediates selective killing of APC-deficient cells in intestinal tumor suppression by nonsteroidal antiinflammatory drugs. *Proc Natl Acad Sci U S A* 2014; : 1–6.
83 Turcotte S, Chan DD a, Sutphin PPD, Hay MMP, Denny W a, Giaccia AJ. A molecule targeting VHL-deficient renal cell carcinoma that induces autophagy. *Cancer Cell* 2008; **14**: 90–102.
84 Chan D a, Sutphin PD, Nguyen P, Turcotte S, Lai EW, Banh A *et al.* Targeting GLUT1 and the Warburg effect in renal cell carcinoma by chemical synthetic lethality. *Sci Transl Med* 2011; **3**: 94ra70.
85 Jacquemont C, Simon J a, D'Andrea AD, Taniguchi T. Non-specific chemical inhibition of the Fanconi anemia pathway sensitizes cancer cells to cisplatin. *Mol Cancer* 2012; **11**: 26.
86 Rabik C, Dolan M. Molecular mechanisms of resistance and toxicity associated with platinating agents. *Cancer Treat Rev* 2007; **33**: 9–23.
87 Dhillon K, Swisher E, Taniguchi T. Secondary mutations of BRCA1/2 and drug resistance. *Cancer Sci* 2011; **102**: 663–669.
88 Agarwal R, Kaye SB. Ovarian cancer: strategies for overcoming resistance to chemotherapy. *Nat Rev Cancer* 2003; **3**: 502–16.
89 Kranz D, Boutros M. A synthetic lethal screen identifies FAT 1 as an antagonist of caspase- 8 in extrinsic apoptosis. 2014; **33**: 181–197.
90 Igney FH, Krammer PH. Death and anti-death: tumour resistance to apoptosis. *Nat Rev Cancer* 2002; **2**: 277–88.
91 Fesik SW. Promoting apoptosis as a strategy for cancer drug discovery. *Nat Rev Cancer* 2005; **5**: 876–85.
92 Josse R, Martin SE, Guha R, Ormanoglu P, Pfister TD, Reaper PM *et al.* The ATR

inhibitors VE-821 and VX-970 sensitize cancer cells to topoisomerase I inhibitors by disabling DNA replication initiation and fork elongation responses. *Cancer Res* 2014.
93 Pommier Y. Topoisomerase I inhibitors: camptothecins and beyond. *Nat Rev Cancer* 2006; **6**: 789–802.
94 Pommier Y. Drugging topoisomerases: lessons and challenges. *ACS Chem Biol* 2013; **8**: 82–95.
95 Scholl C, Fröhling S, Dunn IF, Schinzel AC, Barbie D a, Kim SY *et al.* Synthetic lethal interaction between oncogenic KRAS dependency and STK33 suppression in human cancer cells. *Cell* 2009; **137**: 821–34.
96 Hoffman GR, Rahal R, Buxton F, Xiang K, McAllister G, Frias E *et al.* Functional epigenetics approach identifies BRM/SMARCA2 as a critical synthetic lethal target in BRG1-deficient cancers. *Proc Natl Acad Sci U S A* 2014; **111**: 3128–33.
97 Etemadmoghadam D, Weir B a, Au-Yeung G, Alsop K, Mitchell G, George J *et al.* Synthetic lethality between CCNE1 amplification and loss of BRCA1. *Proc Natl Acad Sci U S A* 2013; **110**: 19489–94.
98 Mayr D, Kanitz V, Anderegg B, Luthardt B, Engel J, Löhrs U *et al.* Analysis of Gene Amplification and Prognostic Markers in Ovarian Cancer Using Comparative Genomic Hybridization for Microarrays and Immunohistochemical Analysis for Tissue Microarrays. *Am J Clin Pathol* 2006; **126**: 101–109.
99 Etemadmoghadam D, Beroukhim R. Integrated genome-wide DNA copy number and expression analysis identifies distinct mechanisms of primary chemoresistance in ovarian carcinomas. *Clin Cancer …* 2009; **15**: 1417–1427.
100 Akli S, Keyomarsi K. Cyclin E and its low molecular weight forms in human cancer and as targets for cancer therapy. *Cancer Biol Ther* 2003.
101 Jones P a, Baylin SB. The fundamental role of epigenetic events in cancer. *Nat Rev Genet* 2002; **3**: 415–28.
102 Bai J, Mei P, Zhang C, Chen F, Li C, Pan Z *et al.* BRG1 is a prognostic marker and potential therapeutic target in human breast cancer. *PLoS One* 2013; **8**: e59772.
103 Schubbert S, Shannon K, Bollag G. Hyperactive Ras in developmental disorders and cancer. *Nat Rev Cancer* 2007; **7**: 295–308.
104 Downward J. Targeting RAS signalling pathways in cancer therapy. *Nat Rev Cancer* 2003; **3**: 11–22.
105 Pylayeva-Gupta Y, Grabocka E, Bar-Sagi D. RAS oncogenes: weaving a tumorigenic web. *Nat Rev Cancer* 2011; **11**: 761–74.
106 Jansen R, Embden JD a. Van, Gaastra W, Schouls LM. Identification of genes that are associated with DNA repeats in prokaryotes. *Mol Microbiol* 2002; **43**: 1565–1575.
107 Wiedenheft B, Sternberg SH, Doudna J a. RNA-guided genetic silencing systems in bacteria and archaea. *Nature* 2012; **482**: 331–8.
108 Sander JD, Joung JK. CRISPR-Cas systems for editing, regulating and targeting genomes. *Nat Biotechnol* 2014; **32**: 347–55.
109 Koike-Yusa H, Li Y, Tan E-P, Velasco-Herrera MDC, Yusa K. Genome-wide recessive genetic screening in mammalian cells with a lentiviral CRISPR-guide RNA library. *Nat Biotechnol* 2014; **32**: 267–73.
110 Szappanos B, Kovács K, Szamecz B, Honti F, Costanzo M, Baryshnikova A *et al.* An integrated approach to characterize genetic interaction networks in yeast metabolism. *Nat Genet* 2011; **43**: 656–62.

111 Jerby-Arnon L, Pfetzer N, Waldman YY, McGarry L, James D, Shanks E *et al.* Predicting Cancer-Specific Vulnerability via Data-Driven Detection of Synthetic Lethality. *Cell* 2014; **158**: 1199–1209.
112 Kaelin WG. The Concept of Synthetic Lethality in the Context of Anticancer Therapy. *Nat Rev Cancer* 2005; **5**: 689–698.
113 Bommi-Reddy A, Almeciga I, Sawyer J, Geisen C, Li W, Harlow E *et al.* Kinase requirements in human cells: III. Altered kinase requirements in VHL-/- cancer cells detected in a pilot synthetic lethal screen. *Proc Natl Acad Sci U S A* 2008; **105**: 16484–16489.
114 Woldemichael GM, Turbyville TJ, Vasselli JR, Linehan WM, McMahon JB. Lack of a functional VHL gene product sensitizes renal cell carcinoma cells to the apoptotic effects of the protein synthesis inhibitor verrucarin A. *Neoplasia* 2012; **14**: 771–7.
115 Wolff NC, Pavía-Jiménez A, Tcheuyap VT, Alexander S, Vishwanath M, Christie A *et al.* High-throughput simultaneous screen and counterscreen identifies homoharringtonine as synthetic lethal with von Hippel-Lindau loss in renal cell carcinoma. *Oncotarget* 2015; **6**: 16951–62.
116 Rotenberg SA, Sun XG. Photoinduced inactivation of protein kinase C by dequalinium identifies the RACK-1-binding domain as a recognition site. *J Biol Chem* 1998; **273**: 2390–2395.
117 Coppin C, Kollmannsberger C, Le L, Porzsolt F, Wilt TJ. Targeted therapy for advanced renal cell cancer (RCC): A Cochrane systematic review of published randomised trials. *BJU Int* 2011; **108**: 1556–1563.
118 Minner S, Rump D, Tennstedt P, Simon R, Burandt E, Terracciano L *et al.* Epidermal growth factor receptor protein expression and genomic alterations in renal cell carcinoma. *Cancer* 2012; **118**: 1268–1275.
119 Zhang Q, Yang H. The Roles of VHL-Dependent Ubiquitination in Signaling and Cancer. *Front Oncol* 2012; **2**: 1–7.
120 Peng XH, Karna P, Cao Z, Jiang BH, Zhou M, Yang L. Cross-talk between epidermal growth factor receptor and hypoxia-inducible factor-1α signal pathways increases resistance to apoptosis by up-regulating survivin gene expression. *J Biol Chem* 2006; **281**: 25903–25914.
121 Leclerc S, Garnier M, Hoessel R, Marko D, Bibb JA, Snyder GL *et al.* Indirubins inhibit glycogen synthase kinase-3β and CDK5/P25, two protein kinases involved in abnormal tau phosphorylation in Alzheimer's disease. A property common to most cyclin-dependent kinase inhibitors? *J Biol Chem* 2001; **276**: 251–260.
122 Zaharevitz D, Gussio R, Leost M, Senderowicz A, Lahusen T, Kunick C *et al.* Discovery and initial characterization of the paullones, a novel class of small-molecule inhibitors of cyclin-dependent kinases. *Cancer Res* 1999; **59**: 2566–9.
123 Lane ME, Yu B, Rice A, Cells C, Lipson KE, Liang C *et al.* A Novel cdk2-selective Inhibitor , SU9516 , Induces Apoptosis in Colon Carcinoma Cells A Novel cdk2-selective Inhibitor , SU9516 , Induces Apoptosis in Colon. *Cancer Res* 2001; : 6170–6177.
124 Sutphin PD, Chan D a, Li JM, Turcotte S, Krieg AJ, Giaccia AJ. Targeting the loss of the von Hippel-Lindau tumor suppressor gene in renal cell carcinoma cells. *Cancer Res* 2007; **67**: 5896–905.
125 Razorenova O V, Finger EC, Colavitti R, Chernikova SB, Boiko AD, Chan CKF *et al.* VHL loss in renal cell carcinoma leads to up-regulation of CUB domain-containing

protein 1 to stimulate PKC{delta}-driven migration. *Proc Natl Acad Sci U S A* 2011; **108**: 1931–1936.
126 Siegel RL, Miller KD, Jemal A. Cancer Statistics, 2016. *Cancer J Clin* 2016; **66**: 7–30.
127 Motzer RJ, Russo P. Systemic therapy for renal cell carcinoma. *J Urol* 2000; **163**: 408–17.
128 Siegel R, Ma J, Zou Z, Jemal A. Cancer statistics, 2014. *CA Cancer J Clin* 2014; **64**: 9–29.
129 Hodorova I, Rybarova S. Multidrug resistance proteins in renal cell carcinoma. *Folia Biol.* 2008; **192**: 187–192.
130 Jonasch E, Futreal P a., Davis IJ, Bailey ST, Kim WY, Brugarolas J *et al.* State of the Science: An Update on Renal Cell Carcinoma. *Mol Cancer Res* 2012; **10**: 859–880.
131 Motzer RJ, Hutson TE, Tomczak P. Sunitinib versus Interferon Alfa in Metastatic Renal-Cell Carcinoma. *N Engl JMed* 2007; **356**: 115–124.
132 Sternberg CN, Davis ID, Mardiak J, Szczylik C, Lee E, Wagstaff J *et al.* Pazopanib in locally advanced or metastatic renal cell carcinoma: Results of a randomized phase III trial. *J Clin Oncol* 2010; **28**: 1061–1068.
133 Motzer RJ, Hutson TE, Tomczak P, Michaelson MD, Bukowski RM, Oudard S *et al.* Overall survival and updated results for sunitinib compared with interferon alfa in patients with metastatic renal cell carcinoma. *J Clin Oncol* 2009; **27**: 3584–3590.
134 Hudes Carducci, M, Tomczak, P, Dutcher, J, Figlin, R, Kapoor, A, Staroslawska, E, Sosman, J, McDermott, D, Bodrogi, I, Kovacevic, Z, Lesovoy, V, Schmidt-Wolf, IGH, Barbarash, O, Gokmen, E, O'Toole, T, Lustgarten, S, Moore, L, Motzer, RJ, the Global ARCC G. Temsirolimus, interferon alpha or both for advanced renal cell carcinoma. *N Engl J Med* 2007; **356**: 2271–2281.
135 Pinto A. Adjuvant Therapy for Renal Cell Carcinoma. *Clin Genitourin Cancer* 2014; **12**: 408–12.
136 Shi J, Wu X, Surma M, Vemula S, Zhang L, Yang Y *et al.* Distinct roles for ROCK1 and ROCK2 in the regulation of cell detachment. *Cell Death Dis* 2013; **4**: e483.
137 Kamai T, Tsujii T, Arai K. Significant Association of Rho / ROCK Pathway with Invasion and Metastasis of Bladder Cancer Significant Association of Rho / ROCK Pathway with Invasion and Metastasis of Bladder Cancer 1. 2003; **9**: 2632–2641.
138 Kamai T, Yamanishi T, Shirataki H, Takagi K, Asami H, Ito Y *et al.* Overexpression of RhoA, Rac1, and Cdc42 GTPases is associated with progression in testicular cancer. *Clin Cancer Res* 2004; **10**: 4799–4805.
139 Lane J, Martin T, Watkins G, Mansel R, Jiang W. The expression and prognostic value of ROCK I and ROCK II and their role in human breast cancer. *Int J Oncol* 2008; **33**: 585–593.
140 Zhang C, Zhang S, Zhang Z, He J, Xu Y, Liu S. ROCK has a crucial role in regulating prostate tumor growth through interaction with c-Myc. *Oncogene* 2013; **33**: 5582–5591.
141 Liu S, Goldstein RH, Scepansky EM, Rosenblatt M. Inhibition of rho-associated kinase signaling prevents breast cancer metastasis to human bone. *Cancer Res* 2009; **69**: 8742–51.
142 Liao JK, Seto M, Noma K. Rho Kinase (ROCK) Inhibitors. *J Cardiovasc Pharmacol* 2007; **50**: 17–24.
143 Mleczak A, Millar S, Tooze S a., Olson MF, Chan EYW. Regulation of autophagosome formation by Rho kinase. *Cell Signal* 2013; **25**: 1–11.
144 Nakagawa O, Fujisawa K, Ishizaki T, Saito Y, Nakao K, Narumiya S. ROCK-I and

ROCK-II, two isoforms of Rho-associated coiled-coil forming protein serine/threonine kinase in mice. *FEBS Lett* 1996; **392**: 189–193.
145 Razorenova O V, Castellini L, Colavitti R, Edgington LE, Nicolau M, Huang X *et al.* The apoptosis repressor with a CARD domain (ARC) gene is a direct hypoxia-inducible factor 1 target gene and promotes survival and proliferation of VHL-deficient renal cancer cells. *Mol Cell Biol* 2014; **34**: 739–51.
146 Maxwell PH, Wiesener MS, Chang GW, Clifford SC, Vaux EC, Cockman ME *et al.* The tumour suppressor protein VHL targets hypoxia-inducible factors for oxygen-dependent proteolysis. *Nature* 1999; **399**: 271–5.
147 Patel R a, Forinash KD, Pireddu R, Sun Y, Sun N, Martin MP *et al.* RKI-1447 is a potent inhibitor of the Rho-associated ROCK kinases with anti-invasive and antitumor activities in breast cancer. *Cancer Res* 2012; **72**: 5025–34.
148 Isler D, Ozaslan M, Karagoz ID, Kilic IH, Karakok M, Taysi S *et al.* Antitumoral effect of a selective Rho-kinase inhibitor Y-27632 against Ehrlich ascites carcinoma in mice. *Pharmacol Rep* 2014; **66**: 114–20.
149 Rikitake Y, Kim H-H, Huang Z, Seto M, Yano K, Asano T *et al.* Inhibition of Rho kinase (ROCK) leads to increased cerebral blood flow and stroke protection. *Stroke* 2005; **36**: 2251–7.
150 Inan S, Büyükafşar K. Antiepileptic effects of two Rho-kinase inhibitors, Y-27632 and fasudil, in mice. *Br J Pharmacol* 2008; **155**: 44–51.
151 Nagatoya K, Moriyama T, Kawada N, Takeji M, Oseto S, Murozono T *et al.* Y-27632 prevents tubulointerstitial fibrosis in mouse kidneys with unilateral ureteral obstruction. *Kidney Int* 2002; **61**: 1684–1695.
152 Lochhead P a, Wickman G, Mezna M, Olson MF. Activating ROCK1 somatic mutations in human cancer. *Oncogene* 2010; **29**: 2591–2598.
153 Liu X, Choy E, Hornicek FJ, Yang S, Yang C, Harmon D *et al.* ROCK1 as a potential therapeutic target in osteosarcoma. *J Orthop Res* 2011; **29**: 1259–1266.
154 Gilkes DM, Xiang L, Lee SJ, Chaturvedi P, Hubbi ME, Wirtz D *et al.* Hypoxia-inducible factors mediate coordinated RhoA-ROCK1 expression and signaling in breast cancer cells. *Proc Natl Acad Sci U S A* 2013; **111**: E384–E393.
155 Greijer AE, van der Groep P, Kemming D, Shvarts A, Semenza GL, Meijer GA *et al.* Up-regualtion of gene expression by hypoxia is mediated predominantly by hypoxia-inducible factor I (HIF-I). *J Pathol* 2005; **206**: 291–304.
156 Turcotte S. HIF-1alpha mRNA and protein upregulation involves Rho GTPase expression during hypoxia in renal cell carcinoma. *J Cell Sci* 2003; **116**: 2247–2260.
157 Takata K, Morishige K-I, Takahashi T, Hashimoto K, Tsutsumi S, Yin L *et al.* Fasudil-induced hypoxia-inducible factor-1alpha degradation disrupts a hypoxia-driven vascular endothelial growth factor autocrine mechanism in endothelial cells. *Mol Cancer Ther* 2008; **7**: 1551–61.
158 Mizukami Y, Fujiki K, Duerr E-M, Gala M, Jo W-S, Zhang X *et al.* Hypoxic regulation of vascular endothelial growth factor through the induction of phosphatidylinositol 3-kinase/Rho/ROCK and c-Myc. *J Biol Chem* 2006; **281**: 13957–13963.
159 Razorenova O V., Ivanov a. V., Budanov a. V., Chumakov PM. Virus-based reporter systems for monitoring transcriptional activity of hypoxia-inducible factor 1. *Gene* 2005; **350**: 89–98.
160 Motzer RJ. Renal cell carcinoma: progress against an elusive tumor. *Semin Oncol* 2000;

27: 113–114.
161 Latif F, Tory K, Gnarra J, Yao M, Duh F-M, Lou Orcutt M *et al.* Identification of the von Hippel-Lindau Disease Tumor Suppressor Gene. *Source Sci New Ser* 1993; **260**: 1317–1320.
162 Tanihara H, Inoue T, Yamamoto T, Kuwayama Y, Abe H, Araie M. Phase 1 Clinical Trials of a Selective Rho Kinase Inhibitor, K-115. *JAMA Ophthalmol* 2014; **131**: 1288–1295.
163 Dong M, Yan BP, Liao JK, Lam Y, Yip GWK, Yu M. Rho-kinase inhibition: a novel therapeutic target for the treatment of cardiovascular diseases. *Drug Discov Today* 2013; **15**: 622–629.
164 Yap TA, Walton MI, Grimshaw KM, Te Poele RH, Eve PD, Valenti MR *et al.* AT13148 is a novel, oral multi-AGC kinase inhibitor with potent pharmacodynamic and antitumor activity. *Clin Cancer Res* 2012; **18**: 3912–3923.
165 Cai A, Zhou Y, Li L. Rho-GTPase and Atherosclerosis: A Effects of Statins. *J Am Heart Assoc* 2015; **4**: e002113.
166 Corsini a, Bellosta S, Baetta R, Fumagalli R, Paoletti R, Bernini F. New insights into the pharmacodynamic and pharmacokinetic properties of statins. *Pharmacol Ther* 1999; **84**: 413–428.
167 Buzková H, Pechandová K, Danzig V, Vareka T, Perlik F, Zak A *et al.* Lipid-lowering effect of fluvastatin in relation to cytochrome P450 2C9 variant alleles frequently distributed in the Czech population. *Med Sci Monit* 2012; **18**: CR512-517.
168 Kim WS, Kim MM, Choi HJ, Yoon SS, Lee MH, Park K *et al.* Phase II study of high-dose lovastatin in patients with advanced gastric adenocarcinoma. *Invest New Drugs* 2001; **19**: 81–83.
169 Larner J, Jane J, Laws E, Packer R, Myers C, Shaffrey M. A phase I-II trial of lovastatin for anaplastic astrocytoma and glioblastoma multiforme. *Am J Clin Oncol* 1998; **21**: 579–583.
170 Rawlings R, Nohria A, Liu PY, Donnelly J, Creager MA, Ganz P *et al.* Comparison of Effects of Rosuvastatin (10 mg) Versus Atorvastatin (40 mg) on Rho Kinase Activity in Caucasian Men With a Previous Atherosclerotic Event. *Am J Cardiol* 2009; **103**: 437–441.
171 Reilly JE, Neighbors JD, Tong H, Henry MD, Hohl RJ. Targeting geranylgeranylation reduces adrenal gland tumor burden in a murine model of prostate cancer metastasis. *Clin Exp Metastasis* 2015; **32**: 555–566.
172 Menter DG, Ramsauer VP, Harirforoosh S, Chakraborty K, Yang P, Hsi L *et al.* Differential effects of pravastatin and simvastatin on the growth of tumor cells from different organ sites. *PLoS One* 2011; **6**.
173 Collisson E a, Kleer C, Wu M, De A, Gambhir SS, Merajver SD *et al.* Atorvastatin prevents RhoC isoprenylation, invasion, and metastasis in human melanoma cells. *Mol Cancer Ther* 2003; **2**: 941–948.
174 Feng J, Ito M, Kureishi Y, Ichikawa K, Amano M, Isaka N *et al.* Rho-associated kinase of chicken gizzard smooth muscle. *J Biol Chem* 1999; **274**: 3744–3752.
175 Garcia MC, Williams J, Johnson K, Olden K, Roberts JD. Arachidonic acid stimulates formation of a novel complex containing nucleolin and RhoA. *FEBS Lett* 2011; **585**: 618–622.
176 Masoud GN, Li W. HIF-1a pathway: Role, regulation and intervention for cancer therapy. *Acta Pharm Sin B* 2015; **5**: 378–389.

177 Kaffenberger SD, Morgan TM, Stratton KL, Boachie AM, Barocas D a., Chang SS *et al.* Statin use is associated with improved survival in patients undergoing surgery for renal cell carcinoma. *BJU Int* 2012; **110**: 21.e11-21.e17.
178 Hamilton RJ, Morilla D, Cabrera F, Leapman M, Chen LY, Bernstein M *et al.* The association between statin medication and progression after surgery for localized renal cell carcinoma. *J Urol* 2014; **191**: 914–919.
179 Hoque A, Chen H, Xu X. Statin Induces Apoptosis and Cell Growth Arrest in Prostate Cancer Cells. *Cancer Epidemiol Biomarkers Prev* 2008; **17**: 88–94.
180 Araki M, Maeda M, Motojima K. Hydrophobic statins induce autophagy and cell death in human rhabdomyosarcoma cells by depleting geranylgeranyl diphosphate. *Eur J Pharmacol* 2012; **674**: 95–103.
181 Yang PM, Liu YL, Lin YC, Shun CT, Wu MS, Chen CC. Inhibition of autophagy enhances anticancer effects of atorvastatin in digestive malignancies. *Cancer Res* 2010; **70**: 7699–7709.
182 Parikh A, Childress C, Deitrick K, Lin Q, Rukstalis D, Yang W. Statin-induced autophagy by inhibition of geranylgeranyl biosynthesis in prostate cancer PC3 cells. *Prostate* 2010; **70**: 971–981.
183 Malenda A, Skrobanska A, Issat T, Winiarska M, Bil J, Oleszczak B *et al.* Statins impair glucose uptake in tumor cells. *Neoplasia* 2012; **14**: 311–23.
184 Smith R, Solberg R, Jacobsen LL, Voreland AL, Rustan AC, Thoresen H *et al.* Simvastatin inhibits glucose metabolism and legumain activity in human myotubes. *PLoS One* 2014; **9**: 1–9.
185 Nowis D, Malenda A, Furs K, Oleszczak B, Sadowski R, Chlebowska J *et al.* Statins impair glucose uptake in human cells. *BMJ open diabetes Res care* 2014; **2**: e000017.
186 Sala SG. HMG-CoA Reductase Inhibitor Simvastatin Inhibits Cell Cycle Progression at the G 1 / S Checkpoint in Immortalized Lymphocytes from Alzheimer ' s Disease Patients Independently of Cholesterol-Lowering Effects. *Pharmacology* 2008; **324**: 352–359.
187 Tsubaki M, Takeda T, Sakamoto K, Shimaoka H, Fujita A, Itoh T *et al.* Bisphosphonates and statins inhibit expression and secretion of MIP-1α via suppression of Ras/MEK/ERK/AML-1A and Ras/PI3K/Akt/AML-1A pathways. *Am J Cancer Res* 2015; **5**: 168–79.
188 Takemi Otsuki, Sakaguchi H, Hatayama T, Fujii T, Tsujioka T, Sugihara T *et al.* Effects of an HMG-CoA reductase inhibitor, simvastatin, on human myeloma cells. *Oncol Rep* 2004; **11**: 1053–1058.
189 Engers R, Zwaka TP, Gohr L, Weber A, Gerharz CD, Gabbert HE. Tiam1 mutations in human renal-cell carcinomas. *Int J Cancer* 2000; **88**: 369–376.
190 Talks KL, Turley H, Gatter KC, Maxwell PH, Pugh CW, Ratcliffe PJ *et al.* The expression and distribution of the hypoxia-inducible factors HIF-1alpha and HIF-2alpha in normal human tissues, cancers, and tumor-associated macrophages. *Am J Pathol* 2000; **157**: 411–21.
191 Zhong H, De Marzo AM, Laughner E, Lim M, Hilton DA, Zagzag D *et al.* Overexpression of hypoxia-inducible factor 1alpha in common human cancers and their metastases. *Cancer Res* 1999; **59**: 5830–5.
192 Ravi R, Mookerjee B, Bhujwalla ZM, Sutter CH, Artemov D, Zeng Q *et al.* Regulation of tumor angiogenesis by p53-induced degradation of hypoxia-inducible factor 1α. *Genes Dev* 2000; **14**: 34–44.

193 Sermeus A, Michiels C. Reciprocal influence of the p53 and the hypoxic pathways. *Cell Death Dis* 2011; **2**: e164.
194 Mazure NM, Chen EY, Laderoute KR, Giaccia AJ. Induction of Vascular Endothelial Growth Factor by Hypoxia Is Modulated by a Phosphatidylinositol 3-Kinase/Akt Signaling Pathway in Ha-ras-Transformed Cells Through a Hypoxia Inducible Factor-1 Transcriptional Element. *Blood* 1997; **90**: 3322–3331.
195 Takacova M, Holotnakova T, Barathova M, Pastorekova S, Kopacek J, Pastorek J *et al.* Src induces expression of carbonic anhydrase IX via hypoxia-inducible factor 1. *Oncol Rep* 2010; **23**: 869–874.
196 Doe MR, Ascano JM, Kaur M, Cole MD. Myc post-transcriptionally induces HIF1 protein and target gene expression in normal and cancer cells. *Cancer Res* 2012; **72**: 949–957.
197 Liu QL, Liang QL, Li ZY, Zhou Y, Ou WT, Huang ZG. Function and expression of prolyl hydroxylase 3 in cancers. *Arch Med Sci* 2013; **9**: 589–593.
198 Astuti D, Ricketts CJ, Chowdhury R, McDonough MA, Gentle D, Kirby G *et al.* Mutation analysis of HIF prolyl hydroxylases (PHD/EGLN) in individuals with features of phaeochromocytoma and renal cell carcinoma susceptibility. *Endocr Relat Cancer* 2011; **18**: 73–83.
199 Thibault A, Samid D, Tompkins AC, Figg WD, Cooper MR, Hohl RJ *et al.* Phase I study of lovastatin, an inhibitor of the mevalonate pathway, in patients with cancer. *Clin Cancer Res* 1996; **2**: 483–491.
200 Siekmeier R, Lattke P, Mix C, Park JW, Jaross W. Dose dependency of fluvastatin pharmacokinetics in serum determined by reversed phase HPLC. *J Cardiovasc Pharmacol Ther* 2001; **6**: 137–145.
201 Fang Z, Tang Y, Fang J, Zhou Z, Xing Z, Guo Z *et al.* Simvastatin Inhibits Renal Cancer Cell Growth and Metastasis via AKT/mTOR, ERK and JAK2/STAT3 Pathway. *PLoS One* 2013; **8**.
202 Ruth MC, Xu Y, Maxwell IH, Ahn NG, Norris D a, Shellman YG. RhoC promotes human melanoma invasion in a PI3K/Akt-dependent pathway. *J Invest Dermatol* 2006; **126**: 862–868.
203 Choi S-K, Min GE, Jeon SH, Lee H-L, Chang S-G, Yoo KH. Effects of statins on the prognosis of local and locally advanced renal cell carcinoma following nephrectomy. *Mol Clin Oncol* 2013; **1**: 365–368.
204 Viers BR, Houston Thompson R, Psutka SP, Lohse CM, Cheville JC, Leibovich BC *et al.* The association of statin therapy with clinicopathologic outcomes and survival among patients with localized renal cell carcinoma undergoing nephrectomy. *Urol Oncol Semin Orig Investig* 2015; **33**: 388.e11-388.e18.
205 Butman; JA, Linehan; WM, Lonser RR. Neurologic manifestations of von Hippel-Lindau disease. Grand Rounds at the Clinical Center of the National Institutes of Health. *JAMA* 2008; **300**: 1334–1342.
206 Li L, Zhang L, Zhang X, Yan Q, Minamishima YA, Olumi AF *et al.* Hypoxia-inducible factor linked to differential kidney cancer risk seen with type 2A and type 2B VHL mutations. *Mol Cell Biol* 2007; **27**: 5381–92.
207 Knauth K, Bex C, Jemth P, Buchberger a. Renal cell carcinoma risk in type 2 von Hippel-Lindau disease correlates with defects in pVHL stability and HIF-1alpha interactions. *Oncogene* 2006; **25**: 370–377.
208 Zundel W, Schindler C, Haas-Kogan D, Koong A, Kaper F, Chen E *et al.* Loss of PTEN

facilitates HIF-1-mediated gene expression. *Genes Dev* 2000; **14**: 391–396.
209 Orgaz JL, Herraiz C, Sanz-Moreno V. Rho GTPases modulate malignant transformation of tumor cells. *Small GTPases* 2014; **5**: e29019.
210 Lin Y, Zheng Y. Approaches of targeting Rho GTPases in cancer drug discovery. *Expert Opin Drug Discov* 2015; **10**: 1–20.
211 Lord-Fontaine S, Yang F, Diep Q, Dergham P, Munzer S, Tremblay P *et al.* Local Inhibition of Rho Signaling by Cell-Permeable Recombinant Protein BA-210 Prevents Secondary Damage and Promotes Functional Recovery following Acute Spinal Cord Injury. *J Neurotrauma* 2008; **25**: 1309–1322.
212 Ogata S, Morishige K-I, Sawada K, Hashimoto K, Mabuchi S, Kawase C *et al.* Fasudil inhibits lysophosphatidic acid-induced invasiveness of human ovarian cancer cells. *Int J Gynecol Cancer* 2009; **19**: 1142–1149.
213 Sadok A, McCarthy A, Caldwell J, Collins I, Garrett MD, Yeo M *et al.* Rho kinase inhibitors block melanoma cell migration and inhibit metastasis. *Cancer Res* 2015; **75**: 2272–2284.
214 Xi Y, Niu J, Shen Y, Li D, Peng X, Wu X. AT13148, a first-in-class multi-AGC kinase inhibitor, potently inhibits gastric cancer cells both in vitro and in vivo. *Biochem Biophys Res Commun* 2016; **478**: 330–336.
215 Ewing RM, Chu P, Elisma F, Li H, Taylor P, Climie S *et al.* Large-scale mapping of human protein–protein interactions by mass spectrometry. *Mol Syst Biol* 2007; **3**: 1–17.
216 Harlander S, Schönenberger D, Toussaint NC, Prummer M, Catalano A, Brandt L *et al.* Combined mutation in Vhl, Trp53 and Rb1 causes clear cell renal cell carcinoma in mice. *Nat Med* 2017; **23**: 869–877.
217 Nargund AM, Pham CG, Dong Y, Wang PI, Osmangeyoglu HU, Xie Y *et al.* The SWI/SNF Protein PBRM1 Restrains VHL-Loss-Driven Clear Cell Renal Cell Carcinoma. *Cell Rep* 2017.
218 Miyata Y, Kanetake H, Kanda S. Presence of phosphorylated hepatocyte growth factor receptor/c-Met is associated with tumor progression and survival in patients with conventional renal cell carcinoma. *Clin Cancer Res* 2006; **12**: 4876–4881.
219 Li B, Qiu B, Lee DSM, Walton ZE, Ochocki JD, Mathew LK *et al.* Fructose-1,6-bisphosphatase opposes renal carcinoma progression. *Nature* 2014.